

THESE DE DOCTORAT

pour obtenir le grade de

Docteur d'AgroParisTech

Spécialité : sciences de l'environnement

École doctorale n° 581

Agriculture, alimentation, biologie, environnement et santé (ABIES)

par

Uday PIMPLE

Spatio-temporal dynamics of mangrove forest in Trat province of Thailand

Directeur de thèse : **Valéry GOND**
Co-encadrante de thèse : **Uta BERGER**

Thèse présentée et soutenue à Paris, le 26 Octobre 2021

Composition du jury :

Samuel CORGNE, Professeur, Université Rennes 2
Frédéric ACHARD, Chercheur (HDR), Joint Research Center (Italie)
Catherine LOVELOCK, Professeure, The University of Queensland (Australie)
Julie BETBEDER, Chercheure, CIRAD
Plinio SIST, Chercheur (assimilé Directeur de recherche), CIRAD
Valéry GOND, Chercheur (assimilé Directeur de recherche), CIRAD
Uta BERGER, Professeure, Technische Universität Dresden (Allemagne)

Président
Rapporteur & Examineur
Rapporteur & Examinatrice
Examinatrice
Examineur
Directeur de thèse
Co-Encadrante de thèse

*It is that range of biodiversity that
we must care for - the whole thing-
rather than just one or two stars*

-David Attenborough

Table of Contents

Preface:.....	6
Summary and thesis structure	9
Résumé et structure de la thèse	12
Background and synthesis.....	15
Abstract:.....	16
1.1 Mangrove ecosystems and their species diversity	17
1.2 Spatial and temporal aspects of mangrove species distribution	22
1.3 Objectives	25
1.4 Demonstration site.....	25
1.5 Difficulties and challenges for diversity monitoring and predictions.....	27
1.5.1 Field inventory data.....	27
1.5.2 Remote sensing data	28
1.5.3 Temporal inconsistencies and gaps in mangrove monitoring	36
1.5.4 Diversity modeling	36
1.6 Discussion on good practices for diversity monitoring and predictions.....	37
1.6.1 Systematic sampling design for characterization of spatial scale diversity	37
1.6.2 Overcoming the challenges of remote sensing data for monitoring mangrove diversity.....	40
1.7 Summary of best practices	47
1.8 Outlook on recent developments in remote sensing.....	50
1.9 Conclusions.....	51
1.10 Research questions.....	53
CHAPTER 2.....	55
Assessing long-term dynamics of in mangrove forest ecosystem	55
Abstract:.....	56
2.1 Introduction	57
2.2 Study site and methodology.....	59
2.2.1 Study area.....	59
2.2.2 Landsat imagery	59
2.3 Training and validation sampling design.....	60
2.4 Pixel based random forest classifier	61

2.5 Validation.....	62
2.6 Post classification change detection	62
2.7 Results	62
2.7.1 Cloud free annual composite of Landsat imagery.....	62
2.7.2 Magnitude of mangrove forest and its surrounding change	64
2.7.3 LULC transition from 1987 to 2017	67
2.8 Discussion	68
2.8.1 Overcoming the limitation of Landsat imagery for monitoring mangrove	68
2.8.2 Change in land use and land cover	68
2.8 Conclusion	69
CHAPTER 3.....	70
Systematic transect plot inventories for species and structural diversity.....	70
Abstract:	71
3.1 Mangrove inventories data specification.....	72
3.2 Value of the data	73
3.3 Data description	73
3.4 Experimental design, materials, and methods.....	73
CHAPTER 4.....	75
Assessing degree of success of rehabilitation interventions	75
Abstract:	76
4. 1 Introduction	77
4. 2 Data and Methods.....	81
4.2.1 Study site description	81
4.2.2 Sampling design	81
4. 3 General description of the methodology	83
4. 4 Species diversity and structural indicators	83
4. 5 Landsat imagery.....	85
4. 6 Mangrove forest normalization	86
4. 7 Sentinel-2 multi-spectral instrument (MSI) high-resolution mask.....	87
4. 8 Masking the mangrove forest area	87
4. 9 Normalized difference infrared index (NDII).....	88
4. 10 Time series of the natural, rehabilitated, and disturbed mangroves	88
4.10.1 Stable mangroves	89

4.10.2 Recovery: development of rehabilitated or naturally regenerated mangroves	89
4.10.3 Disturbance	90
4. 11 Outline of automatic regrowth monitoring algorithm	90
4. 12 Results.....	92
4.12.1 Species diversity and composition.....	92
4.12.2 Structural compositions of the species	96
4.12.3 Landsat annual composite NDII time series assessment	98
4. 13 Discussion	103
4.13.1 Long-term stability of the rehabilitated and natural mangroves	103
4.13.2 Evaluation of the annual composite time series.....	104
4. 14 Conclusions.....	107
CHAPTER 5.....	109
Diversity and intertidal zonation in response to natural, regenerated, and rehabilitated succession.....	109
Abstract:	110
5.1 Introduction	111
5.2 Study site description and sampling design	114
5.3 General description of the methodology	117
5.4 Forest species composition and structure and diversity indices	117
5.5 Species distribution analysis	119
5.5.1 Transect scale distribution	119
5.5.2 Landscape scale distribution	120
5.6 Landsat annual composites (1987–2020).....	121
5.7 Sentinel-2 multi-spectral instrument (MSI) annual composites (2015–2020).....	122
5.8 Normalized Difference Infrared Index (NDII).....	122
5.9 Modified automatic regrowth monitoring algorithm (ARMA).....	122
5.10 Functional indicators of diversity status and secondary succession	123
5.11 Statistical analysis	125
5.12 Results	126
5.12.1 Forest species diversity and composition	126
5.12.2 Structural compositions.....	128
5.12.3 Mangrove species intertidal and landscape scale distribution	132
5.12.4 Mangrove species intertidal and landscape scale distribution	136
5.13 Discussion	139

5.13.1 Intertidal characteristics and distribution of the mangrove ecosystems	139
5.13.2 Indicators of ecosystem diversity state and succession	140
5.14 Implications for mangrove conservation management	142
5.15 Conclusions.....	143
CHAPTER 6.....	144
Spatio-temporal dynamics of mangrove species diversity	144
Abstract:	145
6.1 Introduction.....	146
6.2 Study area and dataset	149
6.2.1 Study area.....	149
6.2.2 Landsat annual composites.....	151
6.2.3 Sentinel-2 MSI composites	151
6.2.4 Sentinel- 1 SAR composites.....	152
6.2.5 DEM	152
6.2.6 Tide gauge data	152
6.3 Data preparation	152
6.3.1 Mangrove forest normalization.....	152
6.3.2 NDVI.....	153
6.3.3 NDII	153
6.3.4 NDWI.....	153
6.3.5 NDWII	154
6.4 Low tide composites.....	154
6.5 Classification approach.....	155
6.5.1 Stratification of mangrove extent.....	155
6.5.2 Sampling design	156
6.6 Modified ARMA	158
6.7 Species distribution mapping: random forest classifier	159
6.8 Accuracy assessment	160
6.9 Results	161
6.9.1 Tidal influence on spectral reflectance of multi-spectral imagery.....	161
6.9.2 Effect of low and high tides on backscatter coefficient of SAR imagery	164
6.10 Mangrove forest gain and secondary successions.....	165
6.11 Species classification performance of multi-source satellite imagery.....	166

6.12 Discussion	169
6.12.1 Effects of tidal inundation on spectral reflectance and backscatter coefficient	169
6.12.2 Sensor performance for discriminating species and their associations	170
6.13 Conclusions.....	172
CHAPTER 7	173
Synthesis and future outlook	173
7.1 Conclusions.....	173
7.2 Implications for future conservation and diversity monitoring.....	177
References	187
Abstract :	214
Résumé:	215

Preface:

Throughout my dissertation, I received considerable support and assistance. Without it, I would not have been able to complete this research. Here, I would like to take some time to express my gratitude.

Merci! I would first like to express my gratitude to my supervisor, Valery Gond, whose expertise and support were invaluable in formulating and completing my Ph.D. Your support, encouragement, and on-demand availability helped me in this great stage of my academic achievement. It is almost six years ago that I met you on ResearchGate! Since then, it has been a great pleasure. You always helped to cope with high-pressure situations during project field surveys, meetings, and report submissions. I really enjoyed your supervision, the countless online meetings (sometimes on weekends), the regular chats on WhatsApp, and all the fieldwork and scientific meetings we did together in Thailand, Vietnam, and Europe. I consider myself very fortunate for being able to work with a very considerate, friendly, and encouraging supervision like you. I could not have imagined having a better advisor and mentor for my Ph.D. study and scientific career. I hope we will continue doing great work together in the future.

Danke! I greatly appreciate my second supervisor, Uta Berger, for her great feedback, excellent encouragement, and guidance. Having you in the supervision team always made me feel confident about mangrove ecology. I am grateful for your guidance, especially during my Ph.D., project proposals, manuscript writing, and whenever I get stuck with research or other ethical issues. We make a great team!

Grazie! The great Dario Simonetti. It has been more than seven years now that we met in one referred email, and since then the rest is history. Over time, you are more like a close friend and colleague who is sitting next door on Skype. I have learned a great deal about remote sensing during our past communications. Your enthusiasm for the subject always pushed me to work harder and achieve better results. We do a great job together.

Khàawp khun! The major of the Thai survey team, Kumrom Leadprathom. Your work ethics, field survey skills, and empathy toward team members in high-pressure work situations inspired me. Without you, it would not be possible to organize and manage all field work. I have learned a great deal of skills from you, including forest field surveys, forest ecology, and interactions with local communities and farmers. We make a great team, and I am sure we will continue to contribute to mangrove ecology and help local communities in Southeast Asia.

Khàawp khun! The commander of the Thai team, Sukan Pungkul. It has been more than eight years since we have met in remote sensing training. Your communication and management skills helped the project to move forward. I always admire your people skills. Without you, it would not be possible to manage bureaucratic situations. I am sure we will continue to contribute to mangrove research and contribute to Thai forest policies.

Khàawp khun! I would like to express my thanks to Asamaporn Sitthi for her support in managing all Thai communications, paperwork, translations, and technical support during this journey. Your role and support were crucial during many phases of this work.

Khàawp khun! I would like to express my thanks to Tamanai Pravinvongvuthi for his official support in managing fieldwork. Your support was crucial from the field survey and the implementation of results point of view. I am positive that we will continue to work in Trat.

Khàawp khun! I would like to express my deep gratitude to Ruchakorn Tanasomboonpan, Thanakrit Bunkoed, and Chaiwat Thaphrik. You guys are the real heroes who made all difficult fieldwork possible in a harsh mangrove environment. I have great admiration for your patience, fieldwork skills, and knowledge about the local ecology of mangroves in Trat. I have learned a great deal of mangrove field inventory measurement and survey navigation skills. In the field, we create a strong team.

Merci! I would like to express my thanks to Johan Oszwald for organizing committee meetings, giving me the opportunity for research stay and sharing my research with the University of Rennes-2, France.

Merci! I would like to express my thanks to Achard Frédéric for giving me the opportunity for a research stay and sharing my research with his team at the Joint Research Center, Europe Commission, Ispra, Italy.

Merci! I would like to express my thanks to Patrick Rousset for his support during the beginning of my Ph.D. Your support was crucial for building a bridge between CIRAD and me.

I would like to express my special thanks to thesis reporters Achard Frédéric and Catherine Lovelock, and examiners Samuel Corgne, Julie Betbeder, and Plinio Sist for their time and petitions to read, providing valuable comments, and critical discussion of my final thesis report.

Special thanks to Prof. Aaron M. Ellison, Harvard Forest, Harvard University, Massachusetts, for his help and suggestions regarding the analysis of randomization test and niche null model interpretation.

I would like to thank to H el ene Dessard and Ronny Peters their participation in field survey and discussions on formal analysis.

I would like to thank to Kraiwut Siri-one, Napaporn Kao-min, Radklao Au-ngern, Ridthichi Namsri, Nitiwut Nilawong, and Surasit Maneetab from the Royal Forest Department, for their support and participation during the ground elevation survey.

Special thanks to the institution and government agencies that were directly or indirectly involved include Department of Marine Coastal Resources, Thailand, Royal Thai Forest Department, Thailand, the Joint Research Center, Europe Commission, Italy, Technische Universit at Dresden, Germany, CIRAD, France, the Joint Graduate School of Energy and Environment, King Mongkut’s University of Technology Thonburi, Thailand, Universit e de Rennes-2, France.

Finally, I am thankful to my parents, brother, sister and friends for their support and encouragement.

This research was funded by the Southeast Asia-Europe Joint Funding Scheme for Research and Innovation (SEA-EU-NET), 2018-2021 as a part of a project entitled, “Monitoring and optimizing the design quality of mangrove restoration towards a sustainable coastal ecosystem management in Thailand and Mekong delta of Vietnam” [Project code :- Thailand (NSTDA): P-18-51184, France (ANR): N0 ANR- 17-ASIE-0003-01, Germany (BMBF): 01DQ18004].

Summary and thesis structure

Mangrove forests are of great ecological importance, have a high capacity for coastal protection under climate change, and have high socio-economic value on a global scale. These highly productive ecosystems are found in tropical and subtropical coastal regions worldwide. Recently, their widespread degradation and loss have led to global attention on enhancing regional-scale biodiversity. To date, species distribution mapping has only been conducted at a local scale without systematic data collection, and consequently, information at national, regional, and global scales remains limited. Mapping and monitoring the spatio-temporal scale of mangrove species biodiversity is one of the most important issues at national and regional level, when determining the degree of success of rehabilitation and enhancement in our general understanding. This Ph.D. thesis is organized into six chapters addressing mangrove species biodiversity and conservation management. Furthermore, it investigates the long-term effects of environmental and anthropogenic settings and processes on the spatio-temporal dynamics of mangrove forest species diversity and zonation.

Synthesis of limitations and current advances in biodiversity assessment: Introduction **Chapter-1** focuses on identifying the status and limitations of existing in situ, remote sensing, and modeling approaches for spatio-temporal assessment of mangrove forest species biodiversity. This chapter also identifies the recent advances in methods for quantifying landscape scale zonation and historic state using remote sensing by integrating a more robust systematic sampling design, environmental and anthropogenic settings, and temporal dynamics. Quantification based on a systematic sampling design could improve the reliability of ecosystem-based spatial and intertidal zonation patterns. Annual gap-free composites and radiometrically corrected time series data provide more accurate information on the historic state and secondary succession of mangrove forests.

Magnitude of mangrove forest and its surrounding landscape change: Understanding the changes in mangrove forests and their surroundings is crucial to determine how mangrove ecosystems are constantly changing and influenced by various natural and anthropogenic stressors. **Chapter 2** elaborates on the methodological approach for monitoring the spatio-temporal dynamics of mangrove landscapes. The main objective of this study was to quantify the evolution of mangrove forests in Thailand's Trat Province over the last 30 years (1987–2017) using the aforementioned methodological framework. The results revealed a significant decrease in agricultural area, while there was an increase in mangrove forests, shrimp/fish farms, and bare land areas. The results indicated that rehabilitation activities change the landscape dynamics of mangrove

forests. This chapter also presents an exploration and potential of annual composites and cloud computing platforms to generate consistent error-free and seamless images that make it possible to achieve fast and accurate classification, making it easier to detect constantly changing ecosystems.

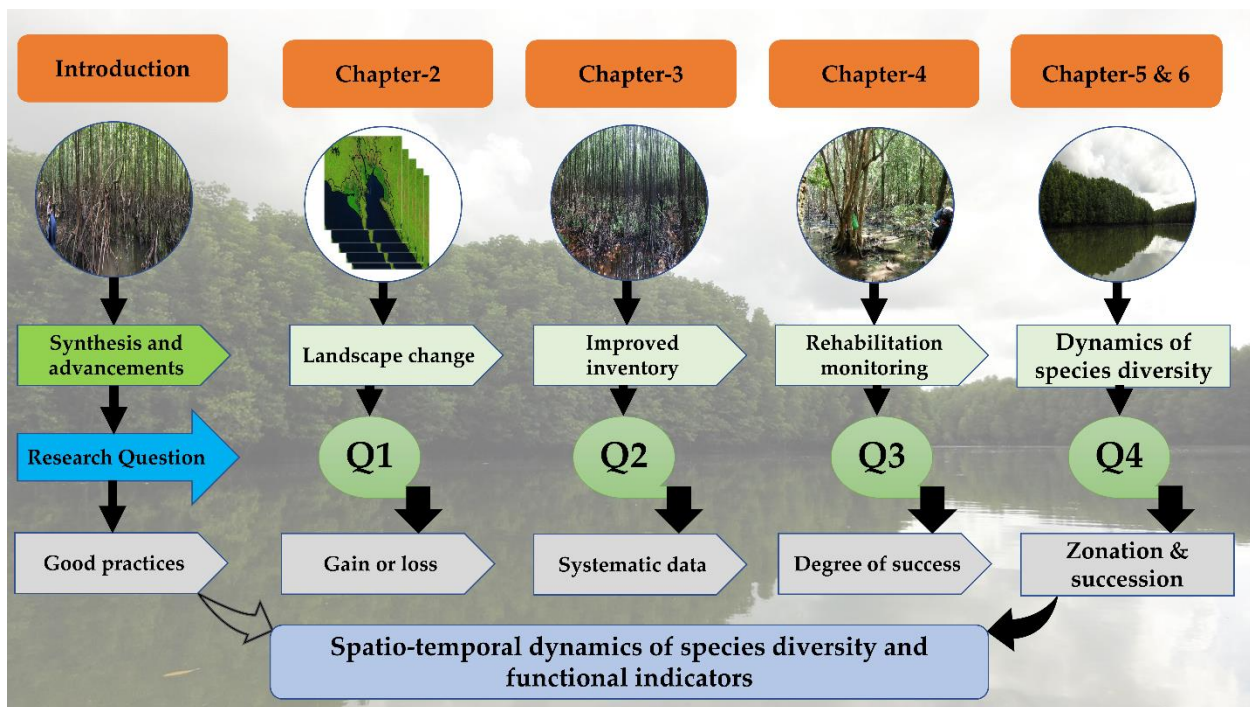
Systematic transect plot inventories for species and structural diversity: Studies focusing on mangrove species diversity and assessment of rehabilitation are often limited to non-systematic field inventories describing spatial species assemblages with very limited data, without considering intertidal zonation and occurrence of species related to the environmental settings. **Chapter 3** presents the field data sampling procedure for assessing species and structural diversity and the success of rehabilitation projects compared with adjacent natural mangroves. These data are freely available to users and can be used to fit site- and species-specific above-ground biomass models and validate satellite-based species height predictions across the intertidal zone.

Assessing the degree of success of rehabilitation interventions: Recent recognition of the importance of mangrove forests has stimulated interest in rehabilitating and restoring deforested mangrove landscapes in several parts of the world. Very few prior studies have assessed the long-term effectiveness of rehabilitation efforts in terms of the time required to stabilize rehabilitated forest stands, their structural development, and species diversity. **Chapter 4** evaluates thirty years of development of structure and species diversity in rehabilitated mangroves using the ARMA algorithm and field survey data in the Trat Province of Eastern Thailand. After thirty years, the rehabilitated mangroves at the study site consisted of monocultures of *Rhizophoraceae*. The rehabilitated forest showed high tree densities, low diameter at breast height, low basal area, and a very low rate of recruitment.

Spatial diversity, intertidal zonation, and functional indicators of succession: Quantitative examination of environmental settings on species zonation and spatio-temporal dynamics at the landscape scale has rarely been attempted. **Chapter 5** presents a novel framework to assess the spatial and intertidal mangrove species diversity and determine the historic state of the ecosystem. There was no single species zonation or group of species zonation along the elevation gradients. However, the structural parameters vary along the elevation gradient. The rehabilitated mangroves (30 years old) appeared to be monocultured (*Rhizophoraceae*), while the species diversity among regenerated forest stands varied at different locations. The effluent from shrimp farms may partially contribute to the disturbance of natural mangrove stands. This chapter also includes the fundamental concepts of modified ARMA. The findings provide insight into

the current state and historic changes in the mangrove ecosystem in the Trat Province in Thailand.

Spatio-temporal dynamics of mangrove species diversity: Regardless of advances in remote sensing, various noise sources affect the satellites in coastal areas, and complex forest structure, understanding of environmental and anthropogenic settings, and lack of proper integration of systematic field inventories make it a notoriously difficult ecosystem to study. To address this, **Chapter 6** combines all information from the aforementioned studies and introduces a state-of-the-art decision-support system that 1) includes a systematic field inventory approach; 2) tests the temporal consistency and change (modified ARMA) while reducing spectral noise caused by various contaminations; and 3) links the field inventory and dynamics to remote sensing for monitoring mangrove species diversity. The proposed approach reveals the potential of freely available satellite sensors, which can be powerful tools, and provides a significant advantage over traditional methods for monitoring complex mangrove species diversity.



Flow diagram of thesis structure

Résumé et structure de la thèse

Les forêts de mangroves sont d'une grande importance écologique car elles ont une grande capacité de protection des côtes dans le contexte des changements climatiques. Elles ont aussi une grande valeur socio-économique à l'échelle mondiale. Ces écosystèmes hautement productifs sont présents dans les régions côtières tropicales et subtropicales du monde entier. Récemment, leur dégradation et leur disparition ont attiré l'attention du public à propos de l'amélioration de la biodiversité à l'échelle régionale. Jusqu'à présent, la cartographie de la répartition des espèces n'a été réalisée qu'à l'échelle locale, sans collecte systématique de données, et par conséquent, les informations à l'échelle nationale, régionale et mondiale restent limitées. La cartographie et le suivi temporel de la biodiversité des espèces de mangrove est l'une des questions les plus importantes au niveau national et régional, lorsqu'il s'agit de déterminer le degré de réussite de la réhabilitation ou de l'amélioration de notre compréhension générale. Cette thèse de doctorat est organisée en six chapitres traitant de la biodiversité des espèces de mangrove et de la gestion de la conservation. En outre, elle étudie les effets à long terme des paramètres et des processus environnementaux et anthropiques sur la dynamique spatio-temporelle de la diversité des espèces et de l'organisation spatiale des forêts de mangrove.

Synthèse des limites et des avancées actuelles en matière d'évaluation de la biodiversité (Introduction). Le chapitre 1 se concentre sur l'identification de l'état et des limites des approches in situ, de télédétection et de modélisation existantes pour l'évaluation spatio-temporelle de la biodiversité des espèces de la forêt de mangrove. Ce chapitre identifie également les progrès récents dans les méthodes de quantification de la zonation à l'échelle du paysage et de l'état historique à l'aide de la télédétection en intégrant un plan d'échantillonnage systématique plus robuste, les paramètres environnementaux et anthropiques et la dynamique temporelle. La quantification basée sur un plan d'échantillonnage systématique peut améliorer la fiabilité des modèles de d'organisation spatiale et intertidale basés sur l'écosystème. Les composites annuels et les données de séries chronologiques corrigées radiométriquement fournissent alors des informations plus précises sur l'état historique et la succession secondaire des forêts de mangroves.

Evaluation des changements au sein de la forêt de mangrove et du paysage environnant.

La compréhension des changements dans les forêts de mangrove et leur environnement est cruciale pour caractériser comment les écosystèmes de mangrove sont en constante évolution et influencés par divers facteurs de stress naturels et anthropiques. Le chapitre 2 détaille l'approche méthodologique pour le suivi de la dynamique spatio-temporelle des paysages de mangrove. L'objectif principal de cette étude était de quantifier l'évolution des forêts de mangrove dans la province de Trat en Thaïlande au cours des 30 dernières années (1987-2017) en utilisant le cadre méthodologique susmentionné. Les résultats ont révélé une diminution significative de la zone agricole, tandis qu'il y avait une augmentation des forêts de

mangrove, des fermes à crevettes/poissons et des zones de sols nus. Les résultats indiquent que les activités de réhabilitation modifient la dynamique du paysage des forêts de mangrove. Ce chapitre présente également le potentiel des composites annuels et des plateformes de *cloud computing* pour générer des images cohérentes, sans erreur et sans raccord, qui permettent d'obtenir une classification rapide et précise, facilitant ainsi la détection des écosystèmes en constante évolution.

Inventaires systématiques de parcelles le long de transects pour caractériser la diversité des espèces et des structures. Les études axées sur la diversité des espèces de mangrove et l'évaluation de la réhabilitation se limitent souvent à des inventaires de terrain non systématiques décrivant les assemblages spatiaux d'espèces avec des données très limitées, sans tenir compte de la zonation intertidale et de l'occurrence des espèces liées au contexte environnemental. Le chapitre 3 présente la procédure d'échantillonnage des données de terrain pour évaluer la diversité des espèces et des structures et le succès des projets de réhabilitation par rapport aux mangroves naturelles adjacentes. Ces données sont librement disponibles pour les utilisateurs et peuvent être utilisées pour ajuster des modèles de biomasse aérienne spécifiques au site et à l'espèce ainsi que pour valider les prédictions de hauteur des espèces mesurées par les satellites dans la zone intertidale.

Évaluer le degré de réussite des interventions de réhabilitation. La reconnaissance récente de l'importance des forêts de mangrove a stimulé l'intérêt pour la réhabilitation et la restauration de ces paysages déboisés dans plusieurs régions du monde. Très peu d'études antérieures ont évalué l'efficacité à long terme des efforts de réhabilitation en termes de temps nécessaire pour stabiliser les peuplements forestiers réhabilités, leur développement structurel et la diversité des espèces. Le chapitre 4 évalue trente ans de développement de la structure et de la diversité des espèces dans des mangroves réhabilitées en utilisant l'algorithme ARMA et des données d'enquête sur le terrain dans la province de Trat, dans l'est de la Thaïlande. Après trente ans, les mangroves réhabilitées sur le site étudié restent constituées de monocultures de Rhizophoraceae. La forêt réhabilitée présente une forte densité d'arbres, un faible diamètre à hauteur de poitrine, une faible surface basale et un très faible taux de recrutement.

Diversité spatiale, zonation intertidale et indicateurs fonctionnels de la succession. L'examen quantitatif des paramètres environnementaux sur la zonation des espèces et la dynamique spatio-temporelle à l'échelle du paysage a rarement été tenté. Le chapitre 5 présente un nouveau cadre pour évaluer la diversité spatiale et intertidale des espèces de mangrove et déterminer l'état historique de l'écosystème. Il n'y a pas eu de zonation unique d'espèces ou de groupes d'espèces le long des gradients d'élévation. Cependant, les paramètres structurels varient le long du gradient d'élévation. Les mangroves réhabilitées (30 ans) semblent être mono-espèce (Rhizophoraceae), tandis que la diversité des espèces parmi les peuplements forestiers régénérés variait à différents endroits. Les effluents des

fermes à crevettes peuvent de leur côté contribuer à la perturbation des peuplements naturels de mangroves. Ce chapitre comprend également les concepts fondamentaux de la méthode ARMA modifiée. Les résultats donnent un aperçu de l'état actuel et des changements historiques de l'écosystème de mangrove dans la province de Trat en Thaïlande.

Dynamique spatio-temporelle de la diversité des espèces de mangrove. Malgré les progrès de la télédétection, diverses sources de bruit affectent les satellites dans les zones côtières. La structure complexe de la forêt, la compréhension des contextes environnementaux et anthropiques et le manque d'intégration des inventaires systématiques sur le terrain en font un écosystème notoirement difficile à étudier. Pour y remédier, le chapitre 6 combine toutes les informations des études susmentionnées et présente un système d'aide à la décision de pointe qui 1) comprend une approche d'inventaire systématique sur le terrain ; 2) teste la cohérence et le changement temporel (ARMA modifié) tout en réduisant le bruit spectral causé par diverses contaminations ; et 3) relie l'inventaire et la dynamique sur le terrain à la télédétection pour surveiller la diversité des espèces de mangroves. L'approche proposée révèle le potentiel des capteurs satellites librement disponibles, qui peuvent être des outils puissants, et peuvent offrir un avantage significatif par rapport aux méthodes traditionnelles pour le suivi de la diversité complexe des espèces de mangrove.

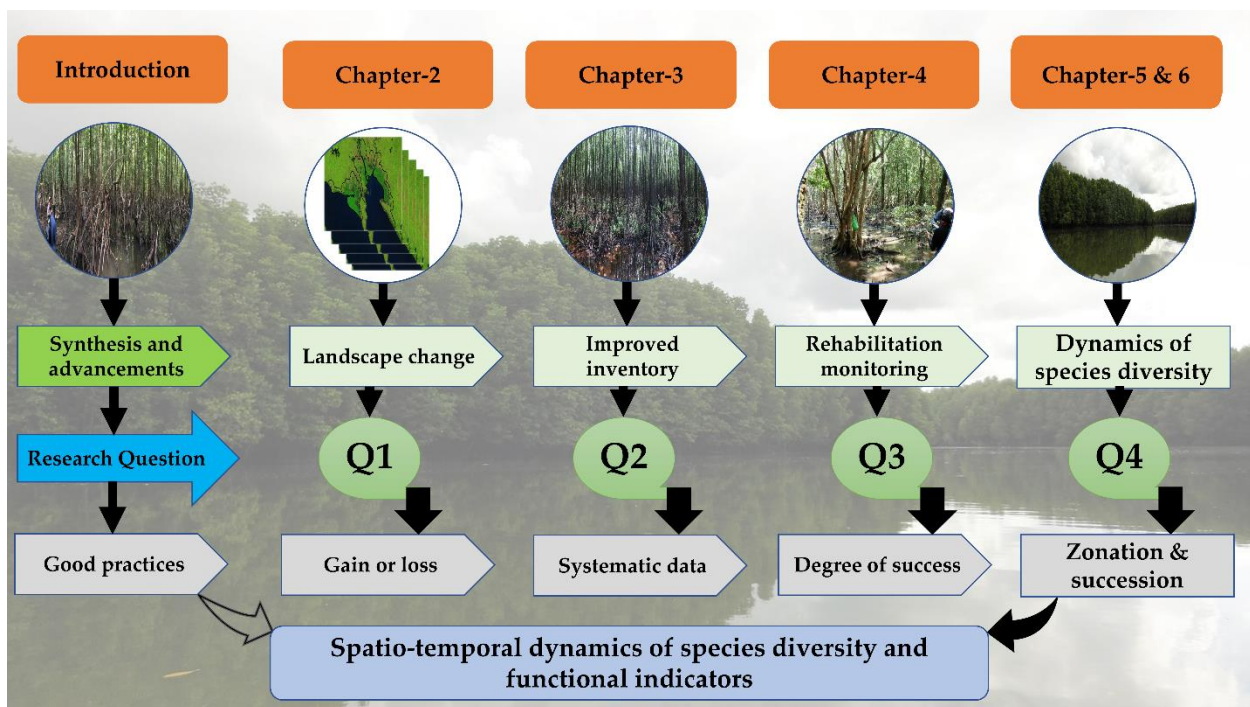


Schéma de la structure de la thèse

General Introduction

Background and synthesis



Mangrove forest in Trat province of Thailand

This chapter has been produced from: Pimple, U., Simonetti, D., Sitthi, A., Podest, E., Peters, R., Berger, U., Leadprathom, K., Gond, V. (2021) Enhancing mangrove spatio-temporal diversity pattern monitoring: a past and future earth observation data perspective, Submitted for publication

Abstract:

The United Nations Decade on Ecosystem Restoration (2021–2030) lists coastal ecosystems such as mangrove forests as a restoration priority. Given the urgent need for mangrove forest restoration, our study objectives were to assess the problems in collecting the large-scale spatial information required for effective restoration interventions and identify appropriate solutions. Spatially explicit knowledge of mangrove species and forests (natural and restored) can help to improve restoration effectiveness and is often needed on a large scale. To date, multiple-species distribution mapping has only been conducted on a small scale without systematic field data collection. Despite advances in applying remote sensing to mangrove forest studies, there are still challenges in understanding and addressing the issues related to the contaminants and other factors affecting satellite observation quality. In addition, the application and effectiveness of modeling approaches are constrained due to inadequate field inventories and a lack of data on temporal changes. An increasing number of studies are reporting field data, using remote sensing, and modeling mangrove species distributions. However, a recent assessment of the status, limitations, and challenges for field data collection caused by coastal environmental conditions and the potential of recent developments in earth observation data is lacking. Here, based on a literature review, we identify and discuss the factors hindering adequate reporting and spatial-scale monitoring. In addition, we identify the factors interfering with remote sensing observation and discuss the best practices to overcome these problems using reproducible examples from a site in eastern Thailand. The results show how inadequate data collection and reporting has led to incomplete information. However, a systematic remote sensing-based sampling design, diversity quantification in relation to environmental gradients, and consideration of secondary succession can provide a complete diversity assessment. Tidal inundation adversely affects the spectral and structural properties of satellite data; however, the consistency and quality of such data can be improved using low tide image composites. Moreover, composite time series are useful in determining historical change. The recent development of earth observation sensors, cloud-computing platforms and machine and deep-learning architectures provide promising possibilities for diversity monitoring.

1.1 Mangrove ecosystems and their species diversity

Mangrove forests consist of a dominant group of woody trees (± 70 species), shrubs, and fern species (25 genera and 19 families) that are distributed in the coastal intertidal areas of tropical and subtropical regions around the world (Alongi, 2009; Duke, 2017; Tomlinson, 2016) with a pronounced gradient of species diversity from the new world (only 12 species) to the Indo-West-Pacific (58 species) (Ellison et al., 2020; Macintosh and Ashton, 2002; Ricklefs et al., 2006). They occupy the interfaces between the land and sea, as they are salt- and flood-tolerant to varying degrees (Kumari et al., 2020). Mangrove forests can be composed of a variety of different tree and shrub species that are not necessarily closely related taxonomically. However, they all possess similar eco-physiological characteristics and structural adaptations that enable them to live in anaerobic and saline soils (Ball, 1988; Tomlinson, 2016). Mangrove forests notably have the following features: (1) trees are a major component of the community; (2) species exhibit morphological adaptations of aerial roots and vivipary; and (3) they exhibit adaptations to saline environment like salt exclusion and secretion (Craft, 2016; Srikanth et al., 2016; Tomlinson, 1986). Mangrove forests are among the most productive ecosystems in the world because they provide several important ecosystem services including storm protection and wave dissipation, food, timber, fuel for local communities, and nursery beds for juvenile fishes, shrimp, and other marine invertebrates (Barbier et al., 2011; Craft, 2016). Mangrove ecosystems also export organic matter to neighboring areas (López-Medellín and Ezcurra, 2012), and are among the most carbon-rich forests in the tropics, serving as long-term carbon sinks for sequestration (Collins et al., 2017). As natural carbon sinks, they play a significant role in the global carbon cycle, accounting for 10–15% of all coastal carbon storage despite covering only 0.5% of the global coastal area (Alongi, 2014; Nóbrega et al., 2019). Furthermore, mangroves play an important role in the functioning of adjacent ecosystems, such as terrestrial wetlands, peat swamps, salt-marshes, seagrass beds, and coral reefs (Macintosh and Ashton, 2002; Sandilyan and Kathiresan, 2012).

Mangrove forests have relatively low levels of species diversity compared to other tropical forest habitats, such as tropical rainforests and coral reefs (Duke et al., 1998; Lee et al., 2017). Despite the low tree species diversity, trees in mangrove forests have a wide range of structural and functional attributes that promote their survival and propagation in the harsh conditions of coastal intertidal zones (Duke et al., 1998). The diversity of

mangrove trees is associated with ecological factors that control species distributions in different environmental conditions (Tomlinson, 2016; Twilley et al., 2017). The distribution of mangrove species is not only determined by the number of species at a certain location but also in the ability of each species to adapt to a wide range of environmental conditions (Fig. 1.1) (Duke et al., 1998; Hogarth, 2013; Twilley et al., 2017). The micro-topography of the landscape and tidal inundation drive the intertidal zonation of mangrove forest species and are considered an ideal proxy for other environmental factors that contribute to tree growth, including salinity, soil texture, and redox potential, and nutrient availability (Hickey and Bruce, 2010; Leong et al., 2018; Ma et al., 2020). Considering the above influencing factors, the mangrove species within each geographical region are largely a product of local scale diversification processes. Random distribution of mangrove species may take place depending on environmental settings and various competing processes offsetting one another (Daru et al., 2013; Ellison et al., 2000).

Mangrove forests occupy only 0.5 % of the world's coastal areas (Giri et al., 2011). However, despite their limited total area, they are widely distributed from 30° N to 30° S (Kuenzer et al., 2011; Zong, 2006). According to Duke et al. (1998), mangrove species are primarily distributed in two hemispheres, the Atlantic East Pacific and the Indo-West Pacific, and in six biogeographic regions (United Nations Environment Program, 2014): (1) western America and the eastern Pacific, (2) eastern America and the Caribbean, (3) western Africa, (4) eastern Africa and Madagascar, (5) Indo-Malesia and Asia, and (6) Australasia and the western Pacific (Fig. 1.2). Mangrove biodiversity is almost five times higher (58 species compared to 12) in the eastern hemisphere than in the western hemisphere (Ellison et al., 2020; Macintosh and Ashton, 2002; Ricklefs et al., 2006). Ricklefs et al. (2006) and (Ricklefs and Latham, 1993) summarized several explanations for species diversity and distribution in this region. The presence of region-specific dominance of geophysical circumstances, adjacent diverse terrestrial flora, and a wet, humid climate may have been contributing factors (Duke, 2017; Macintosh and Ashton, 2002; Ricklefs and Latham, 1993).

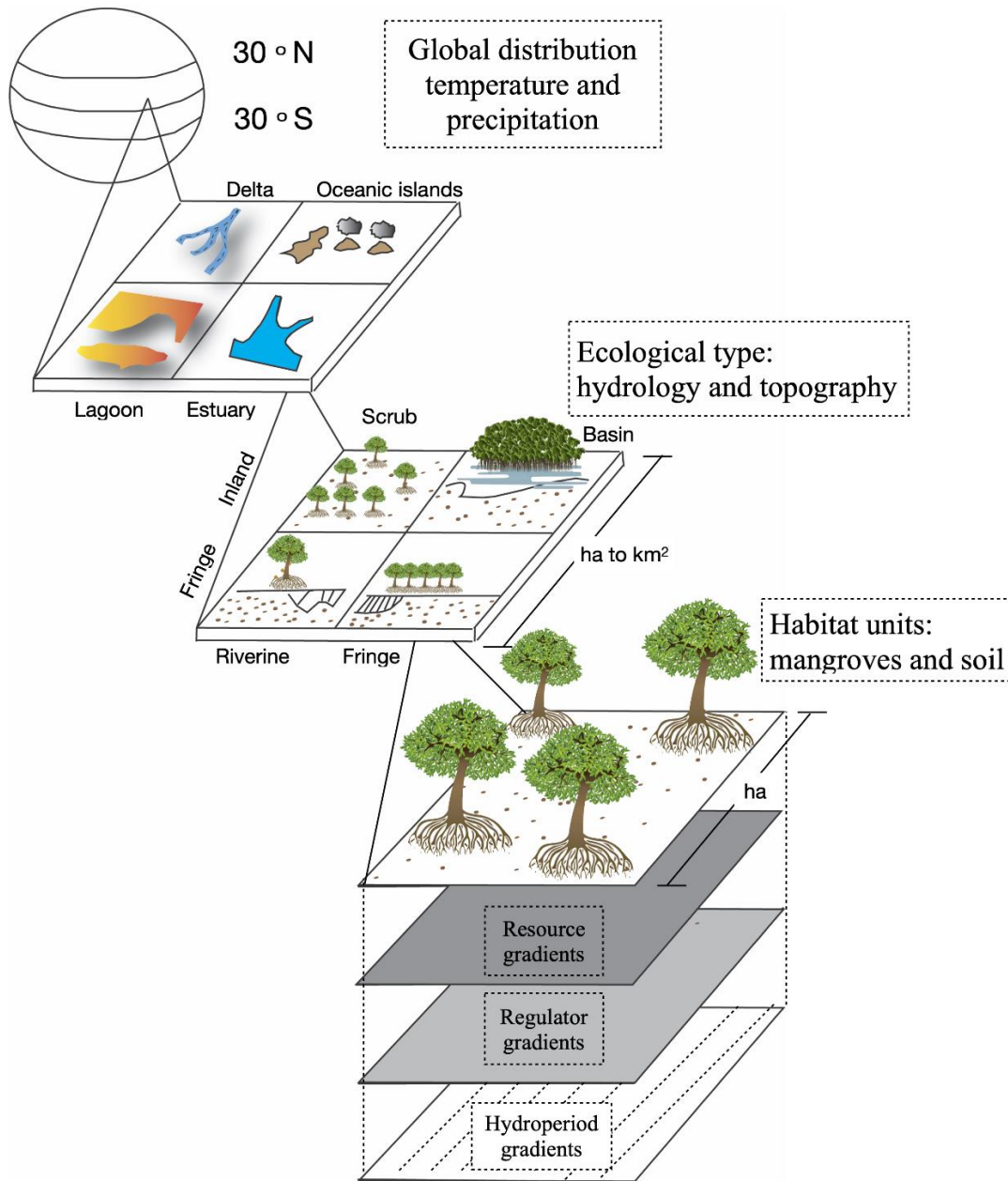


Figure 1.1 Linkage of mangrove biodiversity to local settings (Derived from: (Twilley, 2018, 2008; Twilley et al., 2017; Twilley and Rivera-Monroy, 2005)): hierarchical classification system that describes the structure and function patterns of mangroves based on global (temperature and precipitation) (Osland et al., 2017) geomorphological (regional), and ecological (local) factors that control the concentration of nutrient resources and regulators in soil along gradients from the fringe to more interior locations by the shore. Resource gradient: environmental attributes such as light, water, nutrients, space, and other variables that are consumed and contributed to mangrove growth. Regulator gradient: salinity, sulfide, pH, and redox that are non-resource variables contribute to tree growth. Hydroperiod gradient: the period of time during which mangroves are inundated by tidal water.

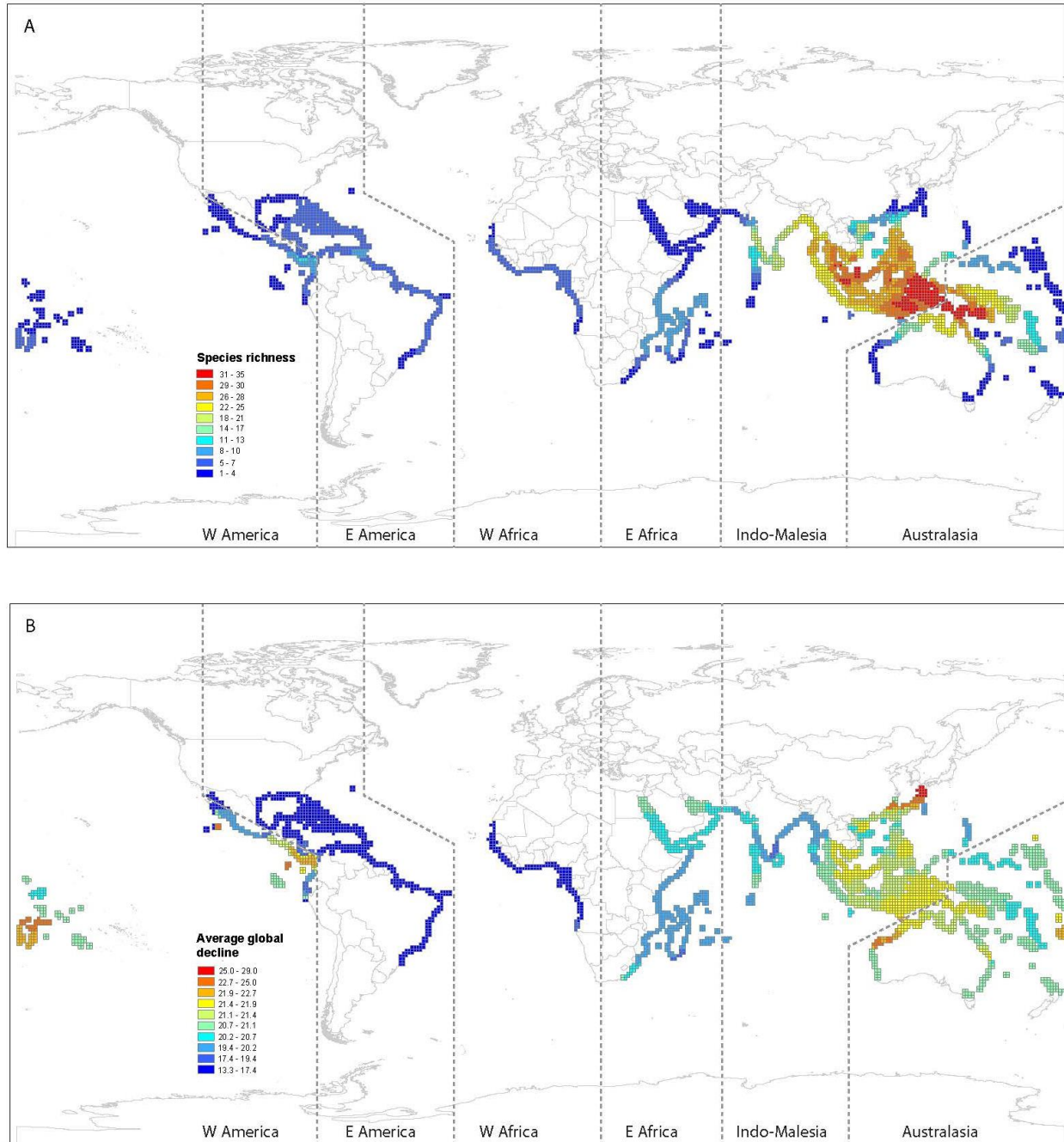


Figure 1.2 Global distribution (1980-2005) of (A) species richness (number of species occupying a grid cell) and (B) global decline in mangrove species across the six biogeographic regions (per quarter degree squares) (Daru et al., 2013). Note: W America: West America, E America: East America, W Africa: West Africa, E Africa: East Africa.

Despite their importance, mangroves are threatened globally, and an estimated one-third of mangrove forests have been lost over the past half-century (Thomas et al., 2018; Valiela et al., 2001). According to the FAO (2007), the extent of mangroves decreased from 18.8 million hectares to 15.2 million hectares between 1980 and 2005. A recent baseline study found that mangroves had a global extent of 13.76 million hectares (Bunting et al., 2018), indicating significant further losses. Rates of mangrove deforestation have declined globally, although countries like Myanmar and Malaysia are still facing high loss (Friess et al., 2019; Goldberg et al., 2020). Furthermore, between 2000 to 2016, 62% of global mangrove losses and 80% of the losses in the Southeast Asian region were the direct result of the replacement of forests with aquacultural and agricultural enterprises (Goldberg et al., 2020). Friess et al.(2019) summarized national and subnational estimates of mangrove loss in the late twentieth century due to aquaculture and other human-induced conversions for various countries across the tropics. Not only are mangroves losing aerial coverage, but they are also declining in terms of species diversity and ecosystem services (Macintosh and Ashton, 2002). According to Polidoro et al.(2010), on a global scale, about 16% of mangrove species are at an elevated threat of extinction, and current mangrove exploitation rates are expected to continue. Considering the accelerating rate of exploitation, the loss of species poses serious ecological and economic consequences, especially in regions with low species diversity and an elevated rate of species loss. For example, the highest percentage of threatened species is observed in the Atlantic and Pacific coastal regions of Central America. Forty percent of mangrove forest species are listed in threatened categories (Polidoro et al., 2010). Under the United Nations Decade on Ecosystem Restoration (2021–2030) lists coastal ecosystems such as mangrove forests as a restoration priority. However, in high diversity regions, regardless of high loss rates, very little is known about the loss of individual localized species or local diversity loss. Bryan-Brown et al.(2020) noted that simply reporting total loss rates or changes in the extent of mangrove forests is inadequate for spatial scale conservation interventions if there is insufficient information on the spatial assemblage of the habitat that remains. However, very limited information is available on the spatio-temporal changes in mangrove species communities (Polidoro et al., 2010). Furthermore, Polidoro et al.(2010) identified the need for species-specific information and the importance of refining conservation practices for threatened species in the Indo-Malesia and Asia region (Fig. 1.2B).

1.2 Spatial and temporal aspects of mangrove species distribution

Mangrove species share a common ability to grow in saline conditions; they appear in predictable mono-specific zones parallel to shorelines, tidal channels, and the banks of rivers and streams influenced by fluvial and marine processes (Polgar and Jaafar, 2018; Snedaker, 1989, 1982). Variation in microtopography and tidal inundation drive the intertidal zonation of mangrove forest species (Hickey and Bruce, 2010; Leong et al., 2018). Several early studies documented zonation patterns perpendicular to the coastline (Peters et al., 2020b; Rabinowitz, 1978) in general accordance with Watson (1928), who showed the zones of different species following shoreline contours. Researchers often try to prove zonation using Watson (1928), but the fact that this concept is purely hypothetical and used to illustrate the concept of inundation classes is not usually stated (Ellison, 2002; Tomlinson, 2016). Moreover, they are not accurate representation zonation because intertidal and spatial patterns are more complex (Buckley, 1982; Bunt et al., 1985; Bunt and Williams, 1980; Peters et al., 2020b). Several studies also note that larger-scale zonation and distribution patterns are still not well understood and that strong zonation patterns are rarely observed in the field (Bullock et al., 2017; Ellison et al., 2000; Snedaker, 1982).

The minimum amount of field data required to assess landscape-scale species diversity and zonation is a complete list of species in the forest, measurements of the edaphic parameters and elevations, as well as the measurements obtained in contiguous quadrats or fixed-area sampling along the intertidal zone of the transects (Castaneda-Moya et al., 2006) (Ellison, 2002). Ellison (2002) provided a detailed review and four possible explanations why many studies have failed to observe zonation patterns: (1) the lack of proper statistical methods to test zonation patterns; (2) the lack of appropriate spatial scales for observation and analysis; (3) the lack of consideration of human impacts that have disrupted zonation patterns; and (4) the “null hypothesis” that zonation does not exist in mangrove forests. Several studies published after 2002 only analyzed randomly sampled plots or transect lines without considering spatial and intertidal zonation. In addition, most of these studies reported only dominant species and structural parameters, and they identified zonation without quantification in relation to inundation level or micro-topography (Ellison, 2002). Furthermore, the consideration of topographic variability and the effects of various anthropogenic settings and factors were sparse. Natural disturbances such as lightning, insects, diseases, tropical storms, and changes in

the sea level could also influence zonation patterns (Bullock et al., 2017; Piou et al., 2006). In addition, land-use changes, such as the conversion of forest to shrimp farms or agriculture, alter the topography or natural elevation gradient, changing the key biophysical variables responsible for zonation (Elwin et al., 2019; Hickey and Bruce, 2010). Among other stressors, shrimp farm waste or effluent from industries also strongly affects ecological functions and negatively impacts species diversity (Capdeville et al., 2018; Vaiphasa et al., 2007). The inclusion of the parameters mentioned above in a systematic field survey and their quantification in relation to various environmental and anthropogenic stressors have rarely been considered while reporting the intertidal and spatial distribution of mangrove species.

Rehabilitation and restoration of mangrove forests are often aimed at conservation, coastal protection, wood production for economic purposes, or the mixed-use of mangroves to produce high sustainable yields (Andradi-Brown et al., 2013). In previous decades, rehabilitation and restoration practices have occurred in several deforested mangrove areas around the world (Andradi-Brown et al., 2013; Ellison et al., 2020; Macintosh and Ashton, 2002; Pimple et al., 2020). Globally, several rehabilitation and restoration projects have been reported, including those in Thailand, Pakistan, Australia, Bangladesh, Sri Lanka, Vietnam, Philippines, Malaysia, Indonesia, India, Florida (USA), Mexico, Columbia, Brazil, China, and Kenya (Asaeda et al., 2016; Bosire et al., 2003; Goessens et al., 2014; López-Portillo et al., 2017; Phan et al., 2019; Pimple et al., 2020; Proisy et al., 2018; Sillanpää et al., 2017).

The terms rehabilitation and restoration are often used synonymously, but they actually have distinct definitions (Schmitt and Duke, 2020). The term “*mangrove rehabilitation*” refers to the simple plantation of mangroves over disturbed, degraded, damaged, or destroyed land, without any site assessment or subsequent evaluation of the functioning of the created ecosystems (Andradi-Brown et al., 2013; Field, 1999; Macintosh and Ashton, 2002). The term “*mangrove restoration*” refers to actively supported measures to return a formerly degraded mangrove ecosystem to its original condition before it became degraded, in terms of species diversity, functioning, and hydrological regime (Andradi-Brown et al., 2013; Dale et al., 2014; Macintosh et al., 2002; Pimple et al., 2020). The term *regeneration* refers to the forest distribution that follows a natural recovery without conservation interventions (FAO, 2019). We reviewed the literature to identify the species responses that could occur during succession in rehabilitated, restored, and regenerated mangrove forests. Numerous studies have compared the native and

rehabilitated mangrove communities and reported significant contrasts in tree density, species composition, and structural diversity (Asaeda et al., 2016; Luo et al., 2010; Pimple et al., 2020; Walters and Walters, 2004). However, there is insufficient scientific information on the secondary succession of species diversity in rehabilitated, restored, and regenerated mangrove forests (Asaeda et al., 2016; Bosire et al., 2003; Luo et al., 2010; Pimple et al., 2020; Reis-Neto et al., 2019; Ren et al., 2008; Smith, 1987; Van Loon et al., 2016). These successions are rarely considered and reported while accessing the spatial scale diversity at specific sites. Furthermore, there are a very few mangrove ecosystem in the world that has not been influenced by human activities (Ellison, 2002). This raises the question of whether the rehabilitated, restored, and regenerated mangroves are truly returned to the species diversity present before degradation occurred. Furthermore, most quantitative baseline studies use single occurrence surveys and lack reports on the temporal changes in species diversity at the study sites.

Numerous natural and anthropogenic stressors or processes could change the assemblages of mangrove species. The reporting of gradual or abrupt changes and their effects on species diversity is crucial for baseline biodiversity monitoring studies, yet such practices are rarely used. Most previous studies also report the species diversity and structural parameters without consideration of proper sampling strategies, surface elevation or tidal regimes, and secondary succession (Abino et al., 2014; Joshi and Ghose, 2014; Nehru and Balasubramanian, 2018; Rahman et al., 2019; Shah et al., 2016; Sillanpää et al., 2017).

The above information implies that many studies have failed to report reliable zonation and diversity distribution patterns due to lack of 1) systematic field data collection, 2) quantification of species diversity pattern in relation to various environmental gradients, 3) effects of conservation and other anthropogenic interventions on the diversity of secondary successions. This leads to complications when such information is used with earth observation data for mapping and monitoring mangrove forest species diversity. Our paper reviews the knowledge gaps and identifies and discusses the best practices for enhancing spatial scale species diversity monitoring using recent developments in earth observation data. Moreover, it discusses 1) the challenges and importance of systematic field surveys, 2) factors affecting the quality of remote sensing data, 3) how to overcome the remote sensing data challenges and the best practices. In addition, we review the possible benefits of integrating earth observation data when predicting spatial scale diversity.

1.3 Objectives

This review intends to identify solutions to the challenges and limitations of quantifying and monitoring spatial scale mangrove species diversity using earth observation data. Knowledge about the best practices for using earth observation data and designing systematic field inventories is helpful for individuals concerned with decision-support systems and mangrove species diversity protection. In particular, such information would be invaluable for conservation and sustainability practitioners, including those working on the United Nations Restoration Declaration Decade (2021–2030) agenda for mangroves, Reducing Emissions from Deforestation and forest Degradation plus (REDD+), or climate change mitigation and carbon sequestration strategies at local, national and regional scale. The objectives of this review are to 1) identify discrepancies and challenges in traditional field inventory data collection approaches, 2) provide an overview on historical and current remote sensing data usage and challenges, 3) provide an overview on current state and challenges associated with prediction and modeling of diversity, 4) Identify the best practices for enhancing the monitoring of spatio-temporal dynamics of mangrove species diversity. An in-depth theoretical and practical understanding of the main factors hindering adequate mapping of mangrove ecosystems was also explored by analyzing recent literature and reproducible examples from a study site in the Trat Province of eastern Thailand (Fig. 1.3).

1.4 Demonstration site

This study site, located along the eastern coast of the Gulf of Thailand and bordering Cambodia, is under investigation by a project entitled “Monitoring and Restoration for Sustainable Coastal Ecosystems (RESCuE: <https://rescue-pro.net/>).” This study site contains a large area of natural mangrove stands characterized by the most common native species found in Thailand, and large areas have been restored without adequate site assessment, resulting in a *Rhizophoraceae* monoculture in most of the rehabilitated zone. Over the past 30 years, these stands have reached the same height as the natural stands but have been unable to reproduce the species diversity found in a natural forest (Pimple et al., 2020). The study area contains a zone of landward forest that had been destroyed for shrimp farming and agricultural activities but has subsequently regenerated naturally (Pimple et al., 2020, 2018). The following 18 mangrove genera occur in the study area: *Sonneratia alba*, *Sonneratia ovata* Backer, *Avicennia alba*, *Avicennia marina*, *Bruguiera cylindrica*, *Bruguiera gymnorhiza*, *Bruguiera sexangula*, *Ceriops tagal*, *Ceriops*

decandra, *Excoecaria agallocha*, *Intsia bijuga*, *Lumnitzera littorea*, *Lumnitzera racemosa*, *Rhizophora apiculata*, *Rhizophora mucronata*, *Xylocarpus granatum*, *Xylocarpus moluccensis*, and *Scolopia macrophylla* (Pimple, 2020; Pimple et al., 2021, 2020). Figure 1.3 presents the available field inventory data used for mangrove species monitoring (Pimple, 2020; Pimple et al., 2021, 2020) and testing the proposed best practices in this review. The locations of Transects 1, 2, and 3 presented in Figure 3 are from recently published studies (Pimple, 2020; Pimple et al., 2021, 2020).

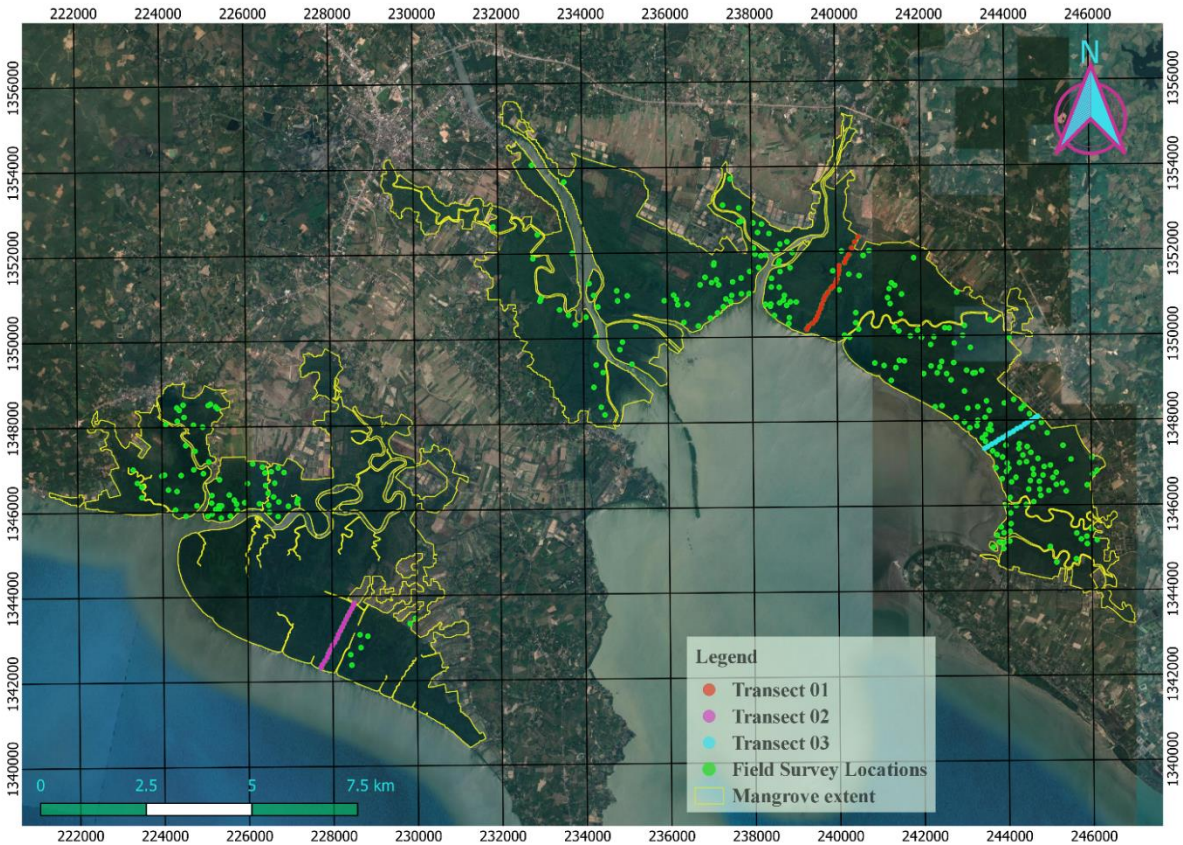


Figure 1.3 Location and available inventory data at the demonstration study site in the Trat Province, Thailand. Transects 1, 2, and 3 indicate the locations for the systematic transect plot placement for intertidal mangrove zonation using Sentinel-1 and -2 data. The green dots are the locations of stratified sample plots collected at a 10 x 10 m size. Note: only locations where the survey was completed are shown here.

1.5 Difficulties and challenges for diversity monitoring and predictions

1.5.1 Field inventory data

Data on mangrove tree species, structure (height and diameter at breast height (DBH)), vegetation complexity, successional stages, and various environmental parameters are important in understanding the requirements for the maintenance of genetic richness, ecological functions, and ecosystem resilience (Dale, 1999; Dale et al., 2014). However, systematic data collection approaches when determining species diversity and zonation in mangrove studies are rarely considered (Dale et al., 2014; Sandilyan and Kathiresan, 2012). Studies focusing on mangrove species biodiversity are often limited to non-systematic field inventories, describing spatial species assemblages with minimal data without considering intertidal sampling or quantifications relating to surface elevation or tidal inundations (Baderan et al., 2018; Ellison, 2002; Sreelekshmi et al., 2020; Torres-Fernández del Campo et al., 2018). The use of inadequate data collection criteria and reporting impacts the study methodology and results in several ways, including sub-optimal location choices and numbers of survey samples, misused resources, and incomplete baseline species zonation and distribution information of mangrove ecosystems (Dale et al., 2014). All these effects can lead researchers to overlook information on rare species unique to specific study sites.

Mangrove forests are notoriously difficult landscapes to study. Besides biting insects and potentially dangerous wildlife, the tidal fluctuations, soft muddy substratum, and complex forest structure present a significant challenge for logistics and field measurements (Kovacs et al., 2011; Lee et al., 2017; Leong et al., 2018). However, samples collected near canals or easy access points may not represent the actual species zonation or assemblage at that particular location. Other problems include sky blockages, caused by dense canopy structures, and challenging ground conditions, which may affect the measurements (real-time kinematic GPS, total station survey, drone), and mean that the spatial accuracy of measurements is not guaranteed (Kaartinen et al., 2015; Rick C. Leong et al., 2018; Pirti et al., 2010). Hence, a highly robust systematic sampling design is required for mangrove species biodiversity assessments. Furthermore, the careful consideration of influencing factors, the history of modified landscapes, and conservation interventions must also be included.

1.5.2 Remote sensing data

Biodiversity is a measure of the number and variety of biotic species found within a defined geographic region (Kuenzer et al., 2014). The species richness of mangrove forests is one of the characteristics of mangrove ecosystems. Environmental conditions and biological factors are responsible for controlling species richness in different geomorphological and ecological settings (Twilley et al., 1996). Traditional in situ mangrove species biodiversity monitoring is limited in time and space and difficult to conduct due to the harsh environment, costs, and time-consuming nature (Wang et al., 2019; Wang and Gamon, 2019). Remote sensing has consequently proved useful in mapping and monitoring mangrove ecosystems (Bunting et al., 2018; Kuenzer et al., 2011; Lucas et al., 2017; Pham et al., 2019b; Wang et al., 2019). In previous decades, remote sensing data such as aerial photographs and satellite imagery have been used extensively to characterize the extent of mangrove habitats, their species composition, health status, and the spatio-temporal changes caused by various stressors and conservation interventions (Adade et al., 2021; Kuenzer et al., 2011; Wang et al., 2019). Since 2011, there have been five major review papers and one book chapter focusing on the remote sensing of mangrove species diversity and related monitoring challenges (Cárdenas et al., 2017; Heumann, 2011; Kuenzer et al., 2011; Lucas et al., 2017; Pham et al., 2019b; Wang et al., 2019). Kuenzer et al.(2011) provided a detailed overview of the sensitivity of optical and Synthetic Aperture Radar (SAR) for detecting mangrove species' spectral signatures, backscatter coefficients, and influencing parameters. They also reviewed the commonly used sensors and their methodologies, advantages, and limitations. Heumann (2011) summarized the new high-resolution and hyperspectral imagery and methods for characterizing mangrove species composition. Cárdenas et al.(2017) provided the status for the usage of freely available satellite imagery, the importance of temporal scale, and the data processing limitations. Lucas et al. (2017) highlighted the range of remote sensing data used in previous studies to describe the multiple dimensions of mangrove forests, including the spatial scales, temporal frequencies, spectral responses, and three-dimensional state. Pham et al. (2019) provided an overview of studies undertaken after 2010, focusing on remote sensing and machine learning applications to distinguish mangrove species. Recently, (Wang et al., 2019) identified key milestones in applying remote sensing for mangrove-species mapping in the previous four decades. They noted that further research was required to determine whether temporal information could be used to identify mangrove species and predicted the future direction that research would

take. The identification of species on a spatial scale or their association is not yet fully defined. Moreover, significant challenges that have not been adequately addressed in remote sensing studies include the spectral characteristics of mangrove species and the effect of environmental conditions on imagery (Wang et al., 2019). Furthermore, despite advances, the integration of environmental conditions and secondary succession has rarely been considered.

1.5.2.1 Spectral reflectance in multispectral imagery

Influence of clouds and shadows

Frequent thick clouds and cloud shadows in mangrove zones are one of the first problems encountered when selecting optical satellite imagery (Baetens et al., 2019; Wang et al., 2019). Cloud cover, shadows, haze, and missing values influence several analysis processes, including atmospheric corrections. Moreover, the effects on spectral reflectance (Fig. 1.4) may cause biased vegetation indexes leading to the misidentification of species and their temporal dynamics. The challenges of cloud cover and shadows have been well-documented in previous studies (Cárdenas et al., 2017; Kuenzer et al., 2011). Cloud shadows change the spectral quality of the pixels under the shadowed area, and some researchers have only performed cloud pixel masking, leaving the shadow pixels untreated (Islam et al., 2019). Despite these challenges, several methods have been developed to automatically screen clouds and cloud shadows from optical images (Zhu and Helmer, 2018). In very cloudy regions, multi-spectral sensors might only provide a few or not even a single cloud-free image throughout the year, which limits the complete monitoring of changes in mangrove ecosystems. Hence, the inclusion of consistent time series to monitor secondary succession in mangrove species is still relatively rare (Hauser et al., 2020).

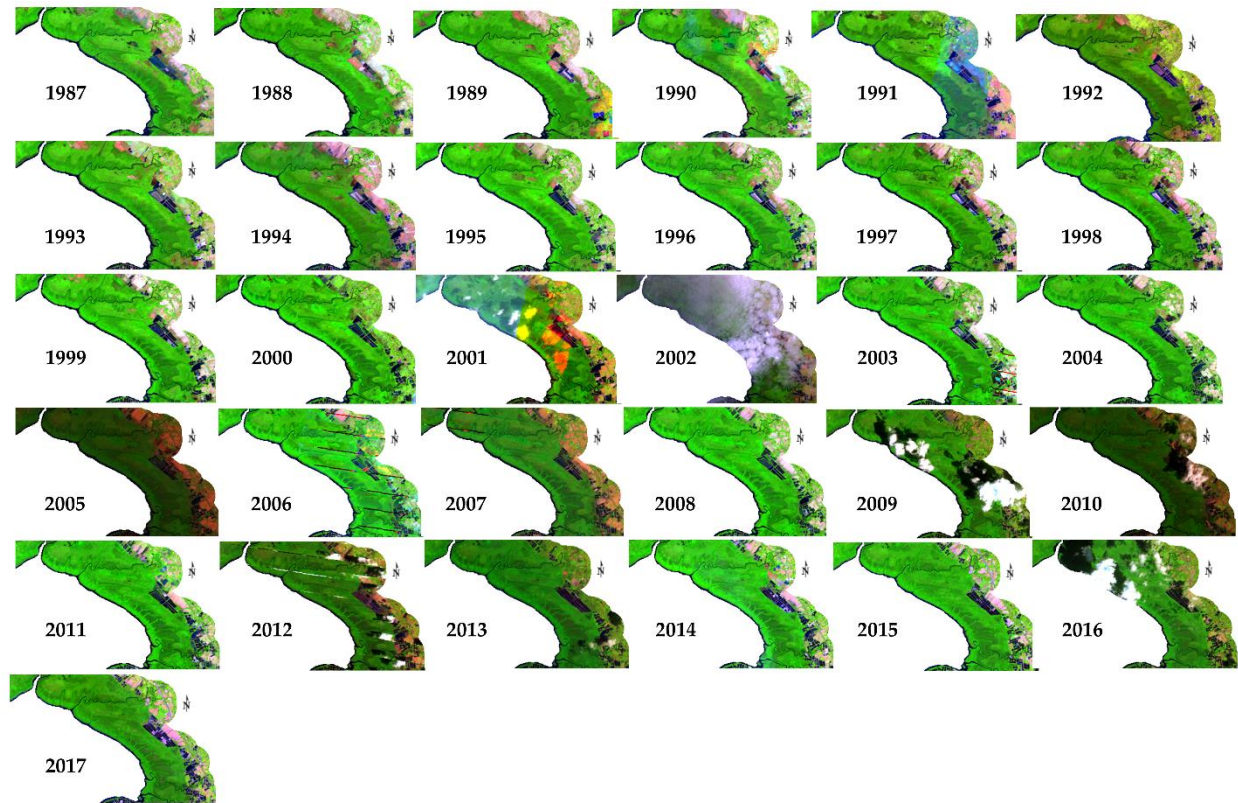


Figure 1.4 The best single date Landsat imagery from 1987 (upper left) to 2017 (bottom left) in Trat province, Thailand, in pseudo-color-composite (SWRI-1, NIR, RED) (Pimple et al., 2018). The cloud, shadow, and other atmospheric contaminants are observed throughout the year.

Changing surface reflectance with tidal inundation

Another challenge in mapping diversity at large spatial scales is the presence or absence of water beneath the mangrove canopy. The spectral reflectance of mangroves is strongly altered by high and low tidal inundations, especially in submerged, sparse, and scrub forest stands (Kuenzer et al., 2011; Lucas et al., 2017; Rogers et al., 2017; Xia et al., 2018). This phenomenon further complicates mangrove zonation across different temporal scales, especially if adjacent cloud-free scenes have been acquired at different tidal stages (Rogers et al., 2017). We also lack an understanding of the effect of tidal levels on spectral reflectance values in mangrove forests (Wang et al., 2019).

The first study focusing on identifying mangrove species (IKONOS and QuickBird) was published in 2004 (Wang et al., 2004; Wang et al., 2019). We have reviewed studies since 2004 that have focused on identifying mangrove species using high (IKONOS, QuickBird, RapidEye, GeoEye, WorldView-3, and Pleiades) and medium resolution multispectral imagery (Landsat, ASTER, SPOT-5, and Sentinel-2 MSI). The benefits of high-resolution

imagery for mangrove species identification have been recognized (Lucas et al., 2017), but the influence of high and low tidal inundations on spectral reflectance have not been considered (Heenkenda et al., 2014; Huang et al., 2009; Jia et al., 2014; Neukermans et al., 2008; Rahman et al., 2019; Wang et al., 2004; Wang et al., 2008, 2016). Furthermore, studies that attempted mangrove species identification using medium resolution satellite data did not account for the tidal influence (Bullock et al., 2017; Ghosh et al., 2016; Myint et al., 2008; Valderrama-Landeros et al., 2018; Wang et al., 2018). However, the lack of availability of tidal data, field-data collection costs, poor accessibility, and the cost of temporal images (for commercial products) may have contributed to these limitations.

Recent studies have tested the performance of various multi-spectral imagery (high and medium resolution) in both low and high tide conditions and identified several improvements that could be made (Proisy et al., 2018; Rogers et al., 2017; Xia et al., 2020, 2018; Zhang et al., 2017). Rogers et al. (2017) reported that spectral properties could become increasingly homogeneous under specific tidal conditions, unlike using a single-date image, which could result in non-homogeneous spectral responses over the same area over different times. Xia et al. (2018) found that the spectral signatures of seaward low-stand mangroves greatly varied during high and low tide. Furthermore, combined high and low tide images may result in the under- or overestimation of mangrove areas (Xia et al., 2020; Zhang et al., 2017). The above review suggests that spatial and temporal data not only aid species identification but that the mapping accuracy extent greatly depends on image acquisition time and tidal level. Figs. 1.5 and 1.6 present examples of the effects of low and high tide on the Landsat OLI-8 and Sentinel-2 MSI imagery observed in the Trat province of Thailand. During low tide, the reflectance values for seaward (orange circle: dominated by *Sonneratia oblongata* and *Rhizophora* zone) and scrub (black circle: dominated by *Ceriops tagel* species with height less than 2 m) mangroves are higher for the NIR (band 5 for Landsat-8 and band 8 for Sentinel-2), SWIR-1 and SWIR-2 (bands 6 and 7 for Landsat-8 and bands 11 and 12 for Sentinel-2) bands than during high tide. Hence, the homogenization of the spatio-temporal spectral signature is crucial in mangrove studies.

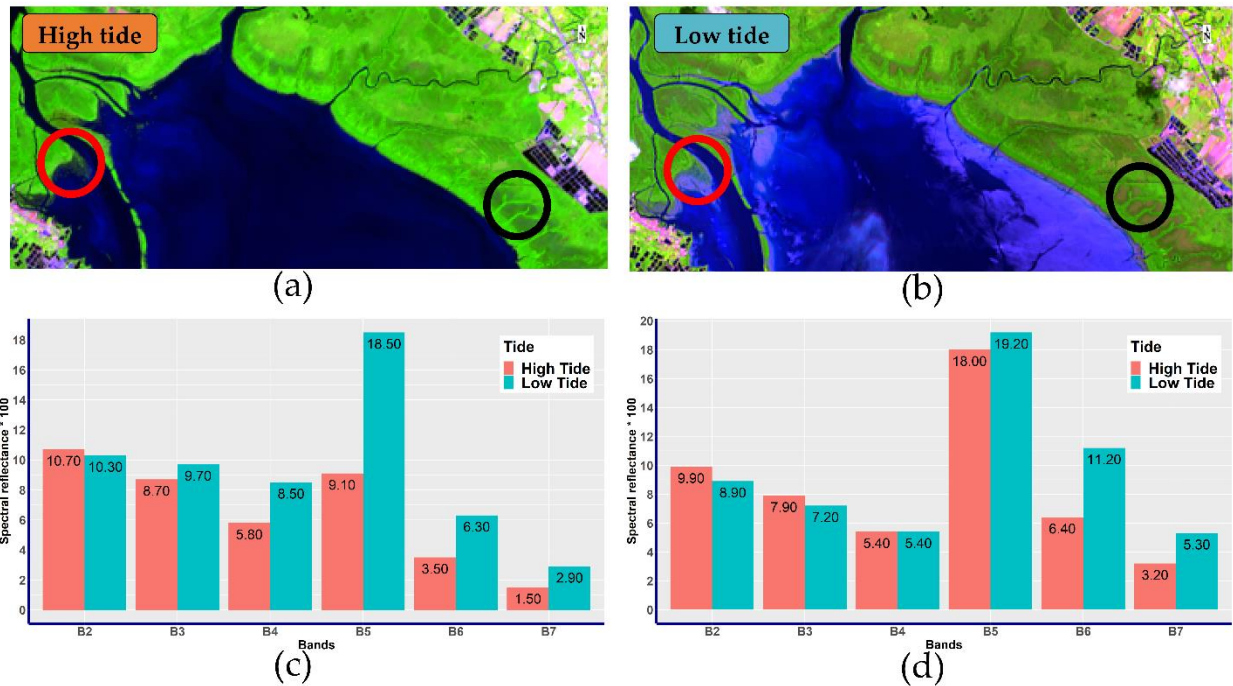


Figure 1.5. Effect of tidal inundation on the reflectance of Landsat-8 (OLI) TOA images. Satellite acquisition time (approximately 10:00–10:30 am local hour) at Trat Province of Thailand. (a) False-color composite (SWIR-1, NIR, and Red) of Landsat-8 (OLI) image (January 27th, 2017) at high tide (3.49 m); (b) False-color composite of Landsat-8 (OLI) image (May 10th, 2017) at low tide (2.00 m); (c) Spectral variability at seaward location during tidal fluctuations (orange circle); (d) Spectral variability at dwarf stand (mid zone) location during tidal fluctuations (black circle). Note: in the graph, the spectral reflectance is scaled by 100 for visualization purposes. The pixel values shown here are the average value of 3 x 3 pixels.

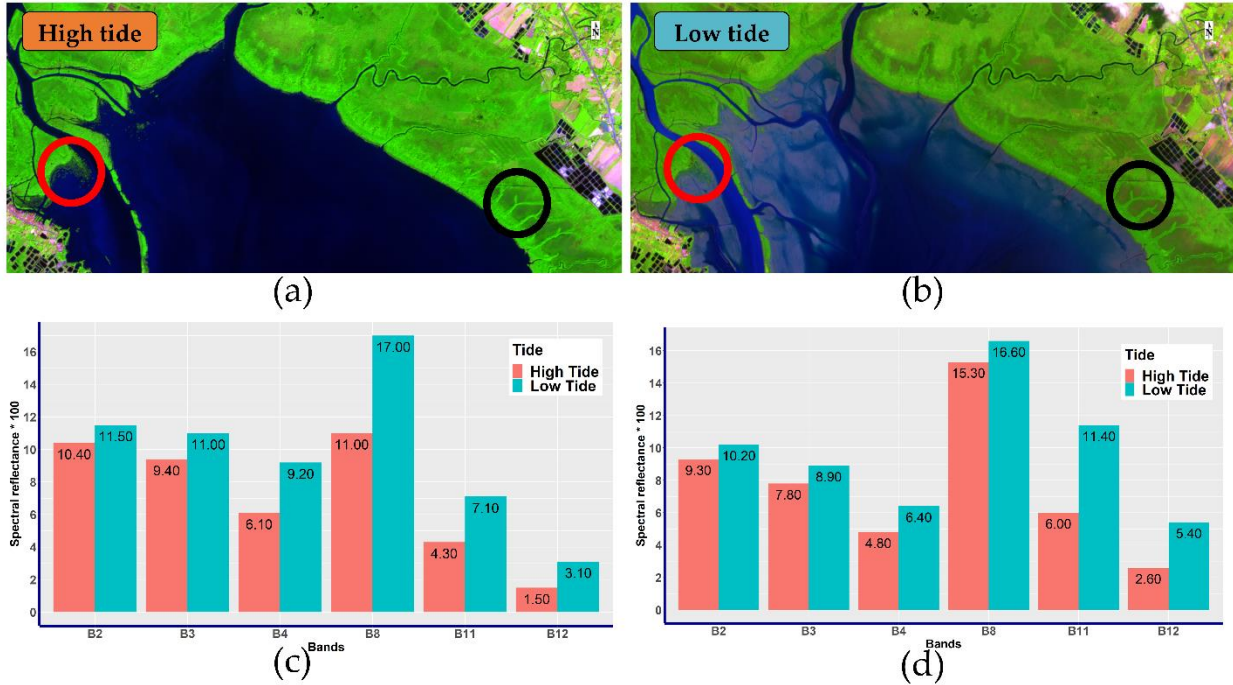


Figure 1.6 Effect of tidal inundation on the reflectance of Sentinel-2 (MSI) TOA images. Satellite acquisition time (approximately 10:00–10:30 am local hours) at Trat Province of Thailand. (a) False-color composite (SWIR-1, NIR, and Red) of Sentinel-2 MSI image (December 25th, 2018) at high tide (3.36 m); (b) False-color composite of Sentinel-2 MSI image (May 4th, 2018) at low tide (1.76 m); (c) Spectral variability at seaward location during tidal fluctuations (orange circle); (d) Spectral variability at dwarf stand (mid zone) location during tidal fluctuations (black circle). Note: in the graph, the spectral reflectance is scaled by 100 for visualization purposes. The pixel values shown here are the average value of 3 x 3 pixels.

1.5.2.3 SAR imagery

In recent years, the use of SAR data in mangrove research has increased. Microwave radar at X, C, L, and P bands has been used to identify different mangroves (Lucas et al., 2017, 2007; H. Zhang et al., 2018). Santiagoa et al. (2013) and Ottinger and Kuenzer (2020) summarized the usage of X, C, L, and P bands for various mangrove applications, including species identification. A combination of the studies by (Lucas et al., 2014) and (Adeli et al., 2020) provides a detailed review of the development of various SAR sensors up to the year 2020. The main benefits of the SAR sensors are that they are consistent and systematic and allow for observations of the land surface by day or night regardless of cloud cover or almost any type of weather condition (Lucas et al., 2014; Zhen et al., 2018). The SAR imagery is sensitive to vegetation structure and moisture content, and the signal can penetrate the canopy and indicate whether the vegetation is inundated. This information is complementary to optical imagery; however, only a few studies have exploited SAR's full potential to identify mangrove species (H. Zhang et al., 2018). Radar backscatter over mangrove ecosystems depends on local environmental conditions, such as tidal inundation, which can affect the backscatter response. Wang and Imhoff (1993) modeled radar backscatter at L-band from mangrove forest stands and reported higher backscatter for inundated conditions than non-inundated conditions. Darmawan et al. (2015) investigated the impact of tidal inundation on ALOS PALSAR polarimetric measurements on HH and HV and found that the tidal regime affected the backscatter coefficient. Furthermore, Lucas et al. (2017) noted that the effect of tidal inundation on L-band HH polarization: the ability of sensors to detect inundation, depends on the amount of overtopping canopy material and the openness of the forest canopy. The partially or fully submerged mangroves and low vegetation areas, such as sparse and dwarf forest stands on the seaward and low elevation areas (inundated during high tide), are likely to show such variations in satellite observations (Fig.1.7). Lucas et al. (2017) also found that backscatter increased with increasing above-ground biomass up to a saturation point (which is frequency-dependent) and, after that, the observed backscatter decreased due to dense aerial root systems. Polarimetric information from SAR images can be used to classify mangrove type and structure (Brown et al., 2016; Hong et al., 2015). However, Simard (2019) states that it is difficult to map the extent of mangroves using SAR alone, especially when the adjacent landcover is another forest type. Instead, Simard (2019) suggests using a combination of optical and SAR methods and optimizing the unique information content of each sensor in order to characterize the mangrove ecosystems.

Herein, literature is reviewed focusing on the application of SAR and combined multi-spectral imagery with SAR for mangrove species identification such as: Landsat-8 and RADARSAT-2 (Zhen et al., 2018); ALOS PALSAR (Santiagoa et al., 2013); Worldview-3 and RADARSAT-2 (H. Zhang et al., 2018); ALOS PALSAR, ALOS PRISM, and IKONOS (Brown et al., 2016); ALOS PALSAR-2 and RADARSAT-2 (Ferrentino et al., 2020); Sentinel-1 SAR and Sentinel-2 MSI (Pham et al., 2019a); Worldview-2 and Tandem-X SAR (Rahman et al., 2019). In these reviews, the tidal influence on SAR backscatter values was not considered. Nevertheless, the recent developments in SAR-based earth observation areas may potentially enhance the spatial scale of mangrove species mapping. The recently added and free public access to the 10-meter resolution Sentinel-1 SAR dense time series could improve mangrove forest monitoring (Wang et al., 2019).

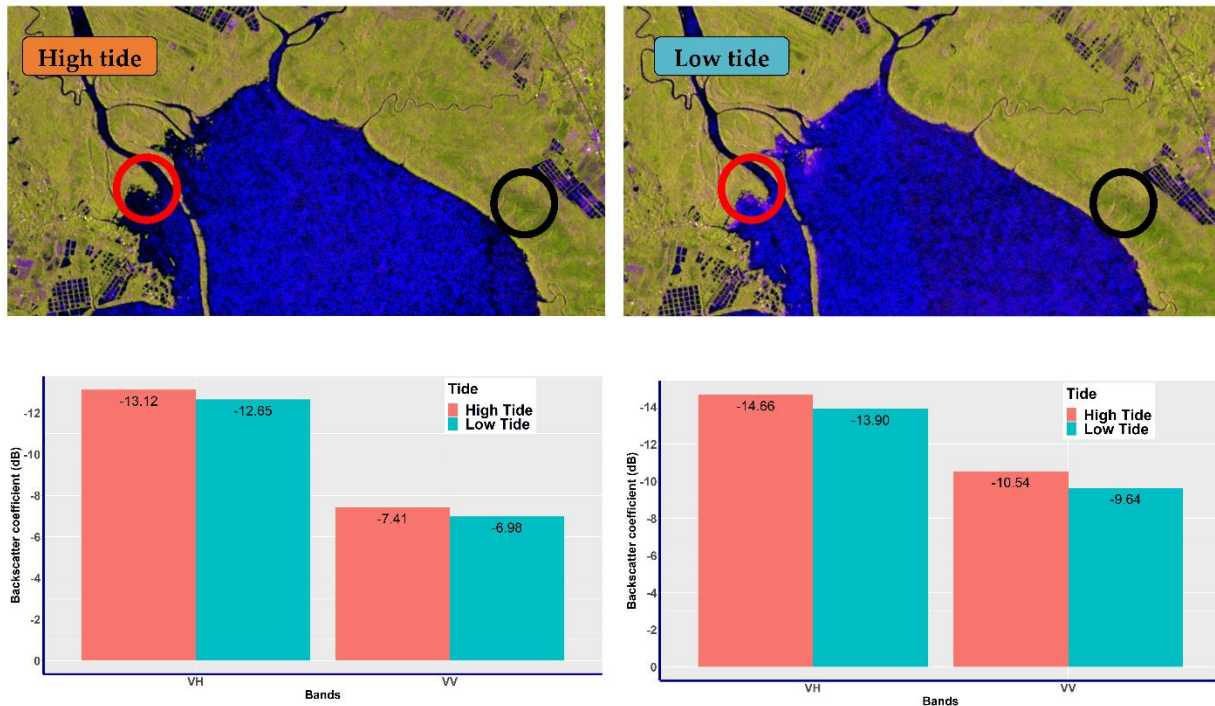


Figure 1.7 Effect of tidal inundation on the backscatter coefficient of Sentinel-1 SAR imagery. Satellite acquisition time (approximately 11:00 am local hours) attributed to tidal heights over a single year (2018) at Trat province of Thailand. (a) RGB composite (VV, VH, and VV/VH) of Sentinel-1 SAR image (December 26th, 2018) at high tide (3.35 m); (b) RGB composite (VV, VH, and VV/VH) of Sentinel-1 SAR image (June 17th, 2018) at low tide (1.12 m); (c) Backscatter coefficient variability at seaward location during tidal fluctuations (orange circle); (d) Backscatter coefficient variability at dwarf stand (mid-zone) location during tidal fluctuations (black circle). Note: the pixel values shown here are the average value of 3 x 3 pixels.

1.5.3 Temporal inconsistencies and gaps in mangrove monitoring

The estimation and consistent monitoring of mangrove diversity provide forest managers, ecologists, and conservationists important information to support forest management and related policy decisions. Despite the importance of multi-temporal changes in mangrove forest management and diversity conservation, the amount of this information is still limited. The lack of consistent field measurements makes remote sensing a valuable tool for mapping temporal dynamics (Thompson et al., 2015; Wang and Gamon, 2019). The influence of clouds, shadows, haze, and missing pixel values limits the temporal consistency in coastal regions (Fig. 4). Furthermore, it becomes more complicated if images are collected in two tidal stages (i.e., low and high tide), as this alters the temporal spectral response of individual pixels. In these situations, submerged or small and sparse mangrove spectral responses can be misinterpreted during the analysis. Remote sensing images are usually influenced by variations in atmospheric conditions, hence the need for radiometric corrections. The relative normalization of multi-temporal images to a common relative scale ensures the spectral homogeneity of each pixel (Bodart et al., 2011). However, the differences in local environmental and atmospheric conditions and the high variability of mangrove ecosystems require standardized and robust image-processing methods (Kuenzer et al., 2011).

1.5.4 Diversity modeling

The analysis given above shows that assessing current mangrove species diversity is essential to inform and enhance the spatial and temporal monitoring capabilities of these ecosystems (Sarker et al., 2019). Modeling approaches, such as stacked species distributions, macro-ecological and ordination and stochastic methods have been used to elucidate mangrove species spatial distribution patterns, stands, richness, and compositions (Mateo et al., 2017; Sarker et al., 2019). Few studies have explored the role of disturbances such as hurricanes or lightning strikes on the maintenance of species richness in mangrove communities or quantified the recovery of the mangroves (Krauss and Osland, 2019; Osland et al., 2018; Piou et al., 2006; Vogt et al., 2014). The lack of information on stressors and biotic and abiotic variables (Victor H Rivera-Monroy et al., 2017b), which are generally assumed to be temporally constant, limits the prediction of mangrove species distributions. Rivera-Monroy et al. (2017) noted that mangrove spatial distribution modeling is still limited to extrapolating small amounts of observational data to the global scale, validation, and uncertainty analysis. Aside from the boundary

conditions of the modeling domain (study site or transect), knowledge of the time series of forest structure and terrain topography is also required. The lack of adequate field inventories and data on temporal changes have constrained the effectiveness and application of modeling approaches (Berger et al., 2008; Victor H Rivera-Monroy et al., 2017b).

1.6 Discussion on good practices for diversity monitoring and predictions

1.6.1 Systematic sampling design for characterization of spatial scale diversity

Mangrove species distribution at any site is attributed to the different responses of individual species to topography, tidal regimes, coastal processes, variability in canal networks, and edaphic variables over a larger spatial scale. The edaphic variables are the physicochemical properties of sediments and water, such as particle size fractions (texture), bulk density, particle density, pH, organic matter, salinity, cation exchange capacity, field capacity, and nutrients (Das et al., 2019; Ellison et al., 2000). As well as the natural factors, anthropogenic controls play an important role in modifying species diversity at specific sites. Depending on the site-specific local settings such as topography, tidal regimes, coastal processes, canal networks, and edaphic variables, mangrove ecosystems can take the form of: (1) a single species zonation: a single tree species monoculture zone systematically arrayed over the landscape; (2) grouped zone: two or more species grouped across the intertidal zone; and (3) random placement or no zonation: species are randomly placed over the landscape (Ellison et al., 2000; Victor H Rivera-Monroy et al., 2017a).

We have found three references describing good sampling practices while reporting intertidal species zonation in mangrove forests (Castaneda-Moya et al., 2006; Dale, 1999; Ellison, 2002). These authors have identified the minimum data and sampling strategies required to assess spatial distribution, as follows: (1) the sampling must be performed in contiguous quadrats or fixed-area sampling along a transect of the intertidal zone; (2) there must be a complete list of species for the study site; (3) there must be a measure of the abundance of each species and where they occur in the given landscape; and (4) a measure of the edaphic parameters and surface elevation. Dale (1999) noted that in zonation studies, researchers should describe and quantify spatio-temporal characteristics and then relate them to observed characteristics and processes, such as growth, succession mortalities, and the species diversity status. The temporal characteristic is rarely considered in mangrove zonation studies. Good sampling practice

must include the four strategies mentioned above (as a minimum) with consideration of anthropogenic settings and the temporal dynamics of succession (Pimple et al., 2021). However, ecological baseline monitoring studies rarely consider the long-term effects of various stressors at the spatio-temporal level. Recently, Pimple et al.(2021) proposed that, in addition to the above-mentioned parameters, the temporal dynamics, anthropogenic settings, and human factors should also be considered when studying the baseline and zonation patterns of mangrove forests (Fig. 1.8).

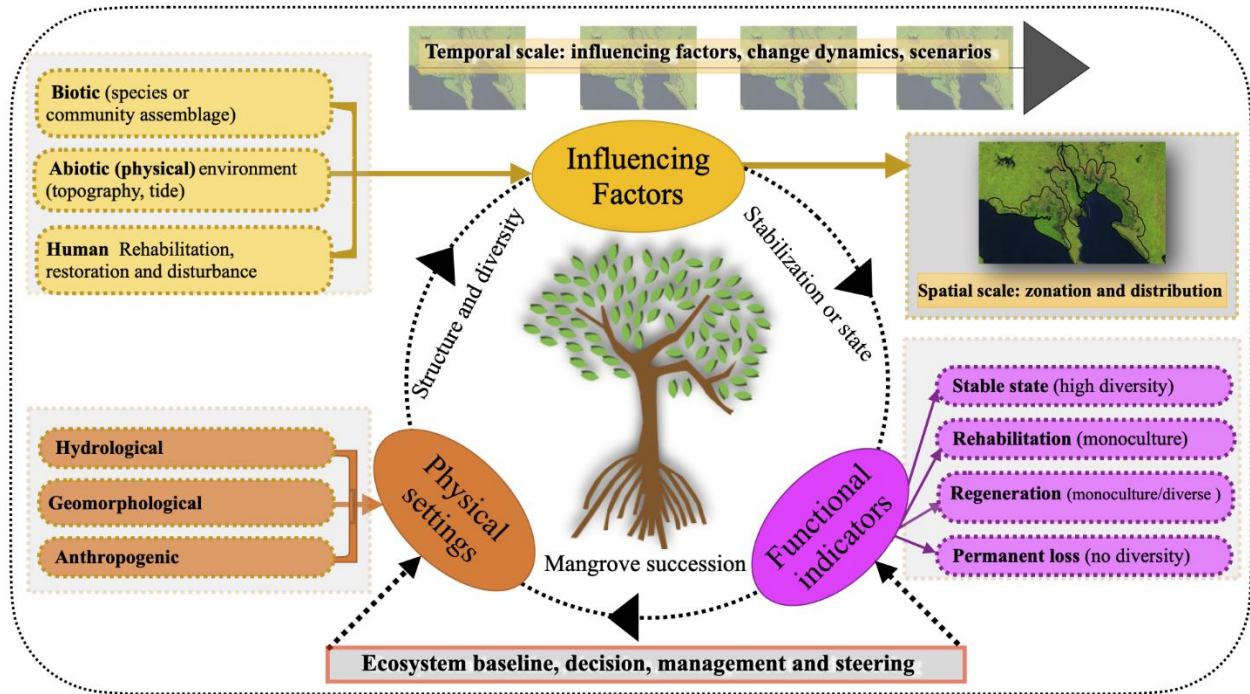


Figure 1.8 Monitoring spatial scale species diversity and zonation using a transect line plot. The orange boxes indicate the physical factors related to elevation, tidal inundation, and landscape modification. The yellow boxes indicate the natural influencing factors as well as those induced by humans. The pink boxes indicate the various phases that could be observed over time in a given ecosystem (Pimple et al., 2021).

A systematic sampling design across mangrove forest landscapes is crucial to obtain a complete species list covering the spatial area, elucidate the intertidal distribution, record changes in mangrove structural features, and knowledge of conservation interventions (Pimple et al., 2020). Considering the difficulties in conducting field inventories, the sampling design needs to be efficient (less time-consuming), precise, and cost-effective. Recently, remote sensing-based spatially balanced sample approaches, such as area proportional stratified random sampling, have been investigated (Grafström et al., 2014; Köhl et al., 2006; Olofsson et al., 2014; Wallner et al., 2018). In such inventories, the study

site can be partitioned into predefined clusters, where the proportion of forest species can be measured using spectral and structural properties of remote sensing imagery. In traditional mangrove ecological studies, the combination of remote sensing-based spatio-temporal dimensions has not been used for zonation and distribution analysis. Distinct spectral and structural heterogeneity of forest landscapes could be useful prior to the sampling design stage. Recent developments, such as low-cost high resolution or freely available high-resolution imagery such as Sentinel- SAR, Sentinel-2 MSI, and PlanetScope, and low-cost UAV (drones), have the potential to significantly improve the sampling design and reduce the associated costs (Hu et al., 2020; Matese, 2019, 2020; Miller et al., 2019; Wang et al., 2019). For example, Pimple et al. (2021) used Sentinel-1 and-2 imagery to establish spectral and structural heterogeneity across the landscape and select the transect line locations. The spectral variations in time series pixels, such as those for Landsat and Sentinel-2 composites, could further relate to the various phenomena that occur at specific sampling locations due to various stressors and processes (Otero et al., 2019; Pimple et al., 2021, 2020). Such an innovative sampling design enables a higher inventory precision, lower number of samples, the identification of possible locations for establishing transect lines (seaward to landward), an understanding of the temporal dynamics, and reduced costs. The spectral and structural variability can be further used in remote sensing-based classification approaches and accuracy assessment. Quantification or statistical testing of zonation (Clarke et al., 2008; Ellison et al., 2000) based on systematic sampling design can yield more reliable outcomes compared with traditional random sampling approaches. Furthermore, mangrove environmental conditions (or characteristics) should be considered for zonation, distribution, and mapping processes. There is considerable uncertainty in the upscaling of small or non-systematic species diversity field measurements to the large spatial scales of remote sensing data.

To understand mangrove biodiversity, it is important to comprehend the extent of mangrove species' habitats at multiple different scales, their interactions, and how they are changing over time (disturbance, rehabilitation, and regeneration) (Lucas et al., 2017). Rivera-Monroy et al. (2017b) provided a macro-ecological conceptual framework dealing with the distribution, abundance, energies, and interactions of networks of individuals and species across a spatio-temporal scale. Advances in satellite remote sensing have opened up new possibilities for monitoring mangrove species at various spatial, temporal, and thematic scales (Cárdenas et al., 2017; Pham et al., 2019b; Wang et al., 2019).

1.6.2 Overcoming the challenges of remote sensing data for monitoring mangrove diversity

Recent studies show that the development of cloud computing services (such as Google Earth Engine (GEE)), composite approaches, and machine learning methods could be used to overcome the above issues for mangrove forests (Chen et al., 2017; Hauser et al., 2020; Pham et al., 2019b; Pimple et al., 2020; Rogers et al., 2017; White et al., 2014). The composite approaches allow for the definition of a set of criteria to select the best observations on a per-pixel basis within defined periods, such as distance to cloud and cloud shadows (Griffiths et al., 2014; Thompson et al., 2015).

1.6.2.1 Obtaining consistent best quality composites

Most previous studies have used single-date cloud-free imagery to determine the forest extent and spatial distribution. Recently, time-series based compositing approaches of medium resolution imagery and the availability of open-source and free-to-use for research, education, and nonprofit cloud-computing platforms such as the GEE, are facilitating the large-scale environmental monitoring, analysis, and processing of high volumes of earth observation imagery, which has limited the number of missing pixels caused by the cloud and shadow masking (Hauser et al., 2020; Pimple et al., 2020; White et al., 2014). Figure 1.9 presents the cloud, shadows, haze, and missing value-free annual composites from 1987 to 2017 at the demonstration site (Pimple et al., 2018). Such gap-free and error-free time series are useful for providing consistent objective information on the changes in the rehabilitated mangrove stands in landward (high elevation areas) (Pimple et al., 2020). The annual composite could be used to provide extensive information on how the mangroves changed over time. The forests with dense canopies can be easily monitored using such composite imagery. However, the sparse canopy, low-height, or scrub intertidal mangroves are likely to be submerged or inundated during high tide (Li et al., 2019; Xia et al., 2020). Therefore, the consistency and quality of such composites may vary depending on observed pixels in low or high tide. However, consideration of tidal fluctuations (low and high tide) during image acquisition is not yet common practice.

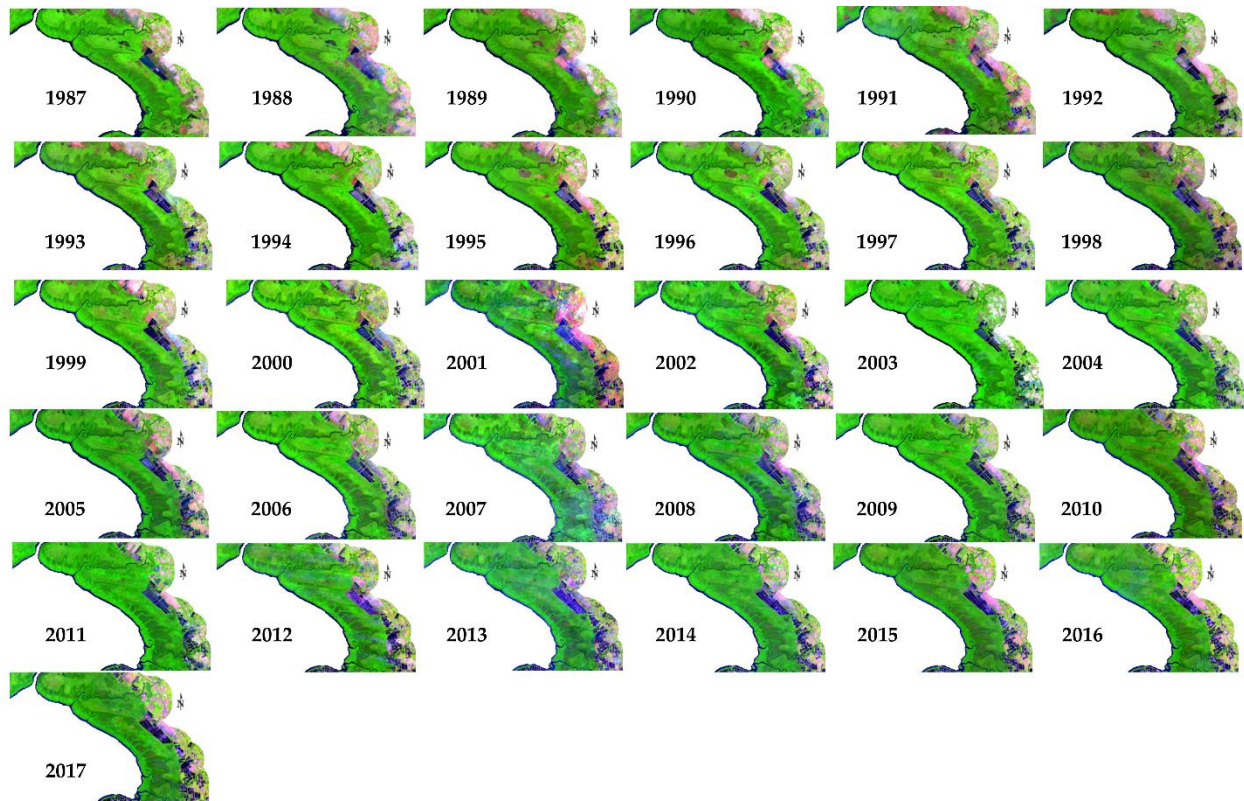


Figure 1.9. The annual cloud-free Landsat composites from 1987 (upper left) to 2017 (bottom left) for Trat province, Thailand, in pseudo-color composite (SWRI-1, NIR, RED). The automatic rule-based algorithm in the Google Earth Engine cloud-computing platform was used to remove contaminated pixels from all the available imagery to create consistent annual composites (Pimple et al., 2018).

The separation of low tide imagery allows for submerged mangroves to be distinguished, as their spectral values are similar to water during high tide (Zhang et al., 2017). In addition, recent studies have demonstrated approaches to extract low tide acquisitions from remote sensing data (Murray et al., 2012; Sagar et al., 2017). A multi-resolution tidal modeling framework can be used to obtain Landsat acquisitions during the low tide period (Sagar et al., 2018, 2017). We can also attribute the image acquisition time of the satellite observations to local tidal gauge station data and further cross-check them with the appropriate spectral signature for the Normalized Difference Water Infrared Index (NDWII), as proposed by (Murray et al., 2012). Furthermore, this approach could be extended to high-resolution time series (e.g., Sentinel-2 MSI, PlanetScope, or commercial high-resolution imagery) to help monitor mangrove ecosystems.

Studies have indicated that the prior stratification of an area of interest (separation of mangrove area) reduces spectral confusion, especially if the subject is terrestrial forest, or

other green vegetation, or cultivated fields (Long and Giri, 2011; Pimple et al., 2017). The prior stratification of mangrove and non-mangrove areas could avoid spectral mixing with other terrestrial forests. A simple vegetation index based on a pixel-by-pixel image multiplication technique with the Otsu threshold could be used for such stratification (Mather and Koch, 2011; Otsu, 1979). The stratified mangrove area of interest can be directly used as a subset for high-resolution imagery (preferably at low tide acquisition time) in combination with machine learning techniques to identify the spatial scale of species distribution. In addition, the Global Mangrove Watch dataset can also be used for stratification at a national or regional scale (Bunting et al., 2018).

Despite the effectiveness of high-resolution techniques, they are often limited to use at local or small scales due to their high purchasing costs, the small number of spectral bands, small swath size, and low temporal frequencies (Lucas et al., 2017; Wang et al., 2018). Therefore, studies with larger-scale spatio-temporal dynamics and species distributions may only become possible with the development of new sensors and algorithms (Wang et al., 2018, 2019). Studies prior to 2008 reported that the discrimination of mangroves using medium resolution satellite sensors such as Landsat and SPOT XS (spatial resolution: 30 m and 20 m; temporal resolution: 16 and 26 days, respectively) was not possible (Neukermans et al., 2008; Wang et al., 2018). However, since the recent launch of Landsat-8 (Pasquarella et al., 2016) and Sentinel-2 MSI (Pasquarella et al., 2016; Wang et al., 2018), many new Landsat-8 OLI time series based-approaches have emerged. Compared to previous medium-resolution sensors, the lengths of the red, NIR, and SWIR bands have been narrowed. In addition, the radiometric resolution and signal-to-noise ratio have been significantly improved. These advances have improved the accuracy of forest discriminations (Wang et al., 2018). Recent studies have explored the potential of medium-resolution satellites (Landsat-8 OLI and Sentinel-2 MSI) for mangrove species identification (Ghosh et al., 2016; Myint et al., 2008; Valderrama-Landeros et al., 2018; Wang et al., 2018). The development of machine learning models, deep learning architecture, and data integration techniques for mangrove species identification is an emerging field. Recent publications show the potential for these new methods and techniques for studying mangrove forest biodiversity using remote sensing (Pham et al., 2019b; Wang et al., 2018). Depending on the type of zonation and species assemblages (single, grouped, no-zonation, or randomly placed), the species extent on the ground, and the diversity of species in the study sites, the homogeneous mangrove species groups

could be well discerned. Furthermore, the integration of SAR-based complementary data with optical imagery may further enhance mangrove species identification.

1.6.2.2 Trajectories of secondary succession of diversity

The spectral variation hypothesis suggests that the spectral variability of multispectral images or vegetation indices could be used as a proxy to assess forest biodiversity (Palmer et al., 2002; Torresani et al., 2019). Satellite image pixels with high spectral heterogeneity correlate with landscape structure and complexity, reflecting forest heterogeneity (Oldeland et al., 2010; Torresani et al., 2019). Similarly, the spectral variation in the time series of a single pixel is related to the various phenomena that occur over a certain period due to various environmental and natural stressors and processes. Therefore, spectral variability of the time-series imagery or vegetation indices could be used as a powerful proxy for temporal changes or the succession of species biodiversity. We have reviewed recent literature focusing on time series analysis to derive a set of possible conditions to characterize temporal dynamics for every single field survey or classification training or testing location and link them to the recently observed species diversity and structural data (Fig. 1.10) (Chazdon et al., 2016; Otero et al., 2019; Pimple et al., 2020; Ryo et al., 2019; Wulder et al., 2019).

Temporal approaches consider the time and magnitude of various natural and anthropogenic disturbances along the spatial and intertidal gradients while reporting spatial zonation patterns. In this case, the changes could be studied through time and used as a proxy to interpret the observed diversity and structural differences and link them to underlying stressors or processes. Furthermore, in complex, diverse landscapes (where many species co-exist), temporal approaches could be used to classify the landscape into natural, rehabilitated, or regenerated forest types. Pimple et al.(2021) used the Normalized Difference Infrared Index (NDII) to characterize succession stages for mangrove species diversity as follows (Fig. 1.10).

1. **Biodiversity of undisturbed forest stands:** The undisturbed mature mangrove forest stands have relatively stable spectral signatures over many years. In this state, mangroves are expected to be structurally more complex and diverse.
2. **Biodiversity of rehabilitated forest stands:** The spectral or vegetation index values are expected to increase gradually and return or come close to those of the undisturbed forest stands or state before the disturbance. The rehabilitated mangroves are usually monoculture stands and structurally less complex. This

characteristic is a good indicator when evaluating the success and failure of rehabilitation projects.

3. **Biodiversity of regenerated forest stands:** The spectral or vegetation index values are expected to increase gradually and return or come close to those of the undisturbed forest stands or the state before the disturbance. Normally, in these forest stands, the disturbance is followed by natural recovery without any rehabilitation or restoration effort, indicating post-disturbance recovery and secondary succession. The regenerated stands are relatively more diverse and structurally more complex. A careful assessment of such sites is required as the final diversity may vary depending on the availability of seedlings.
4. **Biodiversity of permanent disturbed forest stands:** The spectral or vegetation index values drop abruptly with a clear breakpoint, and no gradual increase or return is observed over time. Forest stands are subjected to permanent loss of species biodiversity.

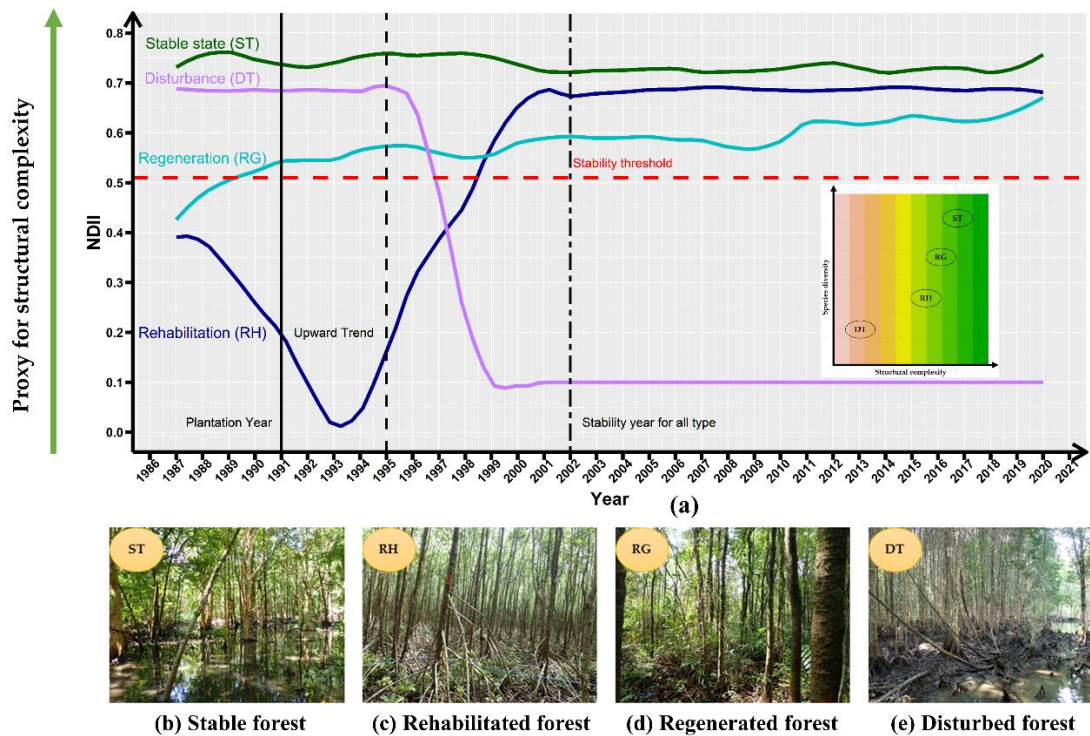


Figure 1.10 Illustration of expected mangrove forest diversity response types following periods of stability or disturbance induced by various biotic, abiotic, and anthropogenic disturbances. ST: stable or undisturbed state (dark green); RH: rehabilitation (dark blue); RG: regeneration (light blue); and DT: disturbance with no recovery (purple); the known plantation year is indicated by a black vertical line; the start of the NDII upward trend after rehabilitation is indicated by a dashed line; the quasi-stability year for

all forest types is indicated by two sized dash lines. In the graph for structural complexity and species diversity, the brown color indicates no diversity and less structural complexity, while the green color indicates high diversity and structural complexity (left to right). Note: b, c, d, and e are the pictures of actual field data of diversity development collected in the Trat province of Thailand (Pimple et al., 2021).

Some studies have shown that both structural and spectral signatures are required to improve mangrove species identification (Zhen et al., 2018). In addition, consistent and gap-free time series without atmospheric contamination and tidal effects are required to provide continuous objective information for the spatial identification, accurate extent assessment, and temporal changes for rehabilitation, regeneration, and disturbances (Hauser et al., 2020; Otero et al., 2019; Pimple et al., 2020, 2018). The consistent annual composites are dependent on the availability of good pixels throughout the year. In the regions where no data were available for annual compositing due to cloud consistent cloud cover, multi-year composites could be generated according to user-predefined rules (White et al., 2014). Furthermore, the Sentinel-1 SAR- and Sentinel-2 MSI-based dense time series may have the potential to interpret the structural variations along with spectral proxy over time. The recent development of cloud-computing platforms such as GEE, Amazon Web Services (AWS), the System for Earth Observation Data Access, Processing and Analysis for Land Monitoring (SEPAL), the Joint Research Center (JRC) Earth Observation Data and Processing Platform (JEODPP), Data and Information Access Service (DIAS) are hosting entire archives of remote sensing data including Landsat, Sentinel-1 and Sentinel-2 and offering high-performance data processing capabilities (Corbane et al., 2020; Gomes et al., 2020). These high-performance computing platforms overcome the limitations associated with data selection, download, pre-processing of raw data, machine learning-based image processing, and classification applications over larger scales. In the demonstration site (Fig 3), we used the GEE platform to develop contamination-free pixel-based annual composites from the Landsat, Sentinel-1, and Sentinel-2 data archives (Fig 1.9).

1.6.2.3 The role of remote sensing to enhance spatial scale biodiversity modeling

The goal of forest simulation models is to predict stand development under assumed or observed environmental conditions or management strategies. As the design of simulation models requires simplifications of selected core processes, an evaluation with measured data is inevitable. Early mangrove models such as FORMAN (Chen et al., 2011) and KiWi (Berger and Hildenbrandt, 2000) focused on interactions between the

individual trees and considered the abiotic environment to be spatially homogeneous and temporally invariable, without any feedback from individual trees. Particularly when dealing with changing environmental conditions, an understanding of the anthropogenic or natural disturbances or regime shifts in the past is required to understand temporal stand development. Field inventories provide the most accurate information but only provide a snapshot as frequent observations are seldom possible. However, there are still discrepancies in current mangrove inventories and reporting. Earth observation data may provide a substantial source for the temporal evolution of mangrove stands, especially when dealing with larger spatial scales. For instance, for the landward expansion of mangroves, Saintilan and Williams (2010) presented results from 28 photogrammetric surveys to document mangrove transgression into saltmarsh areas in Australia. Armitage et al.(2015) classified Landsat-5 data with neural networks to quantify mangrove expansion at the expense of saltmarsh vegetation in Texas. Furthermore, Rodriguez et al. (2016) utilized time-series data from historical aerial photography and high-resolution multispectral satellite imagery from 1942 to 2013 to observe vegetation changes in a mangrove-saltmarsh ecotone in Florida (USA) and related these changes to measurements of rainfall, temperature, and sea level.

Recent model developments considering mechanistic descriptions of abiotic processes, dependencies, and feedback, and spatial gradients and heterogeneity have focused on forecasts of spatially explicit stand phenomena, like a shift in mangrove to freshwater hammock vegetation (Jiang et al., 2012; Sternberg et al., 2007; Teh et al., 2008), and mangrove zonation patterns (Bathmann et al., 2020; Peters et al., 2020b). Such approaches account for species and salinity-dependent water use and the feedback of transpiration on pore water salinity. With increasing consideration of physical parameters like the mass balance of water and related processes as salinization and counteracting dilution processes by water fluxes, such models require more detailed spatial data.

To model and forecast stand development realistically, aside from vegetation maps, researchers need detailed information on the abiotic environment as an inundation regime at high spatial resolution, or digital elevation maps, accurate forest structure, development, or the status of conservation interventions at the site. These models could benefit greatly from the information gained from remote sensing methods. (Peters et al., 2020b) indicated the potential of coupling modeling with remote sensing approaches. Furthermore, Pimple et al. (2020) noted the possibility of using Landsat and Sentinel-2

MSI time-series data to validate the performance of landscape and individual-based models for rehabilitation projects. Data from vegetation and allometry patterns identified from satellite images reflect the characteristic subsurface constraints; for example, mangroves as the visible manifestation of coupled vegetation and hydrological processes indicating subsurface properties. In a similar non-mangrove approach in the Yanqi Basin in the northwestern part of China, Li et al. (2009) used spatial patterns in evaporation maps derived from remote sensing data (NOAA-AVHRR) to deduce the underlying aquifer properties.

Earth observation data has the potential to be used in either parameterizing or evaluating mechanistic mangrove stand models. In addition, satellite data may provide important information about the temporal evolution of mangrove stands, especially at larger spatial scales. The modeling framework could benefit greatly from the recent advances in remote sensing and UAV technologies. Wang et al. (2019) described remote sensing applications such as SAR and LiDAR for mangrove vertical structure monitoring. The recent development of satellite and UAV (Yaney-Keller et al., 2019) based SAR (Fatoyinbo et al., 2008; Simard et al., 2006) and LiDAR (Guo et al., 2021) technologies have proved very useful for the monitoring of mangrove structures. To the best of our knowledge, the integration of earth observation data with the modeling frameworks mentioned above has not yet been attempted for mangrove studies.

1.7 Summary of best practices

The current literature on mangrove species diversity monitoring suggests that many studies based on field inventory focus on small sites. These studies lack a systematic field sampling approach, as well as quantification or statistical testing of species zonation and distribution in relation to various environmental and anthropogenic settings. In addition, secondary succession is not considered while reporting diversity in a given site. Therefore, it is very likely that in several studies, the sampling approaches are not wholly representative of the entire population of mangrove species or their association, and hence the reported findings are inconsistent. Most of the spatial scale diversities have been reported without accounting for micro-topography or inundation regimes. Fassnacht et al. (2016) discussed several issues related to field data collection in forestry, indicating that the sampling strategy and criteria of species classes play a crucial role while reporting forest diversity. Remote sensing-based stratified sampling gives more precise estimates of diversity when spectrally and structurally homogeneous and

individual strata (classes) are identified (Wallner et al., 2018). Furthermore, studies attempting to identify mangrove species using medium or high-resolution satellite data did not account for the tidal influence. In this case, there must be doubt about the accuracy of the estimated mangrove extent or species classification if the images used for analysis are obtained at different tidal stages. The consistency and quality of remote sensing data can be improved using low tide imagery or composites (Rogers et al., 2017; Sagar et al., 2017). In addition, an unbiased field inventory and remote sensing data will undoubtedly improve the parameterization, effectiveness, and spatial application of modeling approaches. Therefore, we recommend using remote sensing and UAV data to facilitate large-scale modeling studies. Figure 1.11 shows the outline of best practices based on this review, the results obtained at the demonstration site, and our experiences that could be used to enhance the monitoring and modeling of mangrove diversity.

Practice 1. Considering low tide images: The selection of low tide imagery allows the identification of submerged mangroves and maintains the spectral and structural heterogeneity within different forest species or their associations. It should be noted that low tide imagery may be affected by haze, clouds, and cloud shadows. Depending on the available imagery, contamination-free annual or biannual median composites could be used in such a situation. In multi-year analysis, radiometric normalization could be performed to reduce variations caused by atmospheric conditions during image acquisition.

Practice 2. Stratification of mangrove and non-mangrove area: The stratification of mangroves as an area of interest reduces the spectral and structural confusion caused by other vegetation categories (Long and Giri, 2011). However, studies using remote sensing techniques to assess in more detail the diversity within mangrove forests are still uncommon (Held et al., 2003). Stratification ensures the spatial scale spectral and structural heterogeneity within mangroves only. The DEM and vegetation indices parameters such as NDVI, NDII, and NDWI are useful to detect low elevation vegetation such as mangroves. A binary vegetation index per pixel image multiplication with the Otsu threshold could be used for such stratification (Mather and Koch, 2011; Otsu, 1979).

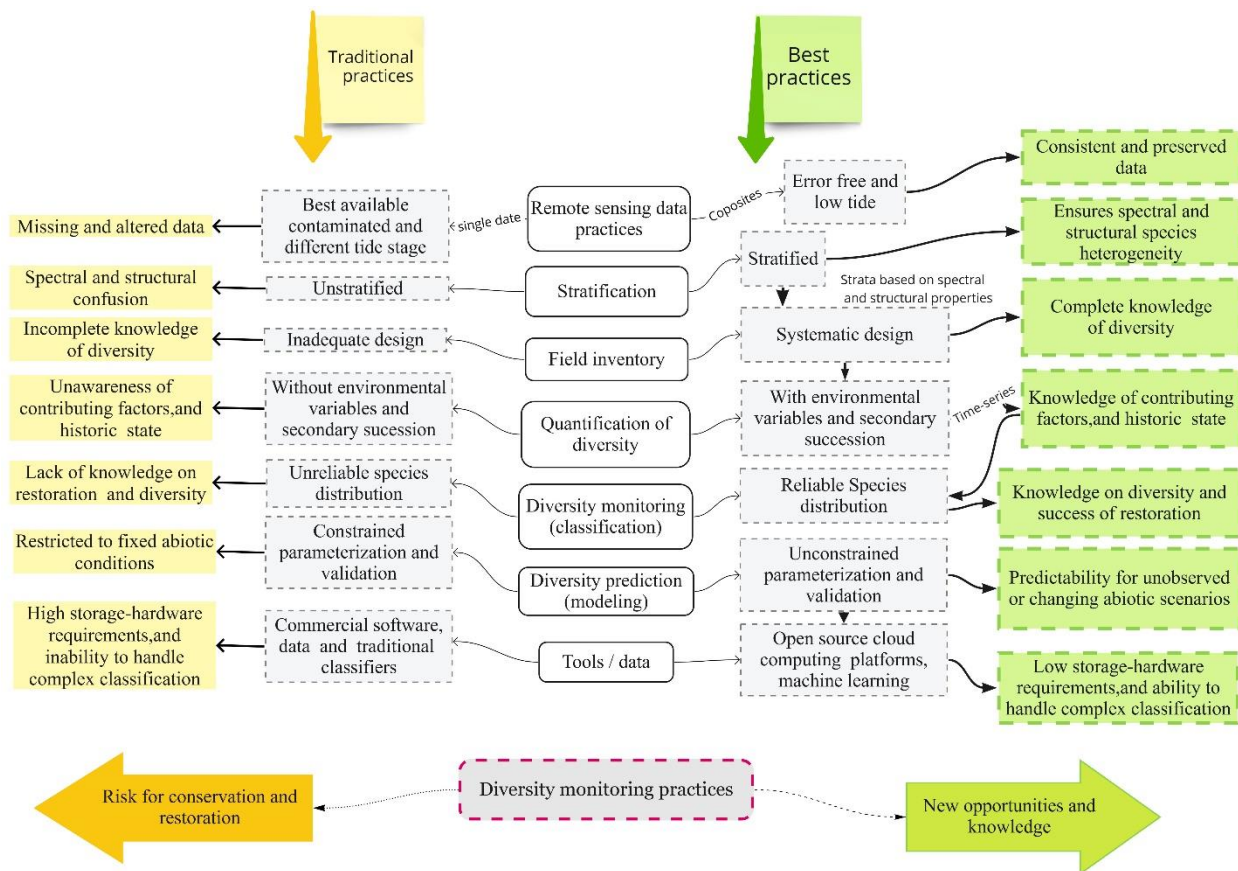


Figure 1.11 Summary diagram highlighting the comparison between reviewed traditional and proposed best practices using earth observation data.

Practice 3. Systematic sampling design: The systematic sampling design must include intertidal (transect plots) and spatial distribution of species and their associations across the landscape. The sampling design is crucial for characterizing either site-specific ecological distribution or remote sensing-based spatial distribution. Stratified sampling can lead to more precise estimates once distinctive mangrove strata or thematic categories of species and their associations are identified (Olofsson et al., 2014; Wallner et al., 2018). Integration of structural and spectral values of Sentinel-1 and-2, UAV, and a preliminary randomly surveyed sample could be useful to establish thematic categories and select the locations, transect line (intertidal), and sampling plots across the landscape (Köhl et al., 2006).

Practice 4: Quantification of diversity distribution (site-specific characterization): For zonation and diversity baseline studies, quantification or statistical testing of species zonation and distribution in relation to various environmental variables (e.g., topography or inundation) must be performed (Clarke et al., 2008; Ellison, 2002; Ellison et al., 2000;

Ma et al., 2020). In addition, the inclusion of anthropogenic settings such as the secondary succession of diversity caused by rehabilitation, restoration, and regeneration must be defined (Pimple et al., 2021). The diversity patterns of secondary succession vary from site to site based on local environmental conditions, land modifications, and rehabilitation practices (Pimple et al., 2020). This quantification enables the definition of mangrove species diversity distributions such as single species zones, group zones (two or more species are grouped), or no zones (random placement). This information is useful in defining satellite spectral response to individual zones.

Practice 5: Remote sensing-based classification: Machine learning and deep learning techniques can be used for classifying mangrove species using multi-spectral and SAR data (Pham et al., 2019b). Cloud-computing platforms such as GEE are equipped with machine learning algorithms (e.g., classification and regression tree (CRAT) and Random Forest). In addition, other freely available open-source platforms such as R, Python, or the Orfeo toolbox facilitate these algorithms (Fassnacht et al., 2016; Wang et al., 2019). Practices 3 and 4 can be used for the selection of training and validation data for classifiers. In addition, time-series-based approaches such as the automatic regrowth monitoring algorithm (ARMA) can be used to distinguish rehabilitated and regenerated mangroves from natural forest stands (Pimple et al., 2020). This information is useful for separating natural *Rhizophoraceae* from rehabilitated stands to avoid spectral confusion with other mangrove species during classification.

Practice 6: Modeling parameterization and validation: The information obtained from Practices 1 to 5 could be used either in parameterizing or evaluating mechanistic mangrove stand models.

1.8 Outlook on recent developments in remote sensing

Recent developments in remote sensing sensors include three major advancements. The new satellite sensors include Landsat-8 OLI, Landsat-9, Sentinel-1 SAR and-2 MSI, and PlanetScope, which are capable of producing larger scale high temporal frequency (Csillik et al., 2019; Fassnacht et al., 2016; Masek et al., 2020). In addition, low-cost Unmanned Aerial Vehicles (UAV) have already become an affordable and cost-efficient tool to map a targeted area for many emerging applications in the arena of ecological monitoring and biodiversity conservation (Adade et al., 2021; Díaz-Delgado and Múcher, 2019). The low altitude UAV flights can easily provide sub-meter scale spatial resolution,

which can be used as complementary information in large-scale surveys. Moreover, the UAV system can be deployed on-demand, providing temporal flexibility to respond to specific needs. For example, it can monitor different inventories and use them during field surveys to identify homogeneity and forest structure to reduce the number of samples (Baena et al., 2017). In addition, upcoming SAR satellites such as NISAR (L-band and S-band sensors), a joint NASA and Indian Space Research Organization (ISRO) mission scheduled to launch in late 2022, as well as the European Space Agency's (ESA) BIOMASS (P-band sensor), scheduled to launch around the same time, will increase the capability of characterizing and monitoring mangrove ecosystems. Finally, ongoing developments in satellites and airborne sensors, such as Light Detection and Ranging (LiDAR) multi-spectral and hyperspectral devices, including UAVs, provide new opportunities in the field of mangrove species diversity monitoring (Dainelli et al., 2021; Fassnacht et al., 2016).

1.9 Conclusions

Mapping, monitoring, and modeling the spatio-temporal scale of mangrove species biodiversity is a critical issue at the global, regional, and national scales when assessing the success of conservation interventions. However, regardless of the current technological advances, there is still a dearth of standardized reporting and monitoring of mangrove species diversity and of reliable scientific data to inform improvements in mangrove management practices. This is partly because the identification and prediction of correct species zonation and spatial patterns is still limited, representing a significant challenge that has not yet been adequately addressed in field-based ecological, remote sensing, and modeling studies. In addition, despite advances in remote sensing, most mangrove studies still lack the proper integration of environmental conditions (or characteristics) and secondary succession.

This review has identified studies focusing on site-specific field inventory, remote sensing, and modeling-based spatial scale mangrove species characterization. Traditional field-inventory-based ecological studies only report the species diversity, zonation, and structural parameters without consideration of (1) a systematic sampling design (not covering heterogeneity in the study site), (2) quantification in relation to topographic or tidal variability, (3) effects of anthropogenic settings, and conservation interventions. However, remote sensing-based mangrove species identification is affected by various environmental and atmospheric contaminants in coastal areas. In optical imagery, the

spectral values are usually influenced by varying atmospheric conditions and tidal inundation stages. In SAR imagery, the backscatter signal in mangrove forests is also influenced by tidal inundation, resulting in poor quality data and unreliable estimates of structural diversity, as well as biomass density of mangroves. In addition, a proper understanding of species and their assemblages and spatially unbalanced insufficient training and validation data affects spatial-scale species classification. Further, the effectiveness and application of modeling-based approaches have been constrained due to inadequate field inventories and data on temporal changes.

Our results showed the potential of using remote sensing-based mangrove stratification to aid systematic sampling design methods. The optical and SAR-based methods could help define heterogeneous mangrove species and their associations at a larger spatial scale. Such stratification based on a systematic sampling design with quantification or statistical testing of spatial zonation patterns could improve the reliability of results for ecological and prediction studies. The cloud-free and low tide composites greatly enhance the spectral and structural discrimination performance of freely available medium and high resolution satellite sensors. In addition, composite-based time-series data could provide comprehensive information on the historical state and secondary succession of conservation interventions. Modeling frameworks could benefit considerably from accurate information on the spatio-temporal evolution of mangrove diversity, especially at larger spatial scales.

1.10 Research questions

The previous sections have provided a comprehensive overview of the interaction of mangrove species diversity and zonation with environmental and anthropogenic settings. The micro-topography drives the extent of tidal inundation and intertidal zonation of mangrove forest species and can be considered ideal proxies for other environmental factors that contribute to forest growth and diversity (such as salinity, soil texture, and redox potential). Studies linking the quantification of mangrove species zonation patterns with respect to microtopography are rarely investigated. In addition, information obtained from site-based biodiversity surveys is often limited to single occurrences and lacks the historical state and dynamics of mangrove forest stands. The inclusion of environmental settings (topography or tidal inundation) and functional indicators when assessing the baseline of mangrove forests is crucial to provide a complete picture of the viability, resilience, and dynamics of secondary succession. The methodological framework based on remote sensing data remains limited and represents a significant challenge for studying species diversity and zonation. Furthermore, despite advances, the effects and uncertainty due to tidal inundation on satellite imagery are poorly understood. This study aims to improve our understanding of the long-term effects of environmental and anthropogenic settings on the spatio-temporal dynamics of mangrove forest species diversity and zonation. Here we investigated the knowledge gaps in terms of potential spatial diversity, intertidal zonation, and the historic state of mangrove forest species and tested the role of environmental as well as anthropogenic settings on diversification. The following hypotheses have been tested (H: Hypothesis; P: Prediction).

Based on a detailed review, synthesis of limitations, current advances, four research question(Q)s have been identified.

Q1. How have the spatio-temporal characteristics of the mangrove forest landscape changed (gain or loss) over a period of three decades?

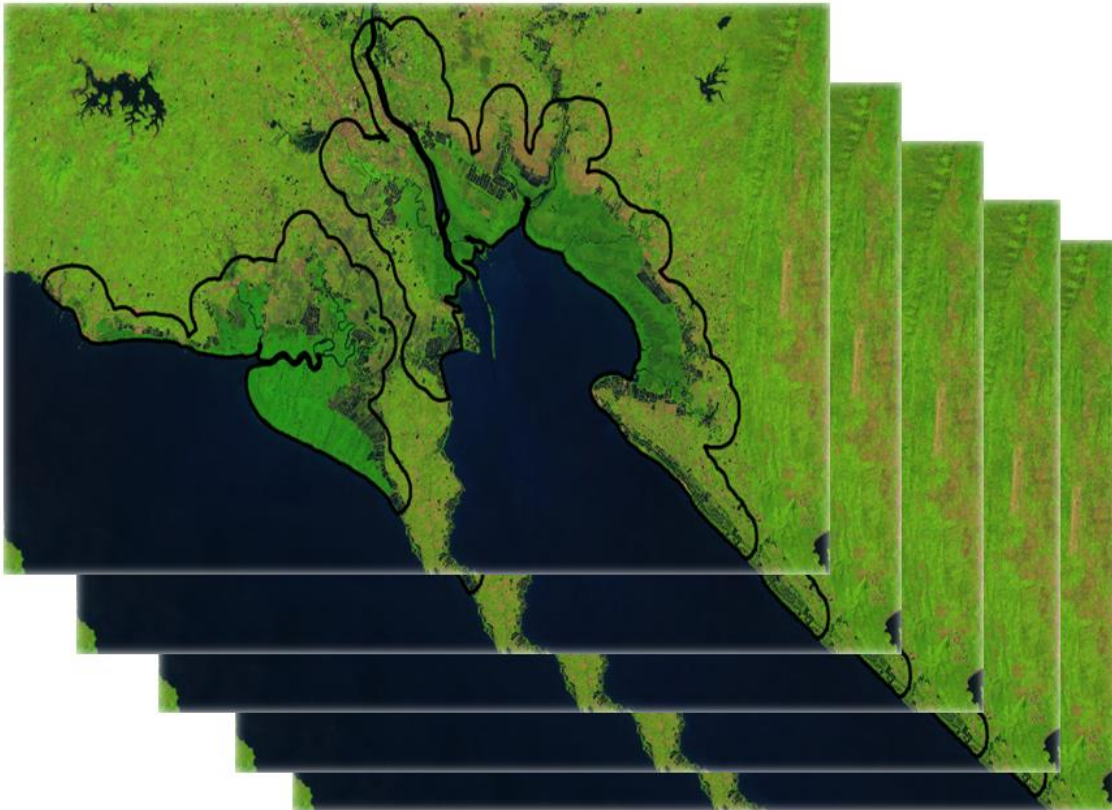
Q2. How did the species biodiversity and structural complexity of rehabilitated (planted) forests develop, compared to the adjacent natural mangrove stands? This question addressed two main issues: (1) How have rehabilitated mangroves develop over the last three decades? and (2) whether the ecological parameters of rehabilitated mangrove forest stands resemble those of the adjacent natural stands.

Q.3 What is the sensitivity of environmental factors and anthropogenic settings (such as topography and rehabilitation) to potential spatial diversity, intertidal zonation, and historic state or knowledge gaps of mangrove forest species diversity? This question addressed three main topics: (1) the species distribution patterns perpendicular to the shoreline, (2) the spatial-scale intertidal zonation patterns in response to the elevation gradient, and (3) the trajectories of functional indicators of diversity in response to secondary succession.

Q.4 What is the potential of multi-source satellites to discriminate the spatial patterns of mangrove forest types? This addressed: (1) evaluating the influence of tidal inundations on satellite imagery, (2) exploring the potential of medium and high resolution freely available satellite spectral response and machine-learning classifiers to select mangrove dominant species, and (3) exploiting the composite-based spectral variability of time series to determine the temporal change or secondary succession.

CHAPTER 2

Assessing long-term dynamics of in mangrove forest ecosystem



Landsat composites over Trat province, Thailand

This chapter has been published as: Pimple, U., Simonetti, D., Sitthi, A., Pungkul, S., Leadprathom, K., Skupek, H., Som-ard, J., Gond, V. and Towprayoon, S. (2018) Google Earth Engine Based Three Decadal Landsat Imagery Analysis for Mapping of Mangrove Forests and Its Surroundings in the Trat Province of Thailand. *Journal of Computer and Communications*, 6, 247-264. <https://doi.org/10.4236/jcc.2018.61025>

Abstract:

Monitoring and understanding the changes in mangrove ecosystems and their surroundings are required to determine how mangrove ecosystems are constantly changing while influenced by anthropogenic, and natural drivers. Consistency in high spatial resolution (30 m) satellite and high-performance computing facilities are limiting factors to the process, with storage and analysis requirements. With this, we present the Google Earth Engine (GEE) based approach for long term mapping of mangrove forests and their surroundings. In this study, we used a GEE based approach: 1) to create atmospheric contamination free data from 1987-2017 from different Landsat satellite imagery; and 2) evaluating the random forest classifier and post classification change detection method. The obtained overall accuracy for the years 1987 and 2017 was determined to be 0.87 and 0.96, followed by a Kappa coefficient 0.80 and 0.94. The change detection results revealed a significant decrease in the agricultural area, while there was an increase in mangrove forest, shrimp/fish farm, and bare land area. The results suggest that major human activities are affecting the landscape dynamics within the study area.

2.1 Introduction

Mangrove forests are located throughout the tropical and sub-tropical regions of the world, and are claimed to be one of the most vulnerable ecosystems to be affected by natural disturbances and human interference (Gilman et al., 2008; Jhonnerie et al., 2015; Kanniah et al., 2015; Kuenzer et al., 2011). Mangrove forests are unique ecosystems that provide important ecological services for coastal habitat and coastal protection (Giri et al., 2007; Son et al., 2015). These ecosystems, however, are under high pressure due to over exploitation, and are declining at an alarming rate (Giri et al., 2007; Kuenzer et al., 2011). Interest in their conservation has increased recently due to their widespread degradation, mangrove forest ecosystems have gained much publicity, particularly in regard to conservation and rehabilitation (Andradi-Brown et al., 2013; Pimple et al., 2020). Quantifying and monitoring the spatial and temporal dynamics of the mangrove ecosystem is essential for a better understanding of the many coastal land and sea processes. Traditionally, mapping a mangrove forest requires intensive field work, which is costly in time and money, as mangroves are inaccessible or difficult to field survey (Kuenzer et al., 2011; Zhang et al., 2014). Satellite remote sensing has a great potential for mapping and monitoring changes in mangrove forests, as the space based technology allows for collecting information from the landscape which is otherwise particularly difficult to access (Jia et al., 2014; Son et al., 2015). Several studies have provided a detailed summary with an overview of remote-sensing research activities, including critical analysis, that has been performed in the last few decades (Kuenzer et al., 2011; Lucas et al., 2017; Pham et al., 2019b; Wang et al., 2019). Also, they highlighted the importance of understanding the local environment when using remote sensing-based mapping and monitoring. In recent years, several studies have been published, illustrating hyper-spectral airborne and space borne data applications, including AISA, CASI, HyMap, AVIRIS, Daedalus, and EO-1 Hyperion (Giri et al., 2007; Green et al., 1998; Jia et al., 2014; Yang et al., 2007). High resolution imagery applications such as IKONOS, QuickBird, RapidEye and WorldView-3, have been very effective in discriminating mangrove forests from other forms of land use (Huang et al., 2009; Myint et al., 2008; Wang et al., 2004; Wang et al., 2004). However, limited spectral bands, complex data collection, and analysis methods, along with their high cost, are major limiting factors in using hyper-spectral and high resolution data (Aslan et al., 2016; Kuenzer et al., 2011; Son et al., 2015). Few studies reported the use of RADAR data, with the inclusion of ALOS PALSAR, ERS-1/2 and Radarsat-1 SAR, as a tool in the mangrove classification framework, having found

that classification and mapping accuracy requires improvement (Kovacs et al., 2006; Kuenzer et al., 2011; Lucas et al., 2009; Rao et al., 1999). In previous studies, optical remote sensing imagery, like the Landsat Multispectral Scanner (MSS), Landsat Thematic Mapper (TM), and Indian Remote Sensing satellites (IRS), SPOT XS, and SPOT-5, have been commonly used for mangrove forest mapping as the data is available via free access, or at a low cost (Jia et al., 2014; Liu et al., 2008). The recent development in the series of Landsat satellites, such as the Operational Land Imager (OLI)-8 and Sentinel-2, have added a new dimension to long term data. The availability of multiple spectral band records over the long term, means the Landsat series can be used for accurate mapping and monitoring of mangrove forests (Shapiro et al., 2015). Additionally, the application of the non-parametric or machine learning classifiers are very efficient for land use and land cover (LULC) mapping, even if still not abundant in mangrove mapping studies (Jhonnerie et al., 2015).

In recent years, there has been an increase in high-performance cloud computing platforms, such as the NASA Earth Exchange (NEX), Amazon Web Service (AWS) and Google Earth Engine (GEE). These high performance cloud computing platforms allow free access to the vast and fast growing earth observation data for global, as well as regional studies (Giri et al., 2015; Midekisa et al., 2017). For example, GEE provides preprocessed Landsat data (1982-present), along with the required disk space and advanced classification machine learning algorithms (Giri et al., 2015).

In Southeast Asia, large areas of the coastal zones have been occupied by mangrove forests (Thampanya et al., 2006). According to the Asian Development Bank Regional Review on the Economics of Climate Change in Southeast Asia (Weiss, 2009), the reduction in the size of mangroves resulted in coastal erosion in Thailand, and in neighboring countries. While the extent of these changes remains limited, means of sustainable management and future rehabilitation remains highly uncertain (Green et al., 1998; Kuenzer et al., 2011; Vo et al., 2012). In recent decades, Thailand's mangrove forest area has substantially decreased as a result of human settlements, transport infrastructure, agriculture, and aquaculture (NESDB, 2000; Thampanya et al., 2006). According to NESDB, while inconclusive in most regions, 30% of mangrove forest was lost during 1961-1996 due to the conversion of mangrove forest to shrimp farms.

Given the above factors, the main objective of this study is to quantify the presence of mangrove forests in Thailand's Trat Province over the last 30 years (1987-2017) using

Landsat imagery and GEE cloud computing, as well as developing an operational wall-to-wall change detection methodology based on long time series analysis.

2.2 Study site and methodology

2.2.1 Study area

The study area is in the Trat Province, eastern Thailand, on the border with Cambodia and along the Gulf of Thailand (Figure 2.1). It covers an area of approximately 240 km² of which 106 km² of mangrove forest. Since ever, local communities have benefit from goods and services provided by the forest but in recent years, mangroves have been heavily exploited for timber extraction, charcoal production and shrimp farms. Chalermchatwilai et al. (2011) reported that, after the 1980's, thanks to the effort of the Department of Marine and Coastal Resources, Thailand has reared this area. Villagers to this day, continue to use mangrove wood for various domestic purposes.

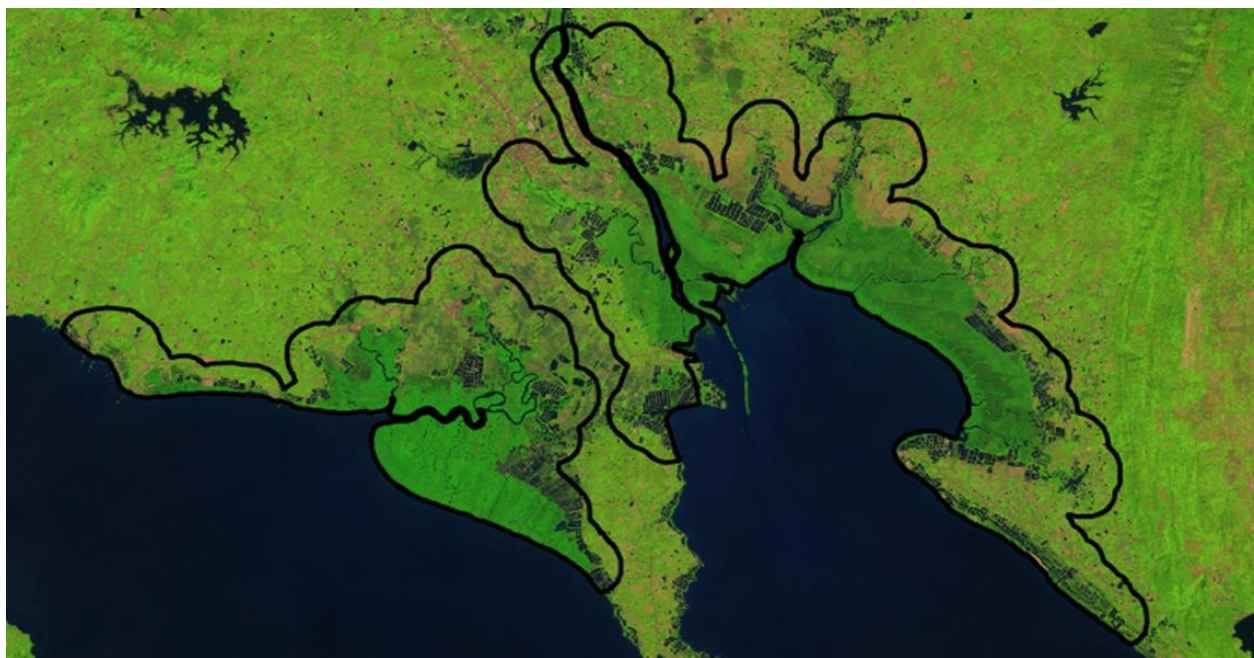


Figure 2.1. Location and extent of mangrove forest in Trat province of Thailand.

2.2.2 Landsat imagery

Data consists of Landsat TM, ETM+, and OLI Tier 1 top-of-atmosphere (TOA) reflectance as obtained from GEE image collections. The red, green, blue, NIR, SWIR-1, and SWIR-2 spectral bands of the TM-5, 7 ETM+, and OLI-8 platforms, were considered in the analysis. Jagged pixels at the edges of Landsat TM-5 images were removed using the 450 m inward

buffer, which ensures the best available reflectance values for image analysis (Robinson et al., 2017). Annual composites were created by using the median reflectance values of the collection (all images for a target year e.g. 1987, from 01/01/1987 to 31/12/1987) (Midekisa et al., 2017), after been cleaned from cloudy or no-data pixels following the algorithm proposed by (Simonetti et al., 2015), and available in GEE. The algorithm is driven by predefined knowledge-based rules built upon the spectral signature collected on a global scale, and generates a thematic output including a cloud mask.

The TOA imagery was atmospherically corrected using a Dark Object Subtraction (DOS) method (Bruce and Hilbert, 2004). Using a forest normalization method, the median value of the mangrove forest pixels was used to apply a linear shift to each spectral band (Bodart et al., 2011) (Pimple et al., 2017). Prior to classification, the Normalized difference vegetation index (NDVI) (Green et al., 1998; Higginbottom and Symeonakis, 2014), and Normalized difference infrared index (NDII) (Jackson et al., 2004), has be computed to mask the composite from residual clouds or no data.

The Landsat imagery used in this study from 1987–2017 was from the Landsat TM-5 (1987–2001, and 2003–2011), Landsat ETM+7 (2002) and Landsat OLI-8 (2013– 2017) sensors respectively. The year 2012 was excluded from the analysis due to missing data.

2.3 Training and validation sampling design

One of the major issues of classifying historical images by using training and validation samples, is often the lack of field data or so called ground-truth (Gomariz-Castillo et al., 2019). The design of a systematic training and validation dataset across a specified area is crucial for identifying major changes in mangrove forests over time. The design must be a good representation of major Land Use Land Cover (LULC) classes, with the dataset sufficiently large to provide reliable estimates (Pimple et al., 2017). The unsupervised classification was performed on the Landsat OLI-8 year 2017 images to establish thematic categories of LULC. The most recent image was chosen for stratification to avoid the effect of the LULC change on training and testing design. Later the stratified random sampling approach was used to estimate the total number of samples per class (FAO, 2016; Olofsson et al., 2014). The stratification and selection of independent sample design focused on each five-year interval to ensure a stable change identification (Olofsson et al., 2014). In total, 414 sample locations (Figure 2.2) were selected for LULC classification: class 1, active agriculture; class 2, bare land and urban areas (some agricultural land without vegetation was included here); class 3, mangrove forest; and class 4, shrimp and

fish farms. To establish each class, training samples were obtained: 150 for agriculture, 50 for bare land and urban areas, 164 for mangrove forest, and 50 for shrimp and fish farms. Among these sample locations, 109 were randomly selected to be set aside as validation samples. In March 2015 and October 2016, a field mission was conducted in the study area to collect training and validation data for mangrove mapping. About 60 mangrove forest samples were collected during these missions and were used along with a combination of Google Earth images, high-resolution satellite imagery, aerial photographs, and prior knowledge, for use as samples of the remaining classes. A distance of 500 meters separated each sample to avoid spatial autocorrelation, while training and validation pixels remained independent of each other. In the process of classification, the reference training and testing data were first developed for each year and then used in the classifier (Peiman, 2011).

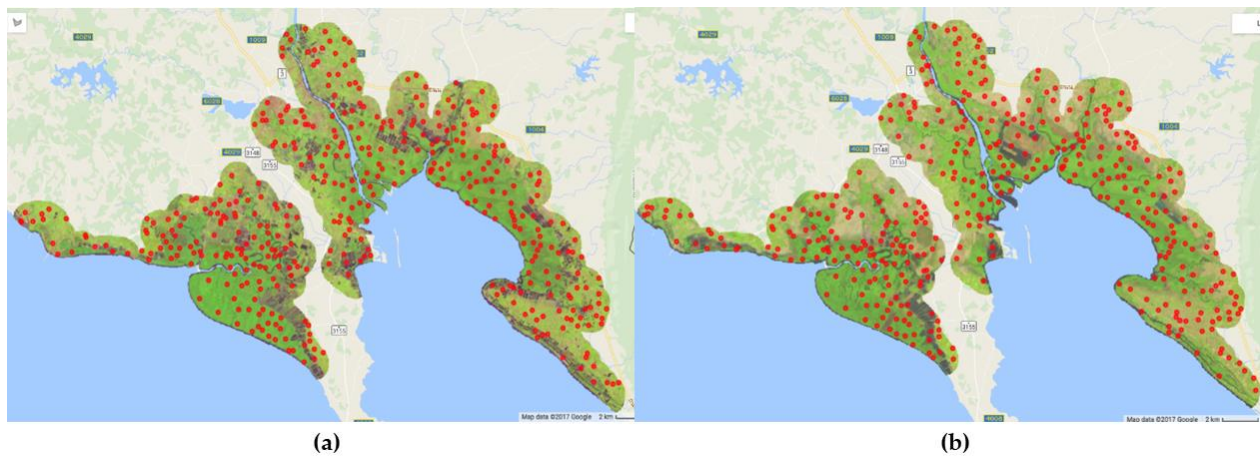


Figure 2.2. Locations of training and testing samples in the study area. (a) training and testing samples for the year 1987; (b) training and testing samples for the year 2017. A total 414 points were created using the stratified approach, of which 109 were used as testing points. The figure contains background of Google earth engine map background.

2.4 Pixel based random forest classifier

We performed a supervised pixel-based classification using a Random Forest (RF), a tree based classifier that includes K-decision trees (Goldblatt et al., 2016; Shelestov et al., 2017). RF overcome the problem of overfitting by constructing an ensemble of decision trees (Shelestov et al., 2017). Pelletier et al. (2016) reported that there are accurate and higher performance RF classifiers in land cover classification studies. The RF classifier was used to classify the extent of mangrove vegetation and other LULC in a study area, as shown in Figure 2.1. We trained the RF classifier (20 trees) in the GEE environment with 305

training samples to then classify the annual composite Landsat images into four LULCs: active agriculture (orchid plants, coconut grows, oil palm and rubber plantation), bare land/urban area/non-active agriculture plots, primary mangrove forest, and water bodies (fish and shrimp farms, and other water resources including water canals within mangrove forest). The categories were based on a detailed analysis of the study area and reviewing previous studies and field surveys conducted for training and testing data. The RF classifier was performed on red, green, blue, NIR, SWIR-1, and SWIR-2 spectral bands of each annual composite.

2.5 Validation

During the classification process, composite from different years are trained and validated individually. About 70% of the sample points are used to train the classifier, while the remaining 30% of samples were used to test the accuracy and validate the RF classifier (Figure 2.2). The RF classifier accuracy and Kappa statistics is assessed by an error matrix. The final maps were compared with high resolution aerial imagery available in Google Earth for visual refinement.

2.6 Post classification change detection

Several methods such as an image overlay, change vector analysis, image rationing, and principal component analysis have been used in LULC mapping studies (Pelletier et al., 2016). In this study, the “From-to” change detection algorithm (Post-classification comparison), has been used to provide detailed information about the type of LULC change (Foody, 2002; Forkuo and Frimpong, 2012; Singh, 1989). The main advantage of post classification change detection is indicating the nature and magnitude of the LULC changes that had taken place over a time.

2.7 Results

2.7.1 Cloud free annual composite of Landsat imagery

Clouds and shadows represent one of the main sources of issue while working with optical remote sensed imagery such as Landsat, particularly when working in tropical regions. Figure 2.3(a) illustrates the influence of clouds, haze and missing pixels on Landsat series imagery, which could be the main limiting factor on the spatial and temporal consistency of long-term mangrove ecosystem changes mapping and monitoring. The cloud cover, shadows, availability of haze and missing data, influence

many data analysis processes including inaccurate atmospheric correction, biased vegetation indexes, mistakes in land cover classification and false detection of land use and land cover change (Zhu and Woodcock, 2012). The cloud free seamless mosaic of Landsat series imagery was created with a predefined knowledge-based rules built upon the spectral signature (Simonetti et al., 2015). Annual composites were created by taking median reflectance values of the collection. Seamless and cloud free image mosaics can be important when mapping mangrove forests, because the cloud and seams can affect the visual interpretation of training sample collection, or leading to erroneous classifications (Zhu and Woodcock, 2012). Cloud free and seamless mosaic images would likely improve the results of the forest normalization method described in section 2.2.2.

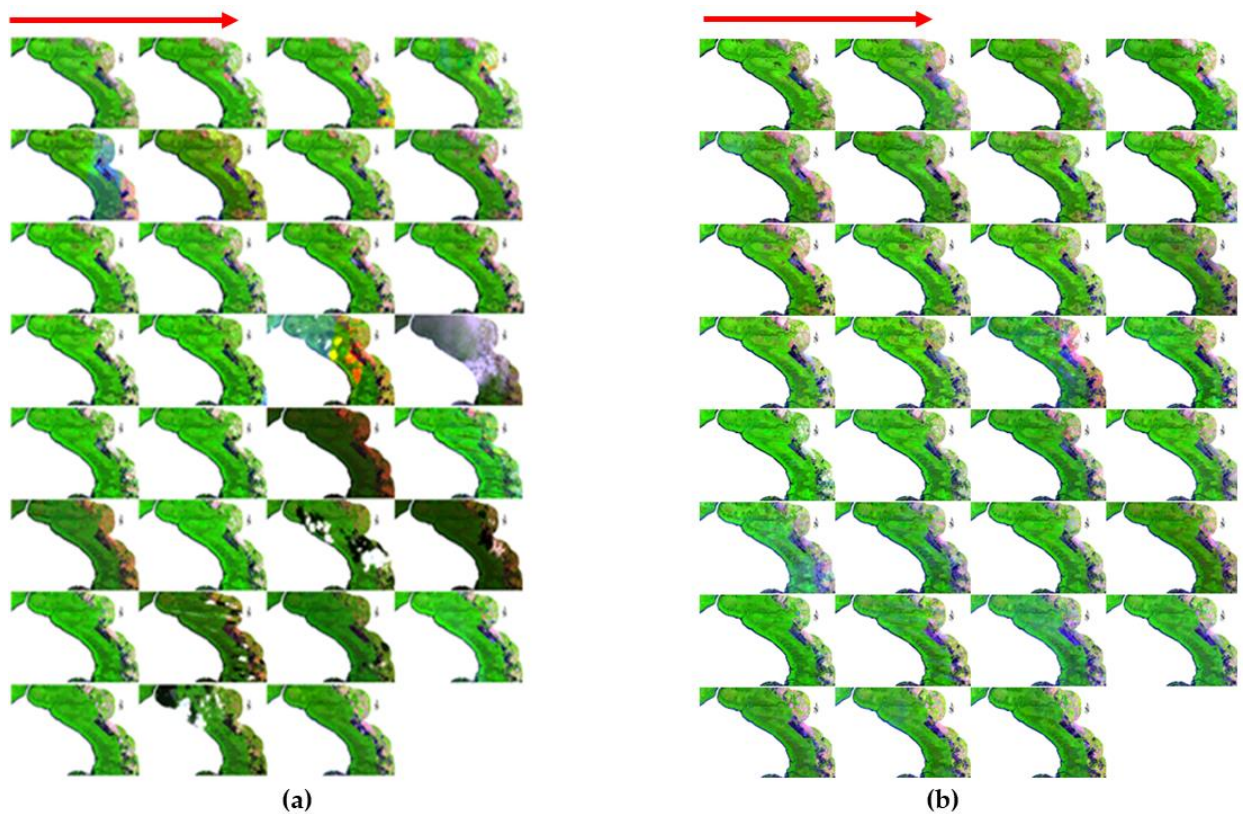


Figure 2.3 Landsat best single date and error free annual composites. (a) Best single date image in each year; (b) Annual cloud free composites. Pseudo color (SWIR1, NIR, Red) Landsat imagery from 1987 (upper left) to 2017 (bottom right). The red line shows the direction in which yearly images are presented.

The comparable visual results presented in Figure 2.3 (a) and (b), were acquired by Landsat TM-5, ETM+ 7, and OLI-8. Their corresponding pseudo color composite (SWIR1, NIR, Red) before and after pre-processing for Landsat TM-5, ETM+ 7 OLI-8 are shown in

Figure 2.3 (a) and (b). Several images in Figure 2.3 (a) contains cloud, shadows, haze and missing data. The automatic rule-based algorithm was used to remove contamination in individual Landsat imagery. Figure 2.3 (b) illustrates the cloud, haze and missing data free annual composite for the period of 1987 – 2017. In addition, the obtained composite revealed more vivid tone when compared with the original imagery. The selected contaminated pixels were tested using NDVI and NDII to mask the composite from residual clouds or no data. Only a selected annual composite image was classified, and stratified random samples generated.

2.7.2 Magnitude of mangrove forest and its surrounding change

In order to test the performance of consistent long-term imagery from different Landsat sensors for mangrove forests and their surroundings, Landsat imagery was used representing two time periods (1987 and 2017). The stratified buffer was generated around the mangrove forest. An 850-meter buffer was generated to delineate the potential loss or gain of mangrove forest (Figure 2.1) within the surrounding landscape. The buffer was designed and based on the change in mangrove pixels within the study area using Normalized Differential Vegetation Index (NDVI), Normalized Difference Infrared Index (NDII), Digital Elevation Model (DEM), and Automatic Classification (Alsaaidh et al., 2013; Green et al., 1998; Higginbottom and Symeonakis, 2014; Jia et al., 2014; Simonetti et al., 2015; Yilmaz et al., 2008) A visual refinement has been carried out for year 1987 and 2017 (Landsat TM-5, ETM+ 7, and OLI-8 imagery respectively), to ensure the high quality of the mask over the time interval.

Independent training and validation data was used for the years 1987 and 2017. The LULC maps for the years 1987 and 2017 were based on Landsat TM-5 and OLI-8 satellite imagery that were prepared with four LULC types: class 1, active agriculture, class 2, bare land and urban area (some agricultural land without vegetation was included here), class 3, mangrove forest and class 4, shrimp and fish farms. Figure 4 shows the final classification of the RF classifier, which consists of classified maps of the study area, for the year 1987 and 2017.

Table 2.1 shows the results obtained from the classified map of 1987 and 2017. An overall accuracy of 0.87 and 0.96, followed by a Kappa coefficient 0.80 and 0.94, were obtained. As a result, the performance of the RF classifier for the year 2017 produced a higher accuracy classification map with an overall accuracy of 0.96. On the other hand, the

classification performance in 1987 was less than that when compared with the year 2017. However, the classification confused agriculture (class 1), and bare land (class2), for the year 1987, due to the similar spectral response and scarcity of ground truth data. Jia et al.(2014), also reported the high performance of Landsat OLI-8 when compared with that of Landsat TM-5 and ETM+ 7.

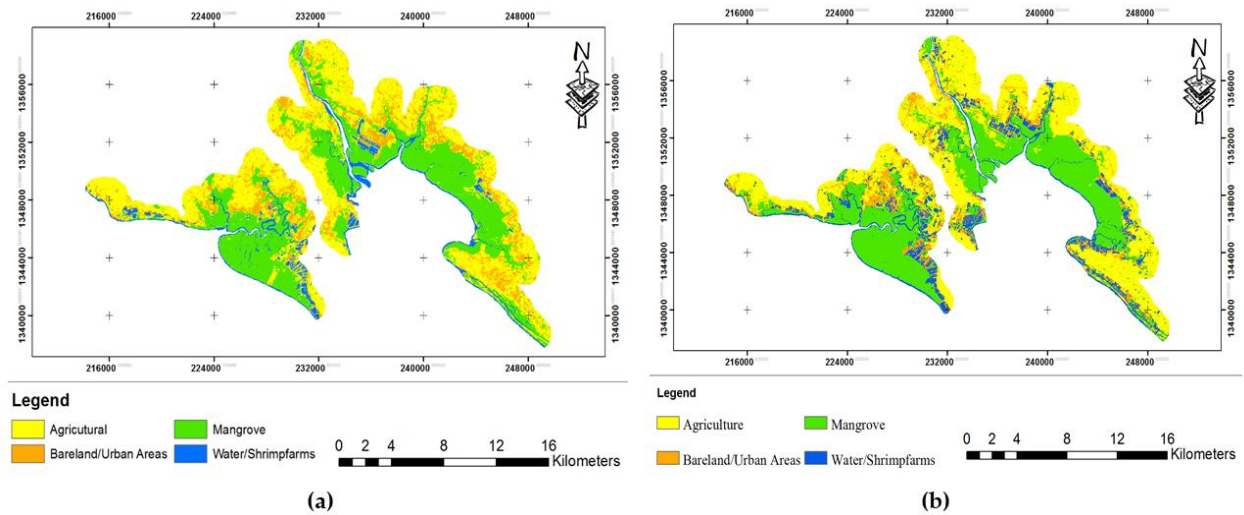


Figure 2. 4 Land use and land cover change from 1987 – 2017. (a) Year 1987; (b) Year 2017

Table 2. 1. Error matrix and accuracy statistics for classification for the years 1987 and 2017

LULU in 1987	Class 1	Class 2	Class 3	Class 4
Class 1	28	5	1	0
Class 2	4	3	2	0
Class 3	2	0	50	0
Class 4	0	0	0	14
Overall accuracy =0.87; Kappa statistics= 0.80				
LULU in 2017				
Class 1	40	0	2	0
Class 2	2	17	0	0
Class 3	1	0	58	0
Class 4	0	0	0	12
Overall accuracy =0.96; Kappa statistics= 0.94				

Note: Class 1, active agriculture; Class 2, bare land and urban area (some agricultural land without vegetation was included here); Class 3, mangrove forest; and Class 4, shrimp and fish farms; LULC: land use land cover

Table 2.2 summarizes the results of the LULC change in the study area of each LULC class. The agriculture and mangrove forest was the main LULC in 1987 with 49.18 % and

34.20%, followed by bare land/urban areas and water bodies/shrimp farms with 9.80 % and 6.82 % respectively. Agricultural area decreased from 49.18% (111.36 km²) in 1987 to 41.25 % (93.40 km²) in 2017, while, mangrove forest area increased from 34.20% (77.43 km²) in 1987 to 36.17 % (81.90 km²) in 2017. Additionally, some of the disturbed mangrove forest area has shown significant recovery (Figure 2.5 a, b, c and d). The bare land/urban areas increased from 9.80% (22.17 km²) in 1987 to 11.08 % (25.10 km²) in 2017. Shrimp/fish farms progressively increased from 6.82 % (15.16 km²) in 1987 to 11.49 % (26.02 km²). The decline in active agriculture was observed to be 7.93% between 1987 and 2017. Bare land/urban areas and shrimp/fish farms did experience an expansion during the period of 1987 to 2017. Another increased rate of change was observed in the mangrove forest.

Table 2. 2. Change in LULC in study area

LULC	1987		2017		Change (1987-2017)
	Km ²	%	Km ²	%	
Class 1	111.36	49.18	93.40	41.25	7.93
Class 2	22.17	9.80	25.10	11.08	-1.28
Class 3	77.43	34.20	81.90	36.17	-1.97
Class 4	15.46	6.82	26.02	11.49	-4.67
Total area	226.42	100	226.42	100	

Note: Class 1, active agriculture; Class 2, bare land and urban area (some agricultural land without vegetation was included here); Class 3, mangrove forest; and Class 4, shrimp and fish farms; LULC: land use land cover

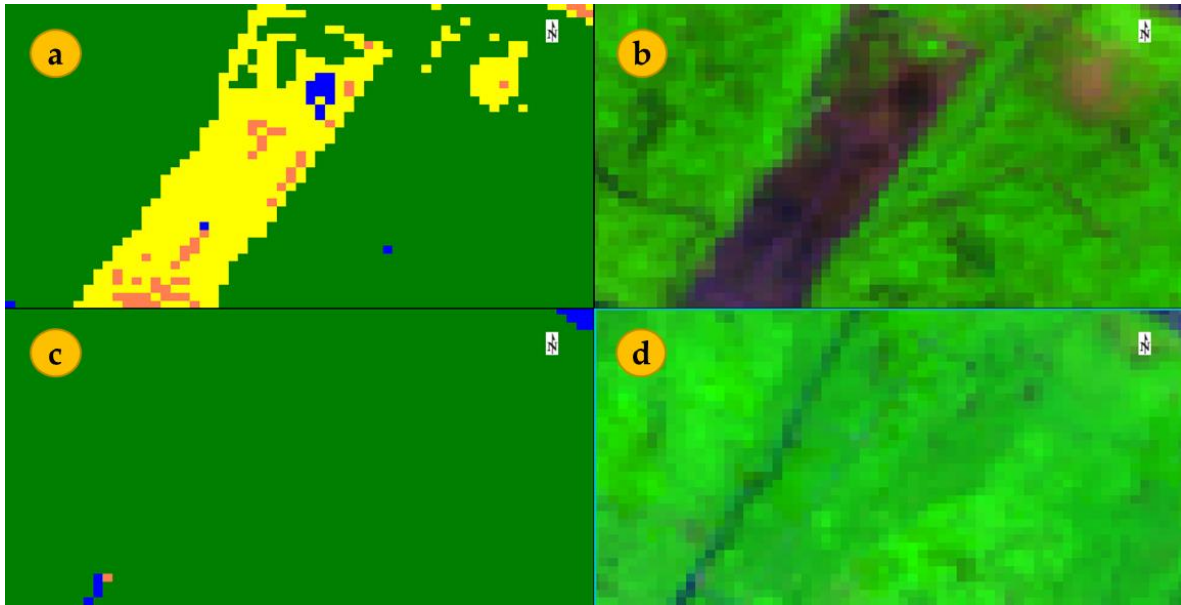


Figure 2. 5. Mangrove recovery over a historic agriculture area. (a) Pixels classified as agriculture in 1987; (b) Original Landsat TM-5 (1987) imagery with Pseudo color (SWIR1, NIR, Red) composites; (c) Pixels classified as mangrove in 2017 (recovery after rehabilitation); (d) Original Landsat OLI-8 (2017) imagery with Pseudo color (SWIR1, NIR, Red) composites

2.7.3 LULC transition from 1987 to 2017

The transition matrix was used to analyse the rates of LULC conversion from one LULC to another for the years 1987 and 2017. The corresponding probabilities of change are shown in Table 2.3. There was a major conversion of agriculture to bare land (15.15 km²) and from agriculture to mangrove forest (8.40 km²) during this period. At the same time, mangrove forest changed to shrimp/fish farm (4.72 km²), and bare land was converted to shrimp/fish farms.

Table 2. 3 Land use land cover change matrix between 1987 and 2017

LULC type	Class 1	Class 2	Class 2	Class 4	Total in 1987
Class 1	68.08	13.57	11.59	7.39	100.64
Class 2	15.15	6.94	3.32	3.45	25.88
Class 3	8.40	3.91	63.97	5.24	81.53
Class 4	0.61	1.59	4.72	8.53	15.46
Total in 2017	92.25	26.02	83.61	24.62	226.42

Note: Class 1, active agriculture; Class 2, bare land and urban area (some agricultural land without vegetation was included here); Class 3, mangrove forest; and Class 4, shrimp and fish farms; LULC: land

2.8 Discussion

2.8.1 Overcoming the limitation of Landsat imagery for monitoring mangrove

Landsat series imagery are very helpful for detecting long term changes in mangrove ecosystems. Wijedasa et al. (2012) have highlighted several limitations of existing Landsat satellites, challenging the wall-to-wall mapping of wetland ecosystems, such as Landsat-5, which no longer has global coverage; and a mechanical fault in the Scan-Line Corrector (SLC-Off) on the Landsat-7 satellite, with a 22–25% data loss with each image. Other limitations also factor into the mix, including the presence of atmospheric contamination such as cloud, haze and missing data in Landsat imagery, which are major limitations in long term mapping and monitoring of coastal ecosystems (Cihlar, 2000; Mwita et al., 2012).

In this study, knowledge-based predefined rules were used to remove the contaminated pixels from all the available imagery and used the annual median reflectance value of the collection for a consistent annual composite. Consistent imagery over a long time series will likely support detection of other spectrally non-stubble changes such as forest clearing, regrowth and undisturbed ecosystems (Helmer and Ruefenacht, 2005). Consistent error free and seamless composite images make it possible to achieve fast and accurate classification, making it easier to detect LULC change (e.g In this study, the machine learning Random Forest classifier was tested).

The annual composites from 1987–2017 are virtually seamless regardless of the presence of atmospheric contamination and sensor artifacts such as the SLC-Off (Landsat-7) and missing pixel data. Benefits introduced by implementing this methodological framework in GEE are threefold: (a) easy and user friendly programming environment; (b) virtually unlimited processing power with high computational efficiency; (c) raw satellite data are already available on GEE servers hence no need to retrieve and download huge amount of data (less local resources). The annual composites from 1987-2017 are not used in this chapter. These composite imagery were used in Chapter-4.

2.8.2 Change in land use and land cover

The results show that a significant change occurred in land cover, particularly in mangrove forests, in the surrounding areas of Trat, between 1987 and 2017. It appears

that agriculture, bare land and shrimp farms had undergone major changes. However, there is very little research has been conducted study of these changes. The mangrove forests made a significant recovery over time. This trend is indicative of the local community's awareness for mangrove forest conservation and in the detrimental effect that shrimp farming can have on mangrove forest conservation. Szuster (2006) reported on the expansion of shrimp farming (1972 -1995), and low-salinity shrimp farming (1996-2002). He also reported that recently (2003-2004), the Thai government's policies restricted the expansion of low-salinity shrimp farming within the freshwater regions of the country. The result of this study suggesting that the rapid change in agriculture, bare land, and shrimp farms, and their interconversion, are a major driver of the change.

2.8 Conclusion

This paper presents a new strategy in attempting to achieve error free 30 year annual composites of Landsat satellites imagery for mapping mangroves and their surrounding LULC changes on the GEE cloud computing platform. This strategy uses pre-defined knowledge-based rules to remove contaminated pixels from all available imagery and uses annual median reflectance values in the collection. A fast, accurate and stable detection of change in agriculture, bare lands, mangrove forests, and shrimp/fish farms generated from consistent seamless mosaic and the RF classifier, demonstrates these results. The study area experienced drastic interchange between agriculture, bare land and shrimp/ fish farms, while mangrove forests had made a recovery over a period of time.

The study contributes to the application of cloud computing GEE and its potential for costal ecosystem mapping and monitoring. The provided reliable and consistent long term satellite data and high-performance classification approach could be beneficial for finding changes in mangrove ecosystems and their surroundings to fill the gaps necessary for forest management, conservation, as well as in understanding their carbon sequestration potential.

CHAPTER 3

Systematic transect plot inventories for species and structural diversity



Transect line plots in mangrove forest of Trat province of Thailand

This chapter has been published as: Pimple, U. (2020) Dataset on plot inventories of species diversity and structural parameters of natural and rehabilitated mangrove forest in the Trat Province of Thailand, *Data in Brief*, Vol.30. <https://doi.org/10.1016/j.dib.2020.105500>

Abstract:

This chapter describes how the rehabilitated mangroves evolved over 28 years and whether the ecological parameters of rehabilitated forest resembled those of the adjacent natural mangroves. This chapter presents the data collection inventories for species and structural composition of rehabilitated and adjacent natural mangrove forests in the Trat Province of eastern Thailand. The species type, their girth at 1.3 m breast height, tree height, and the number of seedlings for each of the thirteen species, (*Avicennia alba*, *Bruguiera cylindrica*, *Bruguiera gymnorrhiza*, *Bruguiera sexangula*, *Ceriops tagal*, *Excoecaria agallocha*, *Intsia bijuga*, *Lumnitzera littorea*, *Lumnitzera racemosa*, *Rhizophora apiculata*, *Rhizophora mucronata*, *Xylocarpus granatum*, and *Xylocarpus moluccensis*), of the mangrove forests were collected. The data were collected in 10 X 10 m size plots from the seaward to landward end along with the stand age of the rehabilitated mangroves. The data was analysed using the Importance Value, Complexity Index, Simpson's Dominance Index of diversity and Simpson's Reciprocal, and Shannon-Weaver Index to distinguish various diversity and structural parameters.

3.1 Mangrove inventories data specification

The Table 3.1 presents the mangrove field inventory data specification.

Table 3. 1 Mangrove field inventory data specification

Subject	Biological sciences
Specific subject area	<i>Forestry, Forest ecology and management, Restoration</i>
Type of data	Excel file
How data were acquired	Species diversity and structural parameters were obtained using the systematic sampling design (fixed-area sampling), across the mangrove forest landscape. Procedure of data sampling described in Sampling design, paragraph 2.2 in Data and methods of Pimple et al.[1].
Data format	Raw, analysed
Parameters for data collection	Mangrove species richness and structural characteristic variables were aggregated at the plot level. The following dendrometric parameters were measured from each tree species of each plot: forest type, tree diameter at breast height, tree height, crown cover, and the number of seedlings
Description of data collection	The systematic sampling design (fixed-area sampling) across the mangrove forest landscape. A transect line was systematically established perpendicular to the coastline (i.e. With seaward and landward limits), recording the species distributions along the intertidal zones
Data source location	The transect line (from 239249 m E, 1350069 m N to 240518m E ,1352337 m N (UTM Zone 48 datum)) was 2.67 km in length, from the shoreline (seaward end) to the end of the forest (landward end).
Data accessibility	URL: http://dx.doi.org/10.17632/tdbm9dgw9r.1
Related research article	Pimple, U., Simonetti, D., Hinks, I., Oszwald, J., Berger, U., Pungkul, S., Leadprathom, K., Pravinvongvuthi, T., Maprasoap, P., Gond, V. (2020). A history of the rehabilitation of mangroves and an assessment of their diversity and structure using Landsat annual composites (1987–2019) and transect plot inventories. <i>Forest Ecology and Management</i> , 462, 118007. https://doi.org/10.1016/j.foreco.2020.118007

3.2 Value of the data

- 1) The species richness, structural parameters, number of seedlings per plot and stand age, between rehabilitated and adjacent natural mangrove stand is very important to assess the degree of success or failure of rehabilitation management practices in the region.
- 2) The data presented here is crucial for understanding the evolution, and potential changes in future ecological variables of rehabilitated mangrove ecosystem.
- 3) The data can be used to compare the structure and species communities in other mangrove forests.
- 4) The data can be used to fit site and species specific above ground biomass models and conversion factors which are very important to estimate the carbon sequestration potential of rehabilitated mangroves compared with adjacent natural stands.
- 5) The data can be used to validate the satellite based species and height predictions across the intertidal zone.

3.3 Data description

The data presented here is the original data that relates to the research article “A history of the rehabilitation of mangroves and an assessment of their diversity and structure using Landsat annual composites (1987-2019) and transect plot inventories” (Pimple et al., 2020). The data is presented as a single .xlsx file, with the title “DataTrat2019”. The data sheet contains parameters of indigenous and rehabilitated mangrove forest that includes plot number, province (location), forest type, species, number of trees in each plot, abbreviations (as used in article (Pimple et al., 2020) for the name of the species), branches, mean girth at breast height, mean height per species, number of seedlings per plot, and age (only applicable for rehabilitated mangroves).

3.4 Experimental design, materials, and methods

A transect line was systematically established perpendicular to the coastline (i.e. with seaward and landward limits), covering the species distributions along the intertidal zones. In total, 24 plots (10 m × 10 m), were established with 100 m apart. Each plot was used to determine the stand composition and diversity, and distributions among the intertidal zones. Field inventories were performed in December 2019. The data were analysed and interpreted. Plots 1 to 15 were in the adjacent natural zone, while plots 16 to 24 were in the rehabilitated mangrove zone. The number of seedlings per plot were counted manually. The plantation dates of the rehabilitated mangroves were obtained

from the Trat provincial office of Department of Marine and Coastal Resources, Thailand. The species in each plot were compared to determine the species diversity and structural variations between the rehabilitated and adjacent natural mangroves. The data was interpreted using diversity and structural indices (Importance value, Complexity index, Simpson's dominance index of diversity and Simpson's reciprocal, and Shannon-Weaver index) to derive species diversity, dominance and structural variability (described in Araujo and Shideler (2019) and Oksanen et al. (2020)).

CHAPTER 4

Assessing degree of success of rehabilitation interventions



Rehabilitated mangrove forest in Trat province of Thailand

This chapter has been published as: Pimple, U., Simonetti, D., Hinks, I., Oszwald, J., Berger, U., Pungkul, S., Leadprathom, K., Pravinvongvuthi, T., Maprasoap, P., Gond, V. (2020) A history of the rehabilitation of mangroves and an assessment of their diversity and structure using Landsat annual composites (1987–2019) and transect plot inventories, *Forest Ecology and Management*, Vol. 462. <https://doi.org/10.1016/j.foreco.2020.118007>

Abstract:

Recently, there has been renewed interest in the ecosystem services of mangroves such as carbon sequestration or coastal protection, and consequently, the development of tools providing an effective and automatic monitoring of the dynamics of mangrove land coverage including rehabilitated or naturally regenerated forest stand is increasingly demanded. Satellite-based time series analysis in coastal areas can be limited by atmospheric contaminations, such as haze, and clouds and their shadows. Here, we present an “automatic regrowth monitoring algorithm” (ARMA) using the Google Earth Engine (GEE), based on Landsat inter-annual median composites from 1987 to 2019 with 30 m spatial resolution. The species and structural diversity were assessed using transect plot inventories. The Landsat-based normalized difference infrared index (NDII) and information obtained from plot inventories were used to assess the characteristics of the natural and rehabilitated mangrove forests. The ARMA identified the starting year of the rehabilitation project using the satellite data, the required stability period after the rehabilitation, and the stand age in the year 2019. The information obtained from the field survey data were linked to the results obtained using the ARMA. After 28 years, the rehabilitated mangroves at the study site consist of monocultures of Rhizophoraceae, while the undisturbed and naturally regenerated mangroves had greater species diversity. Nevertheless, the rehabilitated mangroves were found to reach the height of the adjacent natural mangroves. The period required to reach a stable NDII value (similar to natural stands) after rehabilitation ranged from 7 to 13 years. The careful assessment of the NDII upward trend was crucial for the performance of the ARMA. The application presented here shows, however, that the system can be used to evaluate both small- and large-scale rehabilitation projects. The results of this study provide valuable baseline information for the site assessed and for its comparison with other rehabilitated mangroves in Thailand. Due to the technical potential, we are convinced that the ARMA system is suited to investigate changes in mangrove coverage dynamics, in general, including gain (as presented here), but also mangrove losses, due to disturbances such as degradation or forest diebacks.

4. 1 Introduction

Mangroves are highly productive forest ecosystems, that are found in tropical and subtropical coastal regions around the world (Duke, 2017; Tomlinson, 2016). The trees in mangrove forest provide various services for fauna such as food, breeding grounds, and spawning areas, as well as for people such as fish, medicine or wood for fuel, timber poles, and boats (Asaeda et al., 2016; Bosire et al., 2003; Dahdouh-Guebas and Koedam, 2008). Mangrove forests are also carbon-rich, creating significant carbon sinks that play an important role to mitigate climate change (Donato et al., 2011) (Li et al., 2019). Nevertheless, mangrove ecosystems are currently under high pressure due to both natural and anthropogenic stressors (Li et al., 2019). They are impacted by climatic changes, such as sea-level rise, shifts in temperature patterns, and changes in the atmospheric gas composition and moisture levels, over long temporal scales (Victor H. Rivera-Monroy et al., 2017). Additionally, anthropogenic impacts from land use, rapid urbanization, shrimp farming, overexploitation of wood, and coastal construction significantly affect the spatial distribution and performance of mangroves over time (Barnuevo et al., 2017; Victor H. Rivera-Monroy et al., 2017).

Recent recognition of the importance of mangrove forests has stimulated interest in restoring and rehabilitating deforested mangroves in several areas of the world, including Thailand (Andradi-Brown et al., 2013; Macintosh et al., 2002; Otero et al., 2019). In this context, the term *mangrove restoration* refers often to actively supported measures in order to return a formally degraded ecosystem back, as effectively as possible, to its “original” condition, in terms of its species diversity and hydrological regime (Andradi-Brown et al., 2013; Dale et al., 2014; Macintosh et al., 2002). However, the term *mangrove rehabilitation* refers to the simple plantation of mangrove seedlings over degraded mangrove land, without adequate site assessment or subsequent evaluation of the achieved ecosystem functioning at the ecosystem level (Field, 1999; Macintosh et al., 2002). Moreover, the majority of rehabilitation projects in southeast Asia tend to implement monoculture plantations (usually *Rhizophora apiculata*) (Ellison, 2000), often without an adequate site assessment or consideration of ecological principles. For this, rehabilitation projects are generally not able to sustainably restore ecosystems, but they can provide forest cover and initiate successional sequences. While monoculture or single-species plantations could be the first step towards rehabilitating mangroves (Ellison, 2000), a continuous monitoring and detailed assessments of forest structure and related features (e.g., natural regeneration or succession stages) are required to

understand the recovery processes of the particular rehabilitated ecosystem (Ren et al., 2008).

Several rehabilitation projects throughout the world have previously been reported, including those in Thailand, Pakistan, Australia, Bangladesh, Sri Lanka, Vietnam, and Kenya (Bosire et al., 2003). However, there is limited knowledge regarding the effectiveness of the natural development, survival, and growth characteristics of stands being rehabilitated through these projects, compared to the stands of native (indigenous) forests, over time. For example, Lewis et al. (2019) identified unverified claims of allegedly successful large-scale mangrove rehabilitation projects in Senegal. There had been no previous detailed reports on the monitoring of mangrove rehabilitation projects, and satellite-based analyses failed to identify any success. Alexandris et al. (2013) conducted temporal analyses of 10 projects (24 sites in six countries: United Arab Emirates, Madagascar, Kenya, Senegal, Solomon Islands, and Indonesia), to assess the extent of the recovery of the mangroves after the implementation of the rehabilitation projects. The authors detected no change or only slight changes at these sites. However, the proposed monitoring methods were hindered by persistent cloud coverage and atmospheric contamination, as well as limited field survey data. Nehru and Balasubramanian (2018) summarized the recovery of mangrove ecosystems following a tsunami in the Nicobar Islands. The authors noted that the previously used remote sensing-based approaches in this area lacked integration with the well-documented field surveys. In comparison, Piou et al. (2006) conducted a study to quantify the recovery of the mangroves after hurricane Hattie in Calabash Cay, Belize. They used indirect measurements to estimate mangrove destruction due to a lack of directly available data. Such studies could benefit from using satellite-based time series to track the recovery of mangroves after damage or rehabilitation. The minimum amount of data required to assess the species and structural diversity of the mangrove forests using remote sensing includes a complete list of species in the forest, measurements of the edaphic parameters and elevation, as well as the measurements obtained in contiguous quadrants along the intertidal zone transects (Castaneda-Moya et al., 2006).

Structural heterogeneity is an important attribute of mangrove ecosystems (Luo et al., 2010). Many physical and biological factors influence the population dynamics, community structure, canopy dominance, and succession of rehabilitated mangroves (Proffitt and Devlin, 2005). The spatial patterns of natural mangroves depends on their soil properties, disturbance history, and the displacement of propagules under varying tidal influences (Luo et al., 2010; Proffitt and Devlin, 2005). Hydrological factors, such as salinity and soil inundation, could affect the initial functional outcomes of rehabilitated

mangroves (McKee and Faulkner, 2000). Several studies have reported large contrasts between native and rehabilitated mangroves, in terms of their forest structures, species diversity, and tree density (Asaeda et al., 2016; Barnuevo et al., 2017; Ren et al., 2008; Walter, 2004). The degree of success for rehabilitation projects varies by site. For example, Asaeda et al. (2016) and Barnuevo et al. (2017), among others, reported the failure of rehabilitated mangroves to mimic natural forests over a 60 year period in the Banacon and Olango Islands of the Philippines. Ren et al. (2008) reported the dominance of a single species (or monoculture) in rehabilitated mangroves over a 10-year period in Leizhou Bay, South China. In contrast, Luo et al. (2010) found that, after 50 years of rehabilitation, the mangroves in Shenzhen Bay, South China, had a similar stand structure, spatial arrangement of selected stand characteristics, and species associations, as those of natural mangrove forests. Globally, there is mixed evidence for the effectiveness of rehabilitation projects, due to the limited supporting scientific evidence, the lack of standardized ecological restoration practices, and appropriate socio-political reasoning at local scales. Understanding the structural features and spatial patterns of rehabilitated mangroves is key to assessing the successes and failures of rehabilitation projects. This also leads to an understanding of the processes that underlie mangrove dynamics, including intra- and inter-specific interactions, as well as the effects of various environmental heterogeneities (Luo et al., 2010).

Abundance, as well as relative and absolute density, frequency, and basal area, are commonly used to assess mangrove forest structural parameters. The fundamental Shannon-Weaver diversity, Simpson's diversity, and Simpson's dominance (reciprocal index of Simpson) indices, as well as the importance value and complexity index, are widely used independently and in tandem with other indices, to assess mangrove forest diversity and structure (Blanco et al., 2001; Cintrón and Schaeffer Novelli, 1984; Hill, 1973; Holdridge, 1967; Morris et al., 2014; Shannon and Weaver, 1963; Simpson, 1949). Blanco et al. (2001) confirmed that the maximal tree height is a strong estimator for the development of mangrove forests that are uniformly developed, have closed canopies, or are monospecific (such as rehabilitated mangroves). This is because trees that reach the top of the canopy receive the most sunlight, which prevents shadowed individuals from receiving enough sunlight to compete. Due to the difficulty of estimating tree height within most mangrove forests, the average height of the three tallest trees at a particular site has been found to act as a more reliable estimate of the height of the mangrove canopy (Araujo and Shideler, 2019).

Remote sensing methods have been applied to monitor tree plantations, such as those of rubber, eucalyptus, and pine (McMahon and Jackson, 2019; Ye et al., 2018; Zhu et al.,

2018). Recent developments in cloud computing platforms, advanced cloud and shadow detection algorithms, and time series analyses provide a valuable set of tools with the potential to provide information about the way in which mangroves have developed over time (Chen et al., 2017; Otero et al., 2019; Pimple et al., 2018; Rogers et al., 2017). Time series data from over three decades of freely available satellite-based imagery from sources, such as Landsat, have previously been used to monitor changes in mangrove forests and their associated phenology (Otero et al., 2019; Pimple et al., 2018; Rogers et al., 2017). Satellite-based time series analyses could help assess and quantify the extent of the evolution of mangrove forests, as well as their increasing or decreasing trends over time. This information could be used as an indicator of the changes to the structural features of the forests (Banskota et al., 2014). Understanding the satellite-based spatio-temporal success and failure dynamics of rehabilitation projects or naturally disturbed forests and their recovery, combined with well-documented field surveys, are key in determining the long-term stability and sustainability of forests. Moreover, earth-observation data in combination with field data, can help fill the information gaps that arise from using field data alone (Boisvenue et al., 2016).

In the past, mangroves in Thailand were damaged as they were often converted to agricultural land, bare land, or used for shrimp and fish farming (Pimple et al., 2018). Many of these mangrove forests have made significant recoveries over time. This trend reflects the increased awareness and recognition of the importance of mangroves, the hard work of local communities to rehabilitate mangrove forests, and the Thai government policies that restrict the expansion of low salinity shrimp farming (Szuster, 2006). In this study site, to the best of our knowledge, no prior study has assessed the effectiveness of rehabilitation in this forest type in terms of identifying and reporting the correct starting year of rehabilitation projects; assessing the time required to stabilize the forest; or the structural development, species diversity, and tree density in adjacent natural and rehabilitated mangroves.

This study assessed the viability of a prototype algorithm to identify the starting year of a rehabilitation project, the number of years required to reach stability, and the stand age, structural development, and species complexity, compared to the adjacent natural mangrove stands. We focused on the Trat Province of Thailand and assessed whether the rehabilitated mangroves at this site were able to mimic the diverse structural complexity of the natural mangroves after 28 years. To evaluate the importance of the temporal dynamics using data from the latest biodiversity inventory, we evaluated: (1) how the rehabilitated mangroves evolved over the last 28 years; and (2) whether the ecological parameters of the rehabilitated forests resembled those of the adjacent natural stands.

4. 2 Data and Methods

4.2.1 Study site description

The study area for this investigation was the Trat Province, located along the eastern coast of the Gulf of Thailand and bordering Cambodia (Figure 4.1). The mangrove forest covers approximately 106 km², is located at longitude 102.61° and latitude 12.21°, and has a tropical climate, with seasonal monsoons. The rainy period is from June to November, with an average annual rainfall and mean temperature of 4500 mm and 26.5 – 29.8 °C, respectively (Chalermchatwilai et al., 2011). The study site was selected based on two conditions: (1) the availability of all common natural species (Chalermchatwilai et al., 2011) and (2) the presence of a large rehabilitation area adjacent to the natural mangrove. Preliminary field surveys were conducted during March 2015, October 2016, and December 2017 to determine the availability of the species, the location and extent of the rehabilitated areas, and the structural patterns of the mangroves in a landward direction. In this study site, the mangroves were rehabilitated without adequate site assessment or subsequent evaluation at the ecosystem level; and there was no supporting scientific evidence for the current success or failure of these rehabilitated mangroves.

4.2.2 Sampling design

The systematic sampling design (fixed-area sampling) across the mangrove forest landscape was crucial for the identification of the major mangrove species and the changes in the mangrove structural features. A transect line was systematically established perpendicular to the coastline (i.e., with seaward and landward limits), covering the species distributions along the intertidal zones (Figure 4.1). The transect line (from 239249 m E, 1350069 m N to 240518m E ,1352337 m N (UTM Zone 48 datum)) was 2.67 km in length, from the shoreline (seaward end) to the end of the forest (landward end).

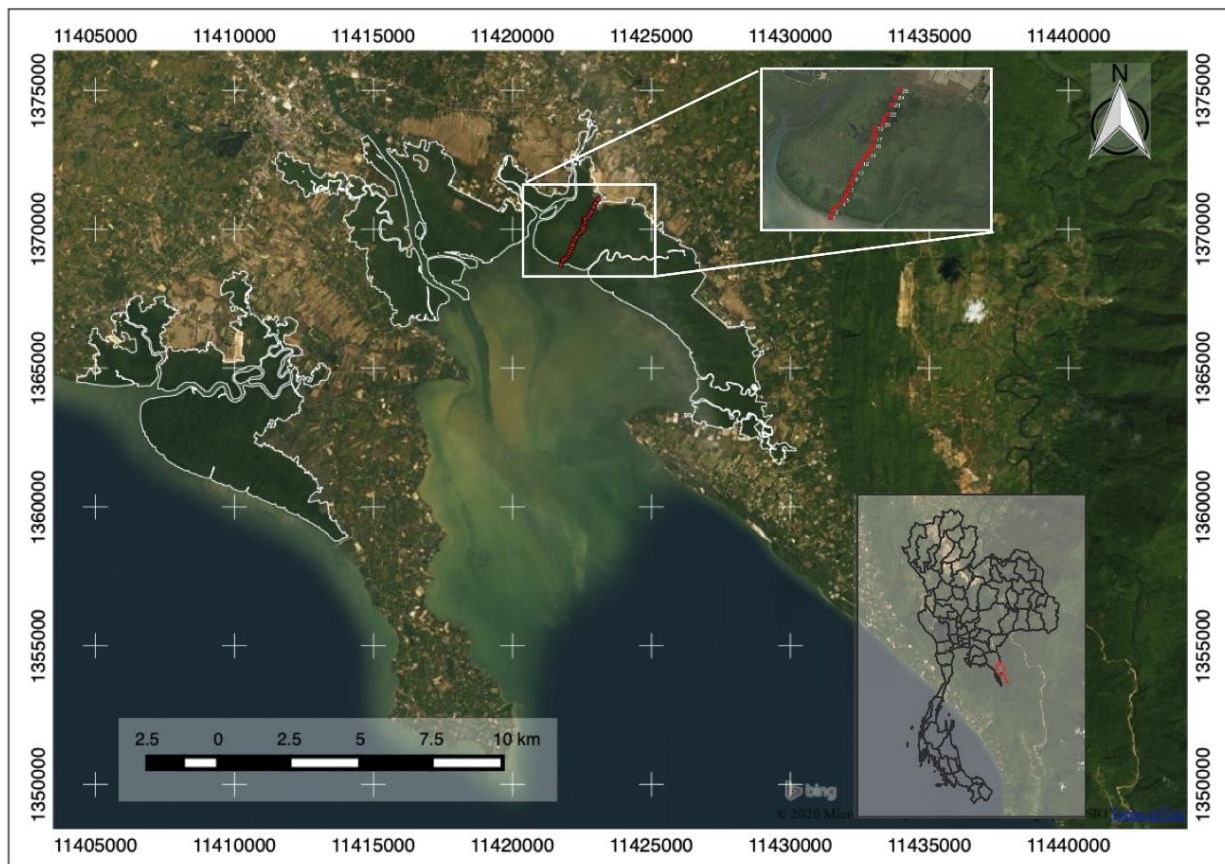


Figure 4. 1. Location of study site in the Trat province of eastern Thailand. The figure presents the spatial distribution of the transect line plots used in the analysis. The red square indicates the locations of the 10 x 10 m transect plots along the transect line.

In total, 25 plots (10 × 10 m), were established with 100 m distances between them, to determine the species composition and diversity of the stands, as well as the distributions among the intertidal zones. The 10 × 10 m plot sizes were chosen because they were manageable to survey, considering the larger spatial scale and sample sizes. This plot size ensured that no species or structural parameters overlapped when comparing the rehabilitated mangroves with the natural stands. The pure spectral values could be achieved if the plot sizes were less than or equal to the spatial resolution of the satellite imagery. Additionally, this plot size fits with the 10 m spatial resolution of the European Space Agency (ESA) Sentinel MSI-2 satellite, launched in 2015, that currently provides free imagery with a spatial temporal resolution of 5 days. Furthermore, several previous studies that have focused on natural and rehabilitated mangroves, have used similar plot sizes to estimate their diversity and structural parameters (Araujo and Shideler, 2019; Asaeda et al., 2016; Barnuevo et al., 2017; Macintosh et al., 2002; Ren et al., 2008). Of these plots, plots 1 to 15 were in the adjacent natural zone and plots 16 to 24 were in the rehabilitated mangrove zone. In each plot, species names, diameters at breast height

(DBH), and tree heights were measured. In addition, the crown **covers** and number of seedlings in the stands was recorded. DBH and tree height were measured with a tape measure and clinometer, respectively. The field inventories data were collected in December 2018. Dead trees were excluded from the height measurements, and in each of these cases, the next living tree was measured instead.

4.3 General description of the methodology

We first evaluated the historical changes along with the transect line plots in the study area by collecting the available satellite data and identifying the spatial extents of the anthropogenic events, both along and adjacent to the transect lines. Second, we conducted a simplified transect line survey. This transect line provided the data with which we benchmarked mangrove development, as precise locations, types, and variations in the structures were identified along the transect line. Third, a detailed analysis of the annual changes over the last 32 years was conducted using a time series of the Landsat imagery. The study placed a strong focus on the long-term fate of the rehabilitated mangroves and the extent to which their structures and diversity resembled the adjacent natural stands. Moreover, we analyzed the possible changes in the transect inventory observations and related these to the degree of success or historical development of the rehabilitation projects. A flow chart of the integrated approach used in this study is presented in Figure 4.2.

4.4 Species diversity and structural indicators

The compiled lists of the species in each plot were compared to determine the species diversity and structural variations between the rehabilitated and adjacent natural mangroves. Forest structural parameters, including abundance and relative and absolute density, frequency, and basal area, were calculated using the data obtained from the plots. The importance value (IV) of each species per plot was calculated using the transect data. The IV was the sum of the relative density, relative dominance, and relative frequency (Cintrón and Schaeffer Novelli, 1984), calculated using equation 4.1:

$$IV_i = \frac{Dens_i}{\sum_{j=1}^s Dens_j} * 100 + \frac{BA_i}{\sum_{j=1}^s BA_j} * 100 + \frac{Fre_i}{\sum_{j=1}^s Fre_j} * 100 \quad 4.1$$

where, IV_i , $Dens_i$, BA_i , and Fre_i are the importance values, relative density, relative basal area, and relative frequency of the mangrove species i , respectively, and s is the number of species.

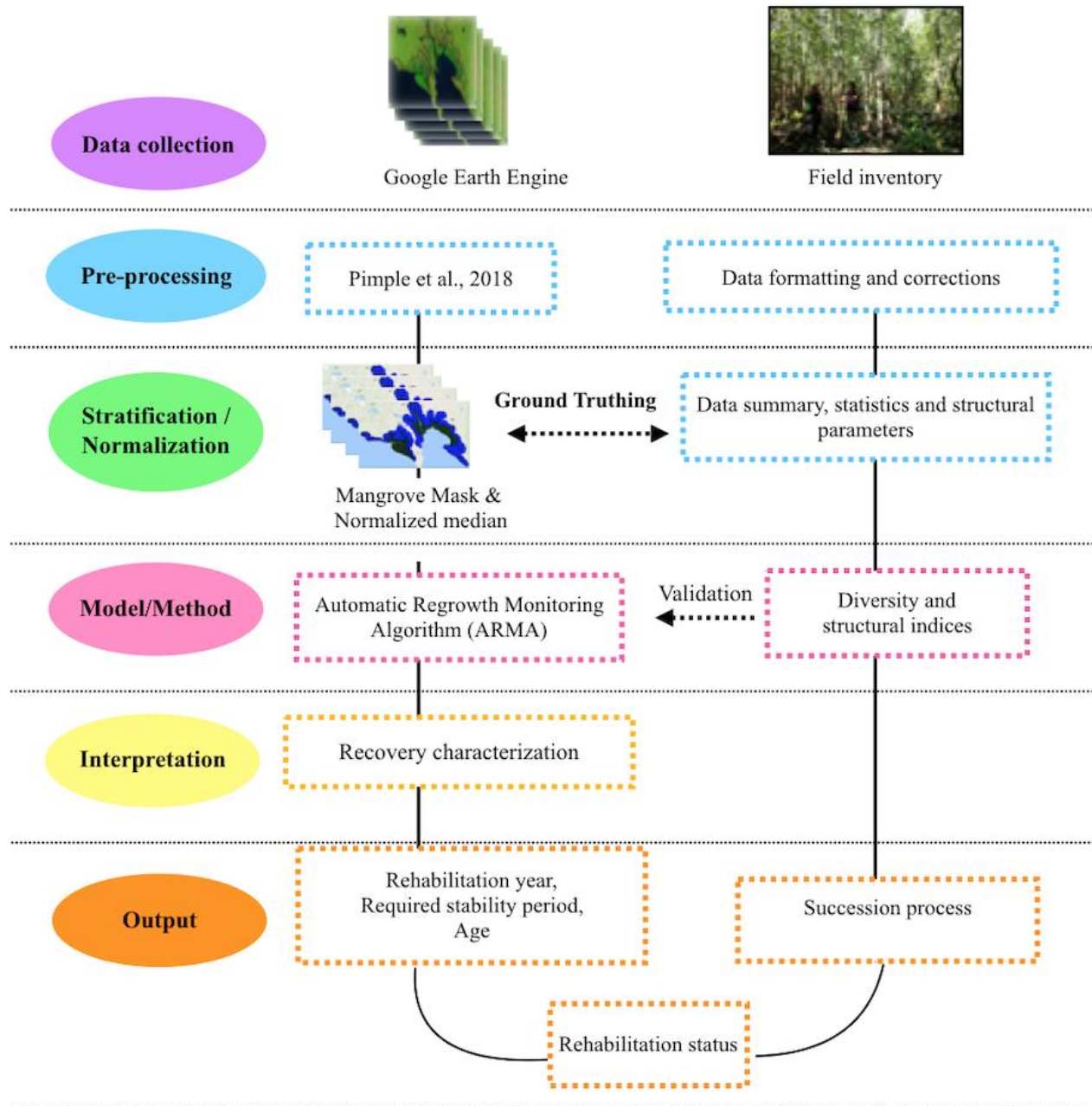


Figure 4. 2. Flow diagram showing the methodological framework. The figure presents the process for the Landsat annual composite preparations, analysis of forest stability parameters, analysis of field inventory data, and derivation of the biodiversity and structural indicators to determine the success of the rehabilitated mangroves.

The complexity index (CI) was developed by Holdridge (1967), and incorporates the number of species, stand density, basal area, and height of the individual trees in the plots of the tropical vegetation and mangrove ecosystems (Pool et al., 1977). The CI was used to estimate the structural development of the planted mangrove forest plots. The CI

uniquely incorporates the height of the individuals, as well as the other parameters of the mangrove trees, to measure the structural complexity of each transect plot (Araujo and Shideler, 2019; Dahdouh-Guebas and Koedam, 2008), and it was calculated using equation 4.2:

$$CI = \frac{(\text{No. species}) * (\text{No. trees}) * (\text{Basal area}) * (\text{Mean height})}{100} \quad 4.2$$

Diversity indices were used to define and enumerate the structure of the ecological communities (Ohlmann et al., 2019). Simpson's dominance index of diversity (1-D) and Simpson's reciprocal Index (1/D) were used to determine species dominance using the basal area at breast height (1.3 m) in each 10 × 10 m plot, occupied by each species. The Simpson's index (D) was calculated using equation 4.3:

$$D = \sum_{i=1}^s \frac{n_i (n_i - 1)}{N(N-1)} \quad 4.3$$

Where n_i is the number of trees of the i^{th} species, and N is the total number of individuals. The Simpson's dominance index of diversity (1-D) ranges from between 0 and 1, with 0 indicating no diversity and 1 indicating a high level of diversity. In comparison, for the Simpson's reciprocal index (1/D), values below 1 represent monoculture mono-specific forests, while values greater than 1 represent higher diversity.

The Shannon or Shannon-Weaver index is widely used to compare the diversity and variance of species distributions between habitats, including mangrove ecosystems (Abino et al., 2014), and is calculated using equation 4.4:

$$H' = - \sum_{i=1}^s p_i \ln p_i \quad 4.4$$

where H' is the diversity index, P_i is the proportion of the individuals of species i , in relation to the total number of individuals in the sample, and \ln is the natural logarithm. This index uses the number of individuals of each species in each 10 × 10 m plot to determine diversity. The higher the Shannon index values are, the higher the levels of richness and evenness in the community; values typically range from 1.5 to 3.5 and rarely reach 4.5 (Ifo et al., 2016).

4. 5 Landsat imagery

The study dataset included data from Landsat TM-5 (1987–2001 and 2003 –2011), ETM+7 (2002, 2013), and OLI-8 (2013 –2019) that was obtained from the Google Earth Engine (GEE) Tier 1 top-of-atmosphere (TOA) reflectance collection. The images were acquired between January 1, 1987 and July 1, 2019. The Tier 1 Landsat collection is considered suitable for the time series analysis, as it includes Level-1 Precision Terrain (L1TP)

processed data with inter-calibrations across the different Landsat sensors. Only red, green, blue, NIR, SWIR-1, and SWIR-2 bands were processed in the Universal Transverse Mercator (UTM) zone 48 N projection. The entire collection was cleaned of clouds, cloud shadows, and pixels with no-data, following the algorithm proposed by Simonetti et al. (2015), which was extended for mangrove forestry by Pimple et al. (2018). This algorithm is driven by predefined knowledge-based rules that have been built on spectral signatures collected at a global scale. It generates a thematic output, including cloud and cloud shadow casting and masking. To ensure that the reflectance values were pure and suitable for long-term analysis, contaminated pixels were aggressively removed from the individual images prior to the annual synthesis. Cases in which there were persistent contaminated pixels (cloud cover with shadows) or no images available, could potentially result in no data. To address this issue, a manual visual inspection of the output images was required to assess whether single- or multi-year composites could be achieved. An additional inward buffer of 450 m was applied to remove the jagged scene edge, ensuring uniform analysis across the different acquisitions and sensors (Pimple et al., 2018; Robinson et al., 2017). It is worth noting that in the cases with persistent contaminated pixels (due to cloud cover, shadows, or haze), the final annual composites might contain no-data values. This issue could be resolved by interpolating values from the previous and following years (Otero et al., 2019). For instance, in 2012, Landsat ETM+ 7 showed large quantities of no- data lines due to the Scan Line Corrector failure (Li et al., 2019). It is impossible to use Landsat ETM+ 7 images for this year, due to the heavy clouds causing missing satellite-imagery pixels in the coastal regions. However, the issue was addressed by visually inspecting the output, to assess whether single or multiple year composites could be achieved. The proposed method in this study was able to select stable annual composite pixels for Landsat ETM+ 7 imagery; thus, no interpolation was required.

4. 6 Mangrove forest normalization

Before calculating the TOA for the annual median composites, every Landsat image was normalized using a dark object subtraction (DOS) method (Bruce and Hilbert, 2004), as described in equation 4.5. This approach used the median values of the mangrove forest pixels to apply a linear correction to each spectral band (Bodart et al., 2011; Pimple et al., 2018), as follows:

$$\varphi_{\text{adjusted}}^{(\lambda)} = \varphi_{\text{original}}^{(\lambda)} - (\bar{X}_{\text{mangrove}}^{(\lambda)} + \bar{X}_{\text{ref}}^{(\lambda)}) \quad 4.5$$

where, $\varphi_{\text{adjusted}}^{(\lambda)}$ is the normalized median for band λ , $\bar{X}_{\text{mangrove}}^{(\lambda)}$ is the median value of the dense mangrove forestry of the sample site for band λ , and $\bar{X}_{\text{ref}}^{(\lambda)}$ is the reference dense mangrove forest value for band λ , as computed for the well-known and stable

locations identified using the Landsat OLI-8 images (2014–2018), and further validated at a 10 m resolution using the sentinel-2 MSI imagery (see section 2.6) across the study area. The per band extracted median reference values were 0.10238 (blue), 0.08208 (green), 0.05340 (red), 0.28267 (NIR), 0.06959 (SWIR-1), and 0.02379 (SWIR-2), respectively, in a TOA reflectance of 0–1, and six processed bands.

Even though the Landsat Tier-1 collection ensured a quality sensor calibration and stability over time, the TOA reflectance was often affected by atmospheric contamination, including haze and residuals of thin clouds (especially in coastal areas). Cloud-free annual composites were then created using the median reflectance values (per band) of the processed data (Pimple et al., 2018; Sagar et al., 2017).

4. 7 Sentinel-2 multi-spectral instrument (MSI) high-resolution mask

The Sentinel-2 MSI images contained 13 UNIT 16 spectral bands, representing the TOA reflectance, that were obtained from the GEE image collection. To ensure meaningful comparisons between the sensors, the red, green, blue, NIR, SWIR-1, and SWIR-2 bands of the Sentinel-2 were selected. Zhang et al. (2018) found that the Sentinel-2A MSI Level-1C cloud mask product was not reliable. The annual composites for 2019 were created using the median reflectance values of the collection, after being cleaned of clouds, cloud shadows, and pixels with no-data. Sentinel-2 SWIR-1 and SWIR-2 bands were acquired at 20 m spatial resolutions (Joint Research Center, 2019). To match the resolution of the red, green, blue, and NIR bands, the SWIR-1, and SWIR-2 bands were resampled at a 10 m resolution, using the nearest-neighbor interpolation methods. Sentinel-2 MSI was used to create a high-resolution mangrove forest mask for the year 2019, and subsequently, to improve the extraction of the reference median values of the mangroves from the Landsat imagery during the DOS normalization phase.

4. 8 Masking the mangrove forest area

As the proposed approach of the mangrove forest monitoring requires long-term earth-observation data to study the success and failure of the rehabilitation projects, it is highly recommended that its applications be limited to mangrove areas only. This is because the separation of the mangrove and non-mangrove areas reduces the computational time and avoids the contamination of other land use or land cover pixels. A “mangrove mask” limits the algorithm to the pixels that were confirmed to be forested at the beginning of the first monitoring period (DeVries et al., 2015), which can be confirmed using field data. The mask of the mangrove forest for the year 2017, as proposed by Pimple et al. (2018), has been improved using a second mask created with Sentinel-2 MSI for the year 2019. The Sentinel-2 MSI high-resolution mask ensures that the stubble and remaining land use

land cover pixels are separated. The Otsu threshold was used to quantify the distribution of the mangrove and non-mangrove areas (Otsu, 1979). Then, visual mangrove forest refinement was performed on Google Earth to produce a high-quality mangrove mask. Pimple et al. (2018) reported the significant recovery of mangroves in the study area. We used the optimal baseline map for the year 2019, where the natural and rehabilitated mangroves were stable. The quality of this map was confirmed using field survey data (conducted in December 2017).

4. 9 Normalized difference infrared index (NDII)

The normalized difference infrared index (NDWI) was introduced by Gao (1996) to obtain the vegetation liquid water status using satellite imagery. However, Ji et al. (2011) noted that in previous research, 13 normalized difference indices were used with the same equation and reported that these indices were designed by independent authors based on near infrared (NIR) and short-wave infrared (SWIR) bands obtained using various satellite sensors, including Landsat TM, Satellites Pour l'Observation de la Terre (SPOT)-VEGETATION, or Moderate Resolution Imaging Spectroradiometer (MODIS). Moreover, Ji et al. (2011) suggested the use of the term normalized difference infrared index (NDII) for the Landsat SWIR wavelength channel between 1.55 and 1.75 μm . In this study we used the NDII based on the Landsat and calculated it as follows:

$$\text{NDII} = \frac{(\text{NIR} - \text{SWIR})}{(\text{NIR} + \text{SWIR})} \quad 4.6$$

where, NIR is the reflectance in the near-infrared wavelength channel (0.70 – 0.90 μm), and SWIR is the reflectance in the shortwave-infrared wavelength channel (1.55 – 1.75 μm) (Alsaaidh et al., 2013; Ji et al., 2011; Yilmaz et al., 2008). Jackson et al. (2004) documented that NDII is sensitive to the mass or volume of water, rather than the fractional percentage of the water. NDII is sensitive to the vegetation moisture content and can be used as an indicator of the water content in the vegetation. It can also enhance the vegetation moisture content in the Landsat imagery. NDII values fluctuate with changes in the water content, ranging from -1 to 1. In this study, the NDII was computed using the annual median composites rather than single images, avoiding post-process filtering or interpolation. The NDII time series was used to analyze the status of the rehabilitated and adjacent natural mangroves over time.

4. 10 Time series of the natural, rehabilitated, and disturbed mangroves

The Landsat interannual time series can be used to characterize and analyze the annual changes in the rehabilitated and natural mangrove forests, including abrupt changes (such as logging, lightning, or a tsunami), disturbance-recovery trajectories, and gradual

changes (Pasquarella et al., 2016). Huang et al. (2010) defined stable forests, disturbances, and post-disturbance processes, as well as their relationships, using their spectral-temporal properties. In this study, we have derived a set of conditions to characterize the state of the forest over time, as described in the proceeding sections.

4.10.1 Stable mangroves

Undisturbed natural mangrove forests maintain relatively stable NDII signatures over many years. Their stable or unchanging state is defined as the median values of all points in the time series of the annual composite, minus one standard deviation. The one standard deviation is used to account for the annual variability in the NDII, as follows:

$$NDII_{stable} = NDII_{median} - NDII_{1SD} \quad 4.7$$

where $NDII_{stable}$ represents stability or no change to the mangrove stand over time, $NDII_{median}$ is the median of all annual median composites of the natural mangroves and rehabilitated mangroves after the year 2002, and $NDII_{1SD}$ is the standard deviation of all annual median composites of the natural mangroves. Additionally, we tested the independent median values of the plantation plots after the year 2002 and compared them with $NDII_{stable}$ to assure the quality of the applied threshold. The years 2002 – 2019 were chosen for this because all the mangrove stand types during this period showed stable NDII values. Visual time series refinement was performed on each plot pixel to ensure the high quality of the threshold.

4.10.2 Recovery: development of rehabilitated or naturally regenerated mangroves

Recovery is the period when the rehabilitated or regenerated mangrove forests reach the stable state of the adjacent natural mangrove forests. The values of the NDII are expected to return, or come close, to those of the adjacent natural mangroves ($NDII_{stable}$) or their state before the disturbance. The recovery time or required stability period is defined as the number of years that the mangrove forest takes to return to a stable state (i.e., $NDII_{stable}$). This is a good indicator of the success of mangrove rehabilitation efforts. To determine the rehabilitation year, we first defined the reference year of the empty land before rehabilitation, using the minimum value of the NDII (< 0.15) corresponding to low photosynthetic activity (i.e., soil or shallow water). Second, we confirmed tree growth using the upward trend of the NDII. Due to the spatial resolution of the Landsat imagery (30 m), the NDII values of the young mangrove stands might remain low (< 0.15) for several years, until the tree crowns and leaves are big enough to be detected. At these early stages of mangrove development, the minimum NDII threshold can be the result of the pixel background values for the soil and water. This limitation may lead to a

significant difference between the satellite derived (predicted) and actual rehabilitation dates. It is thus crucial to carefully assess this at the start of the year when there is a strong upward trend in the NDII values ($NDII_{\min}$ year (adjusted)) from the actual year of rehabilitation. During the first few years of the rehabilitation, young mangroves (lower NDII values) can cause different or multiple lower threshold values for each plot. This situation can lead to significant differences among the lower values or in the rehabilitation years detected in an NDII time series of each plot. Therefore, the lower NDII values may not be effective enough to describe the complicated and diversified regrowth periods of the rehabilitated or naturally regenerated mangroves.

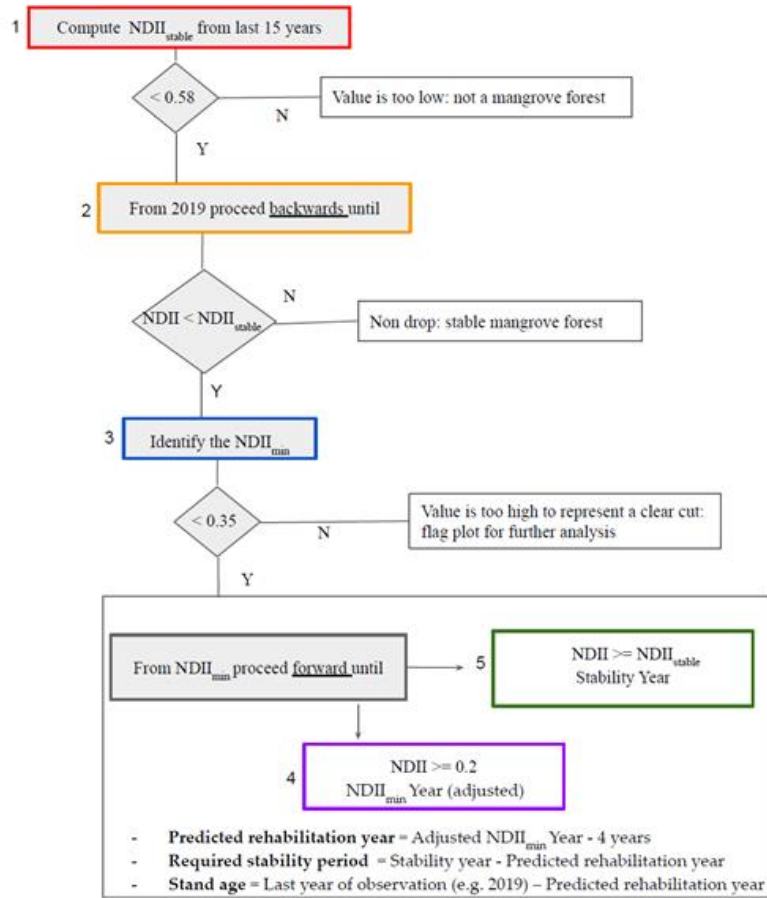
According to the Department of Marine and Coastal Resources, Thailand, in this study area, the rehabilitation projects were initiated in 1991 (DMCR 1991). The pixel-based analysis produced a strong upward trend only four years after the actual plantation year, i.e., an upward NDII trend started in 1994. In this study, we have assumed that four years of time is required to see a strong upward trend after the initial year when rehabilitation began.

4.10.3 Disturbance

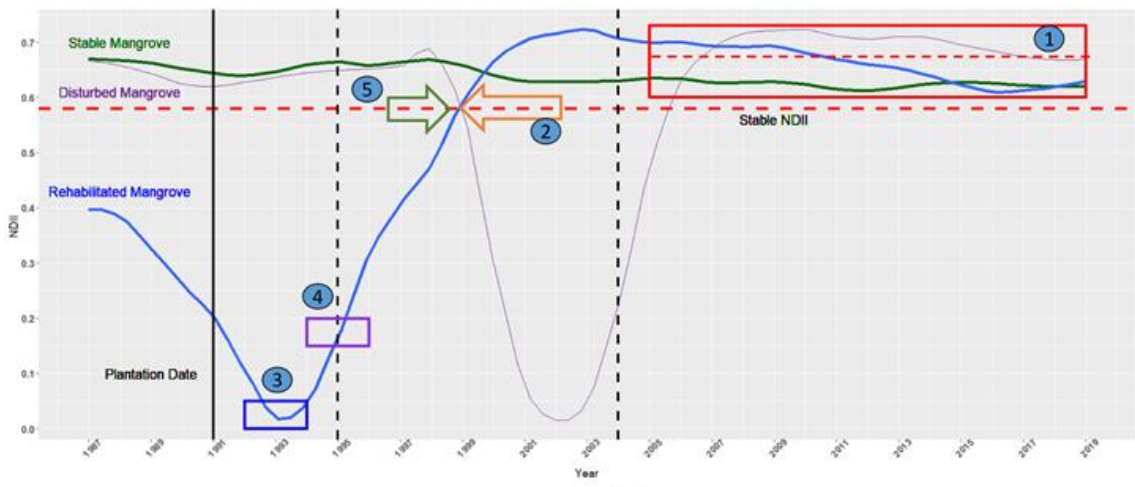
Sudden changes to the mangrove forest canopy (such as the disappearance of the canopy or woody biomass) often results in an abrupt or sudden decline of the NDII values. Forest disturbances were not observed during the study period or along the transect line plots; however, this state was defined, so it may be implemented in disturbance scenarios.

4. 11 Outline of automatic regrowth monitoring algorithm

Section 4.10.2 explains the theory behind the monitoring and recovery of the rehabilitated mangroves, while Figure 4.3 provides a graphical representation of how: 1) the starting year of the rehabilitation project; 2) the number of years required to reach stability; 3) the stability, wherein the NDII is greater than or equal to $NDII_{\text{stable}}$; and 4) the stand age of the rehabilitated mangroves, were automatically computed for every field survey plot using the ARMA. ARMA accounts for an average delay of 48 months (four years) between the Landsat computed and actual rehabilitation years. This approach allows it to overcome the biased estimated rehabilitation year, between the forest cut or rehabilitation and recovery, by analyzing the NDII trend in reverse. The following steps were performed for each plot separately:



(a)



(b)

Figure 4. 3. Illustration of automatic regrowth monitoring algorithm. (a) Flow diagram of the automatic regrowth monitoring algorithm (ARMA); (b) Example plot representation of the normalized difference infrared index (NDII) time series and ARMA-based change matrix.

4. 12 Results

4.12.1 Species diversity and composition

In total, 554 trees were recorded in the 24 plots along the transect line, representing a combined area of 2400 m². The tree counts ranged from 10 to 40 trees per plot (Table 4.1), and the following 14 species were recorded: *Avicennia alba*, *Bruguiera cylindrica*, *Bruguiera gymnorrhiza*, *Bruguiera sexangula*, *Ceriops tagal*, *Excoecaria agallocha*, *Heritiera littoralis*, *Intsia bijuga*, *Lumnitzera littorea*, *Lumnitzera racemosa*, *Rhizophora apiculata*, *Rhizophora mucronata*, *Xylocarpus granatum*, and *Xylocarpus moluccensis*.

The literature and field surveys showed that the dominant species were *Rhizophora apiculata*, *Ceriops tagal*, and *Xylocarpus granatum*. However, *Lumnitzera littorea*, *Excoecaria agallocha*, *Sonneratia caseolaris*, *Avicennia alba*, *Bruguiera gymnorrhiza*, and *Heritiera littoralis* had also previously been documented in the study area (Chalermchatwilai et al., 2011; Suchewaboripont, et al., 2011). The coastline was occupied by *Sonneratia caseolaris* and *Avicennia alba*. The next zone was dominated by *Rhizophora apiculata*, *Rhizophora mucronata*, and *Xylocarpus granatum* (Chalermchatwilai et al., 2011; Suchewaboripont et al., 2011). A third zone was dominated by a mixture of species, including *Bruguiera gymnorrhiza*, *Ceriops tagal*, *Lumnitzera littorea*, and *Excoecaria agallocha*. In the landward area, many of the forest zones were influenced by the mangrove rehabilitation, resulting in monocultures of *Rhizophora apiculata*. However, some of the naturally colonized species, such as *Bruguiera gymnorrhiza*, *Excoecaria agallocha*, and *Intsia bijuga*, were found at the edges of the rehabilitated mangroves.

Table 4. 1 Statistics for the structural parameter

Natural Mangroves											
Plot	No. of Trees	Species	DBH (cm)				Height (m)				Type
			Mean	Min.	Max.	SD	Mean	Min.	Max.	SD	
1	11	Aa, Bg, Rm, Xg, Xm	16.83	9.55**	58.25**	13.93**	11.91	9	18	3.02	ST
2	10	Bg, Ea, Xg	20.16	8.28	35.97	11.75	12.4	10	16	2.41	ST
3	30	Bg, Ea, Xg	10.9	4.77	19.42	3.41	13.1	8	15	1.94	ST

4	10	Bg, Ra, Rm, Xg	18.75	4.77	37.56	9.95	14.7	9	19	2.91	ST
5	13	Ra, Xg	18.82	4.93	34.06	6.83	15.69	7	25	6.32**	ST
6	21	Ea, Ra, Xg	15.64	5.09	25.46	6.62	13.33	5	18	4.2	ST
7	18	Ra, Xg, Xm	15.01	5.73	27.06	5.57	12.17	4	18	3.45	ST
8	13	Ea, Ra, Xg	23.21**	9.55	38.83	10.15	22.23**	12**	30**	4.62	ST
9	14	Ct, Ll, Ra	10.85	5.41	21.33	5.08	6.43	3	10	1.99	ST
10	15	Bg, Ct, Ll, Ra	7.45	2.55	17.19	3.48	5.47*	3*	8*	1.3*	ST
11	30	Bg, Ct, Ea	7.75	1.27*	12.1*	2.27	10.87	6	21	3.06	ST
12	32	Ct, Ea, Ll	8.81	4.77	28.97	5.35	11	7	18	2.63	ST
13	13	Bc, Ea	9.86	4.62	18.46	4.57	11.92	7	22	4.63	ST
14	16	Bc, Ea	13.79	6.05	25.15	5.04	13.75	8	19	3.24	ST
15	26	Ea, Ra	6.48*	4.46	12.73	1.82*	8.38	5	11	1.42	ST
Median	15		13.79	4.93	25.46	5.35	12.17	7	18	3.02	

Rehabilitated Mangroves

Plot	No. of Trees	Species	DBH (cm)				Height (m)				Type
			Mean	Min.	Max.	SD	Mean	Min.	Max.	SD	
16	40	Rm	6.46*	4.77	8.91*	1.23*	6.83*	6*	8*	0.78*	RH
17	33	Lr, Ra, Rm	6.57	4.46	10.19	1.76	9.94	7	13	1.84	RH
18	24	Ra, Rm	7.58	2.55*	11.78	2.48	9.46	6	12	1.64	RH
19	16	Ra, Rm	9.52**	5.41**	12.73	1.98	12.31	10**	14	1.74	RH
20	27	Ra	8	3.18	12.41	2.26	12.04	8	16**	2.38	RH
21	18	Ra	7.36	2.86	13.69**	3.1**	13**	8	15	2.79**	RH
22	33	Ra	7.22	4.14	11.78	1.86	11.67	6	15	2.59	RH
23	32	Ra	7.02	4.14	10.5	1.59	11.88	6	15	2.37	RH
Median	30		7.29	4.14	11.78	1.92	11.78	6.5	14.5	2.11	

Naturally Regenerated Mangroves

			DBH (cm)				Height (m)				Type
			Mean	Min.	Max.	SD	Mean	Min.	Max.	SD	

Plot	No. of Trees	Species	Mean	Min.	Max.	SD	Mean	Min.	Max.	SD	
24	29	Bc, Bg, Bs, Ea, Ib	9.14	4.77	15.6	3.1	9.97	6	12	1.3	RG
Median	29		9.14	4.77	15.6	3.1	9.97	6	12	1.3	

Note: Aa: *Avicennia alba*; Bc: *Bruguiera cylindrica*; Bg: *Bruguiera gymnorrhiza*; Bs: *Bruguiera sexangula*; Ct: *Ceriops tagal*; Ea: *Excoecaria agallocha*; Ib: *Intsia bijuga*; Ll: *Lumnitzera littorea*; Lr: *Lumnitzera racemosa*; Ra: *Rhizophora apiculata*; Rm: *Rhizophora mucronata*; Xg: *Xylocarpus granatum*; Xm: *Xylocarpus moluccensis*. ST: Stable natural stands (1-15); RH: Rehabilitated stands(16-23); RG: Regenerated stands(24). Single asterisk(*): minimum value; Double asterisk (**): maximum value (minimum and maximum values with asterisks are provided for each mangrove stand type).

Of the 524 trees identified at the study site, 293 (56 %) were *Rhizophoraceae* (*Rhizophora apiculata* and *Rhizophora mucronata*), making it the dominant family. *Rhizophora apiculata* was the most frequent species; as it accounted for 209 trees, representing 40 % of the trees in the study area. This species was dominant in both the natural and rehabilitated stands, in terms of basal area and tree density, which were 0.66 m² per 0.1 ha and 87 stems per 0.1 ha, respectively. As a result, *Rhizophora apiculata* had the highest IV (92.90) among all of the observed species, followed by *Xylocarpus granatum* (43.50), *Excoecaria agallocha* (43.40), *Rhizophora mucronata* (33.50), *Bruguiera gymnorrhiza* (28.10), and *Ceriops tagal* (18.40) (Table 4.2).

Table 4. 2 Species composition of the mangrove community along the transect line

Rank	Species	Density (stems per 0.1 ha)	Dominance (m ² per 0.1 ha)	Frequency (%)	Relative Density (%)	Relative Dominance (%)	Relative Frequency (%)	Importance Value (%)
1	Ra	87.00	0.66	62.50	39.70	29.00	24.20	92.90
2	Xg	18.00	0.51	33.33	8.20	22.40	12.90	43.50
3	Ea	23.00	0.38	41.67	10.50	16.80	16.10	43.40
4	Rm	35.00	0.18	25.00	16.00	7.80	9.70	33.50
5	Bg	18.00	0.20	29.17	8.20	8.60	11.30	28.10
6	Ct	17.00	0.09	16.67	7.80	4.10	6.50	18.40
7	Bc	8.00	0.11	12.50	3.70	4.70	4.80	13.20
8	Ll	7.00	0.08	12.50	3.20	3.60	4.80	11.60
9	Xm	1.00	0.03	8.33	0.50	1.20	3.20	4.90
10	Bs	3.00	0.03	4.17	1.40	1.10	1.60	4.10
11	Ib	2.00	0.02	4.17	0.90	0.70	1.60	3.20

12	Aa	0.00	0.00	4.17	0.00	0.00	1.60	1.60
13	Lr	0.00	0.00	4.17	0.00	0.00	1.60	1.60

Note: Aa: *Avicennia alba*; Bc: *Bruguiera cylindrica*; Bg: *Bruguiera gymnorrhiza*; Bs: *Bruguiera sexangula*; Ct: *Ceriops tagal*; Ea: *Excoecaria agallocha*; Ib: *Intsia bijuga*; Ll: *Lumnitzera littorea*; Lr: *Lumnitzera racemosa*; Ra: *Rhizophora apiculata*; Rm: *Rhizophora mucronata*; Xg: *Xylocarpus granatum*; Xm: *Xylocarpus moluccensis*

The biodiversity varied noticeably between the different stands (Table 4.3). Comparisons of the diversity between the different zones with the Simpson's and Shannon's diversity indices, showed that the diversity index was higher in adjacent natural stands (plots 1-15), which had D, 1/D, and H' values of 0.14 – 0.71, 1.17 -3.46, and 0.27 -1.39, respectively. The rehabilitated stands in plots 16 -23 had very low biodiversity indices, as the D, 1/D, and H' values ranged from 0 - 0.30, 1 – 1.44, and 0 – 0.48, respectively. Species diversity is directly related to the number of species present in a given plot, and as such, the D, 1/D, and H' values of 0, 1, and 0, indicate monocultures. In comparison, the naturally regenerated mangrove (plot 24) was more diverse, as D, 1/D, and H' were 0.73, 3.70, and 1.42, respectively. The ecotone between the rehabilitated mangroves and their adjacent natural stands shows low biodiversity indices as D, 1/D, and H' were 0.14, 1.17, and 0.27, respectively.

Table 4. 3 Forest structure indices of mangroves assessed in Trat, Thailand

Plot No	Basal Area (m ² per 0.1 ha)	Simpson's Index		Shannon Index	Complexity Index	Mean Stand Diameter
		1-D	1/D	H'	CI	MSD
Natural Mangroves						
1	3.97	0.71	3.46	1.39	34.91	21.43
2	4.17	0.54	2.17	0.90	19.17	23.03
3	3.06	0.49	1.97	0.84	41.3	11.4
4	3.46	0.66	2.94	1.22	24.89	20.98
5	4.06	0.47	1.90	0.67	24.58	19.92
6	4.72	0.53	2.11	0.88	52.50	16.91
7	3.60	0.54	2.16	0.85	32.38	15.95
8	6.47	0.60	2.52	1.01	70.63	25.17
9	1.56	0.56	2.28	0.90	6.10	11.89
10	0.79	0.62	2.65	1.14	3.46	8.17
11	1.53	0.66	2.92	1.09	23.40	8.06
12	2.65	0.42	1.72	0.69	41.51	10.26
13	1.19	0.26	1.35	0.43	5.76	10.78
14	2.69	0.49	1.97	0.69	15.75	14.62
15	0.92	0.14	1.17	0.27	5.12	6.72
Rehabilitated Mangroves						

16	1.36	0.00	1.00	0.00	4.34	6.57
17	1.20	0.17	1.20	0.36	15.38	6.79
18	1.19	0.08	1.09	0.17	6.87	7.95
19	1.18	0.30	1.44	0.48	5.30	9.71
20	1.46	0.00	1.00	0.00	6.18	8.30
21	0.89	0.00	1.00	0.00	2.41	7.95
22	1.44	0.00	1.00	0.00	7.10	7.44
23	1.30	0.00	1.00	0.00	6.23	7.19
Naturally Regenerated Mangroves						
24	2.11	0.73	3.70	1.42	34.69	9.63

4.12.2 Structural compositions of the species

The species and structural compositions of the transect line plots are presented in Tables 1 and 2. The total tree density and basal area in the transect were 219 stems per 0.1 ha and 2.28 m² per 0.1 ha, respectively. Mangrove forest structures are an important indicator of the degree of success of rehabilitation efforts. Table 1 presents a summary of the natural (1 - 15), rehabilitated (16 - 23), and naturally regenerated (24) mangrove plots. Different compositions of the mangrove species resulted in notably different basal areas. For instance, natural *Rhizophora apiculata*, *Xylocarpus granatum*, and *Excoecaria agallocha* had the greatest basal areas compared with *Ceriops tagal*, *Bruguiera gymnorhiza* and rehabilitated *Rhizophora apiculata* (Table 4.2 and 4.3 and Figure 4.4). Across the transect line, there was a noticeable difference in the species in terms of DBH, basal area, and density values, based on the type of the forest found in each plot.

The results obtained using the Shapiro-Wilk normality test suggested that the values of the DBH and basal areas were significantly smaller for the rehabilitated mangroves (25–28 years) than for the natural stands (Mann–Whitney U test: $W = 126$, and 119 ; p -value = 0.002, and 0.006, respectively). The DBH values of the adjacent natural and rehabilitated mangrove forests were 1.27 - 58.25 and 2.55 -13.69 cm, respectively (Table 1), and their basal areas ranged from 0.79 – 6.47 and 0.89 – 1.46 m² per 0.1 ha. The observed tree densities ranged from 10 – 32 and 16 – 40 per plot. The number of trees per plot tended to be lower in the natural stands, with 10-13 trees per plot, compared to the rehabilitated stands, with 16 - 40 trees per plot. The naturally regenerated plot (plot 24) had a DBH range of 4.47 - 15.60 cm, with a basal area of 2.11 m² per 0.1 ha, and a tree density of 29.

Over the 28 years, for which the rehabilitated mangroves were monitored, their heights did not change significantly compared with heights of the natural stands (Mann–Whitney U test: $W = 98$; $p\text{-value} = 0.1$). The mean heights of the natural and rehabilitated stands along the transect were 5.47 – 22.23 m and 6.83 – 12.31 m, respectively. In comparison, the naturally regenerated plot (plot 24) was found to have a mean height of 9.97 m. Therefore, the rehabilitated (after 28 years) and regenerated mangroves (> 30 years) were able to reach approximately the same heights as those of the natural stands.

The plots of the natural stands were structurally more complex than those of the rehabilitated mangroves (Table 4.3). The high CI values of the natural and regenerated stands could be attributed to their higher species diversities and compositions. The presence of *Rhizophora apiculata*, *Xylocarpus granatum*, and *Excoecaria agallocha*, which characteristically have larger DBH and mean stand diameters compared to those of other local species in the natural and regenerated stands, likely contributed to the high CI values in these plots. Comparatively, the low CI values in the rehabilitated plots could be traced back to the low species diversity in these areas, particularly, the presence of the monocultures of *Rhizophora apiculata*.

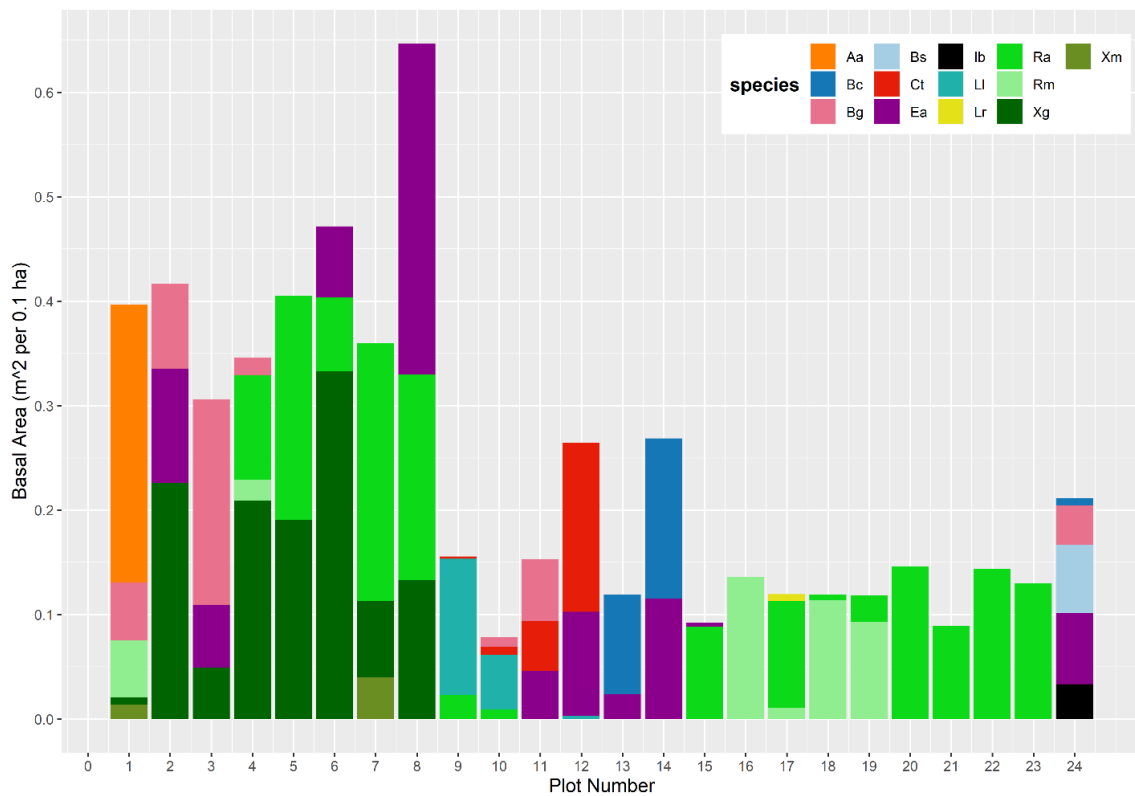


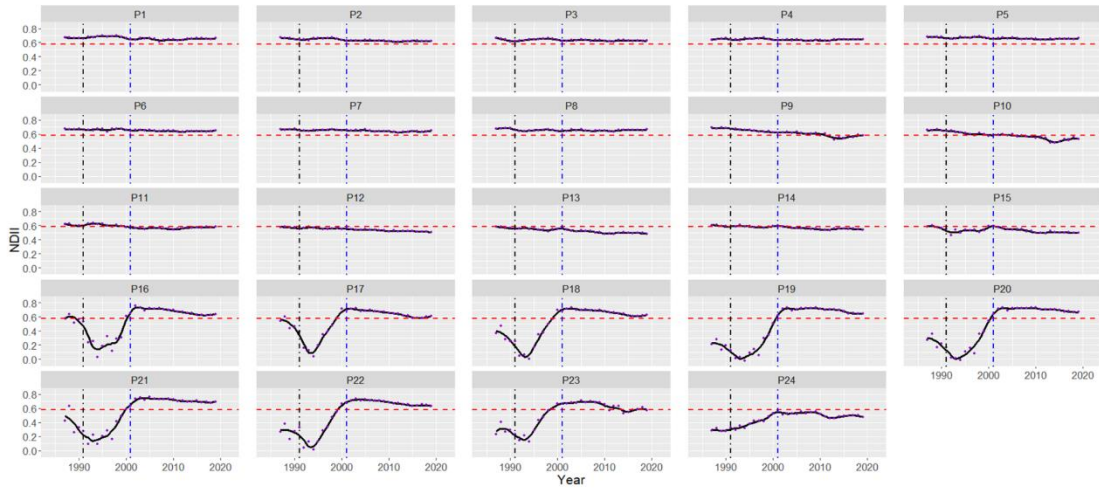
Figure 4. 4 Species composition and basal area per plot, along the transect line. Aa: *Avicennia alba*; Bc: *Bruguiera cylindrica*; Bg: *Bruguiera gymnorrhiza*; Bs: *Bruguiera sexangula*; Ct: *Ceriops tagal*; Ea: *Excoecaria*

agallocha; Ib: *Intsia bijuga*; Ll: *Lumnitzera littorea*; Lr: *Lumnitzera racemosa*; Ra: *Rhizophora apiculata*; Rm: *Rhizophora mucronata*; Xg: *Xylocarpus granatum*; Xm: *Xylocarpus moluccensis*.

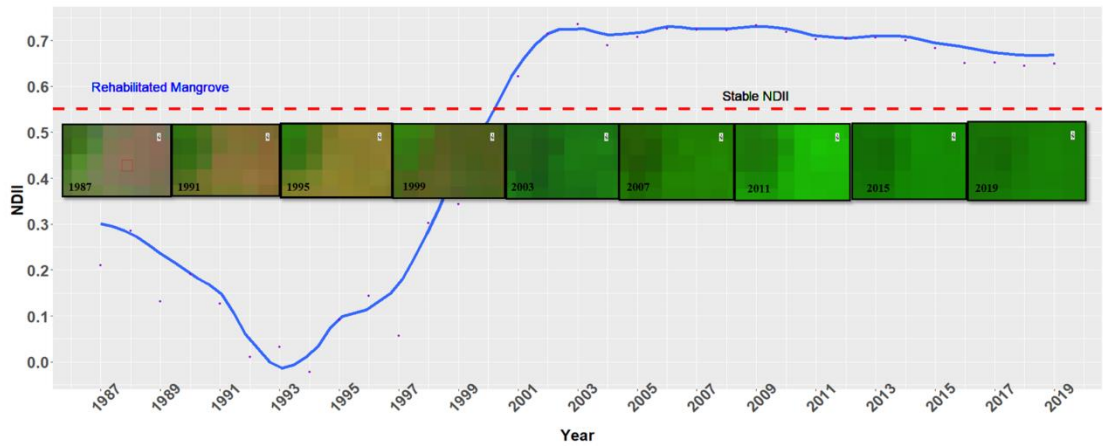
4.12.3 Landsat annual composite NDII time series assessment

Figure 4.5a presents the relative distribution of the changes in the NDII values in pixels within each plot (P1 - P24) along the transect from 1987 – 2019. The graphs were grouped into three scenarios (stable, rehabilitated, and naturally regenerated mangroves) to indicate the temporal dynamics of the NDII on the pixels in each plot. All the pixels within each representative plot were included in our analysis. The NDII annual median composites clearly showed disparities in the amounts of change among the rehabilitated and naturally regenerated stands. Figure 4.5b shows the false color composite image of the rehabilitated mangroves (example plot 19). The figure clearly shows that the rehabilitated pixels appeared brighter at the beginning and became greener over time.

The differences in the NDII values among the stable natural, rehabilitated, and naturally regenerated stands were apparent when the recovery metrics of the mangroves were compared (Figure 4.6). The transect plots of the stable natural mangroves (P1 - P15) showed relatively stable NDII values (≥ 0.58) throughout the monitoring period (Figure 4.5). The stable natural stands had similar NDII values of 0.58 - 0.64 throughout the observation period. The varying recovery tracks shown in the NDII time series indicated that the recovery process was different for the rehabilitated (P16-P23) and naturally regenerated mangroves (P24) (Figure 4.5). The NDII values show high variation during the recovery period, with ranges of 0.034 - 0.73 and 0.27 - 0.57, respectively. After reaching a stable state (i.e., $NDII \geq NDII_{stable}$), the NDII values of the rehabilitated mangroves closely mimicked those of the adjacent natural mangroves (P15-P23) (Figure 4.5). In the Figure 6, all stable forest pixel had high and stable NDII values (≥ 0.58), while the NDII values of the rehabilitated and regenerated forest pixels ranged from 0 - 0.73. This means that the NDII pixel trajectories showed clear distinctions between the stable and the other two types of mangrove investigated.



(a)



(b)

Figure 4. 5 NDII trajectories of all transect plots. Normalized Difference Infrared Index (NDII) trajectories of all the transect plots from 1987 – 2019. (a) time series of a pixel from each of the transect plots. The dotted black lines indicate the actual year of rehabilitation (1991). The dotted blue lines indicate the approximate year in which all the mangroves reached NDIIstable values. The red dotted lines represent the NDIIstable threshold. The dark violet points represent the original NDII values obtained from each annual composite, per year. P1-P24 are the labels that indicate transect line plots. (b) False color composite of the annual median composite showing the historical development of the rehabilitated mangroves (e.g., Plot 19).

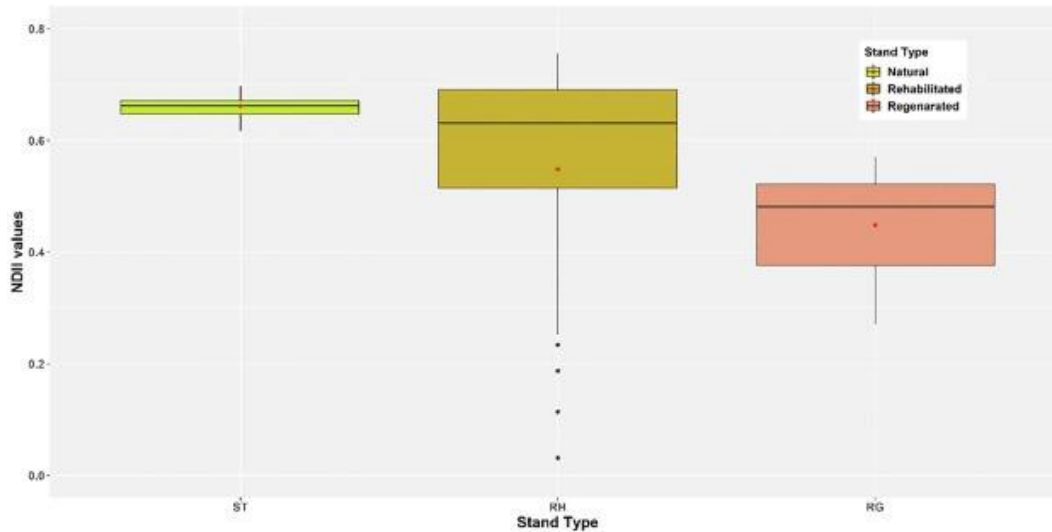


Figure 4. 6 NDII variation for the mangrove stand types. Boxplot of the Normalized Difference Infrared Index (NDII) trends for the mangrove stand types, the values for all pixels of the stable natural (P1-P15), rehabilitated (P16-P23), and regenerated (P24) stands are presented. Where ST means stable natural; RH means rehabilitated; and RG means regenerated stands.

Pixel-based NDII time series were used to assess the rehabilitation year, required stability period, and stand age of the mangroves in each plot. The pixel-based approach method was able to reduce the spectral noise and to extract the NDII time series and their apparent trajectory patterns (G. Chen et al., 2018). The size of the rehabilitated mangroves has no direct impact on the extraction of the time series of Landsat pixels with 30 m spatial resolutions, as the area in which the mangroves were rehabilitated was greater than 900 m². The NDII values of the adjacent natural mangroves were consistent across the time series (i.e., $NDII \geq NDII_{stable}$), which indicated the stability of the natural stands. The predicted and actual observed years (DMCR, 1991) for the mangrove rehabilitation, for all forest plots, are presented in Table 4.4. The main challenge associated with NDII is the identification of the exact starting rehabilitation year. The NDII values in the initial years of the rehabilitation are likely to be affected by background soil and water (G. Chen et al., 2018; Kuenzer et al., 2011). The low NDII values make it challenging to accurately identify the year in which the rehabilitation project began. However, the pixel-based analysis showed a strong upward trend of the NDII values that began four years after the actual year of the rehabilitation. As such, the predicted rehabilitation years were estimated by subtracting four years from the adjusted $NDII_{min}$ year (i.e., the year in which the pixels began to show a strong upward trend in the NDII values). In comparison with the actual rehabilitation year, the NDII-based rehabilitation years ranged from 1989 – 1992, with an error of ± 2 years. Plot 21 showed a relatively higher error in the estimated rehabilitation

year. A detailed assessment of the time series for this plot revealed that the upward trend of the NDII values in the plot were delayed by three years. This may be due to the sensitivity of the low reflectance in the NIR band (Jia et al., 2019) caused by the presence of a large water body next to the plot (Figure 4.7). The Landsat pixels covered 900 m², the sensitivity of the low reflectance of the Landsat in the NIR band may have contributed to the delayed upward trend of the NDII values. The results of the naturally regenerated plot showed that the regeneration process started before 1987. However, the time series showed a consistent increase in NDII values during 1987 – 2019.



Figure 4.7 Effect of water body on NDII trend. Field survey photo (a and b) of plot 21, showing the presence of a large water body near an established plot. The blue line is the border of the plot, and the red circle indicates the available water body.

The period required to reach a stable NDII value (Table 4.4: Required stability period in years), like those of the adjacent natural mangroves (i.e., $NDII \geq NDII_{stable}$), was calculated as the difference between the stability year and the predicated rehabilitation year. The required stability periods for the rehabilitated and regenerated mangroves ranged from 7 to 13 years. The stand age for each plot was determined by subtracting the rehabilitation year predicted based on the NDII from the last year of the time series (i.e., 2019). Most of bias was within a range of ± 2 years and was likely to be caused during the estimation of the starting year, when the NDII value showed an upward trend. The spectral reflectance values of the young mangrove trees were especially susceptible to backgrounds of the wet soil and water, as young mangroves lack canopies that conceal the forest floor from an aerial view. The variation in the NDII values was explained by the low photosynthetic activities and abundance of the water and soil backgrounds within the 30×30 m Landsat pixels.

Table 4. 4 ARMA results for mangroves in each plot of the transect line in Trat, Thailand, from 1987–2019

Plot No.	NDIstable	Actual rehabilitation year	NDIimin Year (adjusted)	Stability Year	Predicted rehabilitation Year	Required Stability period (Years)	Age (Years)	Validity	Status
1	0.65	-	1987	-	-	-	-	0	ST
2	0.62	-	1987	-	-	-	-	0	ST
3	0.63	-	1987	-	-	-	-	0	ST
4	0.65	-	1987	-	-	-	-	0	ST
5	0.65	-	1987	-	-	-	-	0	ST
6	0.64	-	1987	-	-	-	-	0	ST
7	0.64	-	1987	-	-	-	-	0	ST
8	0.66	-	1987	-	-	-	-	0	ST
9	0.57	-	1987	-	-	-	-	0	ST
10	0.53	-	1987	-	-	-	-	0	ST
11	0.57	-	1987	-	-	-	-	0	ST
12	0.52	-	1987	-	-	-	-	0	ST
13	0.49	-	1987	-	-	-	-	0	ST
14	0.55	-	1987	-	-	-	-	0	ST
15	0.50	-	1987	-	-	-	-	0	ST
16	0.65	1991	1995	2001	1991	10	28	1	RH
17	0.61	1991	1995	1999	1991	8	28	1	RH
18	0.64	1991	1995	2000	1991	9	28	1	RH
19	0.69	1991	1998	2002	1994	8	25	1	RH
20	0.70	1991	1996	2002	1992	10	27	1	RH
21	0.70	1991	1993	2002	1989	13	30	1	RH
22	0.65	1991	1996	2000	1992	8	27	1	RH
23	0.58	1991	1995	1998	1991	7	28	1	RH
24	0.49	-	1990	1999	1986	13	33	1	RG

Note: Abbreviations ST, RH, and RG stand for stable, rehabilitated, and regenerated mangroves, respectively.

4. 13 Discussion

This study presented the unique opportunity to assess the historical developments and status (biodiversity and structure) of adjacent natural and rehabilitated mangroves in the Trat province of Thailand. It was found that after 28 years: 1) the rehabilitated mangroves were monocultures of Rhizophoraceae, while the adjacent natural mangroves had higher species diversity; and 2) the rehabilitated mangroves were the same height as the adjacent natural stands. The rehabilitated mangroves required 7 to 13 years to achieve stable NDII values, like those of the adjacent natural stands.

4.13.1 Long-term stability of the rehabilitated and natural mangroves

The diversity and complexity indices had higher values in the adjacent natural and regenerated mangroves than in mangroves that were rehabilitated. These results support the findings of Asaeda et al. (2016) and Barnuevo et al. (2017), who reported that over long periods, the rehabilitated mangroves lacked species diversity. After 28 years of growth, the rehabilitated mangroves in the Trat province of Thailand failed to reflect the diversity of the adjacent natural stands. In contrast, the regenerated plot was more diverse and had a higher CI value. The rehabilitated mangroves had high tree densities and low basal areas, compared with those of the natural mangrove forests (Sillanpää et al., 2017; Walters, 2000). The regeneration potential of the rehabilitated mangrove stands was low at our study site, even though they were adjacent to natural mangrove stands, which could potentially act as sources for the needed propagules (Bosire et al., 2003). The seedlings counted in each plot during the field survey indicated that the natural mangroves had a low rate of recruitment. However, in the rehabilitated mangroves, a single, young *Rhizophora apiculata* tree was surrounded by a mixture of *Bruguiera gymnorhiza*, *Bruguiera cylindrica*, *Lumnitzera racemosa*, and *Excoecaria agallocha* trees, despite the dominance of the *Rhizophora* tree species in the area. However, these seedlings failed to establish and could thus not initialize a succession process so far. In comparison, seedlings grew well in natural mangrove stands. This is in agreement with several studies reported by Asaeda et al. (2016), supporting the theory that the shading effect of the mangrove canopies at plantation sites stops direct sunlight from reaching the ground, which may cause the failure of the seedlings. The rehabilitated forests resulted in monocultures, which may be due to the intense intra-specific competition that only allowed for the survival of homogenous tree communities (Asaeda et al., 2016). Salmo et al. (2013) reported that rehabilitated mangroves tend to follow an asymptotic growth behavior pattern once they reach 18 years of age. The rehabilitated forests in our study area were able to reach heights comparable to those of the natural stands within 28 years.

The tide strongly affected the distribution of the propagules, regardless of the location of the mother trees. Sillanpää et al. (2017) showed that the high tides affected the distribution of the mangroves in West Papua, Indonesia. In our study area, this effect requires further evaluation, in relation to the environmental settings (hydrological, geomorphological, and anthropogenic) and various underlying processes (biotic, abiotic, and human-related) in the region. Additionally, we lack information on the initial planting densities and hydrological structures of the rehabilitated mangroves. The above-mentioned information suggests that there may be better management strategies to promote diversity and structural developments in future rehabilitation projects.

4.13.2 Evaluation of the annual composite time series

The use of the Landsat archives for the mapping and monitoring of the mangrove rehabilitation projects, with respect to the species and structural diversity, remains limited. Wang et al. (2019) reported two main barriers. First, that it was difficult to acquire high-quality data as a result of the consistent presence of clouds and cloud shadows in the mangrove forests. Second, that the operation algorithms required computing facilities and significant amounts of time. Annual gap-free, and seamless time series that are free of atmospheric contamination are needed to provide continuous annual objective information on the changes in the rehabilitated mangrove forests. Several studies have used Landsat-based approaches to monitor the changes in mangrove forests (Abdul Aziz et al., 2015; Li et al., 2019; Rakotomavo and Fromard, 2010). However, these studies used classification or segmentation approaches, which do not provide continuous annual objective information on the changes and cannot be used to determine the dynamics of the rehabilitated mangroves (Otero et al., 2018). The approach proposed in this study proved to be more effective at reducing the spectral noise caused by various types of contamination than the classical mapping and monitoring approaches.

The integration of historical information from the Landsat annual composites and current ecological measurements, can be used to monitor the long-term degree of the success of rehabilitation projects, and compare and assess the species and structural diversities of the rehabilitated stands with those of the adjacent natural mangroves. Forest disturbances such as the effect from tsunamis, lightning strikes, insect damage, and sea level fluctuations, are valuable indicators of the development of forest structures during the growth of rehabilitated stands (Hauff et al., 2006; Matasci et al., 2018). The results obtained during this study are useful for estimating the status of development (change or no change due to any disturbance), biophysical properties (structure), and successional stages (diversity) that are reached by developing rehabilitated mangrove stands. Figure

5 shows the temporal patterns of the stable and rehabilitated mangrove plots. The adjacent natural mangroves appeared to be stable during the monitoring period. Conversely, the long-term NDII values indicated that the growth of the rehabilitated mangrove stands had been consistent over the last 28 years. The findings support the potential use of Landsat annual composites to monitor rehabilitated mangroves and indicate the success of rehabilitated mangroves in the Trat province of Thailand. For instance, Pimple et al. (2018) reported that the mangrove forest made a significant recovery over time, which was the reflection of an increase in the local community's awareness of the importance of mangrove conservation in the region.

In this study, plot 24 showed a steady increase in the NDII values before the actual year of rehabilitation. This indicates that this plot (barren or without rehabilitated stands) may have been colonized naturally. This phenomenon supports a study that reported the natural recolonization of mangroves in abandoned saltworks of the Cear'a Estuary in northwestern Brazil (Reis-Neto et al., 2019). This study documented that a long period (> 10 years) might be required for mangroves to regrow on barren land. However, this observation was made on a single plot during the study period; more field plots are required to confirm the pattern of natural regeneration in different areas.

The Landsat spectral values vary depending on the tidal levels at the time of satellite acquisition. The pixel-based approach used was found to be more effective at reducing spectral noise and extracting the NDII time series, with more apparent trajectory patterns (G. Chen et al., 2018). In this study, we utilized the annual median pixel composite approach, in which the median value of each pixel in a given year accounts for the data gaps and noise across the time series. This, minimizes the effects of the unavoidable inaccuracies in pixel quality and masking processes, as well as the variations in the data coverage and quality (Sagar et al., 2017). A few previous studies have used multi-resolution tidal modeling frameworks to obtain Landsat acquisitions (Sagar et al., 2018, 2017). This approach used five years of Landsat imagery to identify the acquisitions during lowest observed tides, but this is not a very practical approach for monitoring rehabilitated mangroves. This study showed that the mangroves could achieve NDII stability 7-13 years after rehabilitation. The study area, however, did have two major limitations: 1) the tidal records were insufficient to identify the low tide acquisitions; and 2) the low tide acquisition was only possible during May–September; however, this was also the rainy season, during which there are consistently higher cloud densities. These conditions make it difficult to find cloud-free Landsat pixels for creating annual composite images. Future work will focus on the applications of UAV (Wang et al., 2019)

Sentinel-1 and -2, and inundation modeling frameworks to quantitatively address the effects of tidal height on the spectral reflectance of optical imagery.

The results of the NDII time series analysis confirmed that the Landsat annual median composites could be used to provide extensive information on how the mangroves changed (Lymburner et al., 2020). This information allowed us to generate a detailed description of the different aspects of the rehabilitation projects, including the starting year of the rehabilitation project, required period to stabilize rehabilitated mangroves, and the current age of the rehabilitated stands. NDII is a good indicator of recovery when monitoring the rehabilitated mangroves using the long-term Landsat archives. Ultimately, our results provided a precise historical assessment of each location assessed in the ecological survey, allowing us to evaluate the status of the existing rehabilitation project and provided comparative information on the biophysical parameters of mangroves after 28 years of rehabilitation. However, several studies were unable to detect a single suitable diversity index, indicating that more than one index should be used. We recommend using multiple diversity and structural indices to properly assess the diversity and structural developments of the rehabilitation projects. The proposed approach identified the continuous development of the rehabilitated mangroves in the Trat Province. Our field data confirmed that planted mangroves could reach the height of the adjacent natural stands, within a period of 28 years.

The ARMA was developed to monitor the mangrove rehabilitation projects in this study. Stable annual Landsat composites allowed for a more holistic assessment of the forest change dynamics (White et al., 2018). This method can even be used to monitor the rehabilitation of the mangroves that occurred in temporal periods, before the high-resolution data were available (i.e., before 1999). The proposed method has been developed on the Google Earth Engine (GEE) cloud computing platform, which is freely available for public use. The GEE provides fast filtering and sorting capabilities, which allow users to consider millions of individual images and pixels when selecting data to meet specific spatial, temporal, spectral, and other criteria necessary to monitor mangroves (Diniz et al., 2019). The proposed method could be used for accuracy assessments of global or regional mangrove biomass and associated carbon studies (Fatoyinbo et al., 2008; Tang et al., 2018). The ARMA also provides a facility that can be used to understand the historical changes over any planned survey location, prior to the actual survey. The continuous annual observations in each plot provide an effective way to evaluate the history and underlying causes of the changes in the mangrove forests. In addition, these data could be used to validate the landscape and individual-based models for the restoration of the mangrove ecosystems (Berger et al., 2008; Sillanpää et al., 2017).

Furthermore, this method could be extended to high-resolution time series (e.g., Sentinel MSI-2) to monitor mangrove rehabilitation projects, as well as projects in other terrestrial forests, including rubber, eucalyptus, and pine. Our future work will focus on: 1) the implementation of ARMA for Sentinel MSI-2 data (10 × 10 m spatial resolution); and 2) the application of the ARMA and field inventory data in the application of Sentinel MSI-2 allometric models.

4. 14 Conclusions

Assessing the degree of success or failure of mangrove rehabilitation compared with the adjacent natural stand requires a systematic and synoptic approach for long-term monitoring of the forest. We successfully integrated historical information from the Landsat annual composite and current ecological measurements to monitor the long-term evolution of rehabilitated projects and compare and assess the status of development (change or no change), biophysical properties (structure), and successional stages (diversity) reached by developing rehabilitated mangrove stands with those of adjacent natural mangroves. The Landsat NDII-based ARMA algorithm developed in this study is an effective tool for evaluating aspects of the development mangrove forest, including the starting year of the rehabilitation project, required period to stabilize rehabilitated mangroves, and age of the rehabilitated stands.

The period required to reach a stable NDII value (like natural stands) after rehabilitation ranged from 7 to 13 years in the 28-year-old stands, with species biodiversity and structural parameters differing among the management types and with respect to the stand age. After 28 years of growth, the rehabilitated mangroves in the study area failed to reflect the diversity of the adjacent natural stands. The rehabilitated mangrove showed high tree densities, low DBH, and a low basal area and was monoculture in nature. However, the rehabilitated stands reached heights comparable to those in the adjacent natural stands within 28 years. Our findings suggest that even after 28 years, the rehabilitated mangroves were floristically different and still structurally growing compared to adjacent natural mangroves.

The approach developed here could be used in rehabilitation projects at large spatial scales, which could have long-term economic benefits in the monitoring of mangrove wood plantations. As technological approaches advance, a finer spatial and temporal resolution of Sentinel satellite series could provide more information on the various parameters of the rehabilitation projects. Finally, we point to the potential of ARMA to monitor not only the gain of mangroves but also the loss. The algorithm is thus a suitable

tool for monitoring mangrove dynamics in general including rehabilitation projects and disturbances in general.

CHAPTER 5

Diversity and intertidal zonation in response to natural, regenerated, and rehabilitated succession



Mangroves during high tide in Trat province of Thailand

This chapter has been produced from: Pimple, U., Leadprathom, K., Simonetti, D., Sitthi, A., Pungkul, S., Pravinongvuthi, T., Dessard, H., Peters, R., Berger, U., Kraiwut, S., Kemachevahul, P., Gond, V. (2021) Assessing mangrove species diversity, zonation and functional indicators in response to natural, regenerated, and rehabilitated succession: Submitted for publication

Abstract:

The United Nations Decade on Ecosystem restoration (2021-2030) lists mangrove ecosystems as a restoration priority. Interest in their conservation has increased recently due to their widespread degradation. Anthropogenic stressors and rehabilitation practices specifically have resulted in a significant decline in their species compositions. We investigated the knowledge gaps in terms of potential spatial diversity, intertidal zonation and the historic state of mangrove forest species and tested the role of environmental factors such as topography, as well as rehabilitation settings on diversification. Diversity and complexity indices, surface elevation, and species and structural diversities along three simplified transect lines encompassing a broad geographical area and under a variety of management practices were analyzed in Trat province, Thailand. Quantitative statistical zonation analyses within each transect and at the landscape scale were performed using randomization tests and hierarchical cluster analysis. A modified “automatic regrowth monitoring algorithm (ARMA)”, based on Landsat (1987–2020) and Sentinel-2 MSI (2015–2020) annual median composites was also used. Fifteen species were identified, of which *Ceriops tagal* was dominant. The statistical analysis however, failed to identify any significant zonation patterns at transect or landscape-scales at a given elevation. Rehabilitated and naturally regenerated stands showed a gradual increase in their Normalized Difference Infrared Index (NDII) trend with time. After 30 years, the rehabilitated stands made up of Rhizophoraceae monocultures, were the same height as the adjacent natural stands. Depending on the location and propagule availability, the diversity and structure of the regenerated stands showed a high level of variation. Effluent from shrimp farms may have contributed to the disturbance of the forest stands and changes in farming practices may have allowed for their recovery. The results provide a valuable diversity baseline for the study site and secondary succession in rehabilitated and regenerated mangroves. The ARMA algorithm has also been confirmed as a valuable tool for future investigations of secondary succession and state mangrove biodiversity.

5.1 Introduction

Mangrove forest ecosystems have a diverse array of trees and shrubs that are adapted to thrive in the intertidal habitats of their tropical and subtropical coasts (Duke, 2017; Tomlinson, 2016). It is of note that the biodiversity of mangroves in the eastern hemisphere is almost five times higher than that in the western hemisphere (58 species compared to 12; Ashton and Macintosh, 2002). The Indo-Malesia region, which is thought to have the highest biodiversity, was reported by Duke et al. (1998) to have more than forty-nine species. Ashton and Macintosh (2002), however, noted a higher mangrove diversity in the Southeast Asian region. The mangroves along the coastline of southeast Asia have been partially denuded though, due to various anthropogenic stressors causing a loss of natural species. Several rehabilitation projects are currently being carried out in this area to address this (Alexandris et al., 2013; Asaeda et al., 2016; Bosire et al., 2003; McKee and Faulkner, 2000), but these often consist of monoculture *Rhizophoraceae* plantations (Asaeda et al., 2016; Barnuevo et al., 2017; Pimple et al., 2020; Ren et al., 2008). High-zoned areas (landwards or adjacent to natural mangrove stands) are also usually rehabilitated using *Rhizophoraceae* monocultures or sometimes exotic species such as *S. apetala* (Ren et al., 2008). Species level acclimation can occur at different speeds based on the hydro period, propagule availability, and dispersal traits (Di Nitto et al., 2014). This raises questions about whether hydrological modifications for alternative land uses (e.g. shrimp farming) may homogenize the landscape and thereby reduce the suitability for a wide range of species that have a different physiological requirements, and reduce ecological functions in mangrove plantations when compared to natural mixed species mangrove forests (Macintosh et al., 2002, Lee et al., 2017).

Mangrove tree species diversity and vegetation complexity are widely regarded as important for the maintenance of genetic richness, ecological function, and ecosystem resilience (Asaeda et al., 2016; Macintosh et al., 2002). Variations in micro-topography and tidal inundation drive the intertidal zonation of mangrove forest species and are considered to be ideal proxies for other environmental factors that contribute to tree growth, including salinity, soil texture, and redox potentials (Hickey and Bruce, 2010; Leong et al., 2018; Ma et al., 2020). Nevertheless, the quantification or verification of zonation patterns with respect to micro-topography has not yet been widely investigated (Ellison et al., 2000). The conversion of mangrove forests into shrimp farms, agricultural areas, and for other land uses alters the surface elevation gradients, which consequently affects the key biophysical variables responsible for the natural species zonation processes (Elwin et al., 2019; Hickey and Bruce, 2010). Among the other anthropogenic stressors, the effluent and waste discharge from shrimp farms strongly affects ecological

functions, long-term ecosystem stability, and negatively impacts on tree biodiversity (Capdeville et al., 2018; Vaiphasa et al., 2007). Specifically, changes in surface elevation can result in changes to hydroperiod and soil redox (Rybczyk et al., 1998). Several studies have reported that stressful growth conditions may be caused by altered hydrological and geomorphological parameters, and that these could subsequently cause higher mortalities, shorter plant heights, and branched trees (Barnuevo and Asaeda, 2018; Proffitt and Devlin, 2005). The analysis of different scenarios for possible changes in species distributions in natural ecosystems, their regeneration potentials, and the effectiveness of rehabilitated mangroves in response to future climate change and the sustainability of biodiversity, is crucial (Jennerjahn et al., 2017). Regardless of global declines in human-driven mangrove loss (Goldberg et al., 2020), there are very few remaining natural mangrove habitats that are protected and unaffected by human interference. To develop better strategies and resilience for rehabilitation and conservation practices, it is important to understand the sensitivity of mangrove ecosystems in response to various environmental and anthropogenic conditions (Di Nitto et al., 2014; Hickey and Bruce, 2010; Leong et al., 2018; Lovelock et al., 2015; Ma et al., 2020). However, detailed systematic intertidal field observations, quantitative data describing the distribution of species (Ma et al., 2020), and knowledge of the long-term change dynamics in native forests caused by biotic, abiotic, and anthropogenic processes is currently limited and requires further investigation.

Site-based transect sampling, such as fixed area sampling and point-centered quarters, are the most common methods used to assess the compositional, structural, and functional attributes of species diversity (Ma et al., 2020; Nfotabong-Atheull et al., 2013; Rani et al., 2018). However, the information obtained from site-based biodiversity surveys is often limited to single occurrences and lacks information on the temporal dynamics. Several natural and anthropogenic stressors can alter the assemblage of mangrove communities. The knowledge of gradual or abrupt temporal changes is crucial for baseline studies of biodiversity monitoring. Understanding the spatial-scale interrelation between local environmental settings (e.g. tidal inundation and surface elevation) and mangrove species distribution is important to assess the changes in species distribution and sensitivity to sea-level rise (Di Nitto et al., 2014; Leong et al., 2018; Lovelock et al., 2015). The careful consideration of influencing factors, environmental settings with modified landscapes and practiced rehabilitation efforts is also essential.

Satellite-based time-series could help to access and quantify functional indicators as well as their increasing or decreasing trends over time (Lawley et al., 2016; Pimple et al., 2020). There are three decades of free satellite imagery available from sources such as Landsat,

and when combined with future monitoring missions (Landsat-9 and Sentinel-2), they provide a unique opportunity to study functional indicators (Graf et al., 2019; Pasquarella et al., 2016). Recent studies have shown the potential of the Landsat time-series to monitor the stability, recovery, and disturbance of mangrove forests (Abdul Aziz et al., 2015; Cárdenas et al., 2017; Jia et al., 2018; Otero et al., 2019; Pimple et al., 2020, 2018). The newly launched, and freely available Sentinel-2 multi-spectral instrument (MSI) could have monitoring value for various functional indicators of mangrove forests (Manna and Raychaudhuri, 2020). However, the inclusion of temporal dynamics in mangrove species diversity monitoring studies has rarely been attempted. Functional indicators include the ecological processes and vegetation histories, such as disturbances or forest health, and could provide vital information on the natural (Lawley et al., 2016) or anthropogenic processes that occur within ecosystems. The inclusion of functional indicators when assessing the historic state of mangrove forests could provide a complete picture of the viability, resilience, or the trajectories of secondary successions (Gibbons and Freudenburger, 2006; Lawley et al., 2016).

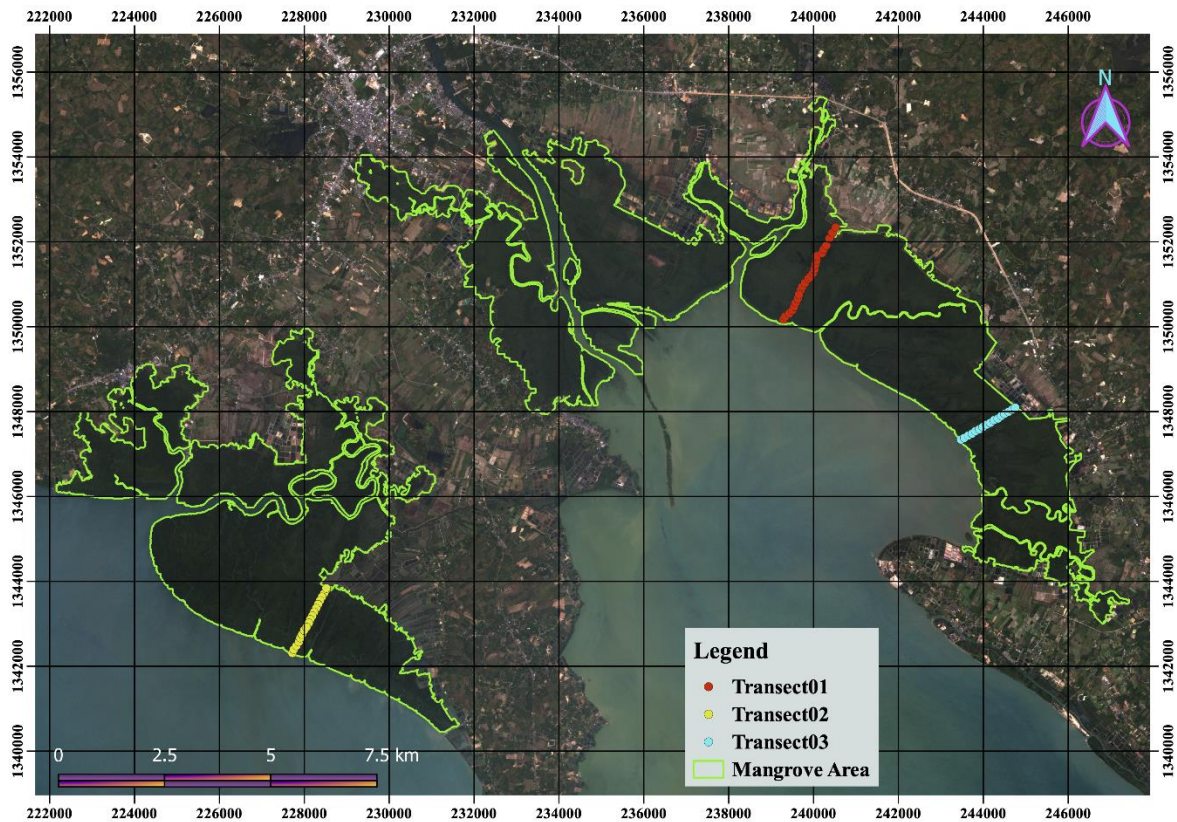
In this paper, we present an innovative approach to improve the understanding of the sensitivity of environmental setting (topography), conservation intervention (rehabilitation) and vegetation histories for mangrove forest species biodiversity. To the best of our knowledge, this is the first study to quantitatively examine the influence of surface elevation on intertidal zones and spatio-temporal species distribution and dynamics at a landscape scale. We have used surface elevation and fixed area quadrants along intertidal zone transect plots to quantify the intertidal zonation of mangrove forest communities. The current species diversity status in the Trat province of Thailand was also explained using thirty-four years of Landsat satellite imagery. The framework was used to determine if the mangrove dominant species zone at a particular location could be defined by abiotic factors such as geomorphological (micro-topography) and anthropogenic factors. Overall, this study: (1) investigates the zonation patterns along transects perpendicular to the shoreline; (2) relates the mangrove species zonation to the elevation gradient; (3) assesses the historical state of forests and links them to species diversity; and (4) establishes the historic state of mangrove forest under various environmental settings and associated processes.

5.2 Study site description and sampling design

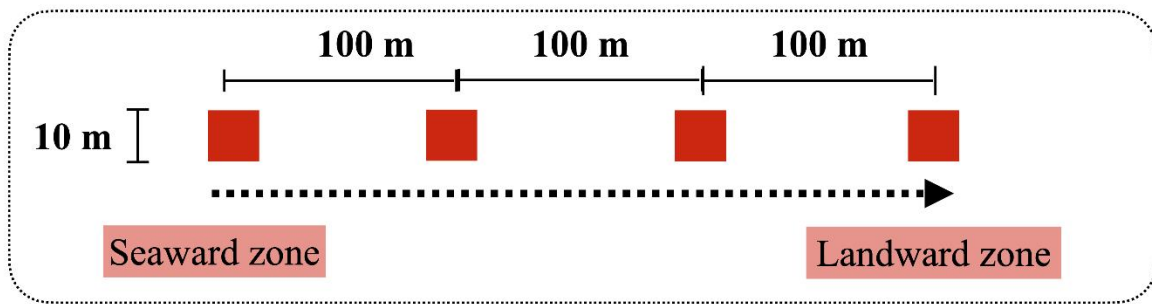
The study area for this investigation was Trat province, Thailand, which is located along the eastern coast of the Gulf of Thailand and borders Cambodia (Fig.5.1; Pimple et al., 2020). The mangrove forests in this province cover approximately 106 km², it is located at longitude 102.61° and latitude 12.21°, and has a tropical climate, with seasonal monsoons (Chalermchatwilai et al., 2011; Pimple et al., 2020, 2018). The study site was selected for the following reasons: (1) it had large rehabilitated mangroves adjacent to natural diverse stands; (2) most natural species found in Thailand could be identified in the area (Pimple, 2020); and (3) it contained a large area of landward forest that had been destroyed for shrimp farming and agricultural activities, but had subsequently been naturally regenerated. Consecutive field surveys were conducted from March 2015 to September 2020, to determine the spatial distribution of the species, as well as the location, extent, structural parameters, and surface elevation of the mangroves. At the study site, most of the mangroves were rehabilitated without adequate site assessment and non-pioneer species (e.g. *Rhizophora* spp.), resulting in most of the rehabilitated zones having monocultures of Rhizophoraceae. Furthermore, natural regeneration was found in the abundant landward area. Recent studies suggest that the rehabilitated mangroves were able to achieve heights similar to those of the natural mangroves over a 28 year of period (Pimple, 2020; Pimple et al., 2020). However, the relationship of the mangroves species zonation in relation to the surface elevation or tidal regime and edaphic parameters, has not yet been investigated.

A systematic sampling design (fixed-area sampling) across the mangrove forest landscape was used, and was crucial for the identification of the major mangrove species and changes in the mangrove structural features (Pimple, 2020; Pimple et al., 2020). A primary forest change map was obtained from (Pimple et al., 2018). The spectral and structural signatures (Sentinel-1 SAR and -2 MSI) were carefully checked to ensure the heterogeneity among the mangrove species and their associations. In addition to the Landsat time-series (see section 5.10), the rehabilitation and regenerated forest records were obtained from the Office of Mangrove Conservation, Department of Marine and Coastal Resources, Trat, Thailand and local communities. The field survey data from March 2015, October 2016, and December 2017 was used to verify the different forest stands. Three transect lines were systematically established perpendicular to the coastline, covering species distributions over a broad geographic area and along the intertidal zones (Fig. 1). The transect lines were located from 239249 m E and 1350069 m N to 240518 m E and 1352337 m N; 227717 m E and 1342309 m N to 228518 m E and

1343837m N; and 243470 m E and 1347340 m N to 244753 m E and 1348091 m N (UTM Zone 48 datum), and were 1.73, 2.67, and 1.51 km in length, from the shoreline to their end in the forest (landward side), respectively. In total, 59 plots (10 × 10 m), were established with 100 m distances between them, to determine the species composition and diversity in each stand, as well as the distributions among the intertidal zones. The 10 × 10 m plot size was chosen because it was manageable to survey when considering the large spatial scale of the area and the required sample sizes. Furthermore, several previous studies that focused on diversity and structural parameters also used similar plot sizes (Araujo and Shideler, 2019; Asaeda et al., 2016; Barnuevo et al., 2017; Macintosh et al., 2002; Pimple, 2020; Pimple et al., 2020; Ren et al., 2008). Of these plots, 45 were in the natural zone considered to have stable or undisturbed forests, 8 were in rehabilitated areas, 3 in naturally regenerated areas, and 3 in partially disturbed plots. In each plot, species names, diameter at breast height (1.3 m), tree height and surface elevation were all measured. The crown cover and number of seedlings within each plot was also recorded. The diameter at breast height (DBH) and tree height were measured with a tape measure and clinometer, respectively. The field inventory data were collected in December 2018, January–July 2020, and February 2021. Dead trees were excluded from the height measurements, and in each of these cases, the next living tree was measured instead (Pimple, 2020; Pimple et al., 2020). Furthermore, extensive ground control points were collected to ensure the distribution of the species around the transect lines.



(a)



(b)

Figure 5.1 Mangrove and sample plot locations used in this investigation. (a) Location of the mangroves in Trat province, eastern Thailand. Transect lines 1, 2, and 3 indicate the locations for the sample plot placements for the mangrove observations. The red, yellow and cyan dot indicates the locations of the 10×10 m plots along the intertidal zone. (b) Overview of transect plot establishment and sampling design.

5.3 General description of the methodology

Detailed surveys of the study sites were first conducted in March 2015, October 2016 and December 2017 to identify the spatial extent of the natural, rehabilitated and regenerated mangroves (Pimple et al., 2018). These transect lines provided the benchmark for the zonation of mangroves, as precise locations, types, and variations were recorded. Surface elevations along the mangrove transect lines were also determined using the RTK GPS surveying. A detailed analysis of the annual changes over the last 34 years was then conducted using a time series of the Landsat and Sentinel-2 MSI annual composites (Pimple et al., 2018). Moreover, we analyzed the relationship between elevation, tidal inundation, and mangrove zonation and related these to the satellite-based functional indicators. A detailed flow chart of the approach used in this study is presented in Fig. 5.2 The Google Earth Engine (GEE) (<https://earthengine.google.com/>), R statistical packages (R Core Team, 2021), and python programming (Python Core Team, 2020) environment were used to carry out all analysis described in the conceptual framework.

5.4 Forest species composition and structure and diversity indices

The Shapiro-Wilk test was used to check the normality of the structural data (stem height, basal area, and DBH) among the different transect lines (Su et al., 2016; Yirdaw et al., 2019). The vegetation data were analyzed using the importance value (IV) (Cintrón and Novelli, 1984; Curtis and McIntosh, 1950). The complexity index (CI) was used to measure the structural complexity of each plot (Holdridge, 1967). The Simpson's index of diversity (1-D) and Simpson's reciprocal Index (1/D) were used to determine species dominance using the basal area at breast height (1.3 m) in each 10 × 10 m plot, occupied by each species. The Shannon or Shannon-Weaver index was used to compare the diversity and variance of the species distributions between the mangrove forest (Shannon and Weaver, 1963). The formulas for the above parameters are as follows:

$$IV_i = RD_i + RBa_i + RF_i \quad 5.1$$

$$RD_i = \frac{n_i}{\sum_{i=1}^s n_i} \times 100 \quad 5.2$$

$$RBa_i = \frac{Ba_i}{\sum_{i=1}^s Ba_i} \times 100 \quad 5.3$$

$$RF_i = \frac{F_i}{\sum_{i=1}^s F_i} \times 100 \quad 5.4$$

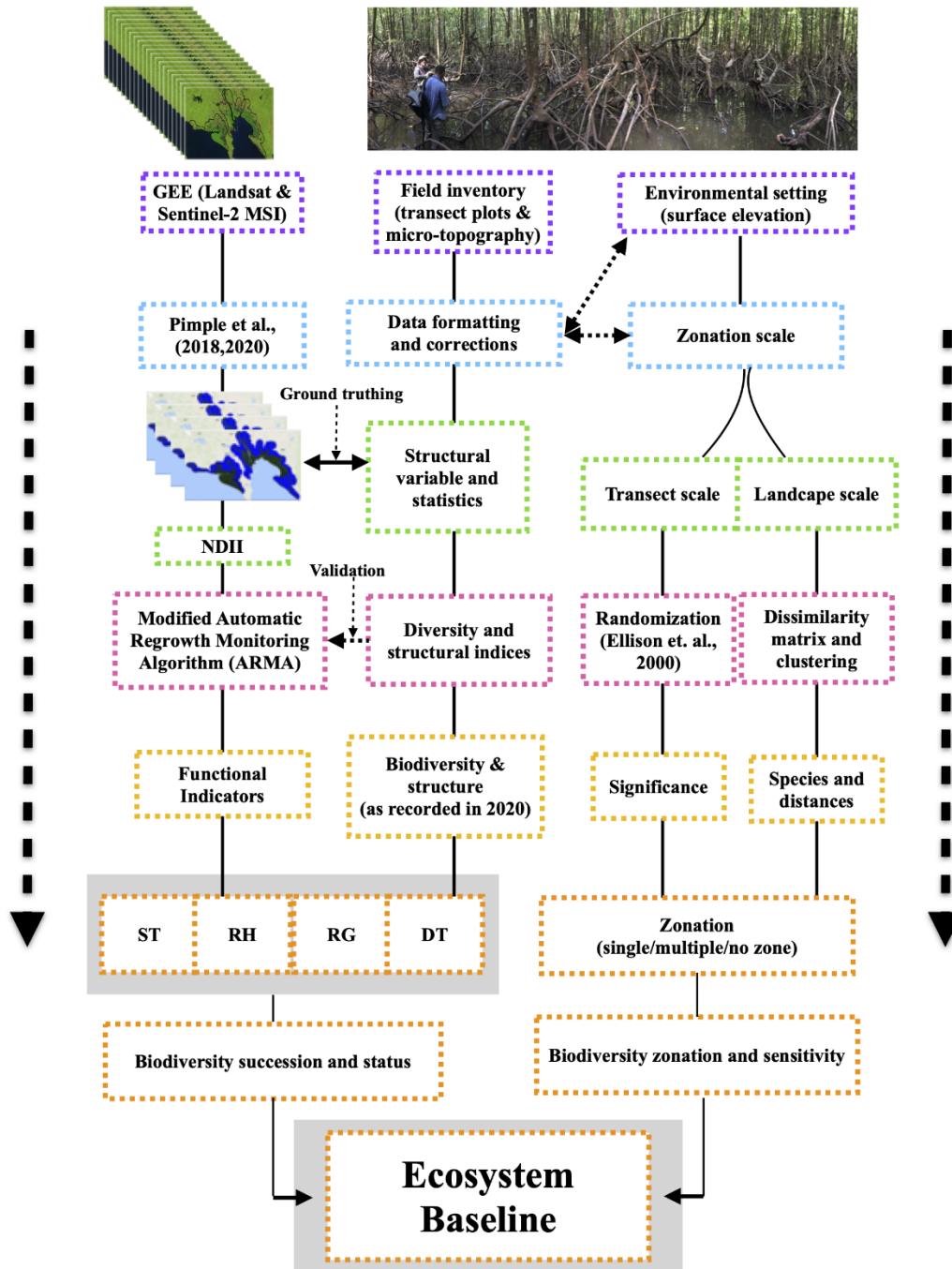


Figure 5.2 Flow diagram of the experimental framework. Flow diagram showing the methodological framework for the transect plot data, preparation of the Landsat and Sntinel-2 MSI annual composites, and the derivation of the biodiversity and succession indicators. Note: GEE: Google Earth Engine; NDII: Normalized Difference Infrared Index; ST: stable or undisturbed forest stands; RH: rehabilitated forest stands; RH: regenerated forest stands; DT: disturbed forest stands

where IV_i is the importance value; RD_i , RBa_i and RF_i are the relative density, relative to the basal area (or dominance), and relative frequency of the mangrove species i ; s is the

number of species; n is number of individuals of a given species i ; $\sum_{i=1}^s n_i$ is the total number of individuals of all species; Ba_i is basal area of species i ; $\sum_{i=1}^s Ba_i$ is the sum of the basal area values for all species; F_i is the frequency of species i ; $\sum_{i=1}^s F_i$ is the sum of the frequency values for all species, respectively.

$$CI = \frac{s \cdot d \cdot Ba \cdot \bar{h}}{1000} \quad 5.5$$

where, s is the number of species per plot, d is the stand density, Ba is basal area in square meter, and \bar{h} the mean height in meter, respectively (Araujo and Shideler, 2019).

$$D = \sum_{i=1}^s \frac{n_i (n_i - 1)}{N(N-1)} \quad 5.6$$

where, n_i is the number of trees of the i^{th} species, and N is the total number of individuals. The Simpson's index of diversity (1-D) and Simpson's reciprocal Index (1/D) were used to determine species dominance.

$$H' = - \sum_{i=1}^n p_i \times \ln p_i \quad 5.7$$

where H' is the Shannon or Shannon-Weaver index diversity index, p is the proportion of the individuals of species i , in relation to the total number of trees (n) in each plot, and \ln is the natural logarithm. This index uses the number of individuals of each species in each 10×10 m plot to determine diversity.

5.5 Species distribution analysis

5.5.1 Transect scale distribution

Mangrove species zones dominated by individual species or association of species may be noticeable on the open shoreline along the steep micro-topography gradient, however, they are not easy to discriminate in many mangrove ecosystems (Robertson and Alongi, 1992). According to Ellison et al. (2000), the mangrove species zoned sequence should occupy a distinct portion of the intertidal and elevation gradient areas. They also identified the importance of surface elevations for most of the edaphic parameters associated with species distributions along the intertidal zones. Furthermore, several previous studies that focused on mangrove zonation used surface elevation as the most common variable (Ellison et al., 2000; Hickey and Bruce, 2010; Leong et al., 2018; Ma et al., 2020; Watson, 1928). A data matrix ($n \times m$) was created with the species (rows) and surface elevation (columns) of each transect line, where each matrix cell indicates the available species at a given surface elevation (Ellison et al., 2000; Gotelli et al., 2015). A zero value indicates the presence of species in the study site but not at the specified location or niche category. To determine how much the measured niche overlap values

differed from what would be expected based on a random sampling of the species data at each transect level, we used randomization tests with the niche overlap model (Gotelli et al., 2015), on individual transect lines. Community niche overlaps were calculated using Pianka's overlap index (Pianka, 1973), which ranges from 0 (no niche overlap) to 1 (complete niche overlap). Randomization algorithm 3 (RA3) was used with 10,000 repetitions to generate a distribution for Pianka's overlap index against the observed measure of the niche overlap for comparison (Ellison et al., 2000). The randomization tests and Pianka's overlap index were carried out using the R package EcoSimR (Gotelli et al., 2015) and then compared with the null model. The possible scenarios for mangrove community zonation include: (1) single species zonation, where the mean pairwise overlap is significantly low and the variance in overlap of such a community is similar; (2) grouped multiple species zones, where the mean pairwise overlap is expected to be high and similar, and the variance was also expected to be high; and (3) no-zonation or random species distribution, where the mean pairwise overlap, and its variance were not expected to differ (Ellison et al., 2000).

5.5.2 Landscape scale distribution

Hierarchical agglomerative clustering was applied to recognise species plots that tended to co-occur in the transect plot samples and group together with similar taxonomic compositions. For multivariate analysis, Danise et al. (2013) suggest that species that occur in only one sample site be removed. However, the removal of rare species can have a similar or greater influence in multivariate analysis (Cao and Thorne, 2001; Poos and Jackson, 2012). In this study, *Bruguiera gymnorrhiza* and *Sonneratia alba* (plots: T2P19 and T3P1) were single monoculture plots that appeared only once in the transect data. We included all plots in the analysis, including sites with no shared species. Data were square-root transformed to further equalize the contributions of the rare and unshared species. The non-parametric cophenetic correlation coefficient (Spearman's r) was computed for different clustering methods and used as a measure of clustering efficiency (Ruokolainen and Blanchet, 2014). The higher the absolute value of the cophenetic correlation, the better the correspondence between the metrics that were compared (Legendre and Legendre, 2012). Based on the cophenetic correlation coefficient, we used a hierarchical average-linkage clustering algorithm. The optimal number of clusters represented the various groups obtained using the Mantel statistical test (Borcard et al., 2011). To detect the groups with site conditions that were almost homogenous inside each cluster, we evaluated the final number of groups using a Silhouette analysis. The Silhouette width ranges from -1 to +1 and the greater this value, the more likely the group is a cluster (Ruokolainen and Blanchet, 2014). Negative values indicate that the samples

might have been assigned to the wrong cluster. If the average Silhouette width was less than or equal to 0.25, this indicates that no substantial structure was found (Kaufman, L. and Rousseeuw, 2009).

The agreement between the Bray–Curtis similarity matrix for species abundance and the Euclidean distance similarity matrices of environmental variables were linked to species assemblages using the Mantel statistical test (Clarke et al., 2008). The Mantel statistical test determines the correlation between two matrices (distance and dissimilarity) and determines whether the species compositions between the samples are correlated with the differences in surface elevation between the samples. In other words, abiotic factors such as elevation select mangrove species communities, which indicates environmental gradients control the distribution of mangrove species through ecophysiological factors (Robertson and Alongi, 1992).

5.6 Landsat annual composites (1987–2020)

In this study, for the time-series data, we obtained a Tier 1 top-of-the atmosphere (TOA) collection from the GEE for Landsat TM-5 (1987–2001 and 2003–2011), ETM+ (2002 and 2013), and OLI-8 (2013–2020). All images were acquired between January 1, 1987 and January 01 2021. The Tier 1 Landsat collection is considered to be suitable for time series analysis, as it includes Level-1 Precision Terrain (L1TP) processed data with inter-calibrations across the different Landsat sensors. Only red, green, blue, NIR, SWIR-1, and SWIR-2 bands were processed in the Universal Transverse Mercator (UTM) zone 48 N projection. The entire collection was cleaned of clouds, cloud shadows, and pixels with no-data, according to previously described algorithms (Pimple et al., 2020, 2018; Simonetti et al., 2015).

Every Landsat image was normalized using a dark object subtraction method (Bruce and Hilbert, 2004), as described in Eq. (6). This approach used the median values of the mangrove forest pixels to apply a linear correction to each spectral band (Bodart et al., 2011; Pimple et al., 2020, 2018).

$$\varphi_{adjusted}^{(\lambda)} = \varphi_{original}^{(\lambda)} - (\bar{X}_{mangrove}^{(\lambda)} - \bar{X}_{ref}^{(\lambda)}) \quad 5.8$$

where, $\varphi_{adjusted}^{(\lambda)}$ is the normalized median for band λ , $\bar{X}_{mangrove}^{(\lambda)}$ is the median value of the dense mangrove forestry of the sample site for band λ , and $\bar{X}_{ref}^{(\lambda)}$ is the reference dense mangrove forest value for band λ . The per band extracted median reference values were 0.10238 (blue), 0.08208 (green), 0.05340 (red), 0.28267 (NIR), 0.06959 (SWIR-1), and 0.02379 (SWIR-2), respectively, in a TOA reflectance of 0–1, and six processed bands.

5.7 Sentinel-2 multi-spectral instrument (MSI) annual composites (2015–2020)

The Sentinel-2 MSI images contained 13 UNIT 16 spectral bands, representing the TOA reflectance, and were obtained from the GEE image collection. To ensure meaningful comparisons between the sensors, the red, green, blue NIR, SWIR-1, and SWIR-2 bands were selected. The annual composites for the period 2016–2020 were created using the median reflectance values of the collection, after being cleaned of clouds, cloud shadows, and pixels with no data (Simonetti et al., 2021). Sentinel-2 SWIR-1 and SWIR-2 bands, were originally acquired at 20 m spatial resolutions and later resampled at 10 m resolutions, using the nearest-neighbor interpolation method. The Sentinel-2 MSI time series (2015–2020) was used to cross verify the recovery dynamics of the plots T3P5–T3P7 (T:transect number and P:plot number) as observed from the Landsat annual composites. Manual checks were performed to assess the available reflectance values over the plots T3P5–T3P7.

5.8 Normalized Difference Infrared Index (NDII)

In this study we used the NDII based on the Landsat and sentinel-2 MSI NIR and SWIR-1 bands, and it was calculated as follows:

$$\text{NDII} = \frac{(\text{NIR}-\text{SWIR})}{(\text{NIR}+\text{SWIR})} \quad 5.9$$

where NIR is the reflectance in the near-infrared wavelength channel (0.70–0.90 μm), and SWIR is the reflectance in the shortwave-infrared wavelength channel (1.55–1.75 μm ; Jackson et al., 2004; Ji et al., 2011). The sensitivity of NDII to the forest water content provided a measure of all water contained in the foliage canopy. Water content is an important quality for vegetation as higher water contents indicate healthier vegetation that is likely to grow faster and be more stable over time (Jackson et al., 2004). The NDII can detect physiological responses to sudden changes or stresses over very small intervals of time.

5.9 Modified automatic regrowth monitoring algorithm (ARMA)

Continuous Landsat annual observations in each plot provide an effective way in which to evaluate the history and underlying causes of the changes in forest stands (Pimple et al., 2020). To understand the temporal dynamics, we have modified ARMA, which was first introduced by Pimple et al. (2020). Previously, ARMA was used to characterize annual changes in rehabilitated mangroves. In this study however, we have modified its

performance using the three transect lines, to include abrupt changes, disturbance-recovery trajectories, and gradual changes. This has allowed the status of the functional indicators of the mangrove forests to be defined.

5.10 Functional indicators of diversity status and secondary succession

According to the spectral variation hypothesis, the spectral variability of multispectral images or vegetation indices could be used as a proxy to assess forest biodiversity (Palmer et al., 2002; Torresani et al., 2019). Images with high spectral heterogeneity in their pixels corresponded to a higher number of available ecological niches where multiple tree species could be found (Torresani et al., 2019). The spectral variations in the time-series pixel data were related to the various phenomenon that occurred over time due to various stressors and processes. Most previous ecological studies of mangrove species and their relations to the environmental gradients focus on the patterns observed at a single or specific time point, and do not include a long term understanding of environmental settings, vegetation histories, and anthropogenic processes. Lightning, insects, diseases, tropical storms, sea level, timber extraction, waste discharge from aquaculture, and other industries are natural and anthropogenic factors that affect mangroves at varying spatial and temporal scales (Allen et al., 2001; Ellison and Farnsworth, 1996; Tian et al., 2018; Vaiphasa et al., 2007). The results often show a clear interaction between ecological processes and spatial patterns, usually as patches of different species compositions (Dale and Fortine, 2014). In this study, plot T1P24 (T:transect number and P:plot number) was an example of such processes. Initially, this plot was barren or had not been rehabilitated, but it was later colonized by more diverse species (Pimple et al., 2020). In ecological studies, the main question that arises is whether there was an event in the past that might have triggered secondary succession which subsequently changed the species diversity. The understanding of temporal dynamics of diversity during the successional processes could provide insights into the current differences in forest species, structures, and their interactions with various ecological processes.

In this study, we propose a satellite-based approach that considers the timing and magnitude of various ecological disturbances along the intertidal gradients while reporting the zonation patterns. In this case, the changes could be studied through time to interpret the observed diversity and structural differences. Here we have derived a set of possible conditions to characterize the temporal dynamics of every single field survey plot and linked them to the currently observed ecological diversity and structures (Fig 5.3).

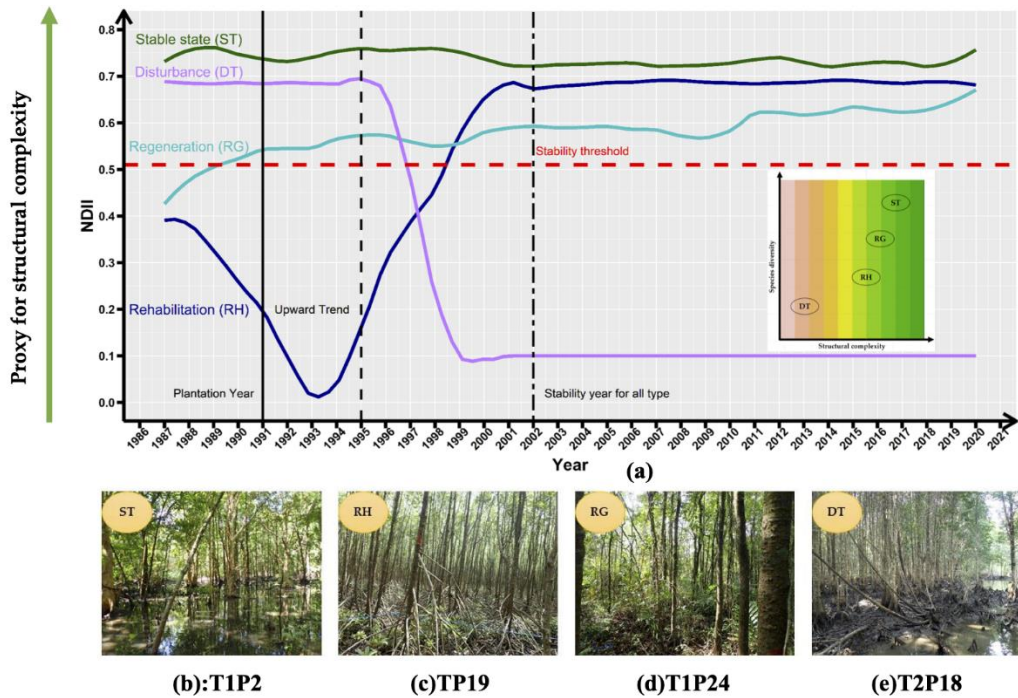


Figure 5.3 Illustration of expected mangrove forest diversity response types. (a) state and temporal dynamics, ST: stable or undisturbed state (dark green); RH: rehabilitation (dark blue); RG: regeneration (light blue); and DT: disturbance with no recovery (purple); the known plantation year is indicated by a black vertical line; the start of the Normalised Difference Infrared Index (NDII) upward trend after rehabilitation is indicated by a dashed line; the quasi-stability year for all forest types is indicated by two sized dash line. In the subset graph for structural complexity and species diversity, the brown colour indicates no diversity and less structural complexity while the green colour indicates high diversity and structural complexity (left to right). (b), (c), (d) and (e) are the field photo of ST (T1P2), RH (T1P19), RG (T1P24), and DT(T2P18), plots showing the example diversity and structure, where T: transect no. and P: plot no)

The stable state mangroves forest stands were defined as the median values of all points in the time series of the annual composite, minus one standard deviation (Pimple et al., 2020):

$$NDII_{stable} = NDII_{median} - NDII_{1SD} \quad 5.10$$

where $NDII_{stable}$ represents stability or no change to the mangrove stand over time, $NDII_{median}$ is the median of all annual median composites of the natural mangroves and rehabilitated mangroves after the year 2002, and $NDII_{1SD}$ is the standard deviation of all annual median composites of the natural mangroves (Pimple et al., 2020). Additionally, we tested the independent median values of the natural, rehabilitated, and regenerated plots after the year 2002, and compared them with $NDII_{stable}$ to ensure the applicability of the threshold over all mangrove types. The years 2002–2020 were chosen for this as most

types of mangrove stand during this period (except disturbed stands), showed relatively stable NDII values. Visual quality control was performed on each plot to test the stability of the applied thresholds as follows:

Stable state: The undisturbed mangrove forest stands have relatively stable NDII signatures over many years. In this state, mangroves are expected to be structurally more complex and diverse.

Rehabilitation: The planted mangroves are usually monoculture stands. The values of the NDII are expected to increase gradually and return, or come close, to those of the natural mangroves or their state before the disturbance. This is a good indicator of the success or failure of mangrove rehabilitation efforts. The rehabilitated mangrove stands are subjected to less structurally complex monocultures, which are not found in nature. However, outcomes may vary due to management practices and the duration of the rehabilitation project.

Regeneration: Disturbed mangroves followed by natural recovery without any conservation intervention. Unlike the sustained abrupt changes in the recovery phase, the values of the NDII are expected to increase gradually, return, or come close, to those of the natural mangroves or their state before the disturbance. This is a good indicator of forest recovery or secondary succession. The regenerated mangrove stands were subjected to more structurally complex and diverse conditions. However, outcomes may vary depending on the availability and dispersal limitations of the propagules at given sites.

Disturbance and no recovery: The sudden changes to the mangrove forest canopy caused by abiotic, biotic, and anthropogenic disturbance. This condition often results in an abrupt or sudden decline of the NDII values with a clear breakpoint between the before and after conditions. Mangrove stands are subjected to a permanent loss of diversity.

5.11 Statistical analysis

The NDII time series was used to quantify the temporal dynamics observed in the successional process of each plot. Here we have derived a set of conditions and grouped them into four mangrove forest categories: stable state (undisturbed), rehabilitated, regenerated, and partially disturbed and recovered. One-way analysis of variance (ANOVA) was used to test the differences across forest categories in four measures of forest species diversity indices (D , $1/D$, H') and complexity index (CI). A Post-hoc (Tukey Honest Significant Differences) test was used to determine the differences in diversity

among the forest categories. R statistical packages (version 4.0.2) were used to carry out statistical analysis (R Core Team, 2021).

5.12 Results

5.12.1 Forest species diversity and composition

In total, 1600 trees were recorded in the 59 plots along the three transect lines, which represented a combined area of 5900 m². The tree count ranged from 5–63 per plot (Fig. 5.4), and the following 15 species were recorded: *Sonneratia alba* (Sa), *Avicennia alba* (Aa), *Avicennia marina* (Am), *Bruguiera cylindrical* (Bc), *Bruguiera gymnorrhiza* (Bg), *Bruguiera sexangula* (Bs), *Ceriops tagal* (Ct), *Excoecaria agallocha* (Ea), *Intsia bijuga* (Ib), *Lumnitzera littorea* (Ll), *Lumnitzera racemose* (Lr), *Rhizophora apiculata* (Ra), *Rhizophora mucronata* (Rm), *Xylocarpus granatum* (Xg), and *Xylocarpus moluccensis* (Xm) (Pimple et al., 2020). A recent survey conducted in February 2021 by the authors reports the presence of *Sonneratia ovata* Backer (So), however their occurrence is quite rare at this study site. The Rap and Rmp stand for *Rhizophora apiculata* plantation and *Rhizophora mucronata* plantation.

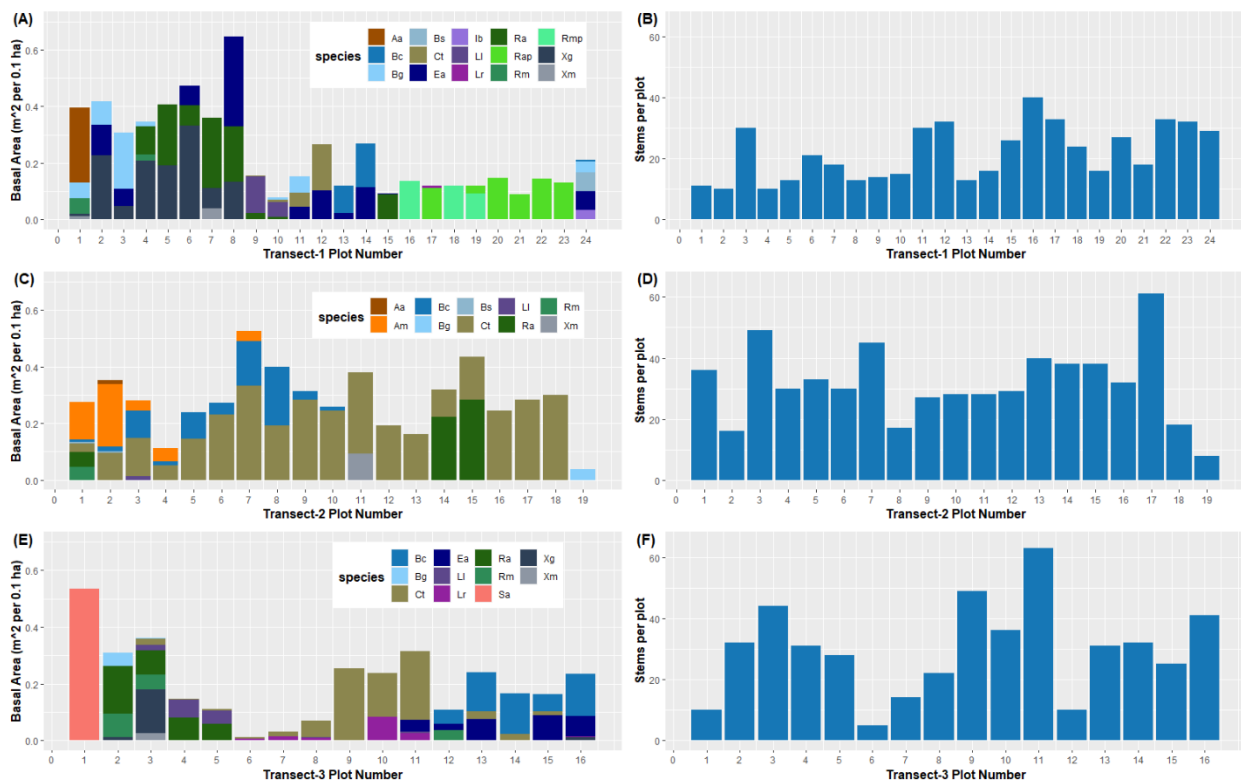


Figure 5. 4 Mangrove species composition, basal area, and stems per plot along the three transect lines investigated. A, C, and E indicate the basal stem area (m² per 0.1 ha) per plot per transect; B, D, and F indicate the stem counts per plot, per transect. The x-axis indicates the plots per transect line from seaward to landwards. Note: Aa: *Avicennia alba*; Am: *Avicennia marina*; Bc: *Bruguiera cylindrical*; Bg: *Bruguiera gymnorrhiza*; Bs: *Bruguiera sexangula*; Ct: *Ceriops tagal*; Ea: *Excoecaria agallocha*; Ib: *Intsia bijuga*; Ll: *Lumnitzera*

littorea; Lr: *Lumnitzera racemosa*; Ra: *Rhizophora apiculata*; Rap: *Rhizophora apiculata* plantation; Rm: *Rhizophora mucronata*; Rmp: *Rhizophora mucronata* plantation; Sa: *Sonneratia alba*; Xg: *Xylocarpus granatum*; and Xm: *Xylocarpus moluccensis*.

The detailed species composition parameters and their relative ranks are presented in Table 5.1 Of the 1600 trees identified at the study site, 677 (41.69%) were *Ceriops tagal* making it the dominant species, both in terms of basal area (4.50 m² per 0.1 ha) and tree density (677 stems per 0.1 ha). As a result, *Ceriops tagal* had the highest importance value (IV) (96.22) of all the observed species. Of the combined rehabilitated and natural trees, 431 (26.94%) were *Rhizophoraceae* (319 *Rhizophora apiculata* and 112 *Rhizophora mucronata*), making it the second most dominant genus with an IV of 68.99. The results also showed that the *Bruguiera* plant genus in the family *Rhizophoraceae* (172 *Bruguiera cylindrical*, 58 *Bruguiera gymnorhiza*, and 11 *Bruguiera sexangula*) had the third highest IV of 49.40, followed by *Xylocarpus* (*Xylocarpus granatum* and *Xylocarpus moluccensis*; 24.47), *Excoecaria agallocha* (23.72), *Lumnitzera* (*Lumnitzera littorea*, *Lumnitzera racemosa* 18.8), *Avicennia* (*Avicennia alba* and *Avicennia marina*; 11.46), *Sonneratia alba* (5.01), and *Intsia bijuga* (1.14).

Table 5. 1 Mangrove community species compositions

Rank	Species	Density (stems per 0.1 ha)	Dominance (m ² per 0.1 ha)	Frequency (%)	Relative Density (%)	Relative Dominance (%)	Relative Frequency (%)	Importance Value (%)
1	Ct	677	4.51	0.58	42.31	31.39	22.52	96.22
2	Ra	174	1.90	0.25	10.88	13.23	9.93	34.04
3	Bc	172	1.47	0.31	10.75	10.22	11.92	32.89
4	Ea	86	1.21	0.25	5.38	8.41	9.93	23.72
5	Xg	54	1.40	0.19	3.38	9.72	7.28	20.38
6	Rap	145	0.65	0.10	9.06	4.50	3.97	17.54
7	Bg	58	0.54	0.17	3.63	3.78	6.62	14.02
8	Ll	41	0.34	0.17	2.56	2.35	6.62	11.54
9	Rmp	77	0.35	0.05	4.81	2.42	1.99	9.22
10	Rm	35	0.29	0.10	2.19	2.05	3.97	8.21
11	Am	24	0.47	0.08	1.50	3.25	3.31	8.06
12	Lr	26	0.15	0.12	1.63	1.01	4.64	7.27
13	Sa	10	0.54	0.02	0.63	3.73	0.66	5.02
14	Xm	4	0.17	0.07	0.25	1.21	2.65	4.11
15	Aa	2	0.28	0.03	0.13	1.95	1.32	3.40
16	Bs	11	0.08	0.05	0.69	0.54	1.99	3.21
17	Ib	4	0.03	0.02	0.25	0.23	0.66	1.14

Note: Aa: *Avicennia alba*; Am: *Avicennia marina*; Bc: *Bruguiera cylindrical*; Bg: *Bruguiera gymnorhiza*; Bs: *Bruguiera sexangula*; Ct: *Ceriops tagal*; Ea: *Excoecaria agallocha*; Ib: *Intsia bijuga*; Ll: *Lumnitzera littorea*; Lr: *Lumnitzera racemosa*; Ra: *Rhizophora apiculata*; Rap: *Rhizophora apiculata* plantation; Rm: *Rhizophora mucronata*; Rmp: *Rhizophora mucronata* plantation; Sa: *Sonneratia alba*; Xg: *Xylocarpus granatum*; and Xm: *Xylocarpus moluccensis*.

Mangrove species biodiversity varied noticeably among the different transect lines. The obtained diversity between the different transect lines with the Simpson's (1-D and 1/D) and Shannon's (H') indices ranged from 0.00–1.00, 1.00–4.70, and 0.00–1.65, indicating the presence of a monoculture and diverse species. In transect 1, the diversity index was higher in adjacent natural and naturally regenerated stands (plots T1P1-T1P15, and TP24, where T: Transect and P: Plot), which had 1-D, 1/D, and H' values of 0.14–0.73, 1.17–3.71, and 0.27–1.41, respectively. The rehabilitated stands in plots T1P16–T1P23 had very low biodiversity, as the 1-D, 1/D, and H' values ranged from 0.00–0.30, 1.00–1.43, and 0.00–0.13, respectively, indicating a monoculture (Pimple et al., 2020). The rehabilitated stands were mostly dominated by *Rhizophora apiculata* (plots T1P20-T1P23) but they also contained some *Rhizophora mucronata* (plots T1P16-T1P17, T1P19; Fig.5.4). Transect 2, plots T2P1–T2P10 and T2P14–T215 appeared to be more diverse compared with plots T211–T2P13 and T2P16–T219, which had 1-D, 1/D, and H' values of 0.12–0.77, 1.14–4.38, and 0.24–1.57 and 0.00–0.06, 1.00–1.07, and 0.00–0.15, respectively. Transect 2 had the highest number of *Ceriops tagal* with natural monoculture stands, and *Ceriops tagal* was the most dominant. Plot T219 was dominated by the monoculture stands of *Bruguiera gymnorhiza*. In transect 3, the fringe zone facing towards the sea was dominated by pioneering *Sonneratia alba* (plot T3P1). The diversity index was higher among the plots T3P2–T3P8 and T3P10–T3P16, which had 1-D, 1/D, and H' values of 0.12–0.79, 1.13–4.70, and 0.23–1.65, respectively. Plot T3P9 was a natural monoculture stand of *Ceriops tagal*. Table A.1 presents the detailed tabular values of the 1-D, 1/D, and H' indices for the individual plots of all transect lines.

5.12.2 Structural compositions

The detailed species and structural compositions of all transect line plots are presented in Tables 5.1 and 5.2 and Fig.5.4. The total tree density and basal area in the three transects was 272 stems per 0.1 ha and 2.42 m² per 0.1 ha, respectively. Based on the Shapiro test of normality the forest structure parameters including height, DBH, and basal area were significantly different among the transect lines ($p < 0.05$). The height values of the three transect lines ranged from 4–24, 5.50–13.75, and 1.90–12.57 m, respectively (Fig. 5.5), DBH ranged from 4.61–58.23, 5.69–34.68, and 4.29–22.77 cm, respectively, and their basal areas ranged from 0.02–3.33, 0.05–3.33, and 0.014–5.36 m² per 0.1 ha, respectively (Table 5.2).

Table 5. 2 Forest structural and diversity indices

Type	Plot number	Basal	1-D	1/D	H'	CI	MSD
ST	T1P1	1.19	0.71	3.46	1.39	34.91	21.43
ST	T1P2	1.25	0.54	2.17	0.90	19.17	23.03
ST	T1P3	0.92	0.49	1.97	0.84	41.30	11.40
ST	T1P4	1.04	0.66	2.94	1.22	24.89	20.98
ST	T1P5	1.22	0.47	1.90	0.67	24.58	19.92
ST	T1P6	1.42	0.53	2.11	0.88	52.50	16.91
ST	T1P7	1.08	0.54	2.16	0.85	32.38	15.95
ST	T1P8	1.94	0.60	2.52	1.01	70.63	25.17
ST	T1P9	0.47	0.56	2.28	0.90	6.10	11.89
ST	T1P10	0.24	0.62	2.65	1.14	3.46	8.17
ST	T1P11	0.46	0.66	2.92	1.09	23.40	8.06
ST	T1P12	0.79	0.42	1.72	0.69	41.51	10.26
ST	T1P13	0.36	0.26	1.35	0.43	5.76	10.78
ST	T1P14	0.81	0.49	1.97	0.69	15.75	14.62
ST	T1P15	0.28	0.14	1.17	0.27	5.12	6.72
RH	T1P16	0.41	0.00	1.00	0.00	4.34	6.57
RH	T1P17	0.36	0.06	1.06	0.14	10.25	6.79
RH	T1P18	0.36	0.00	1.00	0.00	3.43	7.95
RH	T1P19	0.36	0.30	1.44	0.48	5.30	9.71
RH	T1P20	0.44	0.00	1.00	0.00	6.18	8.30
RH	T1P21	0.27	0.00	1.00	0.00	2.41	7.95
RH	T1P22	0.43	0.00	1.00	0.00	7.10	7.44
RH	T1P23	0.39	0.00	1.00	0.00	6.23	7.19
RG	T1P24	0.63	0.73	3.70	1.42	34.69	9.63
ST	T2P1	0.82	0.77	4.38	1.58	76.07	9.85
ST	T2P2	1.06	0.69	3.20	1.33	40.42	16.75
ST	T2P3	0.84	0.54	2.16	0.90	71.31	8.53

ST	T2P4	0.33	0.52	2.07	0.87	12.01	6.87
ST	T2P5	0.72	0.50	2.00	0.69	19.00	9.62
ST	T2P6	0.82	0.12	1.14	0.24	21.52	10.75
ST	T2P7	1.58	0.20	1.25	0.40	97.01	12.20
ST	T2P8	1.20	0.29	1.41	0.47	17.16	17.28
ST	T2P9	0.94	0.14	1.16	0.26	21.97	12.15
ST	T2P10	0.77	0.13	1.15	0.26	19.26	10.83
ST	T2P11	1.14	0.07	1.07	0.15	27.66	13.14
ST	T2P12	0.57	0.00	1.00	0.00	4.99	9.17
ST	T2P13	0.48	0.00	1.00	0.00	4.20	7.17
ST	T2P14	0.96	0.50	1.99	0.69	32.38	10.35
ST	T2P15	1.30	0.49	1.95	0.68	42.89	12.06
ST	T2P16	0.74	0.00	1.00	0.00	7.85	9.88
ST	T2P17	0.85	0.00	1.00	0.00	16.39	7.68
RG	T2P18	0.90	0.00	1.00	0.00	5.42	14.59
RG	T2P19	0.11	0.00	1.00	0.00	0.19	7.75
ST	T3P1	1.61	0.00	1.00	0.00	5.45	26.12
ST	T3P2	0.92	0.65	2.86	1.18	60.48	11.07
ST	T3P3	1.08	0.79	4.70	1.65	142.02	10.22
ST	T3P4	0.44	0.40	1.66	0.67	9.52	7.75
DT	T3P5	0.33	0.58	2.40	0.95	4.90	7.05
DT	T3P6	0.03	0.64	2.78	1.05	0.04	5.27
DT	T3P7	0.09	0.46	1.85	0.65	0.22	5.35
ST	T3P8	0.21	0.24	1.32	0.49	1.85	6.32
ST	T3P9	0.76	0.00	1.00	0.00	15.97	8.12
ST	T3P10	0.71	0.46	1.86	0.65	21.87	9.15
ST	T3P11	0.94	0.28	1.39	0.59	103.03	7.97
ST	T3P12	0.33	0.54	2.17	0.90	3.80	11.76
ST	T3P13	0.72	0.52	2.07	0.88	26.71	9.92

ST	T3P14	0.50	0.12	1.13	0.23	10.60	8.12
ST	T3P15	0.49	0.42	1.73	0.71	13.83	9.10
ST	T3P16	0.70	0.46	1.85	0.79	46.06	8.53

Note: 1-D: Simpson's index of diversity; 1/D: Simpson's reciprocal Index; H': Shannon-Weaver index; CI: Complexity index; MSD: Mean stem diameter; T: Transect; P:Plot

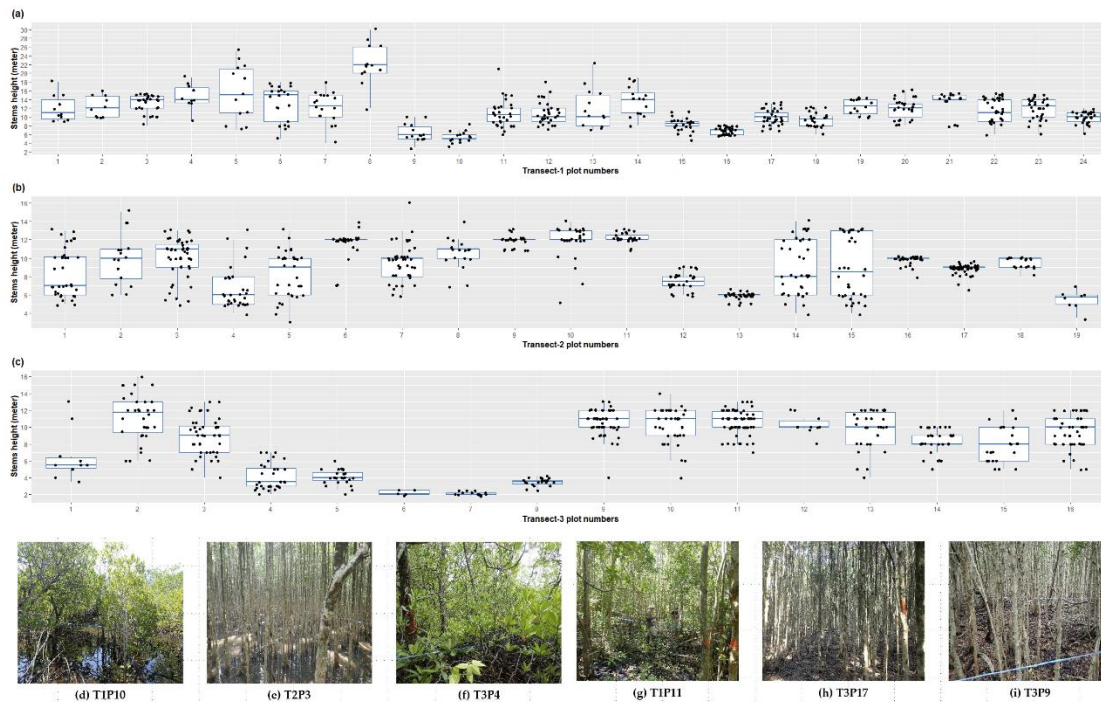


Figure 5.5 Boxplot of the height distribution per plot among the three transect lines in Trat province, Thailand. In subplot, a, b, c, the black dots indicate the height of the individual stems in each plot, which shows the structural diversity within each plot and along the intertidal zones. The median stem height in each plot is identified by the bold line in the middle of each box. The subplot, d, e, f, g, h, i field photo showing the structural (height) variation between the dwarf zones, monocultures, and diverse *Ceriops tagel* species in Trat Thailand; (d) diverse dwarf species; (e) monoculture of tall species; (f); diverse dwarf species; (g) diverse tall species; (h) monoculture of tall species; (i) monoculture of tall species. note: The x-axis indicates the plots per transect line from seaward to landwards, T: transect number; P: plot number.

Most of the natural stand plots were structurally more complex (Table 5.2, Fig. 5.4 and 5.5). The high CI values of the natural stands could be attributed to their higher species diversity and composition. In comparison, the low CI values in the rehabilitated plots could be traced back to their low diversity and the presence of the monoculture (Pimple et al., 2020). The field data also verified the significant differences in height, DBH, and diversity among the *Ceriops tagel* (Fig. 5.4 and 5.5). The result showed the presence of several monocultures and dwarf *Ceriops tagel* plots (Fig. 5.5). The height values of the

three transect lines for available *Ceriops tagal* ranged from 3.00–16.00, 4.00–13.00, and 1.80–13.00 meters and DBH ranged from 1.27–18.93, 2.23–25.45, and 3.50–14.96 cm, respectively. In general, the dwarf and tall *Ceriops tagal* exhibited a higher biodiversity and number of seedlings in Transects 1 and 3 when compared with the tall monocultures in Transect-2. However, the monoculture stands were taller and had larger DBH and basal areas (Table 5.2 and Fig. 5.4).

5.12.3 Mangrove species intertidal and landscape scale distribution

The randomization tests performed within the transect lines indicated that there was no single species zonation, the mean overlap is significantly larger than expected at random. The pairwise observed and simulated mean overlaps were not significant ($p = 0.50, 0.63,$ and 0.60) and the variance was low. The values of the standardized effect sizes indicate the non-significant tail probabilities. The results indicate that the species occurred in groups in distinct patches, and that they were not zoned over the elevation gradient. The randomization test failed to identify any significant patterns of species zonation at the given elevation gradients.

For landscape scale assessment, hierarchical agglomerative clustering was applied to recognise species plots that tended to co-occur in the transect plot samples and group together with similar taxonomic compositions. For linkage based hierarchical clustering, the average linkage method shows the highest cophenetic correlation coefficient (0.75), when compared with the single, complete, and ward's coefficients (0.70, 0.68, and 0.39). Therefore, the average linkage method was selected for clustering. Based on Mantel statistics, the hierarchical cluster analysis generated nine assemblage groups. The hierarchical structure of the clustering and the relative similarities of the mangrove species assemblages are shown in Fig. 5.6. The global average silhouette width value obtained from the nine clusters was relatively low (0.46), indicating that the general affinity among the transect plots was not strong. Only three groups had average silhouette widths greater than 0.50. As expected, there was a stronger affinity among the rehabilitated plots. The average silhouette width values for these groups (8 and 9) were 0.80 and 0.96. The single plots with no shared species (T2P19 and T3P1) showed zero average silhouette width values, indicating that the sample plot could belong to more than one group.

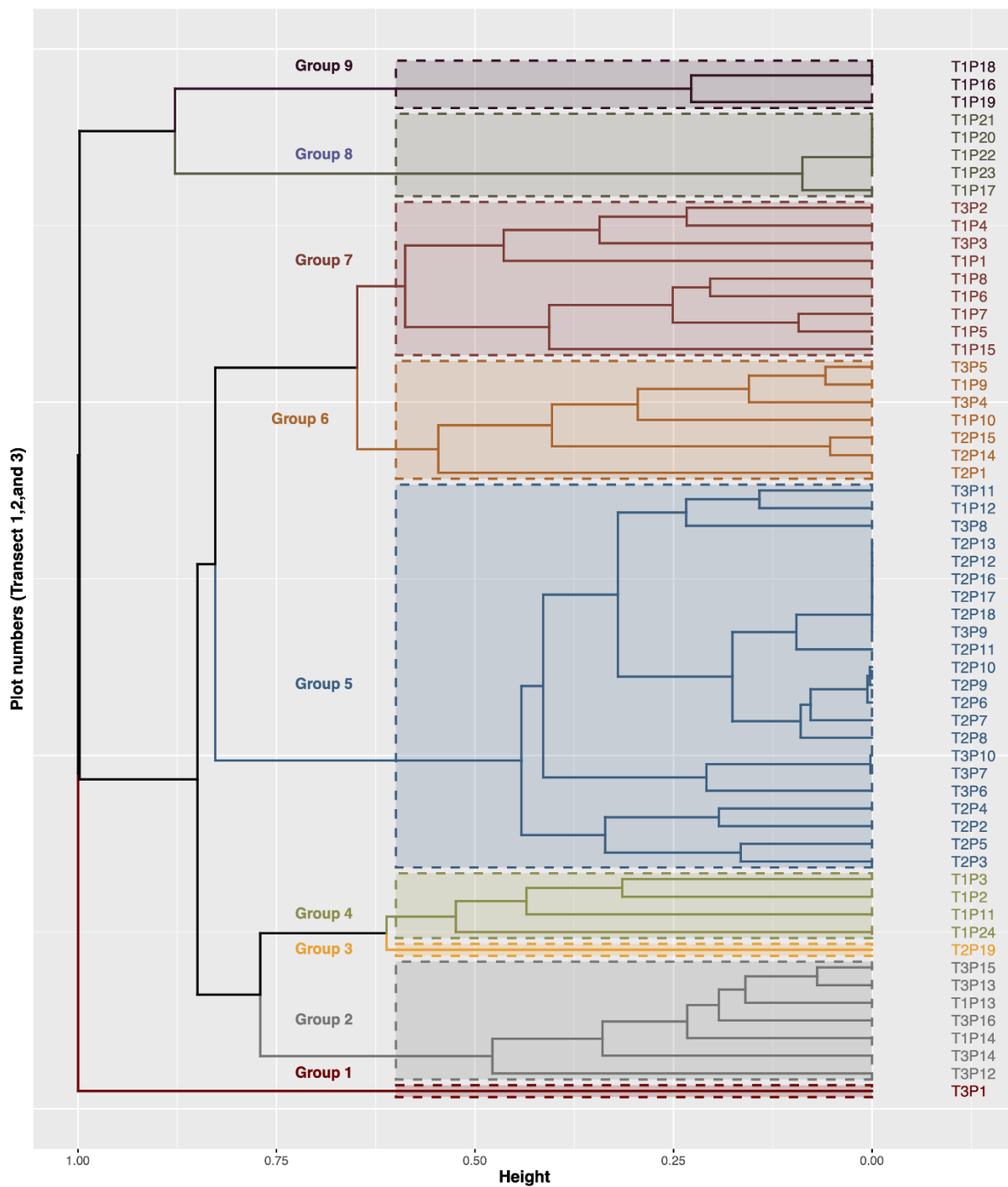


Figure 5.6 Dendrogram generated by average linkage hierarchical clustering, representing the groups identified in the sample plots in Trat province, Thailand. Groups indicate those plots that species tended to co-occur in the transect plot samples and group together with similar taxonomic compositions. Note: T: transect number; P: plot number.

The nine clusters obtained from the hierarchical clustering showed the following characteristics: Group 1 (T3P1), contained a single plot of *Sonneratia alba*. This is a pioneer species that usually prefers high salt conditions, mostly grows on the seaward side, and these areas inundated daily with tidal water (Göltenboth and Schoppe, 2006). Normally, *Sonneratia alba*, *Avicennia alba*, and *Avicennia marina* are observed at the seaward zone. Compared to other locations, the mature stands of this group were considered a monoculture. Group 2 (T1P13-T1P14 and T3P12-T3P16) contained *Bruguiera cylindrical*, *Excoecaria agallocha*, *Rhizophora mucronata*, and *Ceriops tagal* (11.86% of the total sampled area) and was dominated by *Bruguiera cylindrical* and *Excoecaria agallocha*. These plots were in the mid and landward zone. Group 3 (T2P19), contained a single monoculture plot of *Bruguiera gymnorhiza*. This plot was located on the landward side, unlike most of the others that were found on the seaward side. The landscape of this plot was modified and disconnected from the natural mangroves. A single mother tree was observed which is likely to be the source of the propagules. Group 4 (T1P2-T1P3, T1P11, and T1P24) included 6.78% of the total sample area, and was occupied by *Bruguiera gymnorhiza*, *Excoecaria agallocha*, and *Xylocarpus granatum*. The plot T1P24 was present in a modified landscape and appeared to be more diverse compared to other plots available in this group. Group 5 (T1P12, T2P2-T2P13, T2P16-T2P18, and T3P6-T3P11) was the largest cluster in the analysis (37.29% of the total sampled area), was mostly dominated by *Ceriops tagal*. Continuous overlapping positions were observed across all species, and because of this *Avicennia alba* and *Avicennia marina* may have clustered in this group. Group 6 (T1P9-T1P10, T2P1, T2P14-T2P15, and T3P4-T3P5), included 11.86% of the total sampled area with several mixed species. Group 7 (plots: T1P1, T1P4-T1P8, T1P15, T3P2-T3P3), the second largest cluster in the analysis (15.25% of the total sampled area), occupied the seaward zone, and contained *Avicennia alba*, *Bruguiera gymnorhiza*, natural *Rhizophoraceae*, *Xylocarpus granatum*, and *Excoecaria agallocha*. The grouping of T1P15 could be explained by the negative average silhouette width value, which indicates that the sample might have been assigned to the wrong cluster. Group 8 and 9 (T1P16-T1P23) were the largest rehabilitated monocultures of *Rhizophoraceae* (13.56 % of the total sampled area) and were present in the landward zone. The agreement between the Euclidean distance similarity matrix of the elevation indicates a statistically significant positive correlation between the Bray–Curtis similarity matrix for species abundance (Mantel statistics $r = 0.38$ and $p = 0.0001$). This implies a limitation to recruitment, that the plots were more dissimilar in terms of surface elevation, and that they were also dissimilar in term of mangrove species groups. However, the result failed to identify any single or group of species in the discrete zones.

Further, the relationship between the surface elevation and species occurrence was explored based on the average elevation of each species along three transects (Fig.5.7). The lower surface elevations were inhabited by *Sonneratia alba*, *Avicennia alba*, *Avicennia marina*, and natural *Rhizophoraceae*. The seaward zone was occupied by *Bruguiera gymnorrhiza*, *Xylocarpus granatum*, and *Rhizophoraceae*. The *Bruguiera cylindrica* and *Excoecaria agallocha* dominated groups were present from the mid to landward elevation zone. The *Ceriops tagal* is dominant and overlapped throughout the elevation gradient and was observed to have the highest surface elevation (>1.1 m). Apart from *Sonneratia alba* and natural monocultures of *Ceriops tagal*, continuous overlapping positions were observed across all species. The noticeable zones of the rehabilitated *Rhizophoraceae* were located in the most landward zone however the observed mean surface elevation of the plots ranged from 0.5–0.6 m. The topographic variation within this rehabilitated region is attributed to the historic modifications to the landscape for shrimp farming and agriculture (Pimple et al., 2018).

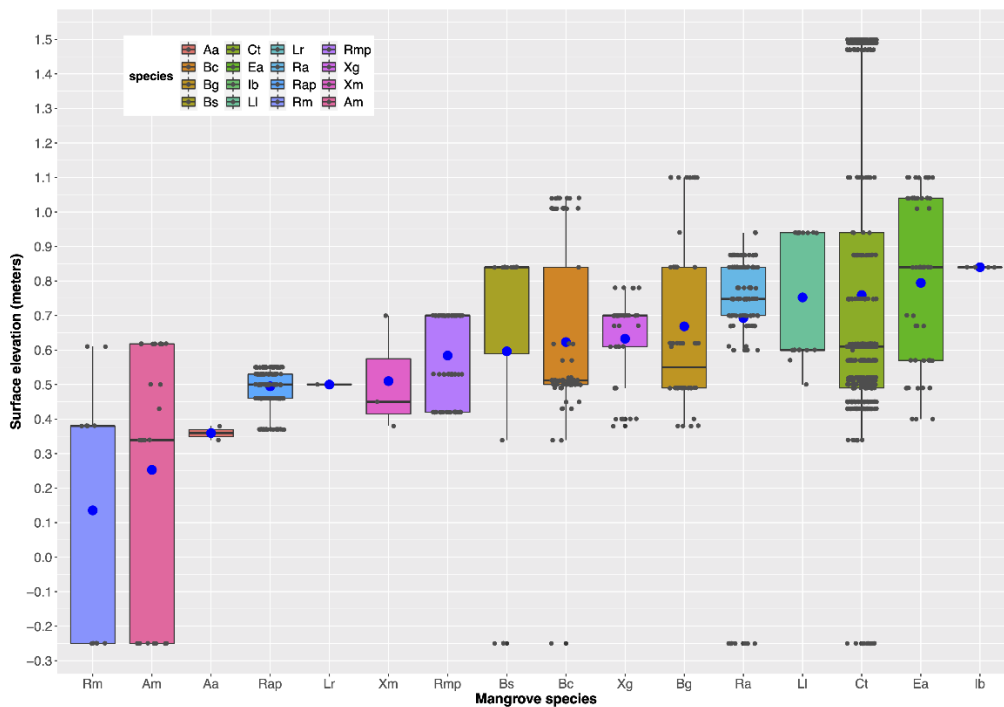


Figure 5. 7 Mangrove species distributions along the average elevation gradients of all three transect lines. Mean and median elevation values for each species are identified using bold blue dots and black bold lines, respectively. Note: Aa: *Avicennia alba*; Am: *Avicennia marina*; Bc: *Bruguiera cylindrica*; Bg: *Bruguiera gymnorrhiza*; Bs: *Bruguiera sexangula*; Ct: *Ceriops tagal*; Ea: *Excoecaria agallocha*; Ib: *Intsia bijuga*; Ll: *Lumnitzera littorea*; Lr: *Lumnitzera racemosa*; Ra: *Rhizophora apiculata*; Rap: *Rhizophora apiculata plantation*; Rm: *Rhizophora mucronata*; Rmp: *Rhizophora mucronata plantation*; Xg: *Xylocarpus granatum*; and Xm: *Xylocarpus moluccensis*.

5.12.4 Mangrove species intertidal and landscape scale distribution

The relative distribution of the temporal dynamics in the NDII pixel values along the three transects from 1987–2020 are presented in Fig. 5.8 and 5.9. The NDII time-series clearly showed the disparities of change among the different forest stands. The result suggests four distinct scenarios as follows: stable undisturbed, rehabilitated, regenerated, and partially disturbed mangroves. The varying tracks in the NDII time series indicated that the recovery process was different in the rehabilitated (Pimple et al., 2020), naturally regenerated, and partially degraded mangroves. The transect plots of the stable undisturbed natural mangroves showed relatively stable NDII values of 0.45–0.78 throughout the observation period (Fig.8). In plot T3P1, the high NDII values during the initial years could be connected to high SWIR reflectance and the lower levels of canopy cover provided by *Sonneratia alba* and *Avicennia alba*. This plot was in the shallow part of the sea and was mostly underwater. The time series pixels for NDII ranging from $0.45 \geq$ and ≤ 0.51 ($NDII \leq NDII_{stable}$) were indicators of scrub mangroves plots and plots underneath mangrove canopy presence of dense of *Acrostichum aureum* (the golden leather fern) in the plots.

The naturally regenerated plots were situated on the landward side which was abandon and not rehabilitated. The naturally regenerated mangroves showed a gradual increase in NDII values with time (1987–2020) (Fig 5.9b). The plot adjacent to rehabilitated mangroves (T1P24) showed relatively lower NDII values and appeared to be more diverse (Fig. 5.4 and 5.9a). The NDII values of the regenerated plots showed high variation during the recovery period among the different transects, with ranges from 0.27–0.67. While the plots adjacent to the natural stable mangroves appeared to be monocultures that were able to maintain higher threshold values than $NDII_{stable}$ ($NDII \geq NDII_{stable}$). After reaching the stable state ($NDII \geq NDII_{stable}$) the rehabilitated stands could closely mimic the NDII values of the stable mangroves. The NDII values of the rehabilitated mangroves ranged from 0–0.76.

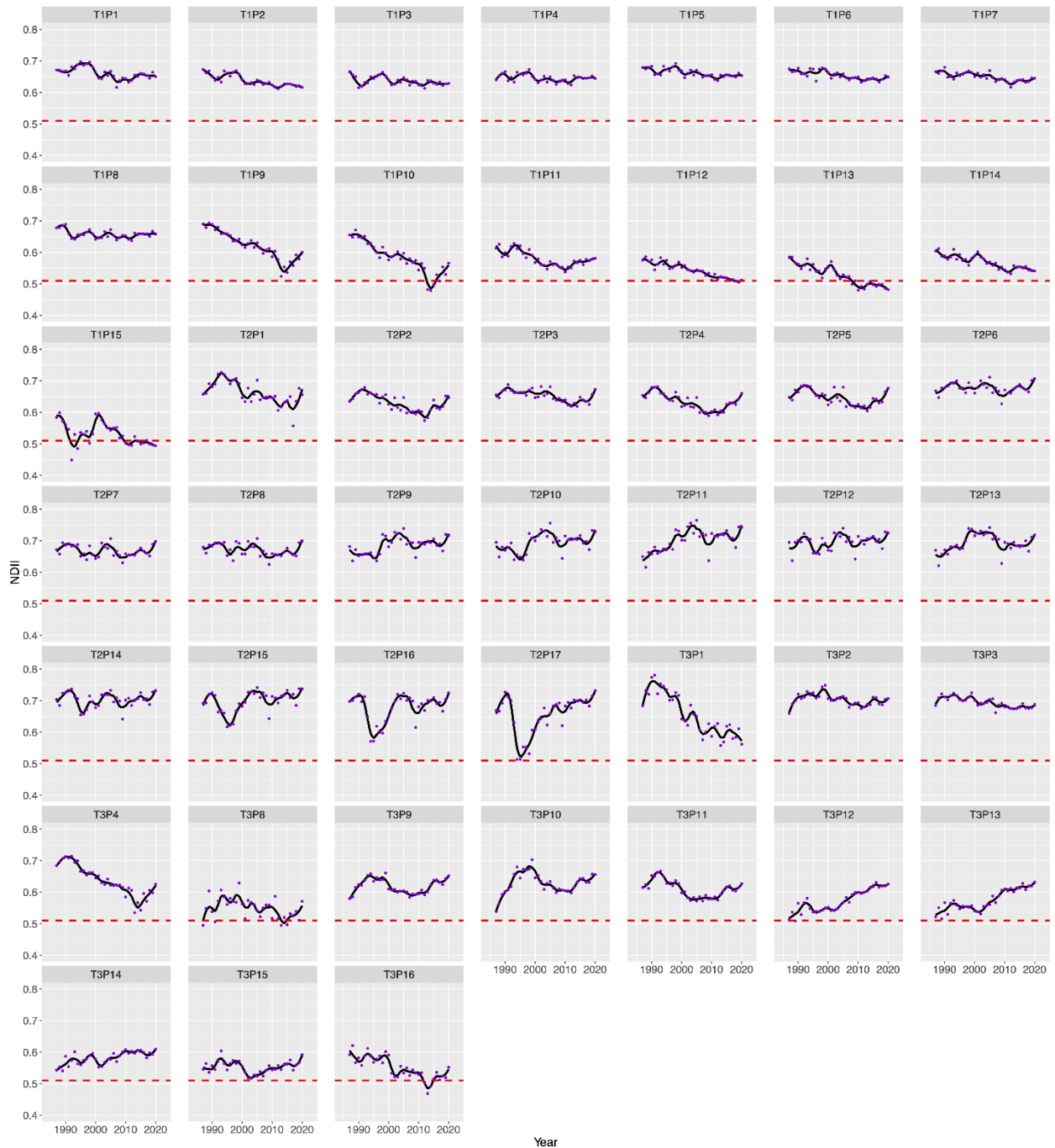


Figure 5.8 Normalized Difference Infrared Index (NDII) trajectories of stable (undisturbed) mangrove stands from 1987–2020. The red dotted lines indicate the stability thresholds. T: transect number; P: plot number.

In the third transect line, plots with scrub *Ceriops tagal* and *Lumnitzera* species showed abrupt changes over time (T3P5–T3P7) (Fig.9 c). Between 1987–2014, these plots continued their downward trajectories ($NDII < NDII_{stable}$), however, after the year 2015, a

continuous upward trend was observed. This indicates that these plots had experienced partial degradation, but that secondary succession processes were likely to have been initiated. The scrubmangrove plots experienced a relatively faster recovery (3–6 years). A similar post-disturbance upward trend was also observed with Sentinel-2 MSI annual composites. Although the Sentinel-2 MSI temporal window used to observe the recovery was relatively short, it allowed for cross-validation of the upward trend identified with the Landsat.

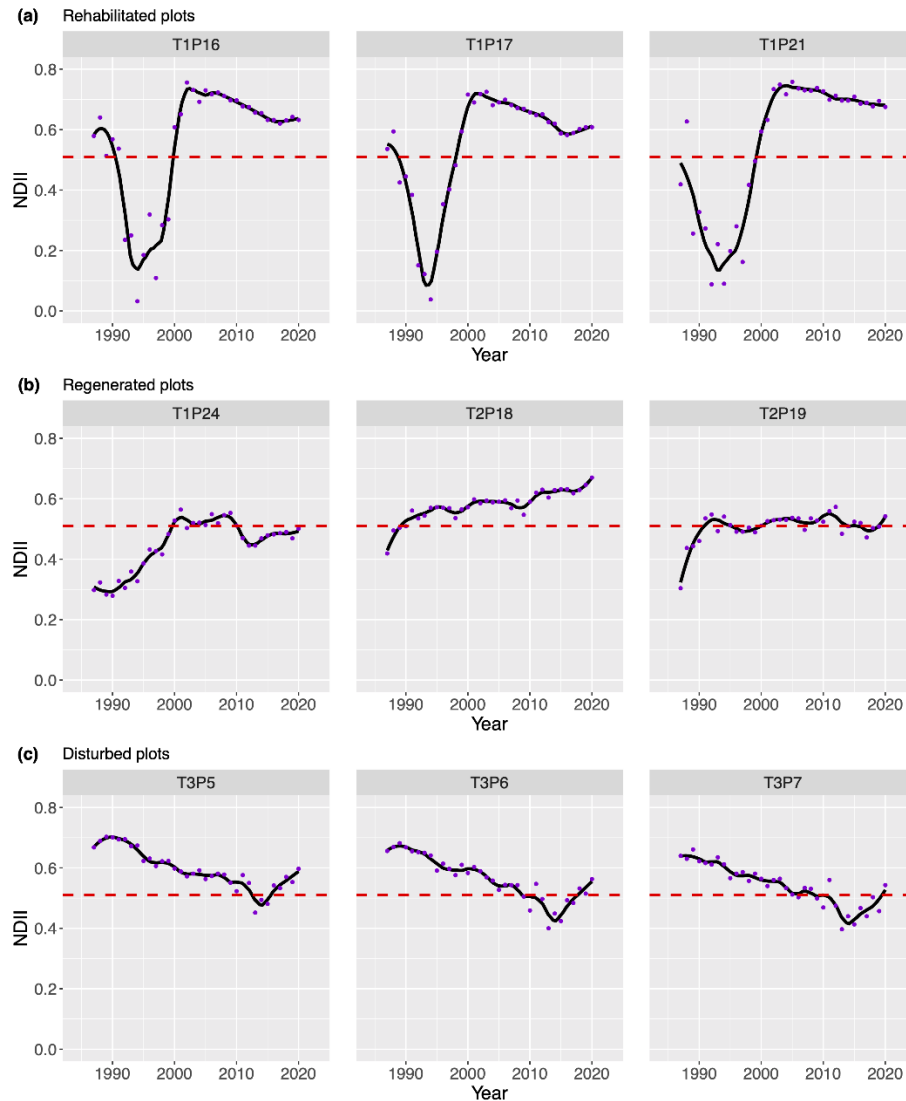


Figure 5.9 Normalized Difference Infrared Index (NDII) trajectories of (a) rehabilitated, (b) regenerated, and (c) disturbed mangrove stands from 1987–2020. The red dotted lines indicate the stability threshold. T: transect number; P: plot number.

A significant association was found between forest categories and species diversity (D , $1/D$, and H') ($F = 6.08, 2.88, \text{ and } 5.02; P = 0.012, 0.04, \text{ and } 0.03$). The complexity index followed a similar pattern ($F = 3.04$ and $P = 0.03$). Higher species diversity was observed in the natural and partially disturbed forests when compared to the rehabilitated and regenerated mangroves. Mixed biodiversity patterns (diverse and monoculture) were observed in the regenerated mangroves, depending on the location of the plots. Overall, the NDII values of natural, rehabilitated, regenerated and disturbed plots showed high variation both among the plot and over a time.

5.13 Discussion

This study provided the unique opportunity to establish a baseline for the mangrove ecosystems in the Trat province of Thailand. It was found that: (1) mangrove ecosystems did not show any systematic zonation patterns for individuals or groups of species; and (2) the temporal dynamics observed indicated that there were different successional processes among the rehabilitated, partially degraded, and naturally regenerated mangroves.

5.13.1 Intertidal characteristics and distribution of the mangrove ecosystems

Findings indicate that mangrove species apportion niche spaces, but there is limited evidence of the zonation patterns for any single species at a given elevation gradient. Interpretation of within transect and landscape-scale clustering indicated that there were significant overlaps. Five large groups were detected using the spatial dissimilarities in the taxonomic and composition assemblages. The average silhouette width indicated that species zonation might not be present in this study site. It is worth noting that the monoculture stands (no shared or rehabilitated species) could yield low or high average silhouette widths, which affected the global average. Therefore, careful evaluation is crucial to identify any unintended influences on the results from the landscape-scale analysis.

The findings are in agreement with the hypothesis of limited zonation or the random placement of mangrove communities, that was previously proposed by (Ellison et al., 2000). Recently, Leong et al. (2018) and Schmiegelow and Ganesella (2014) reported significant species overlap along the elevation gradient of the Mandai mangroves in Singapore and the absence of zonation in southern Brazil. However, significant differences in tree height were observed, particularly between the seaward-mid-landward zones (Fig. 5.5). The structural differences (Table 5.2) indicated that the

growing conditions may vary along the elevation gradient, and differences in soil structure and nutrient availability may have a notable influence (Ewel et al., 2013; Feller et al., 2010). The regimes for tidal flooding are considered the important determinants of mangrove species distribution. However, tidal regimes are not likely to be homogenous over a larger spatial scale, due to the variability and modifications in topography and canal networks. In such conditions species distribution patterns likely to be determined by flooding regimes that are experienced at much finer spatial scales (Raulings et al., 2010). Raulings et al. (2010) reported that the heterogeneity of water regimes at small spatial scales drives the vegetation patterns. Furthermore, modifications of surface elevation, artificial canals, and effluent discharges may have contributed to changes in the hydrodynamics and nutrient availability (Hickey and Bruce, 2010; Vaiphasa et al., 2007). Interspecific competition and propagule dispersal may also play a more important role than edaphic variables in controlling the size and abundance of co-occurring species (Ellison et al., 2000). Nevertheless, in this study site our understanding of the spatial zones and intertidal distributions of mangrove species at the landscape scale is still limited in relation to edaphic properties. Further investigations and soil measurements would help to improve our understanding of the role of edaphic variables in mangrove biodiversity.

5.13.2 Indicators of ecosystem diversity state and succession

The term “state” has been commonly used to indicate the shift of vegetation or dominant species (Fu et al., 2017). We used “state” to identify a present status of the mangrove as characterized by a set of temporal (Beisner et al., 2003) dynamics using the NDII variable and to provide an algorithm (ARMA) to quantify the changes in the ecosystem. This study provides empirical evidence of species diversity along the intertidal zone and its secondary succession. We evaluated Landsat annual composite based temporal dynamics, and the results obtained in this study will be useful when identifying the status, biophysical properties, and state of diversity after secondary successions. The species diversity, complexity, and NDII of the natural undisturbed mangroves had higher values than the other stands.

The long-term NDII values indicated that the growth of rehabilitated mangrove stands was consistent over the previous 30 years (Pimple et al., 2020). The obtained biophysical properties showed that the rehabilitated mangroves appeared to be monocultures (*Rhizophoraceae*), had high tree densities, and seedlings of natural species failed to establish there (Pimple et al., 2020). The rehabilitated mangroves had a thinner canopy layer than the natural stands. This is because the seedlings were planted with a spacing

of less than or equal to 1.5×1.5 m (Macintosh et al., 2002). Several studies reported similar behavior in rehabilitated mangroves (Asaeda et al., 2016; Barnuevo et al., 2017; Chen et al., 2012; Proffitt and Devlin, 2005). However, these stands were able to reach the same height as those of the natural stands. Furthermore, they did not differ in their available canopy gaps. The high tree density in the rehabilitated plots reflects aspects of the rehabilitation practices in the study site (Walters, 2000). First, the high number of stems and the low basal area could be due to the high planting density and geomorphic location. Second, there was negligible evidence that rehabilitated stands facilitated the growth of natural mangrove seedlings.

The naturally regenerated plots were located to the landward area that was abandoned. The NDII trajectories of the naturally regenerated mangroves showed a gradual recovery over the 34-year period, but species diversity varied based on location. For example: 1) species were diverse in the areas adjacent to the rehabilitated mangroves; 2) there were monocultures adjacent to the natural mangrove stands (T2P18); and 3) open patches detached from the mangrove stands resulted in monocultures that originated from the available mother tree (T2P19). The first phenomenon supports previous studies that reported the natural recolonization of diverse species along the edges of rehabilitated mangroves in Vietnam and Brazil (Reis-Neto, et. al., 2019; Van Loon et al., 2016). This could be explained by the phenomenon of propagule dispersal limitation. Artificial drainage canals were observed on the border between the mangrove forest and the mainland area, and they were connected to natural canals. These canals enabled the inflow of propagules during high tides and facilitated natural regeneration (Di Nitto et al., 2014; Triest et al., 2020). Consequently, regeneration could be slow due to restrictions that limit tidal inundations, dispersal, and the establishment rate of other seawards species (McGuinness, 1997; Oh et al., 2017; Robert et al., 2015). The adjacent natural forest or the presence of parental trees could provide an adequate propagule supply for dispersal to the nearest colonisable areas (Di Nitto et al., 2014). The plot T2P18 and T2P19 shows a similar growth response. T2P18 is located adjacent to the natural zone of the *Ceriops tagal* and resulted in monocultures of the same species. While T2P19 is a modified landscape that was occupied by a monoculture of *Bruguiera gymnorhiza*. This behavior can be attributed to the presence of parent trees, which were most likely to be the source of the propagules. Smith (1987) reported the best seedling establishment when the adult conspecific was least abundant on the landward side. Bosire et al. (2003) reported natural colonization and high-density seedling establishment for other mangrove species due to the availability of adult trees.

Our analysis of plots T3P5–T3P7 revealed that the partial disturbance and recovery affected the scrub *Ceriops tagal*. Although this disturbance was not reported in previous literature or the local database, there is sufficient temporal evidence to speculate that the development of shrimp farming and dredged shrimp farms waste in the mangrove canals may have contributed to this disturbance. These results support the recent findings of (Vancutsem et al., 2020), who reported disturbances in similar locations. Recent studies have reported the short-term and direct effects of shrimp farm waste discharge (excess sediments) on mangrove growth, mortality, and colonization (Capdeville et al., 2018; Tian et al., 2018; Vaiphasa et al., 2007). However, very little is known about the long-term impacts on mangrove ecological functions (Wolanski et al., 2000). In this study, the recovered mangroves were found to have moderate diversity and were structurally less complex when compared to the natural stands.

5.14 Implications for mangrove conservation management

The temporal effects on mangrove biodiversity have not received the same amount of research attention as the spatial distribution of biodiversity (Wang and Gamon, 2019). This is in part because of: (1) the limited mangrove species data available for intertidal zones; (2) considerations of environmental (Ellison et al., 2020) and anthropogenic settings; and 3) the limited knowledge available on the temporal changes in biodiversity due to biotic, abiotic, and anthropogenic stressors (Sarker et al., 2019). The proposed methodological framework will be beneficial when developing action plans to monitor the health and diversity of natural as well as restored mangrove ecosystems in the region. Understanding the long-term effects, underlying processes, and baselines of the ecosystem is fundamental when trying to improve management practices. Furthermore, this information could provide a more realistic spatial validation for restoration modeling. Recent approaches combined hydrodynamic modeling with mangrove vegetation modelling, such as the MANGA modeling framework, and predicted mangrove growth from the ground elevation, flooding regime, and subsurface water flow such as the MANGA modeling framework (Bathmann et al., 2020; Peters et al., 2020a). In particular, the reconstruction of the recent history of mangrove stands and the identification of the causes for their disturbances and developments may help to verify mechanist modelling approaches and improve our understanding of the drivers behind forest development. The temporal dynamics may also help ecologists or forest practitioners to identify the field observations that should be collected, the analytical approach to be used, and the interpretation of the results of independent of single observations. Our approach, thus, provides a more robust method to monitor restoration efforts and the ecosystems in general.

5.15 Conclusions

Mangrove forest status, such as the intertidal patterns of the species assemblages, long-term effects underlying the biotic, abiotic, and environmental settings, and the effects of conservation interventions are crucial for ecosystem sustainability, future conservation efforts, and policy development. Assessing the complete historic dynamics and present status requires a robust systematic and synoptic approach. We successfully integrated historic multi-satellite annual composites with current ecological and micro-topography measurements to establish a historic change and present status for mangrove forests in the Trat province of Thailand, that could be summarized using the type of functional indicator.

The current baseline or state of diversity was identified and included the results of previous rehabilitation efforts. The results showed that there was no zonation of single species or group of species along the elevation gradient, which suggested that the mangrove communities occurred randomly. However, structural diversity varied greatly along the elevation gradients. The stable or undisturbed natural mangroves were consistent, and no abrupt changes were observed. The required stability period for the rehabilitated mangroves ranged from 7–13 years. Regardless of the gradual recovery over the 34-year period assessed, the species diversity varied greatly among the naturally regenerated mangroves. The effluent from the shrimp farming may partially disturb the dwarf *Ceriops tagal*. However, observations in recent years have shown a significant recovery.

The approach developed here and the modified ARMA algorithm provide comprehensive information on the historic state of mangrove ecosystems, that could have several potential applications in restoration management planning, and therefore, is a useful tool to measure and evaluate biodiversity to characterize ecosystem-based mangrove forest management.

CHAPTER 6

Spatio-temporal dynamics of mangrove species diversity



Mangroves during high tide in Trat province of Thailand

This chapter has been produced from: Pimple, U., Simonetti, D., Leadprathom, K., Podest, E., Sitthi, A., Pungkul, S., Pravinongvuthi, T., Dessard, H., Peters, R., Berger, U., Gond, V. (2021) Spatio-temporal dynamics of mangrove species diversity using multi-source Earth observations and improved ground inventories in the Google Earth Engine; Submitted for publication

Abstract:

The United Nations decade on ecosystem restoration (2021 to 2030) lists coastal ecosystems such as mangroves as a priority for restoration. Understanding the spatial patterns of species is crucial for predicting ecosystem health, viability, and resilience against a changing climate, as well as for the modeling of restoration measures. Regardless of the advances in remote sensing technologies, various sources of noise affect satellite imagery in coastal areas, rendering it difficult to discriminate large scale spatial species typologies and their temporal changes. Besides, the complex structure, environmental and anthropogenic settings, and lack of proper integration of systematic field inventories render it a notoriously difficult ecosystem to examine. To address this, we developed a systematic workflow based on a robust systematic sampling design, homogenized Landsat 34-year time-series, modified Automatic Regrowth Monitoring Algorithm (ARMA), and the use of error-free spectral and backscatter composites (Sentinel-1 and -2) in the Trat Province, Thailand. Tidal inundation alters the spectral and backscatter properties of an image and thus the heterogeneity of species features. The low tide Landsat-8 and Sentinel-1 and -2 composite-based classification resulted in an overall accuracy of 0.85 and 0.65. The spectral confusion was attributed to the presence of rehabilitated and mixed Rhizophoraceae, which resulted in a reduced producer's accuracy. Further, the ARMA system was suited to recreate the secondary succession history (i.e., discriminating rehabilitated and regenerated stands) and identify unchanged nature forest stands. The combination of the Sentinel-1 and -2 composites achieved better results than Landsat-8 alone and was able to discriminate among six classes, including three single species and three species associations. Our approach demonstrates the full potential of the Landsat time-series, as well as the error-free Sentinel multi-spectral and synthetic aperture radar sensors with improved systematic field inventories, which can all discriminate mangrove species and their associations.

6.1 Introduction

Mangrove ecosystems can be found throughout the tropical and subtropical regions of the world (Duke, 2017; Tomlinson, 2016). Mangrove forests are one of the most vulnerable ecosystems to natural and anthropogenic disturbances. Lightning, insects, disease, tropical storms, changes in sea level, agriculture, wood and wood product extraction, waste discharge from shrimp farms and other industrial waste, industrialization, and tourism are the natural and anthropogenic factors that affect mangroves at varying spatial and temporal scales (Allen et al., 2001; Ellison and Farnsworth, 1996; Giri et al., 2015; Vaiphasa et al., 2007). Mangroves are critically endangered in 26 out of 120 countries (Duke et al., 2007). Rates of mangrove deforestation have declined globally, although countries like Myanmar and Malaysia are still facing high loss (Friess et al., 2019; Goldberg et al., 2020). Besides, knowledge on species diversity remains limited in many parts of the world. Mapping mangrove species is crucial for understanding their fundamental biology, responding to environmental change, aiding conservation efforts, and observing their integrity for providing goods and services (Wang et al., 2018; Wang et al., 2004). Therefore, efficient conservation efforts require a suitable decision support system tool for a local to regional scale assessment.

Remote sensing has been widely used in mangrove studies, such as mapping of the areal extent, identifying species, and estimating parameters, such as the leaf area, canopy height, and biomass (Spalding et al., 1997; Wang et al., 2019). Recently, many studies have provided comprehensive historical overviews based on aerial photography, optical and Synthetic Aperture Radar (SAR), and methodologies highlighting the current limitations in mangrove research (Cárdenas et al., 2017; Dat Pham et al., 2019; Kuenzer et al., 2011; Lucas et al., 2017; Wang et al., 2019). Several studies have focused on mapping the mangrove extent at various landscape scales using medium-low resolution imagery (Alsaaidh et al., 2013; Baloloy et al., 2020; Bunting et al., 2018; Giri et al., 2011; Nguyen et al., 2013; Rogers et al., 2017; Wang et al., 2019; Zhao and Qin, 2020). However, in the past decade, most studies have focused on mangrove extent mapping (Wang et al., 2019), whereas studies on remote sensing based mangrove species or species association mapping have been limited.

Moreover, identifying mangrove species and their associations using remote sensing imagery is challenging (Heenkenda et al., 2014; Heumann, 2011) as there are only few studies that have focused on long-term classification (Wang et al., 2004). In the past,

studies that compared the performance of medium resolution imagery (such as Landsat and SPOT) indicated that high-resolution imagery is important for identifying mangroves species (Gao, 1998; Green et al., 1998; Wang et al., 2004). Studies that have assessed the performance of high-resolution satellite imagery, such as IKONOS, QuickBird, RapidEye, GeoEye, and WorldView-3, found that these images can discriminate among mangrove species zones (Huang et al., 2009; Roslani et al., 2013; Wang et al., 2004; Wang et al., 2008; Wang et al., 2016). Viennois et al. (2016) used a time-series of four very high-resolution multispectral images to show the fine-scale spectral response of four Asian mangroves species. Spatial coherence is an important attribute for large-scale mapping, especially with the involvement of multi-temporal data (Jia et al., 2018). Aerial photographs, high-resolution imagery, and hyperspectral imagery often have several limitations that restrict their application to mangrove ecosystems. The major limitations involve the availability of relatively few spectral bands, a very high spatial resolution that only covers a small area and lower frequency imagery, the presence of persistent clouds and their shadows in coastal areas, radiometric inconsistencies, and on-demand access with high associated costs (Aslan et al., 2016; Kuenzer et al., 2011; Son et al., 2015).

Several studies have used Landsat, SPOT, and Sentinel-2 multispectral instrument (MSI) imagery for mangrove extent mapping, but few studies have attempted to harness its full potential for species-based classification (Aslan et al., 2016; Bullock et al., 2017; Ghosh et al., 2016; Rogers et al., 2017; Wang et al., 2018). Recently, Giri et al. (2014) and Rogers et al. (2017) explored the potential of Landsat data, in which they were able to discriminate the extent of five mangrove zones. Jusoff (2006) reported on the sensitivity of the near-infrared range (700–900 nm) to mangrove species identification. However, there are four major barriers: 1) persistent cloud cover and its shadows (Wang et al., 2019), 2) the effect of periodic inundation on satellite imagery, 2) mangrove classification using sensors with a relatively low radiometric resolution (8 bit or 256 grey levels), and 3) the ability of the mangrove classification methods (Aslan et al., 2016). Several classification approaches have emerged (Lucas et al., 2017; Pasquarella et al., 2016; Pham et al., 2019a; Wang et al., 2018) since the recent launch of freely available (high temporal and spectral resolutions) Landsat-8 OLI, Sentinel-1 (SAR) and -2 (MSI), and PlanetScope time-series imagery and the development of high performance cloud computing platforms (such as Google Earth Engine).

Another challenge for mangrove mapping is the presence or absence of water underneath the mangrove canopy. Tidal inundation may affect the texture analysis and the reflectance values for a sparse canopy or scrub mangroves (Kuenzer et al., 2011; Lucas et al., 2017; Proisy et al., 2007; Rogers et al., 2017). Areas with changes in tidal levels often result in contrasting spectral signatures and different mapping outcomes (Li et al., 2019; Zhang et al., 2017). Hence, there is a lack in the understanding of the effect of tidal inundation or their periodic fluctuations on satellite spectral reflectance values in mangrove forests (Maurya et al., 2021; Wang et al., 2019). This phenomenon further limits the temporal assessment of mangrove distribution, if adjacent cloud-free scenes have been acquired at different tidal stages (Rogers et al., 2017). Rogers et al. (2017) proposed that the image composites of high and low tides should improve the capacity to detect a community composition by leveraging the spectral differences between mangrove zones at low and high tides. The best method to overcome these problems is to create cloud free composites from all available scenes at a similar tidal stage and use the statistical robustness of the median over the composites (Pimple et al., 2018; Rogers et al., 2017; Sagar et al., 2017).

Studies have also used pixel-based supervised classifiers, such as Maximum Likelihood, for mangrove species classification (Giri et al., 2014; Sulong et al., 2002), but they often result in “salt-and-pepper” effects. Object-based image classification (OBIC) has been shown to be more accurate and robust than pixel-based classifiers (Jia et al., 2019; Son et al., 2015). However, OBIC requires extensive prior knowledge of the study area, which may be a limiting factor with respect to the classification accuracy (Son et al., 2015). Recently, the application of non-parametric classifiers for studying mangroves has increased (Pham et al., 2019b; Pimple et al., 2018; Rogers et al., 2017; Wang et al., 2018, 2016). Machine-learning classifiers have the capability and robustness to resolve complex classification problems for high dimensional data. Recently, the random forest has become one of the most popular classifiers (Jhonnerie et al., 2015). The advantages of random forest are its potential to determine the importance of variables, its robustness to data reduction, no tendency to over-fit, the production of an unbiased accuracy estimate, and a higher accuracy than decision trees with a lower sensitivity to tuning parameters (Jhonnerie et al., 2015; Shen et al., 2016). However, the application of a machine learning classifier (Jhonnerie et al., 2015), deep learning architecture, and data integration techniques for mangrove species classification remain limited.

The selection of a systematic sampling design across a mangrove forest landscape is crucial in obtaining a complete list of species covering their spatial and intertidal distribution (Pimple et al., 2020). Recently, several remote sensing-based area proportional stratified random sampling approaches have been investigated in forestry (Grafström et al., 2014; Köhl et al., 2006; Olofsson et al., 2014; Wallner et al., 2018). However, such systematic sampling strategies have rarely been used in mangrove studies, thus resulting in a limited understanding of the species and species associations in each ecosystem, as well as limited or uncertain data to train and test the classifiers.

The above information implies that the mapping accuracy of mangrove forests evidently depends on 1) the tide level when using a single date image (Zhang et al., 2013), 2) the availability of clouds and their shadows, 3) the temporal consistency and radiometric stability of the spectral reflectance, 4) the classifiers used, 5) the selection of the systematic sampling design, and 6) the temporal dynamics of conservation interventions. Therefore, a more robust and suitable image selection, classifier training and testing, and systematic field data collection approach is required for discriminating mangrove species. This study aims to develop a novel systematic approach to determine the gap and error free wall-to-wall change dynamics and current spatial pattern of mangrove typology in the Trat Province, Thailand. The specific objectives are to 1) evaluate the influence that tidal inundations have on satellite imagery; 2) exploit the annual composite-based time-series to determine the temporal changes or secondary successions; and 3) explore the full potential of freely available medium- (Landsat) and high-resolution (a combination of Sentinel-1 SAR and -2 MSI) satellite imagery and the machine-learning classifier to identify mangrove species and their associations. The proposed framework not only aids in obtaining species distribution information at each study site, but will also provide a tool for enhancing larger spatial scale monitoring capabilities.

6.2 Study area and dataset

6.2.1 Study area

The study area was the Trat Province, which is located along the eastern coast of the Gulf of Thailand and borders Cambodia (Figure 6.1) (Pimple et al., 2020, 2018). The mangrove forest covers approximately 106 km² and is located at longitude 102.61° and latitude 12.21°. The region experiences a tropical climate with seasonal monsoons (Pimple et al., 2020, 2018). The rainy period is from June to November, with an average annual rainfall and mean temperature of 4,500 mm and 26.5–29.8 °C, respectively (Chalermchatwilai et

al., 2011). This study site contains a large area of natural mangrove stands characterized by the most common natural species found in Thailand and large areas have been rehabilitated without adequate site assessment, resulting in a *Rhizophoraceae* monoculture in most of the rehabilitated zone. However, over the past 30 years, these stands have been able to reach the same height as those of the natural stands, but have been unable to mimic the diversity found in a natural forest. The study contains a zone of landward forest that had been destroyed for shrimp farming and agricultural activities, but has subsequently been naturally regenerated (Pimple et al., 2020, 2018). The following 18 genera of mangroves can be found in the study area: *Sonneratia alba* (Sa), *Sonneratia ovata* Backer (So), *Avicennia alba* (Aa), *Avicennia marina* (Am), *Bruguiera cylindrica* (Bc), *Bruguiera gymnorhiza* (Bg), *Bruguiera sexangula* (Bs), *Ceriops tagal* (Ct), *Ceriops decandra* (Cd), *Excoecaria agallocha* (Ex), *Intsia bijuga* (Ib), *Lumnitzera littorea* (Ll), *Lumnitzera racemosa* (Lr), *Rhizophora apiculata* (Ra), *Rhizophora mucronata* (Rm), *Xylocarpus granatum* (Xg), *Xylocarpus moluccensis* (Xm), and *Scolopia macrophylla* (Sm) (Pimple et al., 2021; Pimple, 2020; Pimple et al., 2020). Section 3.4.1 presents the detailed data collection procedure.

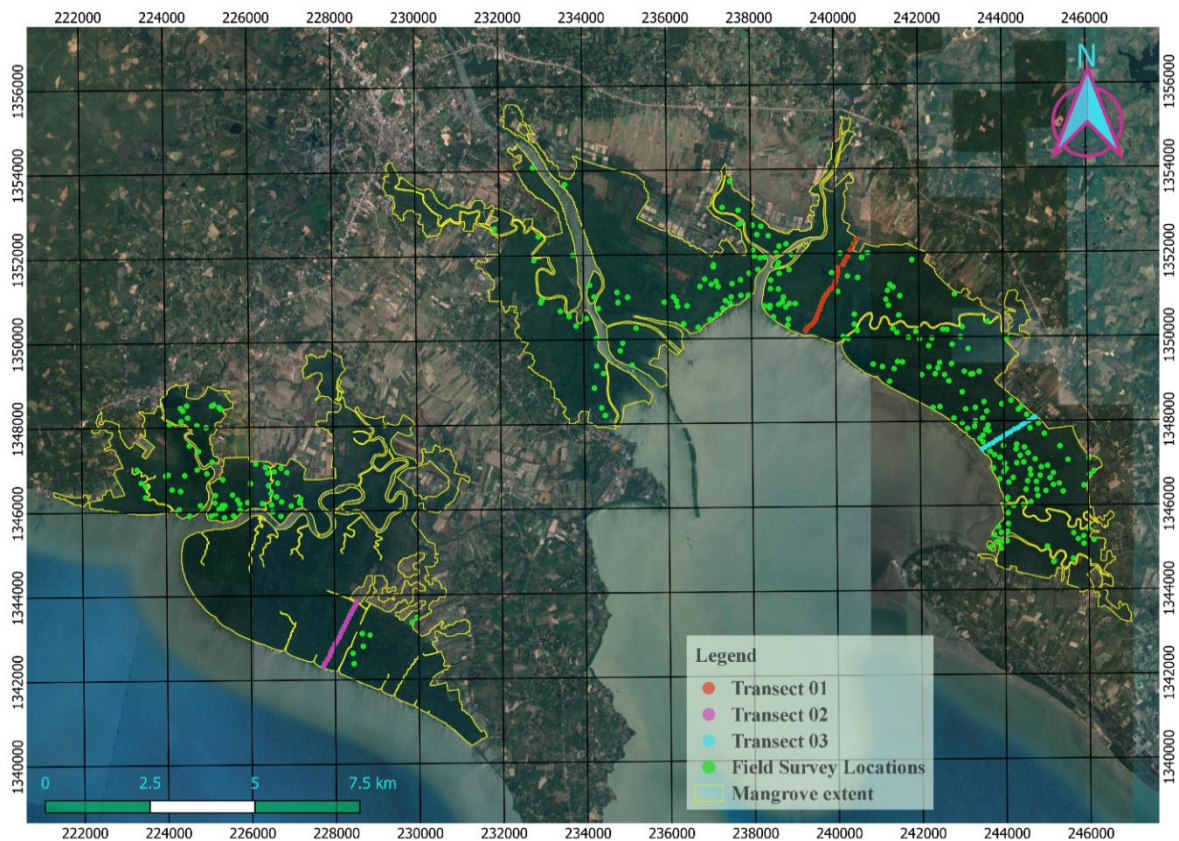


Figure 6.1 Location of the study site in the Trat Province, Thailand, and the spatial distribution of mangroves along three transect lines with the field inventory plots.

6.2.2 Landsat annual composites

In this study, for the time-series data, we obtained the Tier 1 top-of-the atmosphere (TOA) collection from the Google Earth Engine (GEE) for Landsat TM-5 (1987–2001 and 2003–2011), ETM+ (2002 and 2013), and OLI-8 (2013–2020). All images were acquired between January 1, 1987, and January 1, 2021. The Tier 1 Landsat collection is suitable for time-series analyses, as it includes Level-1 Precision Terrain processed data with inter-calibrations across the different Landsat sensors. Only the red, green, blue, near-infrared (NIR), shortwave infrared (SWIR)-1, and SWIR-2 bands were processed in the Universal Transverse Mercator zone 48N projection. Clouds, cloud shadows, and pixels with no-data were removed from the entire collection following the algorithm proposed by (Pimple et al., 2020, 2018). Jagged pixels at the edges of Landsat images were removed using a 450 m inward buffer, which yielded the best available reflectance values for image analysis (Pimple et al., 2018; Robinson et al., 2017). Seasonal low tide annual composites were created using the median reflectance values from the collection (Pimple et al., 2018, Sagar et al., 2017), after removing clouds, cloud shadows, and no-data pixels following the algorithm proposed by (Simonetti et al., 2015) available in GEE and further adopted to mangrove forests (Pimple et al., 2020, 2018). This algorithm is driven by predefined knowledge-based rules built upon the spectral signature collected at a global scale, which then generates a thematic output, including a cloud and cloud shadow mask. Considering the sensitivity of the mangrove pixels to various environmental and atmospheric variables, potentially contaminated pixels were aggressively removed to ensure a meaningful classification.

6.2.3 Sentinel-2 MSI composites

The Sentinel-2 MSI imagery contains 13 UNITS 16 spectral bands representing the TOA reflectance obtained from the GEE image collection. To ensure a meaningful comparison of data obtained from the different sensors, the red, green, blue, NIR, SWIR-1, and SWIR-2 bands of Sentinel-2 were selected. Zhang et al. (2018) noted that the Sentinel-2A MSI Level-1C cloud mask product is not currently reliable. In this study, similar to Landsat, the clouds, cloud shadows, and no-data pixel masks were generated using predefined knowledge-based rules built upon the spectral signature collected at a global scale. The low tide composites were created using the median reflectance values from the collection, after removing clouds, cloud shadows, and no-data pixels. The Sentinel-2 SWIR-1 and SWIR-2 bands, which are acquired at a 20-m spatial resolution, were resampled to 10-m

resolution to match their resolution to the red, green, blue, and NIR bands and obtain a layer stack of six spectral bands.

6.2.4 Sentinel- 1 SAR composites

The Sentinel-1 data was obtained from a dual-polarization C-band SAR instrument. Within the GEE environment, the images were pre-processed for border noise removal, thermal noise removal, and radiometric calibration and orthorectification (Slagter et al., 2020). Further pre-processing included additional border noise correction and speckle filtering (Mullissa et al., 2021). Terrain normalization was not applied considering the uncertainty in the Shuttle Radar Topographic Mission (SRTM) and Advanced Spaceborne Thermal Emission and Reflection Radiometer Global Digital Elevation Model (ASTER GDEM) elevation data over a mangrove forest.

6.2.5 DEM

The National Aeronautics and Space Administration SRTM 30 m x 30 m high-resolution DEM was obtained from the U.S. Geological Survey and resampled using a nearest neighborhood transformation (Wu et al., 2016). Mangrove forests can grow above mean sea level in the intertidal zones of marine coastal environments and estuaries. An additional elevation parameter DEM was used to discriminate between mangrove forests and other vegetation. The DEMs allowed the separation of mangrove pixels located within lowlands and other vegetation located in highland areas (Alsaaidh et al., 2013).

6.2.6 Tide gauge data

Tidal gauge station data from Laem Ngop station in Trat Province (12°10'7" N, 102°12'45" E) were obtained from the Marine Department (Bangkok office), Ministry of Transport, Thailand. For this study, hourly tide level records were used to obtain the high and low tides during the satellite acquisition period.

6.3 Data preparation

6.3.1 Mangrove forest normalization

The TOA imagery was atmospherically corrected using a Dark Object Subtraction (DOS) method (Bruce and Hilbert, 2004). For the DOS, all images were adjusted using a forest normalization method, (Eq. [6.1]), which uses the median value of a mangrove forest to apply a linear shift to each spectral band (Bodart et al., 2011; Pimple et al., 2020):

$$\varphi_{\text{adjusted}}^{(\lambda)} = \varphi_{\text{original}}^{(\lambda)} - \bar{X}_{\text{forest}}^{(\lambda)} + \bar{X}_{\text{ref}}^{(\lambda)} \quad 6.1$$

where $\bar{X}_{\text{forest}(\lambda)}$ is the median value of a dense mangrove forest in the sample size for band λ and $\bar{X}_{\text{ref}(\lambda)}$ is the reference dense mangrove forest value for band λ computed from representative areas visually selected in 30 images (1987–2020) across the study area.

6.3.2 NDVI

The normalized difference vegetation index (NDVI) is the most widely used spectral vegetation index to indicate vegetation density or greenness and differentiate areas with non-vegetation or non-mangrove with mangrove based on satellite imagery (Kuenzer et al., 2011). NDVI is calculated using the red and NIR bands (Green et al., 1998) as follows:

$$\text{NDVI} = \frac{(\text{NIR} - \text{Red})}{(\text{NIR} + \text{Red})} \quad 6.2$$

where red is the reflectance in the visible wavelength channel (0.63–0.69 μm) and NIR is the reflectance in the near-infrared wavelength channel (0.70–0.90 μm). The NDVI equation is based on the fact that the chlorophyll present in vegetation absorbs red while the mesophyll leaf structure scatters NIR. NDVI values range from -1 (no vegetation) to $+1$ (dense vegetation).

6.3.3 NDII

The normalized difference infrared index (NDII) is sensitive to the mass or volume of water and not the fractional percentage of water. The NDII is sensitive to the vegetation moisture content and can be used as an indicator of the water content in vegetation (Jackson et al., 2004). In this study, we used the NDII based on the Landsat and Sentinel SWIR bands, which was expressed (Pimple et al., 2020) as follows:

$$\text{NDII} = \frac{(\text{NIR} - \text{SWIR})}{(\text{NIR} + \text{SWIR})} \quad 6.3$$

where NIR is the reflectance in the near-infrared wavelength channel (0.70–0.90 μm) and SWIR-1 is the reflectance in the shortwave-infrared wavelength channel (1.55–1.75 μm). The NDII values increase with the increase in water content, and they range from -1 to 1 . The NDII was used to detect vegetation water content and one of the parameters to differentiate the mangrove and non-mangrove area to enhance the stratification process.

6.3.4 NDWI

The normalized difference water index (NDWI) was designed to analyze water information from satellite imagery. The NDWI was derived using a principle similar to the NDVI and NDII (McFeeters, 1996) as follows:

$$\text{NDWI} = \frac{(\text{Green} - \text{NIR})}{(\text{Green} + \text{NIR})} \quad 6.4$$

where the green band is the reflectance in the green wavelength channel (0.53–0.59 μm) and NIR is the reflectance in the near-infrared wavelength channel (0.70–0.90 μm). This spectral index is designed to: 1) maximize the typical spectral reflectance of water features using green wavelengths; 2) minimize the low reflectance of NIR resulting from water features; and 3) use the high NIR reflectance resulting from vegetation and soil features. The values range from -1 to $+1$, where water features have positive values and terrestrial vegetation and soil have zero or negative values.

6.3.5 NDWII

Murray et al. (2012) noted that the land-water threshold of the normalized difference water infrared index (NDWI) can vary between images in multi-temporal studies. The NDWI and NDVI show opposite trends in mudflats and seawater; hence, subtracting the NDWI from the NDVI can highlight mudflat locations during low tides. The NDWII was calculated as follows:

$$\text{NDWII} = \text{NDWI} - \text{NDVI} \quad 6.5$$

where NDWII values < 0 indicate mudflats (low tide) and NDWII values > 0 (high tide) represent the presence of seawater in the image pixel. We used this index only to perform manual checks and cross-verify low tide pixel values during the image screening process.

6.4 Low tide composites

The majority of previous studies have used single date cloud-free imagery to map the extent and spatial distribution patterns of mangrove forests regardless of high or low tides during the acquisition time (Zhang et al., 2017). Mangrove forests are periodically inundated by seawater, and thus, the spectral signatures of multi-spectral satellite sensors usually differ with changes in the tide (water) levels (Li et al., 2019; Zhang and Tian, 2013). In our proposed methodology, we matched the image acquisition time of the satellite observations to the tidal gauge station data and the appropriate variations in the NDWII values. To maximize the accuracy of pixel extraction during low tide, three selection criteria were: 1) using tidal height value at the satellite acquisition time, which can reduce short-term tidal variations, 2) manually verifying the NDWII values to cross-check the tidal fluctuations at predetermined locations during the field survey, and 3) removing cloud shadows to ensure the selection of good quality pixels in the seasonal composites. Pixels unaffected by tidal fluctuations, clouds, and shadows were considered as good quality pixels. The final low tide composite was achieved by taking the median

value at each pixel. The median values accounted for the remaining temporal noise or outliers, which may affect the reflectance values (Sagar et al., 2017).

6.5 Classification approach

A detailed classification approach is a prerequisite for grouping the pixels to their corresponding species clusters. This is because of spectral similarity between mature rehabilitated, regenerated, and mixed forest stands in narrow strips. The detailed ecological characterization, biodiversity, and spectral response of each forest type was adopted from (Pimple et al., 2020, 2021).

6.5.1 Stratification of mangrove extent

Previous studies have indicated that the stratification of an area of interest reduces the spectral confusion, especially in terrestrial forests or green vegetation (Long and Giri, 2011). Therefore, we employed a pixel-by-pixel image multiplication technique (Mather et al., 2001). The vegetation indices, i.e., the NDVI, NDII, NDWI, and DEM, were used to categorize the mangrove forests from other vegetation. The Otsu threshold (Otsu, 1979) method was used to identify the distribution of mangrove forests from each spectral index. To create a stratified mangrove extent, we first created a binary mask of the NDVI, NDII, NDWI, and DEM covering the mangrove pixels using Otsu thresholding. The pixel values above the threshold were labeled as 1 (mangrove) and the pixel values below the threshold were labeled as 0 (non-mangrove). For the DEM, pixel values < 12 m were considered as lowland area.

In the second stage, we performed multiplication of the binary masks using Eq. (6.6) (Figure 6.2). The multiplication of the same two suitability pixels, with values of 1, resulted in a suitable feature of interest, whereas multiplication by 0 set resulted in the corresponding pixels in the masked image to 0 (Mather et al., 2001). Using the pixel-by-pixel multiplication technique, the image pixels that presented non-mangrove features were replaced by zero while pixels with mangrove forests were unaltered. The multiplication of $NDVI_{Binary}$ and $NDII_{Binary}$ yielded vegetation with a high *moisture* content. Further, multiplication by DEM_{Binary} ensured that the pixels lay in the lowland areas. Finally, the outcomes were multiplied by $NDWI_{Binary}$ to remove water pixels. Visual refinement was performed in Google Earth and aerial imagery in Bing Maps were used to ensure the quality of the derived mangrove extent. We also obtained the mangrove extent from Pimple et al. (2018) for cross verification. The final subset of homogenous mangrove pixels was then used for further analysis. The mangrove extent was calculated as follows:

$$\text{Mangrove Extent} = (\text{NDVI}_{\text{Binary}} * \text{NDII}_{\text{Binary}}) * \text{DEM}_{\text{Binary}} * \text{NDWI}_{\text{Binary}}$$

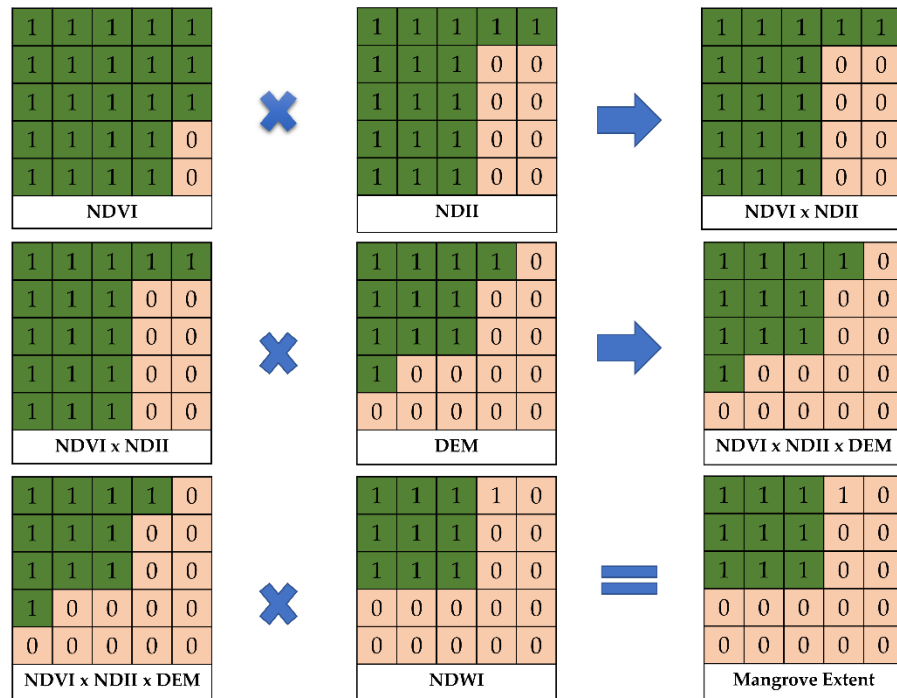


Figure 6.2. Illustration of the pixel-by-pixel image multiplication technique used to obtain the mangrove extent. NDVI: normalized difference vegetation index; NDII: normalized difference infrared index; DEM: digital elevation model; NDWI: normalized difference water index.

6.5.2 Sampling design

The systematic sampling design across the mangrove forest landscape is crucial for discriminating species and their associations. Practices to assess the mangrove spatial diversity must include a complete list of the species and their associations, an understanding of the micro-topography or tidal regimes, measures taken in contiguous quadrants or fixed area sampling along a transect of the intertidal zone (Castaneda-Moya et al., 2006; Dale, 1999; Ellison, 2002), and cover the spatial heterogeneity of mangroves at the landscape scale. Thus, to identify areas of mangrove species and their associations, it was important to design a well-planned field inventory strategy that adequately covered the spatial and intertidal variability in the mangrove species and was sufficiently large to provide reliable estimates for integration with the satellite imagery.

An important objective was to specify strata based on satellite images that represented thematic categories of mangrove species and their associations using the spectral and structural heterogeneity. The integrated backscatter coefficient and spectral reflectance

values of the Sentinel-1 and 2 bands, i.e., VH, VV, red, green, blue, NIR, SWIR-1, and SWIR-2, and preliminary field survey data were used to establish thematic categories and select the sampling locations. We used a three-stage sampling approach to obtain a good spatial and intertidal sample proportion of the total available species and their associations.

The preliminary field survey was conducted in March 2015, October 2016, and December 2017. A handheld GPSMAP 64 SC SiteSurvey (Garmin) and MapPlus offline navigation system were used to collect 40 randomly placed survey points at the landscape scale. Later, these survey points were used to extract the spectral signature from the satellite imagery. The sample unit was chosen as a group of 3 × 3 pixels to minimize the effect of positional error (Xiong et al., 2017). The spectral and structural signatures (Sentinel-1 and -2) were carefully checked to ensure the heterogeneity among the mangrove species and their associations; these signatures were then passed through the RF classifier to generate the reference thematic categories.

Further, three perpendicular transect lines were systematically established from seaward to landward, covering the heterogeneous landscape-scale species distribution along the intertidal zones (Figure 6.1). The transect lines were located from 239249 m E and 1350069 m N to 240518 m E and 1352337 m N; 227717 m E and 1342309 m N to 228518 m E and 1343837m N; and 243470 m E and 1347340 m N to 244753 m E and 1348091 m N (UTM Zone 48 datum). These transects were 1.73, 2.67, and 1.51 km in length, from the shoreline to their terminus in the forest (landward side), respectively. In total, 59 plots (10 × 10 m) were established, with 100 m distances between them, to determine the species composition and diversity in each stand, as well as the distributions among the intertidal zones (Pimple et al., 2021).

Finally, a stratified random sampling approach was used to estimate the total sample size per strata (Olofsson et al., 2014). In total, 367 sample locations were selected for all of the predefined strata, among which 235 were collected in the field and 129 were determined using high-resolution satellite imagery, Google Earth, and Bing VirtualEarth map. At each location, the species names, numbers, diameter at breast height (DBH), and tree height were measured with a tape measure and clinometer. The field inventory data were collected during December 2018, June 2019, January-July-September-November 2020, and February 2021. Further, the basal area was used to determine the most dominant species or their associations within each plot. Table 6.1 lists the grouping of species and their associations based on the spectral and structural variability and frequency in the field inventory plots.

Table 6.1 Species classification categories.

Group	Forest type	Dominant Species and their associations	Allocated Class	Field inventories plot	Points by high-resolution imagery
1	Rehabilitated	<i>Rap; Rmp</i>	Class-1	36	26
2	Natural	(Bc, Ea); (Bg, Ea). (Bs, Ea, Ra); (Bc, Ct, Ea); Bc; Bg; Ea; (Ct, Bg, Ea); (Ct, Am, Bc)	Class-2 (Bg or Bc or Bs associated with Ct, Ea, Ra. Rarely with Am and Rm)	57	20
3	Natural	(Lr, Ra); (Ll Ra); Lr; Ll (Ct, Ll); (Ll, Ra, Ct); (Ct, Ll, Lr); (Lr, Ct); (Ll Ra Lr);	Class-3 (Ll or Lr associated with Ct and Ra (scrub stand))	50	43
4	Natural	(Ra, Xg); (Ra, Xg, Bg); (Xg, Bg, Bc); (Bg, Xg, Ra); (Xg, Ra, Ea); (Xg Xm, Ra); (Xm, Ea, Ct); (Xg, Ll, Xm, Ea)	Class-4 (Xg and Xm associated with Ra, Bg, Bc and Ea. Rarely with Ct and Ll)	33	9
5	Natural	Ra Rm	Class-5 (<i>Ra; Rm</i>)	43	23
6	Natural	Aa, Sa (Am, Ra, Rm); (Am, Aa, Ct)	Class-6 (Aa, Am or Sa. Rarely with Ra and Rm)	16	11

6.6 Modified ARMA

The automatic regrowth monitoring algorithm (ARMA) was originally developed to monitor the mangrove rehabilitation project and the state of natural undisturbed mangroves (Pimple et al., 2021; Pimple et al., 2020). This Landsat-based algorithm allowed a more holistic assessment of mangrove forest dynamics at the study site. This can even be used to identify rehabilitated, regenerated, and naturally undisturbed forest stands. The separation of these categories was crucial to avoid the spectral overlap of similar species. For example, at our study site, rehabilitated mangroves are a monoculture of Rhizophoraceae, which is also one of the most dominate species (Pimple et al., 2021; Pimple et al., 2020). Regenerated stands can be found as single species or mixed with multiple species. We modified the ARMA algorithm to group the mangrove stands into three main categories before classification, including natural undisturbed, rehabilitated,

and regenerated stands. Figure 6.3 presents an illustration of ARMA. An independent visual assessment was performed using the field inventory and high-resolution data to ensure the quality of these categories.

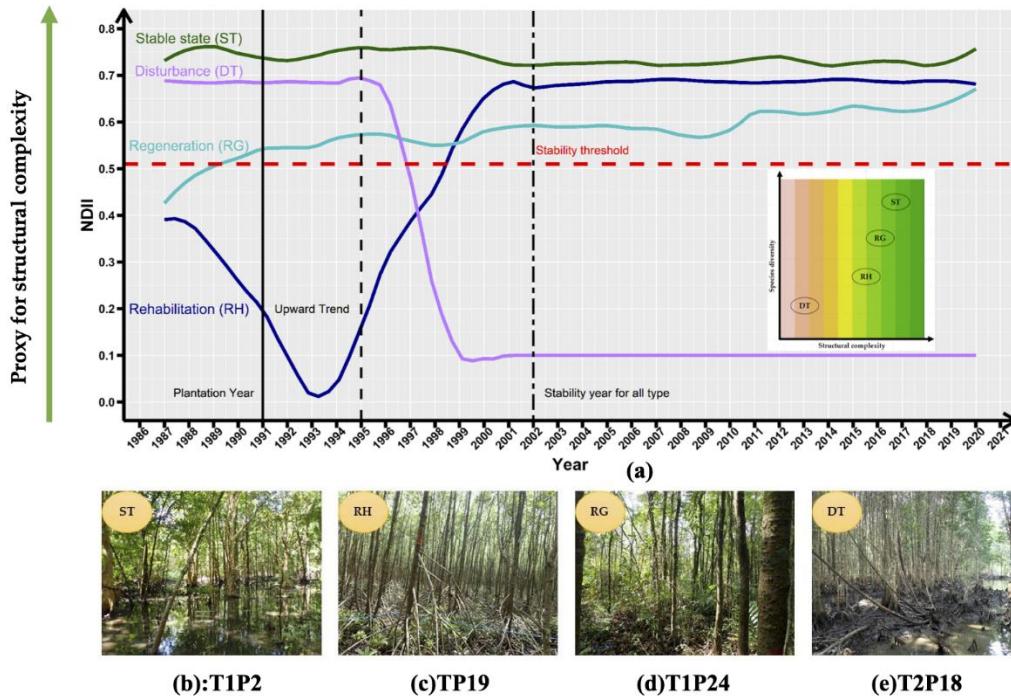


Figure 6.3 Illustration of the expected temporal behavior of Landsat pixels of mangrove forests. Note:(a) State and temporal dynamics, ST: stable or unchanged pixels (dark green); RH: rehabilitated pixels (dark blue); RG: regenerated pixels (blue); and DT: disturbance pixels with no recovery (purple); the known planting year is indicated by a black vertical line. The dashed line indicates the NDII upward trend after rehabilitation. The sub-graph indicates the link between the structural complexity and species diversity. Brown indicates no diversity and less structural complexity while green indicates high diversity and structural complexity. (b), (c), (d), and (e) are (left to right) field photos of ST (T1P2), RH (T1P19), RG (T1P24), and DT (a disturbed area adjacent to T2P18), presenting the observed species in each forest type after 34 years.

6.7 Species distribution mapping: random forest classifier

A pixel-based RF classifier was used to test the multi-sensor performance for discriminating mangrove species and their associations. It is a non-parametric machine learning classifier used to examine mangroves and other terrestrial forests (Pimple et al., 2017; Wang et al., 2018), which consists of an ensemble of decision trees and bootstrapping with replacements. This classifier can manage high-dimensional and confusing objects, and is less sensitive than other streamlined machine learning classifiers

to the quality of the training data and overfitting (Belgiu and Drăgu, 2016; Wang et al., 2018).

Considering that the locations of the plots acquired during the field inventory may occur at the boundary of a pixel (Liu et al., 2018), and the positional error of a single satellite pixel may impact the training and testing of the classifiers (Gu and Congalton, 2020), we used a 3 x 3-pixel window from the center of each plot to train and test the classifier. Before classification, a rigorous assessment of each plot was carried out to ensure the spectral and structural variability available for a single species or species association (see section 3.4.2). Species association is defined as the occurrence of more than one species in the spatial distribution based on their spectral similarity. The dominance of individual species and/or species associations within each plot was determined using forest structural and diversity parameters. These dominant species within each plot contribute significantly to the observed spectral values. Table 6.1 presents the dominance-based observed spectral and structural categories. Additionally, the Landsat annual composite-based NDII time-series was used to test the temporal consistency of each plot from 1987–2020 (Figure 6.3). The spectral variations in the time-series pixel data were related to various phenomena that have occurred over time, which can be used as an indicator of the natural forest pixel stability. For the final classification, low tide image composites between 2019 and 2020 were used.

6.8 Accuracy assessment

We used a two-stage accuracy assessment. First, we used the field inventory data to verify the mangrove strata of natural, rehabilitated, and regenerated stands produced by ARMA. The selected pixels were manually tested and compared with the plot inventories. Second, the accuracy of the random forest classifier was derived from a confusion matrix. Widely used measures, such as the overall, producer's, and user's accuracies (OA, PA, and UA, respectively) were used (Congalton, 1991). Consistent with previous recommendations (Foody, 2020; Olofsson et al., 2014), owing to reported redundancy with the overall accuracy and other limitations, the kappa coefficient was not considered in the accuracy assessment. Instead, per class accuracy and detailed confusion matrix assessments were used. During the classification process, approximately 70 % of the sample points were used to train the classifier while the remaining 30 % of the sample points were used to test the accuracy of the classifier (Figure 6.1).

6.9 Results

6.9.1 Tidal influence on spectral reflectance of multi-spectral imagery

Landsat-8 and Sentinel-2 are in a sun-synchronous, near-polar orbit with an equatorial crossing time of 10:00 am and 10:30 am local time (± 15 min). We assigned each of the satellite acquisition times with a tidal height value at 10:00 am (local time). Figures 4 and 5 present the tidal heights during the Landsat and Sentinel-2 image acquisition time and the effects of tidal fluctuations over the scrub forest (mid-zone) and low elevation areas (seaward-zone). During high tide, in low elevation partially submerged areas, sparse and scrub forests were inundated. The Landsat-8 and Sentinel-2 images showed visible effects in the false color composites obtained during high and low tides. During high tide, the submerged, sparse, or scrub canopy forest areas inundated with seawater absorbed light and appeared darker while during low tides they appeared brighter. Mudflats were visible in the low tide images and not in the high tide images. The spectral reflectance during high tide showed high blue band values while lower values were observed from the NIR, SWIR-1, and SWIR-2 bands. This was attributed to the strong absorption of water, which weakened the spectral features of the high NIR reflected by the inundated mangroves (Q. Chen et al., 2018). In contrast, the spectral reflectance of green, NIR, SWIR-1, and SWIR-2 was higher under low tide conditions (Figures. 6.4 and 6.5b and d). This spectral reflectance variability can be attributed to the presence of background sediments and soil exposed during low tide conditions (Rogers et al., 2017).

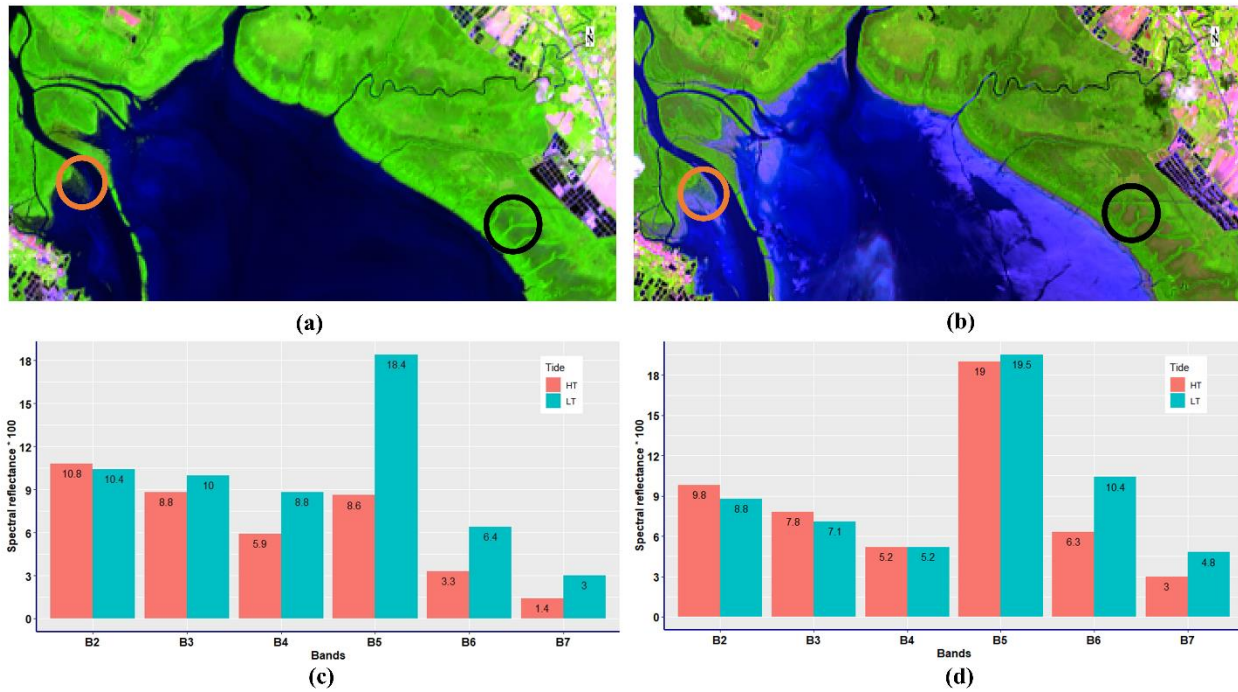


Figure 6.4 Effect of tidal inundation on the reflectance of Operational Land Imager (OLI)-8 images. (a) False color composite of a Landsat OLI-8 high tide image (01/27/2017); (b) spectral variability at a seaward location during tidal fluctuations (orange circle); (c) false color composite of a Landsat OLI-8 low tide image (05/10/2017); and (d) spectral variability at a scrub stand (mid zone) location during tidal fluctuations (blue circle). Note: HT: High tide; LT: Low tide. In the graph, the spectral reflectance is scaled by 100 for visualization purposes. The pixel values shown here are the average value of a 90 m buffer around the point.

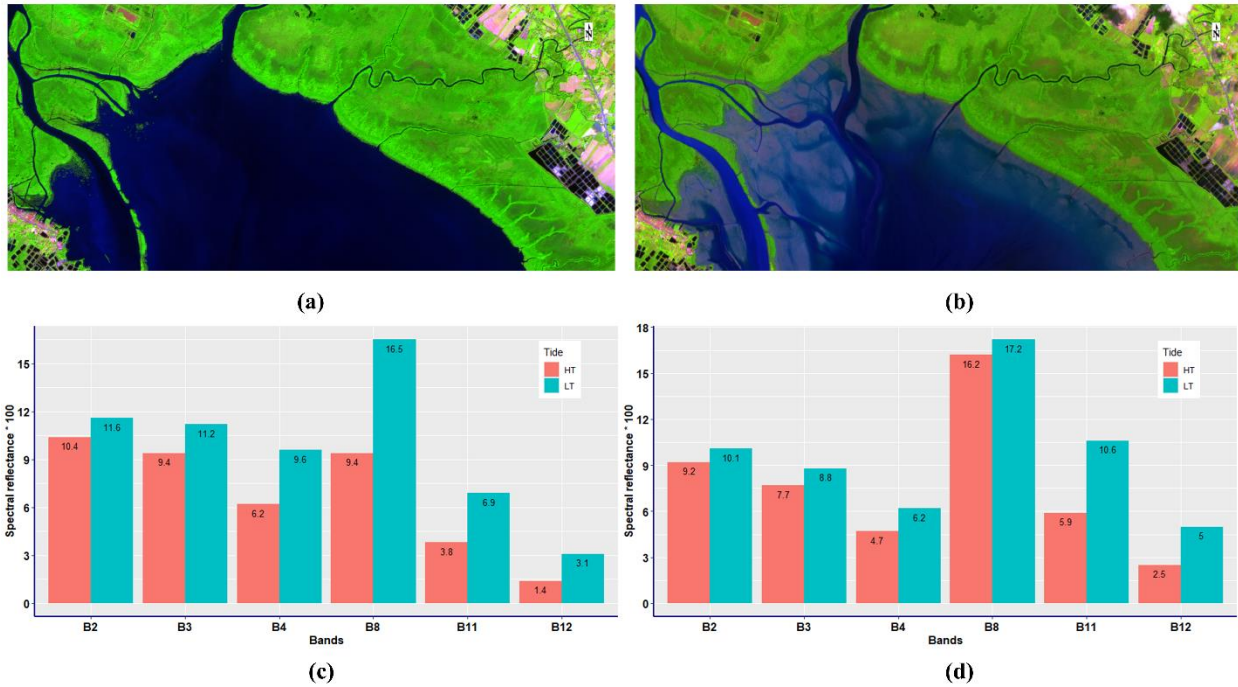


Figure 6.5 Effect of tidal inundation on the reflectance of Sentinel-2 (MSI) TOA images. Note: (a) False color composite (SWIR-1, NIR, and Red) of a Sentinel-2 MSI image (December 25, 2018) at high tide (3.36 m); (b) false color composite of a Sentinel-2 MSI image (May 4, 2018) at low tide (1.76 m); (c) spectral variability at a seaward location during tidal fluctuations (orange circle); and (d) spectral variability at a scrub stand (mid zone) location during tidal fluctuations (black circle). Note: HT: High tide; LT: Low tide. In the graph, the spectral reflectance is scaled by 100 for visualization purposes. The pixel values shown here are the average value of a 90 m buffer around the point.

6.9.2 Effect of low and high tides on backscatter coefficient of SAR imagery

Sentinel-1 SAR has a sun-synchronous near-polar orbit with an equatorial crossing time of 11:00 am and 11:00 pm local time. We assigned each of the satellite acquisition times with a tidal height value at 11:00 am (local time). Figure 6.6 presents the tidal heights during the Sentinel-1 image acquisition time and the effects of tidal fluctuations on submerged, sparse, and scrub forest stands. During low and high tides, an average of 90 m buffered pixels values were extracted to assess the tidal influence. At seaward locations, the average backscatter values (VH and VV) under high and low tide were -7.77 and -6.97 , and -13.22 and -12.94 , respectively. At mid-zone locations, the average backscatter values (VH and VV) under high and low tide were -10.52 and -10.63 , and -14.86 and -14.06 , respectively. During low tide, the average VH and VV values varied from 0.11 to 0.8, and 0.28 to 0.8, respectively. However, the backscatter VH and VV values of single pixels were slightly higher from 3.04 to 4.97 and 0.08 to 1.46, respectively, indicating that single pixels may show a higher variation. The backscatter increased in the VH and VV values owing to the presence of water beneath the mangrove canopy.

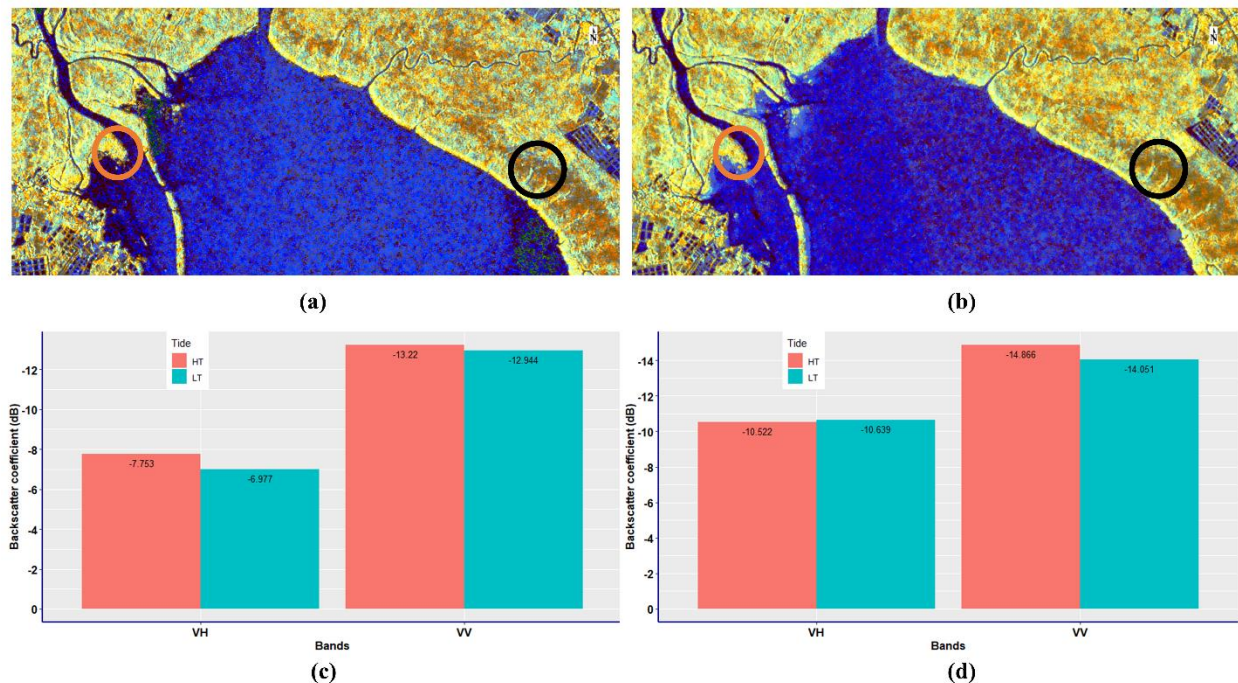


Figure 6.6 Effect of tidal inundation on the backscatter coefficient of Sentinel-1 SAR imagery. (a) RGB composite (VV, VH, and VV/VH) of a Sentinel-1 SAR image (June 17, 2018) at high tide (3.35 m); (b) RGB composite (VV, VH, and VV/VH) of a Sentinel-1 SAR image (December 26, 2018) at low tide (1.12 m); (c) backscatter coefficient variability at a seaward location during tidal fluctuations (orange circle); and (d) backscatter coefficient variability at a scrub stand (mid-zone) location during tidal fluctuations (black

circle). Note: HT: High tide; LT: Low tide. The pixel values shown here are the average value of a 90 m buffer around the point.

6.10 Mangrove forest gain and secondary successions

This study produced a 30-m mangrove extent and change (gain or loss) map for 1987 and 2020, derived using the Landsat annual composite for Trat Province, Thailand (Figure 6.7). The proposed mangrove extent detection method (Eq. [6.6]) utilized the DEM and vegetation indices. This method could easily distinguish mangroves from non-mangroves areas, regardless of the presence of terrestrial and agricultural vegetation. Figure 6.7 indicates the unchanged (orange) and gained (green) mangrove areas. Over the past three decades, approximately 2,047 ha of mangrove forest has grown. The mangrove forest area has increased from 7,131 ha in 1987 to 9,178 ha in 2020. The accuracy of the mangrove forest area obtained in this study was assessed based on the previously estimated mangrove area for 2017 and 2019 in the same study area by Baloloy et al. (2020) and Pimple et al. (2018). Owing to the 30-m resolution, adjacent small agricultural field, shrimp farms, and canals within the forest contributed to the slight overestimation of the calculated area than that estimated from Sentinel-2 data. For further analysis, we used the Sentinel-based extent.

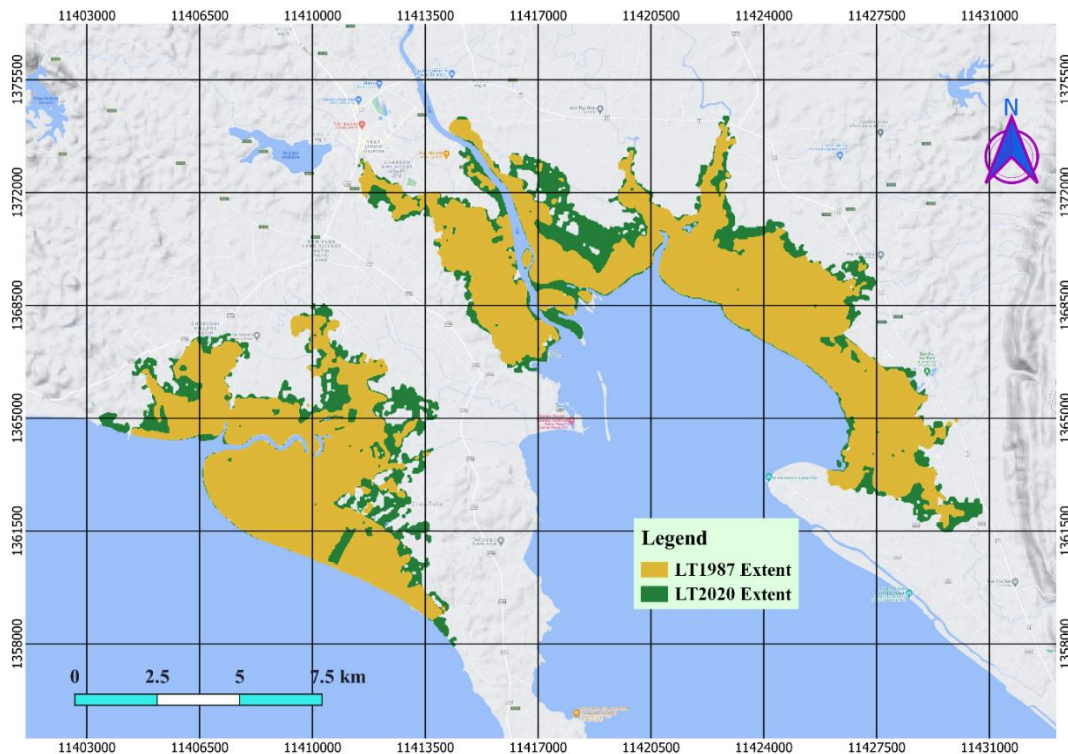


Figure 6.7 Mangrove forest gain and secondary succession from 1987 to 2020. Note: The green color indicates forest gain.

The detailed analysis of the NDII using the modified ARMA indicated variations in the secondary succession of these mangrove stands (Figure 6.8). Over the past three decades, approximately 886.47 and 308.81 ha of mangrove forest have been rehabilitated and regenerated, respectively. A further detailed analysis revealed that approximately 851.72 ha of mangrove were partially disturbed and recovered over time. The NDII time-series cannot capture such dynamics of small patches, i.e., < 900 m², within partially disturbed or natural mangroves.

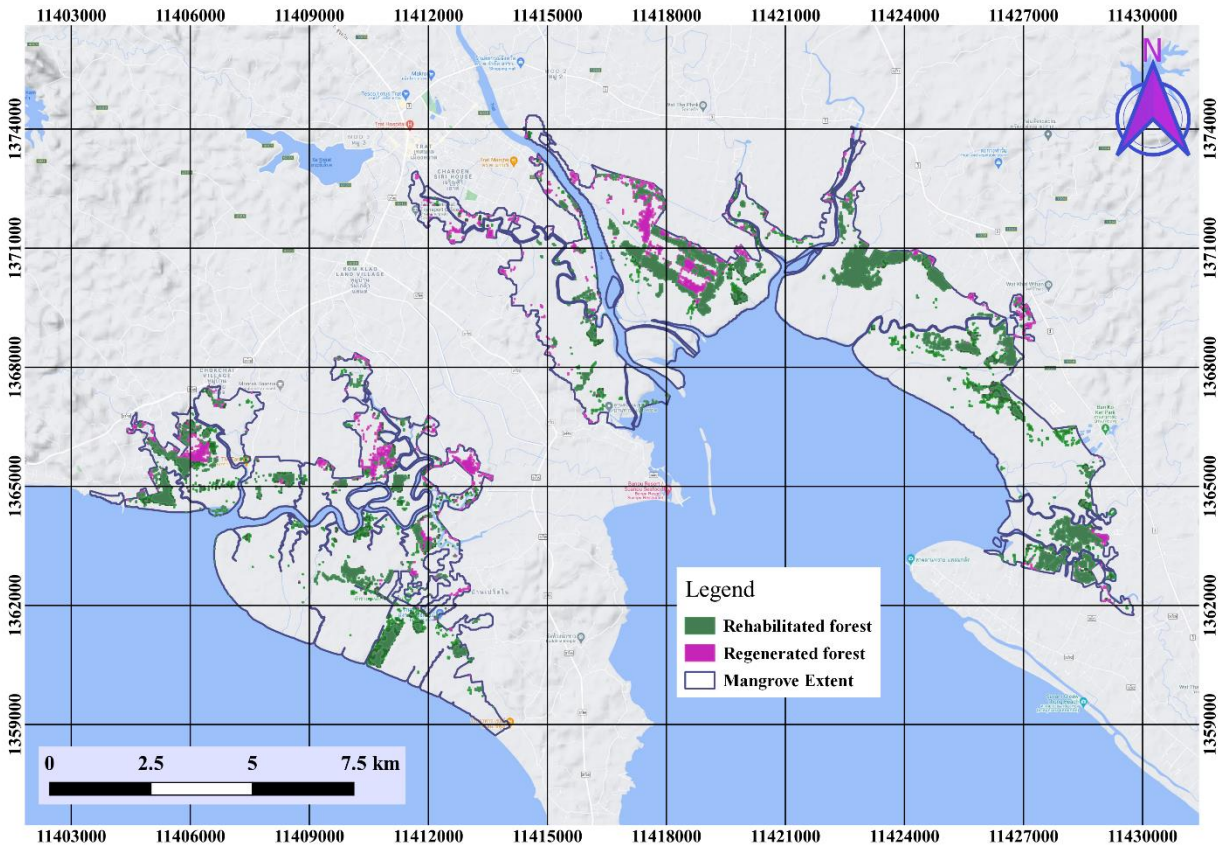


Figure 6.8. Rehabilitated and regenerated (secondary succession) mangrove forest gain from 1987 to 2020. Note: The green and pink color indicates rehabilitated and regenerated forest stands respectively.

6.11 Species classification performance of multi-source satellite imagery

Figure 6.9 shows the resulting species distribution map obtained from low tide Sentinel-1 and -2 composites. Most of the study area was occupied by species associations in Class-2 and -3 (45 and 14 %, respectively), followed by Class-5 (23 % also dominated by Rhizophoraceae), and Class-4, -1 and -6 (7, 6, and 5 %, respectively). Herein, we have only presented the results obtained from Sentinel-1 and -2 owing to its improved accuracy compared to Landsat-8 OLI. We generated two independent confusion matrices to test

the performance of the above two satellite sensors. Table 6.2 lists the confusion matrix for the Sentinel-1 and -2 classifications. Notably, the classification obtained by the combination of Sentinel-1 and -2 performed the best, with an OA of 0.85. Among the class categories presented in Table 6.1, the maximum difference between the PA and UA was exhibited by the rehabilitated (Class-1) mangroves (0.73 and 0.90, respectively) and Class-4 (0.69 and 0.77, respectively), with the exception of Class-1 and -4, where the PA for each class ranged from 0.88 to 0.94. The results showed that compared with other classes, Class-1 and -4 had a relatively lower PA. These categories included rehabilitated mangroves (mostly Rap) and associations of Xg, Ra, and Bg, which had a greater inter-species omission error than the commission error; the spectral confusion among the other classes mainly occurred as a result of the dominant presence of Ra species among these categories. Further, their random assemblage (Pimple et al., 2021) in narrow strips may have contributed to spectral confusion.

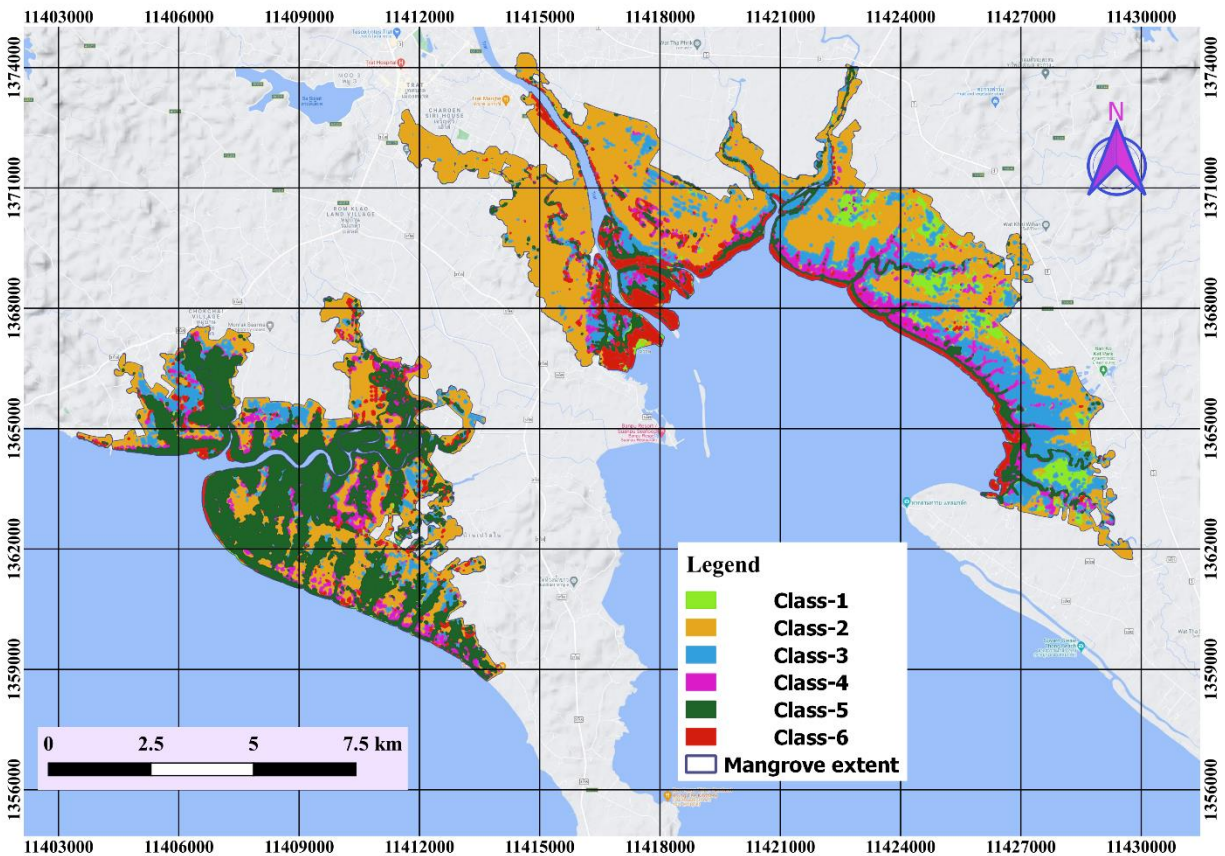


Figure 6.9 Mangrove forest species classification based on Sentinel-1 and -2 low tide composites. Class-1: Rap, Rmp; Class-2:Bg,Bc, Bs associated with Ct, Ea and Ra, Class-3: Ll, Lr associated with Ct and Ra; Class-4: Xg, Xm associated with Ra, Bg, Bc and Ea; Class-5: Ra,Rm (natural); Class-6: Aa and Sa (Note: Aa: *Avicennia alba*; Bc: *Bruguiera cylindrica*; Bg: *Bruguiera gymnorrhiza*; Bs: *Bruguiera sexangula*; Ct: *Ceriops tagal*; Ea: *Excoecaria agallocha*; Ll: *Lumnitzera littorea*; Lr: *Lumnitzera racemosa*; Ra: *Rhizophora apiculata*; Rap:

Rhizophora apiculata plantation; Rm: *Rhizophora mucronata*; Rmp: *Rhizophora mucronata* plantation; Sa: *Sonneratia alba*; Xg: *Xylocarpus granatum*; and Xm: *Xylocarpus moluccensis*).

Table 6.2 Accuracy assessment and confusion matrix based on Sentinel-1 SAR and -2 MSI for species classes.

	Class-1	Class-2	Class-3	Class-4	Class-5	Class-6	Total	PA	OE
Class-1	131	12	18	5	14	0	180	0.73	0.27
Class-2	1	200	3	4	3	2	213	0.94	0.06
Class-3	8	12	220	6	3	1	250	0.88	0.12
Class-4	3	6	12	86	16	1	124	0.69	0.31
Class-5	2	3	5	5	172	3	190	0.91	0.09
Class-6	1	2	0	5	0	78	86	0.91	0.09
Total	146	235	258	111	208	85	1,043		
UA	0.90	0.85	0.85	0.77	0.83	0.92		OA :0.85	
CE	0.10	0.15	0.15	0.23	0.17	0.08			

The OA obtained from Landsat-8 was 0.65. Compared with the combination of Sentinel-1 and -2, Landsat-8 produced the largest omission and commission errors (Table 6.3). Class-1 and -4 produced the lowest PA (0.13 and 0.58, respectively) and UA (0.25 and 0.50, respectively), followed by Class-4 and -5 (PA: 0.58 and 0.60, respectively; UA: 0.50 and 0.53, respectively). The random dominant species assemblage (Ra) in narrow strips and a 30 m pixel resolution may have contributed to the spectral confusion. In contrast, Class-2 and -3 showed a relatively high PA (0.76 and 0.87, respectively) and UA (0.76 and 0.74, respectively). The larger spatial scale distribution and inter-species variability produced high accuracies for these categories; for example, Class-1 (Ra) leaves were dark green compared with Class-3 (Ll, Lr, and Ct).

Table 6.3 Accuracy assessment and confusion matrix based on Landsat -8 OLI for species classes.

	Class-1	Class-2	Class-3	Class-4	Class-5	Class-6	Total	PA	OE
Class-1	2	3	6	2	2	0	15	0.13	0.87
Class-2	1	19	2	1	2	0	25	0.76	0.24
Class-3	2	0	26	1	1	0	30	0.87	0.13
Class-4	1	1	0	7	3	0	12	0.58	0.42
Class-5	1	2	0	2	9	1	15	0.60	0.40
Class-6	1	0	1	1	0	6	9	0.67	0.33
Total	8	25	35	14	17	7	106		
UA	0.25	0.76	0.74	0.50	0.53	0.86		OA: 0.65	
CE	0.75	0.24	0.26	0.50	0.47	0.14			

6.12 Discussion

Using a robust data cleaning method, Landsat time-series, cloud computing, and machine learning algorithm to leverage a large-scale systematic field inventory dataset, as well as the species discrimination potential of two freely available satellite sensors, this study provides four main contributions to remote sensing research on mangrove biodiversity. First, we proposed a satellite-based robust systematic sampling design, which accounted for landscape-scale spectral and structural variability in species and their associations. Further, the sampling design considered the environmental setting, landscape modification, and conservation interventions (Pimple et al., 2021; Pimple et al., 2020). Second, this study affirms the importance of accounting for the factors that influence satellite imagery, such as various atmospheric contaminants and periodic tidal inundations, which enhances species or their association-level spectral variability. Third, the modified ARMA algorithm used 34 years of Landsat archives as a powerful proxy to determine temporal changes and secondary successions. Fourth, we explored the full spectral potential of freely available satellite sensors for species-level classification. Previous studies have investigated mangrove species classifications, which are based on a commercial product and non-systematic field data (Heenkenda et al., 2014; Rahman et al., 2019; Wang et al., 2018; Xia et al., 2020). Our approach overcomes several previous limitations, not only recording the spatial and intertidal scale species distribution, but also creating a historical state for the ecosystem.

6.12.1 Effects of tidal inundation on spectral reflectance and backscatter coefficient

In mangrove extent or diversity mapping studies, the influence of the tidal inundation on spectral reflectance and backscatter coefficient is not well understood (Maurya et al., 2021; Wang et al., 2019) and is rarely considered during image processing. Our results revealed that the most important bands for mangrove species classification, such as NIR, SWIR-1, and SWIR-2, show altered spectral reflectances in Landsat-8 and Sentinel-2 images. During high tide, the most significant reduced spectral responses were observed between seaward and mid-zone areas occupied by partially submerged, sparse, and scrub mangrove stands. This suggests that the spectral properties of these bands can be homogenous if the satellite acquisition time was during high tide. Recent studies have reported on the limitations of distinguishing submerged mangroves during high tide; such mangrove stands usually lead to misclassification or cannot be detected during high tides (Jia et al., 2019; Li et al., 2019; Xia et al., 2018). To the best of our knowledge, this is the first study that demonstrates the effects that tides have on detecting scrub mangroves using remote sensing imagery. In this study, during low tide, higher spectral values were

observed, which is consistent with recent studies that identified an enhanced spectral response compared with high tide imagery (Chen et al., 2017; Li et al., 2019; Rogers et al., 2017; Xia et al., 2020). We also found that the Sentinel-1 backscatter response was altered during high tide (Figure 6.6). Previous studies have reported changes in the backscattering coefficient of the C-band due to flooding beneath trees (Landuyt et al., 2020). The sensitivity of the backscatter is highly dependent on the forest complexity and tidal level at the time of acquisition (Darmawan et al., 2015). The above findings indicated that the remote sensing capabilities for mangrove species and the mapping of their extent in periodically inundated complex ecosystems, such as partially submerged and sparse stands, are highly dependent on the image acquisition time and tidal level (Proisy et al., 2018; Xia et al., 2018).

Recent developments in standardized image products and cloud computing platforms have enabled pixel-based composite approaches (White et al., 2014). Besides cloud and atmospheric contamination-free pixels, these approaches do not account for the tidal influence on individual pixels. For example, at the current study site, we can find several cloud-free images from September to December, which correspond to a very high tide period. The species classification accuracy and temporal consistency of such composite pixels depend on the tidal levels at the time of acquisition. This study thus suggests that species classifications based on low tide spectral and backscatter composite images can more accurately enhance the identification of species or their associations. Low tide composites also preserve the band value at each pixel.

6.12.2 Sensor performance for discriminating species and their associations

In this study, low tide composite-based Sentinel-1 and -2, and Landsat-8 images can better distinguish the inter-species variability. Compared with Landsat-8 (OA: 0.65), the combination of Sentinel-1 and -2 (OA: 0.85) produced better and comparable results with the field inventory plots and intertidal zonation reported in Pimple et al. (2020, 2021). Owing to the 30-m coarse resolution of Landsat-8, identifying the species or their associations in narrow strips or small patches is difficult (Classes 1 and 4–6; Table 6.3) (Valderrama-Landeros et al., 2018). Classes covering large spatial areas were more accurately classified than class assemblages in narrow strips and overlapping species; Class-1 and -4 especially showed low PA values in both sensors. Spectral confusion can be attributed to the presence of Rhizophoraceae, i.e., Ra and Rm (natural), and Rap and Ram (rehabilitated). At the study site, several plnated Rhizophoraceae (Class-1: Rap and Rmp) have been rehabilitated across the area. Over last 30 years, these stands have reached a height similar to adjacent natural mangroves (Pimple et al., 2020). The spectral

response of Rhizophoraceae can be similar if the rehabilitated stands are adjacent or mixed with natural stands. Class-4 had an association of dominant mangrove groups, i.e., Xg, Ra, or Rm, and Bg; such plots or pixels can yield similar spectral responses as other locations if *Rhizophoraceae* is the dominant species. Studies using very high-resolution imagery, such as World View-2 and GeoEye-1, have also reported spectral discrimination limitations with respect to species in complex structural situations (Heenkenda et al., 2014; Leempoel et al., 2013). This indicates that even with very high-resolution imagery, it is challenging to distinguish a single species of mangroves from an association or mixed group. Also, some species can be more common in the subcanopy such as *Bruguiera*. In such a situation, higher spectral resolutions and the SAR capabilities of Sentinel may provide an advantage. Limited spectral bands, non-systematic, and limited field inventory data can yield spectral confusion during species classification and may contradict field-based studies (Ellison et al., 2000; Rahman et al., 2019).

Regardless of whether the spectral variability has been shown to be useful for mapping mangrove-associated species, several challenges remain for spatial-scale studies, which are usually not considered when collecting and linking field inventory data. These include the effects of topography or intertidal zonation (transect line), a complete list of species and their site-specific distributions, the abundance of each species, where and how they occur in a given landscape (single, grouped, or no-zonation), or the present strata (Castaneda-Moya et al., 2006; Ellison, 2002; Lucas et al., 2017; Pimple et al., 2021). Furthermore, several studies have been based on single-date analysis and the lack of knowledge on the temporal changes in species diversity caused by natural and anthropogenic stressors (Miettinen et al., 2014). Lucas et al. (2017) summarized several limitations associated with the temporal dynamics of mangrove monitoring. However, recent studies have used Landsat-based time-series to evaluate trends in species zonation and regeneration dynamics (Bullock et al., 2017; Otero et al., 2019). Further, studies have demonstrated the species discrimination capabilities of Sentinel-2 (Wang et al., 2018), but did not include Sentinel-1. The method introduced in this study 1) included a systematic sampling approach (determination of the spatial and intertidal species dominance); 2) tested the temporal consistency and changes (ARMA) while reducing spectral noise caused by various contaminations; and 3) linked the field inventory and temporal dynamics at a resolution of 10-m based on Sentinel-1 SAR and-2 MSI data to more realistically determine the species, their associations, and their histories at a larger scale. Obtaining the mangrove species and their association information were possible owing to a combination of Sentinel SAR and MSI imagery. This indicated that the combination of the 34-year Landsat archive, systematic field survey, and machine learning classifiers

with Sentinel-1 SAR and-2 MSI can be a powerful tool and provide significant advantages for monitoring complex mangrove ecosystems.

6.13 Conclusions

In this study, we successfully explored the potential of freely available satellites to distinguish between mangrove species. We 1) explored the use of Sentinel-1 SAR and -2 MSI features to design a systematic sampling approach; 2) developed and integrated 34 years of error-free homogenized Landsat time-series with a modified ARMA algorithm to recreate the history; 3) assessed the effect that tidal levels have on spectral and backscatter values and the importance of low tide images for discriminating mangrove species; and 4) explored the potential of freely available low tide composites of Landsat and Sentinel-1 SAR and-2 MSI imagery to discriminate mangrove species or communities in Trat Province, Thailand.

We obtained an OA of 0.65 and 0.85 for the results from Landsat and Sentinel- 1SAR and-2 MSI, and was able to discriminate six categories, including three single species and three species associations. Generally, the PA was lower in narrow strips and patchy forest stands where similar species were dominant. Our results acknowledge the limitations of Landsat imagery while revealing the capabilities of integrating Sentinel-1 SAR and -2 MSI imagery for mangrove species discrimination. With spatial resolutions suitable for the reliable characterization of secondary successions, a time-series of Landsat archives can provide a historical overview of rehabilitated, regenerated, and undisturbed forests. Such a record is critical for many mangrove studies as high-resolution imagery was not available in the past. However, the potential of Landsat has been underestimated. Based on a comparison with other very high-resolution imagery studies, we can conclude that if the species assemblage is in association with or mixed over the landscape, then identifying a single species with remote sensing remains challenging. However, using the dominant species reflectance and structural variability can provide a reliable discrimination of mangrove species or their associations at the landscape scale. This study thus demonstrates the potential of Landsat time-series and Sentinel- 1 SAR and -2 MSI for monitoring the historical state, degree of success or failure of restoration interventions, and landscape-scale discrimination of mangrove species and their associations.

CHAPTER 7

Synthesis and future outlook

7.1 Conclusions

This research aimed to improve our understanding of the long-term effects of environmental and anthropogenic settings on the spatio-temporal dynamics of mangrove forest species diversity, while also developing a decision-support system to assess the succession trajectories of natural, rehabilitated, and regenerating mangrove forest stands. The introduction chapter provides a detailed review of the background of mangrove species biodiversity and synthesis on key limitations, advances, and research gaps for biodiversity assessment at both local and regional scales. Based on a review and preliminary ecosystem analysis, four main research topics were identified: (1) spatio-temporal characterization of the mangrove forest landscape in terms of gain and loss; (2) degree of success of conservation interventions; (3) assessment of spatial diversity, intertidal zonation, and functional indicators of succession; and (4) development of a state-of-the-art decision-support system using multi-satellite and improved field inventories.

Q1. How have the spatio-temporal characteristics of the mangrove forest landscape changed (gain or loss) over a period of three decades?

Chapter 2 provides thirty years of explicit quantification of mangrove forest landscape characterization in the Trat Province in Thailand. Mangrove forests have experienced significant recovery over the past thirty years. Bare land and urban areas increased from 9.80% in 1987 to 11.08% in 2017. In addition, shrimp farms progressively increased from 6.82% in 1987 to 11.49% in 2017. The agricultural area decreased from 49.18% in 1987 to 41.25% in 2017, while mangrove forest area increased from 34.20% in 1987 to 36.17% in 2017. Most agricultural land within the mangrove forest areas was converted to rehabilitated mangroves by local communities through conservation efforts. In addition, the disturbed mangrove forest area showed significant recovery. This recovery could be attributed to the adaptation of low-salinity shrimp farming practices. This chapter also presents a cloud computing-based methodological approach in attempting to achieve error-free annual composites of Landsat imagery for mapping wall-to-wall changes in mangrove forest landscapes and their surroundings. The obtained composite imagery is free from cloud cover, shadows, haze, missing value pixels, and the effect of the presence or absence of water underneath the mangrove canopy.

Q2. How did the species biodiversity and structural complexity of rehabilitated (planted) forests evolve, compared to the adjacent natural mangrove stands?

Chapters 3 and 4 address two main issues: (1) How the rehabilitated mangroves have evolved over the last three decades, and (2) whether the ecological parameters of the rehabilitated mangrove forest stands resemble those of the adjacent natural stands. In the study site, the significant gain of mangrove forests (Chapter 2) is attributed to larger scale rehabilitation practices. The rehabilitated stands were composed of Rhizophoraceae monoculture. The degree of success of such rehabilitation projects varied significantly. Very few of these projects have a systematic field inventory or monitoring plans, and there are no reports on success or failure assessment or future recommendations for good rehabilitation practices. A systematic design of field inventories across the mangrove forest landscape is crucial to collect species list in study sites, their occurrence in rehabilitated stands, intertidal distribution, change in mangrove structure along various environmental gradients, and detailed knowledge of conservation intervention practices. Chapter 3 presents the experimental design, transect line establishment, data collection for species and structural diversity, and usage of such information for assessing the degree of success and failure of rehabilitation efforts and carbon sequestration potential estimations. Chapter 4 assesses the historical developments and status of species and structural diversity of rehabilitated and adjacent natural mangroves in the Trat Province in Thailand. This study shows that after thirty years, the rehabilitated mangroves were still a monoculture of Rhizophoraceae, and natural mangroves had a higher species diversity. The forest plot trajectories demonstrated that the period required to stabilize rehabilitated mangrove stands ranged from 7 to 13 years (after plantation year). The rehabilitated mangrove forest stands were able to reach comparable heights to the natural stands, while tree density was significantly higher in rehabilitated mangroves. The seedling recruitment and secondary succession rates were very low, regardless of the presence of mixed forest species seedlings. These facts indicate that the rehabilitated mangrove may provide forest cover, but still lacks the functionality of the adjacent natural forest. Thus, to improve mangrove rehabilitation and management, adequate site assessment, such as hydrologic patterns and species suitability, is crucial. The assessment of the degree of success provides valuable information on the effects of biological, ecological, and hydrological variables and restoration trajectories at specific sites.

Q.3 What is the sensitivity of environmental factors and anthropogenic settings (such as topography and rehabilitation) to potential spatial diversity, intertidal zonation, and historic state or knowledge gaps of mangrove forest species diversification?

Q3 addressed the following topics: (1) the species distribution patterns perpendicular to the shoreline, (2) the spatial-scale intertidal zonation patterns in response to the elevation gradient, and (3) the trajectories of functional diversity indicators in response to secondary succession. Environmental settings and biological factors are responsible for controlling mangrove species diversity in different landscapes. Mangrove forest ecosystem assessment based on a systematic sampling design with quantification of spatial and intertidal species diversity could improve the results of ecological and prediction studies. Furthermore, the inclusion of functional indicators such as the underlying ecological process and historic forest state could provide a complete picture of the viability, resilience, and trajectories of secondary succession required for better conservation practices and management. Chapter 5 advances the baseline assessment of the whole ecosystem by 1) quantitatively examining the influence of surface elevation on spatial and intertidal distribution of mangrove species, and 2) understanding the temporal dynamics of diversity during successional stages. Fifteen species were identified in the Trat Province of Thailand, in which the landscape is dominated by *Ceripos tagel* (including tall and dwarf forest stands). However, the analysis failed to identify any significant patterns at the transect or landscape scale. This indicates that the species may have occurred randomly. The direct effects of anthropogenic activities, such as topography modification, canal network, and waste from shrimp farms, on species diversification were observed. The trajectories of rehabilitated mangroves are discussed in the paragraph above and in Chapter 2. The species diversity of naturally regenerated mangroves in landward abandonment areas varies greatly. This behavior is attributed to the availability of seedlings. The waste from shrimp farms caused partial disturbances in the dwarf *Ceripos tagel*. The adaptation of low salinity shrimp farming has allowed the recovery of partially disturbed forest patches. The methodological approach proposed in Chapter 5 is beneficial when developing management plans to monitor the diversity and health of forests, as well as conservation projects in the field of mangrove forestry.

Q.4 What is the potential of multi-source satellites to discriminate the spatial patterns of mangrove forest typology?

Q.4 and Chapter 6: 1) Evaluate the influence of tidal inundation on satellite imagery, 2) explore the potential of medium resolution freely available satellite spectral response and machine-learning classifiers to selected mangrove dominant communities, and 3) exploit the composite-based spectral variability of time series to determine the temporal change or secondary succession. This chapter concludes that remote sensing-based mangrove species and extent mapping capabilities can be significantly reduced during periodic inundation. In addition, low-tide imagery enhances the spectral and structural

capabilities. With Landsat-8, it is possible to discriminate species association to a certain extent, but its coarse resolution limits the performance. However, this spatial resolution is suitable for recreating the history of ecosystems and provides valuable insights into secondary succession caused by natural or human-induced stressors. The integration of Sentinel-1 SAR and-2 MSI shows promising potential for mangrove species discrimination.

7.2 Implications for future conservation and diversity monitoring

Despite extensive discussion of the need for spatio-temporal monitoring of mangrove species diversity and conservation interventions, the large-scale practical implementation of such an approach is still limited. Current literature on mangrove species monitoring suggests that the past attempts to monitor mangrove species diversity have indeed been conducted on a small spatial scale and lack temporal consistency. Understanding the development of rehabilitated forests, landscape scale species diversity, and long-term changes within the mangrove ecosystem remains a poorly explored topic in developing countries globally. This is in part because of (1) the limited data and knowledge of proper data collection practices, (2) consideration of the relationship between local environmental and anthropogenic settings in monitoring approaches, (3) assumption about species zonation without scientific analysis, (4) dependence on commercial satellite-based products and their limitations, and (5) tools of scientific knowledge to monitor changes over time. To address this, this study introduces a state-of-the-art decision-support system (Fig 7.1) that 1) includes a systematic field inventory approach; 2) derive the secondary succession, temporal consistency, and change (modified automatic regrowth monitoring algorithm: ARMA) while reducing spectral noise caused by various contaminations, and 3) links the field inventory and dynamics to remote sensing for monitoring mangrove species diversity.

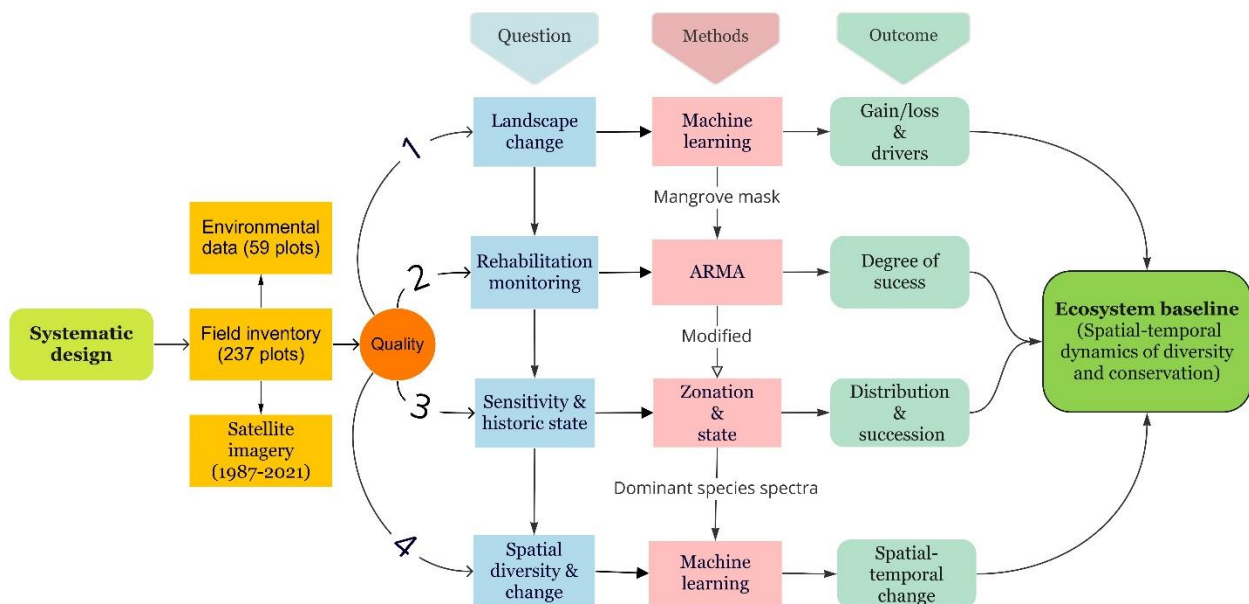


Figure 7.1 General flow diagram of the methodological framework for ecosystem baseline monitoring. A flow diagram is showing the use of systematic sampling design, multisource satellite, and environmental data required to obtain mangrove spatio-temporal dynamics of species and conservation activities. Note: ARMA :automatic regrowth monitoring algorithm.

Rates of mangrove deforestation have declined globally, although countries like Myanmar and Malaysia are still facing high loss (Friess et al., 2019; Goldberg et al., 2020). However, the spatio-temporal scale driver (natural and anthropogenic)-response relationships are not necessarily constant through time, but they can change over time due to recent and past experiences (Ryo et al., 2019). The understanding of temporal dynamics of such drivers has proven difficult, with most of the attempts relying without time-series of remotely sensed data, existing field information from the literature, or national government agencies in single-point time. The expected response of these drivers may vary from regional to local scale such as high or no deforestation in conservation zones, low or intensive shrimp farm, or agricultural activities. The response of mangroves to these drivers has become a vital component of forest management as it helps in understanding the outcome of historic decision support systems and implemented restoration or conservation policies. In addition, the understanding of undisturbed or stable forests and predicting near-future risks of anthropogenic drivers may play a crucial role in biodiversity conservation and enhancing carbon sequestration capabilities (Funk et al., 2019). Temporal inconsistencies and data gaps in remotely sensed caused by various atmospheric and local conditions are discussed in Chapter-1. Further, this chapter also discusses the time-series based compositing approaches of medium resolution imagery and the availability of open-source and free-to-use cloud-computing platforms such as the Google Earth Engine (GEE), are facilitating the large-scale environmental monitoring, analysis, and processing of high volumes of earth observation imagery, which has limited the number of missing pixels caused by the cloud and shadow masking. The annual composite could be used to provide extensive information on how the mangroves changed over time (Chapter-2). In this study, the time series composite-based analysis indicated that 1) the mangrove forests made a significant recovery over time, 2) no forest disturbance was found within the conservation zones. This trend is indicative of the local community's awareness and the Thai government's policies restricted the expansion and deforestation of mangrove forests. However, it appears that agriculture, bare-land, and shrimp farms had undergone major changes. The interconversion to shrimp farms could pose a serious threat to mangrove forest diversity as waste from these farms is directly discharged into the forest. Without attention to past dynamics, we may fail to recognize key such variables explaining a given phenomenon. There is an urgent need to improve local scale driver pressure mapping for mangrove habitats, specifically direct threats like conservation to shrimp farms, agriculture, and oil palm plantations (Turschwell et al., 2020). The rate of change of drivers and responses may vary when considered in local and national contexts. Future diversity studies should

consider the forest landscape dynamic. Understanding such impacts will help to inform how the driver dynamics changed in relation to rehabilitation or conservation efforts.

A systematic sampling design across mangrove forest landscapes is crucial to obtain reliable information on species diversity and its patterns. This must include the complete species list that covers the spatial area, elucidate the intertidal distribution, record changes in mangrove structural features, and knowledge of conservation interventions. However, such approaches when determining species diversity and zonation in mangrove studies are rarely used (Dale et al., 2014; Sandilyan and Kathiresan, 2012). The natural factors and anthropogenic controls play an important role in modifying species diversity at specific sites. The use of inadequate data collection criteria and reporting yields incomplete information on species diversity and the distribution of mangrove forests. In this study, we have identified the minimum data and sampling strategies required to assess spatial distribution, as follows (Fig. 7.2) : (1) the sampling must be performed in contiguous quadrats or fixed-area sampling along a transect of the intertidal zone; (2) there must be a complete list of species for the study site; (3) there must be a measure of the abundance of each species and where they occur in the given landscape; (4) a measure of the edaphic parameters and surface elevation; (5) anthropogenic settings and human factors for example landscape modification (Chapter-3 and-4); and (6) the temporal dynamics of the forest (Chapter-4 and-5).

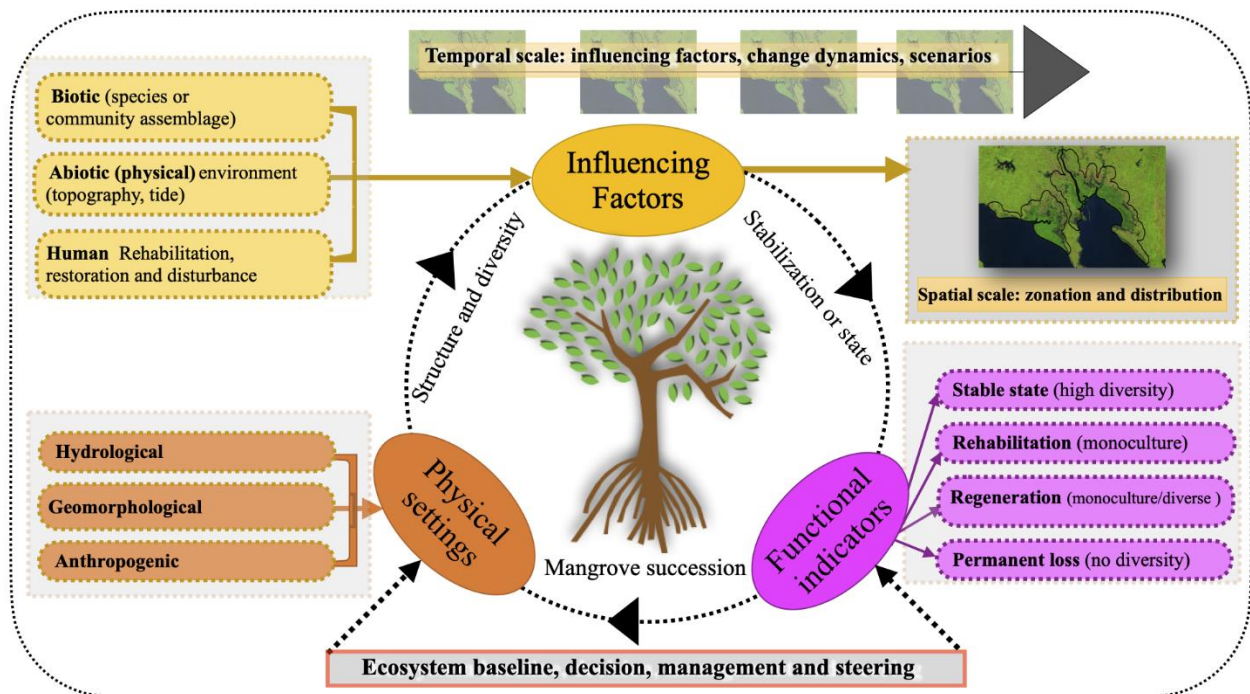


Figure 7.2 Monitoring spatial scale species diversity and zonation using a transect line plot. The orange boxes indicate the physical factors related to elevation, tidal inundation, and landscape modification. The yellow boxes indicate the natural influencing factors as well as those induced by humans. The pink boxes indicate the various phases that could be observed over time in a given ecosystem (Pimple et al., 2021).

In traditional mangrove diversity studies, the combination of remote sensing-based spatio-temporal dimensions has not been used for sampling design. Distinct spectral and structural heterogeneity of forest landscapes could be useful prior to the sampling design stage such as Sentinel-1 SAR, Sentinel-2 MSI, and PlanetScope, and low-cost UAVs (drones). Remote sensing-based spatially balanced sample approaches, such as area proportional stratified random sampling, can be used for systematic sampling design (Grafström et al., 2014; Köhl et al., 2006; Olofsson et al., 2014; Wallner et al., 2018). Such an innovative sampling design enables a higher inventory precision, lower number of samples, the identification of possible locations for establishing transect lines (seaward to landward), an understanding of the temporal dynamics of natural, rehabilitated, and regenerated forest stands, and reduced costs. The spectral and structural variability can be further used in remote sensing-based classification approaches and accuracy assessment. To understand mangrove species diversity, it is important to comprehend the extent of mangrove species' habitats at multiple scales, their interactions with local environmental and anthropogenic settings, and how they are changing over time (disturbance, rehabilitation, and regeneration).

Mangrove forest rehabilitation projects are increasingly undertaken in the context of diversity conservation. With different rehabilitation practices, it is difficult to access the effectiveness of such rehabilitation compared to natural stands on species diversity. Under the United Nations Decade on Ecosystem Restoration (2021–2030) lists coastal ecosystems such as mangrove forests as a restoration priority. Due to this assessing long-term impacts of rehabilitation on species diversity are crucial. In order to assess the effectiveness of rehabilitation in this forest type requires: (1) the starting year of rehabilitation projects, (2) assessing the time required to stabilize the forest; (3) the structural development, species diversity, and tree density in comparison to adjacent natural mangroves. This study (Chapter-4) assessed the viability of a prototype algorithm to identify the starting year of a rehabilitation project, the number of years required to reach stability, and the stand age, structural development, and species complexity, compared to the adjacent natural mangrove stands. Further, we evaluated: (1) how the rehabilitated mangroves evolved over the last three decades; and (2) whether the ecological parameters of the rehabilitated forests resembled those of the adjacent natural stands. The automatic regrowth monitoring algorithm (ARMA) was developed to

monitor the mangrove rehabilitation projects in this study. Stable annual Landsat composites allowed for a more holistic assessment of the forest change dynamics. The integration of historical information from the Landsat annual composites and current ecological measurements, can be used to monitor the long-term degree of the success of rehabilitation projects, and compare and assess the species and structural diversities of the rehabilitated stands with those of the adjacent natural mangroves. The methodological framework developed during this study is useful to generate a detailed description of the different aspects of the rehabilitation projects, including the starting year of the rehabilitation project, the required period to stabilize rehabilitated mangroves, the current age, the status of development (change or no change due to any disturbance), biophysical properties (structure), and successional stages (diversity) that are reached by developing rehabilitated mangrove stands. This method can even be used to monitor the rehabilitation of the mangroves that occurred in temporal periods before the high-resolution data were available (i.e.,1999). The proposed method could be used for monitoring large spatial scale rehabilitation projects. In addition, forest disturbances such as the effect of tsunamis, lightning strikes, insect damage, and sea-level fluctuations could be monitored during the growth of rehabilitated stands. Furthermore, this method could be extended to high-resolution time series (e.g., Sentinel MSI-2) to monitor mangrove rehabilitation projects.

Assessing mangrove species diversity, zonation, and functional indicators in response to natural, regenerated, and rehabilitated succession are important for reporting the baseline of mangrove forest diversity. Most of the reported species diversity at the site scale did not account for various environmental settings. Although usually not stated in studies, the collection of sampling plots might have been biased convenient data collection conditions (e.g. access points from land and water, solid terrain, low degree of species diversity, and limited samples on rehabilitated vs natural mangroves). As a result, inadequate sampling methods have been used to report spatial scale diversity baseline. In addition to the above-mentioned minimum data requirements and sampling strategies, the inclusion of local environmental and anthropogenic settings is required (Fig 7.2). Depending on the site-specific local settings such as topography, tidal regimes, coastal processes, canal networks, edaphic variables, modified landscapes, and rehabilitations mangrove ecosystems can take the form of (1) a single species zonation: a single tree species monoculture zone systematically arrayed over the landscape; (2) grouped zone: two or more species grouped across the intertidal zone; and (3) random placement or no zonation: species are randomly placed over the landscape.

In this study (Chapter-5), we investigated the knowledge gaps in terms of potential spatial diversity, intertidal zonation, and the historic state of mangrove forest species and test the role of environmental settings such as topography, as well as rehabilitation settings on species diversity. We have successfully integrated historic multi-satellite annual composites, current ecological (transect plot), and micro-topographical measurements to establish a historic state and zonation for the mangrove forests in the Trat province of Thailand. In addition, we have developed a modified “automatic regrowth monitoring algorithm (ARMA)” and summarized the functional indicators by type for a realistic baseline assessment of species diversity and their temporal dynamics. Findings of this study indicate that the mangrove species apportion niche spaces, but there is limited evidence of the zonation patterns for any single species at a given elevation gradient. This indicates that the different species of mangrove respond differently to local environmental settings, edaphic gradients, and climate conditions (Duke et al., 1998; Ellison et al., 2000; Twilley, 2008; Twilley et al., 2017). The non-systematic sampling strategy and qualitative assessment may not capture the species distribution and zonation patterns at the landscape scale. In contrast, quantification or statistical testing of zonation (Clarke et al., 2008; Ellison et al., 2000) with a systematic sampling design can yield more reliable outcomes compared with traditional random sampling and qualitative approaches. Quantitative studies reported significant species to overlap along the elevation and other environmental gradients (Ellison et al., 2000; Leong et al., 2018; Schmiegelow and Ganesella, 2014). To understand mangrove species diversity spatial and intertidal patterns, it is important to consider the environmental conditions. Furthermore, the detailed temporal analysis revealed that the diversity among natural stable, rehabilitated, regenerated, and partially disturbed mangrove stands is greatly varied. The recovered or secondary succession mangroves were found to have moderate or no diversity and were structurally less complex when compared to undisturbed ones. Considering the complex processes involved in mangrove restoration, incorporate, and consider, aspects of the consequences of conservation interventions for the diversity, structure, and function of coastal ecosystems. Thus, the spatial diversity reporting methodological framework must include reliable sampling design, quantification of diversity in relation to environmental variables, and temporal dynamics. Such approaches will improve our ecological understanding of the complex environmental and anthropogenic settings and how only by improving our spatial scale understanding of the interlinking of these processes can we improve conservation measures in the future for mangroves. In addition, the complete information has the potential to be used in either parameterizing or evaluating mechanistic mangrove stand models (Chapter-1).

Identifying large spatial scale mangrove species and their associations using remote sensing imagery is a greater challenge as there are only a few studies that have focused on long-term classification (Heenkenda et al., 2014; Heumann, 2011; L. Wang et al., 2004). The mapping accuracy of mangrove species identification evidently depends on 1) the tide level when using a single date image 2) the availability of clouds and their shadows, 3) the temporal consistency and radiometric stability of the spectral reflectance, 4) the classifiers used, 5) the selection of the systematic sampling design, and 6) the temporal dynamics of conservation interventions (Chapter-1). In addition, we suspect that much remote sensing-based literature on species classification does not accurately account for the truly complex species patterns. For example, the mangrove species can be found 1) a single species zonation; 2) grouped zone; 3) random placement or no zonation, and 4) single species and species associations. Limited spectral bands, non-systematic, and limited field inventory data can yield spectral confusion during species classification and may contradict field-based studies (Ellison et al., 2000; Rahman et al., 2019). To address this it is important to recognize species that tended to co-occur as single species and/or in associations with similar taxonomic compositions. In this study (Chapter-6), we have explored the potential multisource satellite for mangrove species identification. The spatial scale statistical quantification was used to determine species grouping and distribution (Chapter-5). In addition, Landsat-based time-series to evaluate trends in species zonation and secondary succession. Obtaining the mangrove species and their association information was possible owing to a combination of Sentinel SAR and MSI imagery. Results revealed that the combination of the 34-year Landsat archive, systematic field survey, and machine learning classifiers with Sentinel-1 SAR and-2 MSI can be a powerful tool and provide significant advantages for monitoring complex mangrove ecosystems. In addition, the consistency and quality of such composites may vary depending on observed pixels in low or high tide. However, inclusion of low tidal images will enhance the spectral and structural discrimination performance of freely available.

Based on results obtained from this study, we outline good practices that could be used to enhance the monitoring and enhancing modeling of mangrove diversity (Fig 7.3). The high-performance open-source computing platforms overcome the limitations associated with data selection, download, pre-processing of raw data, machine learning-based image processing, and classification applications over larger scales. In this study, we used the GEE platform to develop contamination-free pixel-based annual composites from the Landsat, Sentinel-1, and Sentinel-2 data archives, and run the machine learning classifiers. The selection of low tide, atmospheric contamination-free, and radiometrically corrected imagery allows the identification of submerged mangroves and maintains the

spectral and structural heterogeneity within different forest species or their associations. The stratification of mangroves as an area of interest reduces the spectral and structural confusion caused by other vegetation categories. Integration of structural and spectral remote sensing data could be used to establish thematic categories for a spatially balanced sampling strategy. Further, this can be used to select the locations of transect lines and sampling plots across the landscape. The quantification or statistical testing of species zonation and distribution in relation to various environmental variables (e.g., topography or inundation) must be performed. In addition, the inclusion of anthropogenic settings such as the secondary succession of diversity caused by rehabilitation, restoration, and regeneration must be defined to understand the dynamics of diversity change. The above information can be integrated with machine learning and deep learning techniques can be used for classifying mangrove species. The information obtained from above the practices could be used either in parameterizing or evaluating mechanistic mangrove stand models.

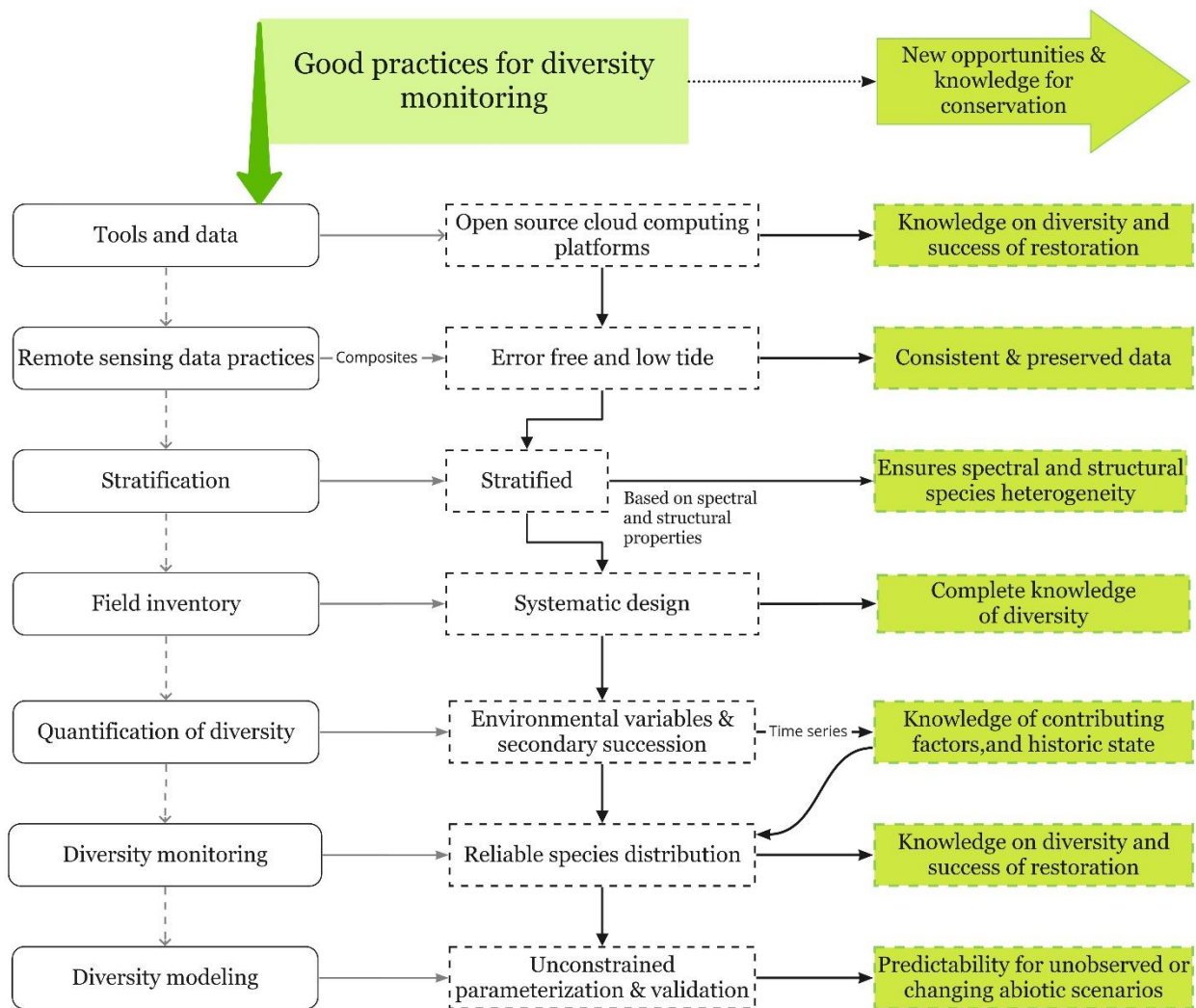


Figure 7.3 Summary diagram highlighting the proposed good practices using earth observation data, systematic sampling design, and environmental variables to monitor species diversity and enhance the performance of modeling approaches.

Overall, this study provides a novel and state of the art decision-support-system for monitoring various ecological and management aspects of mangrove forestry (Fig 7.4). This framework will be beneficial when developing action plans to monitor the health and diversity of natural and restored mangroves. Furthermore, the tools developed in this study could provide a more realistic spatial validation for various restoration and biodiversity prediction models. Further, such a decision-support system may help ecologists or forest practitioners around the world to plan and conduct field inventories in a more systematic way, which could further be linked to spatial and temporal scale studies to improve the usability of resources to improve regional-scale knowledge. In addition, modeling approaches could benefit considerably from accurate information on the spatio-temporal evolution of mangrove diversity, especially at larger spatial scales.

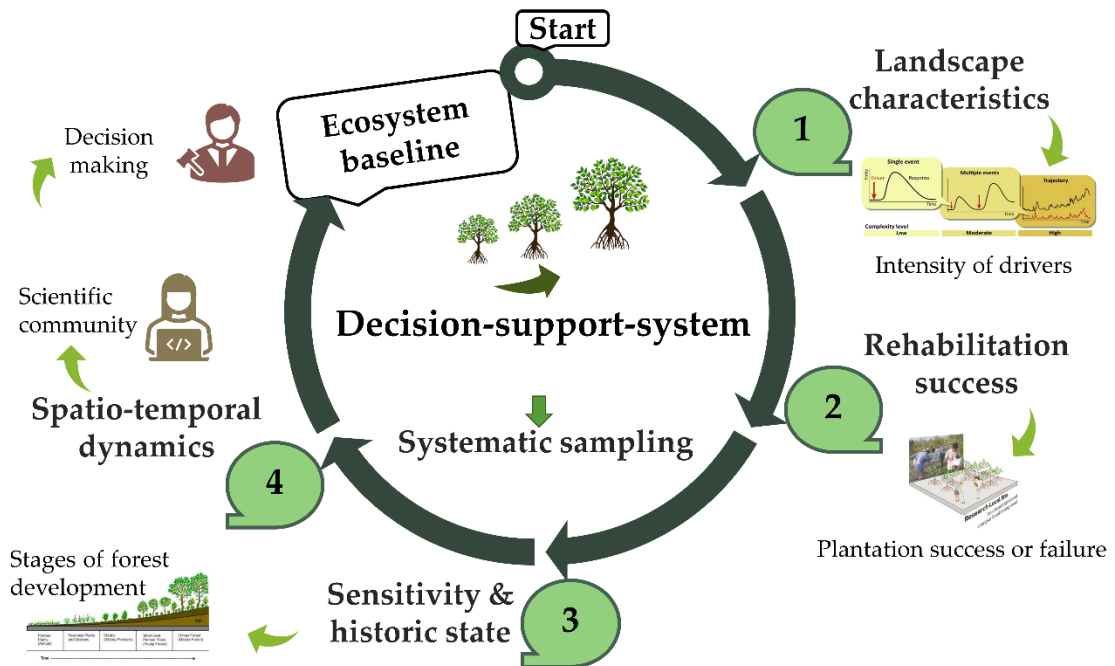


Figure 7.4 The general framework of decision-support-system for monitoring various ecological, species diversity, and management aspects of mangrove forestry.

References

- Abdul Aziz, A., Phinn, S., Dargusch, P., Omar, H., Arjasakusuma, S., 2015. Assessing the potential applications of Landsat image archive in the ecological monitoring and management of a production mangrove forest in Malaysia. *Wetl. Ecol. Manag.* 23, 1049–1066. <https://doi.org/10.1007/s11273-015-9443-1>
- Abino, A.C., Castillo, J.A.A., Lee, Y.J., 2014. Assessment of species diversity, biomass and carbon sequestration potential of a natural mangrove stand in Samar, the Philippines. *Forest Sci. Technol.* 10, 2–8. <https://doi.org/10.1080/21580103.2013.814593>
- Adade, R., Aibinu, A.M., Ekumah, B., Asaana, J., 2021. Unmanned Aerial Vehicle (UAV) applications in coastal zone management—a review. *Environ. Monit. Assess.* 193. <https://doi.org/10.1007/s10661-021-08949-8>
- Adeli, S., Salehi, B., Mahdianpari, M., Quackenbush, L.J., Brisco, B., Tamiminia, H., Shaw, S., 2020. Wetland monitoring using SAR Data: A meta-analysis and comprehensive review. *Remote Sens.* 12. <https://doi.org/10.3390/rs12142190>
- Alexandris, N., Chatenoux, B., Lopez Torres, L., Peduzzi, P., 2013. Monitoring Mangroves Restoration from Space. UNEP/GRID- Geneva.
- Allen, J.A., Ewel, K.C., Jack, J., 2001. Patterns of natural and anthropogenic disturbance of the mangroves on the Pacific Island of Kosrae. *Wetl. Ecol. Manag.* 9, 279–289. <https://doi.org/10.1023/A:1011125310794>
- Alongi, D.M., 2014. Carbon cycling and storage in mangrove forests. *Ann. Rev. Mar. Sci.* 6, 195–219. <https://doi.org/10.1146/annurev-marine-010213-135020>
- Alongi, D.M., 2009. *The Energetics of Mangrove Forests*. Springer, Dordrecht, Netherlands. <https://doi.org/10.1007/978-1-4020-4271-3>
- Alsaaidh, B., Al-Hanbali, A., Tateishi, R., Kobayashi, T., Hoan, N.T., 2013. Mangrove Forests Mapping in the Southern Part of Japan Using Landsat ETM+ with DEM. *J. Geogr. Inf. Syst.* 5, 369–377. <https://doi.org/10.4236/jgis.2013.54035>
- Andradi-Brown, D.A., Howe, C., Mace, G.M., Knight, A.T., 2013. Do mangrove forest restoration or rehabilitation activities return biodiversity to pre-impact levels? *Environ. Evid.* 2, 1–8. <https://doi.org/10.1186/2047-2382-2-20>
- Araujo, R.J., Shideler, G.S., 2019. An R package for computation of mangrove forest structural parameters using plot and plotless methods. *Madera bosques* 25. <https://doi.org/10.21829/myb.2019.2511696>
- Armitage, A.R., Highfield, W.E., Brody, S.D., Louchouart, P., 2015. The contribution of mangrove expansion to salt marsh loss on the Texas Gulf Coast. *PLoS One* 10, 1–17. <https://doi.org/10.1371/journal.pone.0125404>
- Asaeda, T., Barnuevo, A., Sanjaya, K., Fortes, M.D., Kanesaka, Y., Wolanski, E., 2016. Mangrove plantation over a limestone reef - Good for the ecology? *Estuar. Coast. Shelf Sci.* 173, 57–64. <https://doi.org/10.1016/j.ecss.2016.02.017>

- Ashton, E.C., Macintosh, D.J., 2002. Preliminary assessment of the plant diversity and community ecology of the Sematan mangrove forest, Sarawak, Malaysia. *For. Ecol. Manage.* 166, 111–129. [https://doi.org/10.1016/S0378-1127\(01\)00673-9](https://doi.org/10.1016/S0378-1127(01)00673-9)
- Aslan, A., Rahman, A.F., Warren, M.W., Robeson, S.M., 2016. Mapping spatial distribution and biomass of coastal wetland vegetation in Indonesian Papua by combining active and passive remotely sensed data. *Remote Sens. Environ.* 183, 65–81. <https://doi.org/10.1016/j.rse.2016.04.026>
- Baderan, D.W., Utina, R., Lapolo, N., 2018. Vegetation structure, species diversity, and mangrove zonation patterns in the Tanjung Panjang Nature Reserve Area, Gorontalo, Indonesia. *Int. J. Appl. Biol.* 2. <https://doi.org/10.20956/ijab.v2i2.5752>
- Baena, S., Moat, J., Whaley, O., Boyd, D.S., 2017. Identifying species from the air: UAVs and the very high resolution challenge for plant conservation. *PLoS One* 12, 1–21. <https://doi.org/10.1371/journal.pone.0188714>
- Baetens, L., Desjardins, C., Hagolle, O., 2019. Validation of copernicus Sentinel-2 cloud masks obtained from MAJA, Sen2Cor, and FMask processors using reference cloud masks generated with a supervised active learning procedure. *Remote Sens.* 11, 1–25. <https://doi.org/10.3390/rs11040433>
- Ball, M.C., 1988. Ecophysiology of mangroves. *Trees* 2, 129–142. <https://doi.org/10.1007/BF00196018>
- Baloloy, A.B., Blanco, A.C., Raymund Rhommel, R.R.C., Nadaoka, K., 2020. Development and application of a new mangrove vegetation index (MVI) for rapid and accurate mangrove mapping. *ISPRS J. Photogramm. Remote Sens.* 166, 95–117. <https://doi.org/10.1016/j.isprsjprs.2020.06.001>
- Banskota, A., Kayastha, N., Falkowski, M.J., Wulder, M.A., Froese, R.E., White, J.C., 2014. Forest Monitoring Using Landsat Time Series Data: A Review. *Can. J. Remote Sens.* 40, 362–384. <https://doi.org/10.1080/07038992.2014.987376>
- Barbier, E.B., Hacker, S.D., Kennedy, C., Koch, E.W., Stier, A.C., Silliman, B.R., 2011. The value of estuarine and coastal ecosystem services. *Ecol. Monogr.* 81(2), 169–193.
- Barnuevo, A., Asaeda, T., 2018. Integrating the ecophysiology and biochemical stress indicators into the paradigm of mangrove ecology and a rehabilitation blueprint. *PLoS One* 13, 1–17. <https://doi.org/10.1371/journal.pone.0202227>
- Barnuevo, A., Asaeda, T., Sanjaya, K., Kanesaka, Y., Fortes, M., 2017. Drawbacks of mangrove rehabilitation schemes: Lessons learned from the large-scale mangrove plantations. *Estuar. Coast. Shelf Sci.* 198, 432–437. <https://doi.org/10.1016/j.ecss.2017.02.015>
- Bathmann, J., Peters, R., Naumov, D., Fischer, T., Berger, U., Walther, M., 2020. The MANgrove–GroundwAter feedback model (MANGA) – Describing belowground competition based on first principles. *Ecol. Modell.* 420, 108973. <https://doi.org/10.1016/j.ecolmodel.2020.108973>
- Beisner, B.E., Haydon, D.T., Cuddington, K., 2003. Alternative Stable States in Ecology. *Front. Ecol. Environ.* 1, 376. <https://doi.org/10.2307/3868190>
- Belgiu, M., Drăgu, L., 2016. Random forest in remote sensing: A review of applications and future directions. *ISPRS J. Photogramm. Remote Sens.* 114, 24–31. <https://doi.org/10.1016/j.isprsjprs.2016.01.011>
- Berger, U., Hildenbrandt, H., 2000. A new approach to spatially explicit modelling of forest dynamics:

- Spacing, ageing and neighbourhood competition of mangrove trees. *Ecol. Modell.* 132, 287–302. [https://doi.org/10.1016/S0304-3800\(00\)00298-2](https://doi.org/10.1016/S0304-3800(00)00298-2)
- Berger, U., Rivera-Monroy, V.H., Doyle, T.W., Dahdouh-Guebas, F., Duke, N.C., Fontalvo-Herazo, M.L., Hildenbrandt, H., Koedam, N., Mehlig, U., Piou, C., Twilley, R.R., 2008. Advances and limitations of individual-based models to analyze and predict dynamics of mangrove forests: A review. *Aquat. Bot.* 89, 260–274. <https://doi.org/10.1016/j.aquabot.2007.12.015>
- Blanco, J.F., Bejarano, A.C., Lasso, J., Cantera, J.R., 2001. A new look at computation of the complexity index in mangroves: Do disturbed forests have clues to analyze canopy height patchiness? *Wetl. Ecol. Manag.* 9, 91–101. <https://doi.org/10.1023/A:1011115220126>
- Bodart, C., Eva, H., Beuchle, R., Raši a, R., Simonetti, D., Stibig, H.-J., Brink, A., Lindquist, E., Achard, F.A., 2011. Pre-processing of a sample of multi-scene and multi-date Landsat imagery used to monitor forest cover changes over the tropics. *ISPRS J. Photogramm. Remote Sens.* 66, 555–563. <https://doi.org/10.1016/j.isprsjprs.2011.03.003>
- Boisvenue, C., Smiley, B.P., White, J.C., Kurz, W.A., Wulder, M.A., 2016. Integration of Landsat time series and field plots for forest productivity estimates in decision support models. *For. Ecol. Manage.* 376, 284–297. <https://doi.org/10.1016/j.foreco.2016.06.022>
- Borcard, D., Gillet, F., Legendre, P., 2011. Numerical Ecology with R. *Numer. Ecol. with R.* <https://doi.org/10.1007/978-1-4419-7976-6>
- Bosire, J.O., Dahdouh-Guebas, F., Kairo, J.G., Koedam, N., 2003. Colonization of non-planted mangrove species into restored mangrove stands in Gazi Bay, Kenya. *Aquat. Bot.* 76, 267–279. [https://doi.org/10.1016/S0304-3770\(03\)00054-8](https://doi.org/10.1016/S0304-3770(03)00054-8)
- Brown, I., Mwansasu, S., Westerberg, L.O., 2016. L-band polarimetric target decomposition of mangroves of the rufiji delta, Tanzania. *Remote Sens.* 8. <https://doi.org/10.3390/rs8020140>
- Bruce, C.M., Hilbert, D.W., 2004. Pre-processing Methodology for Application to Landsat TM/ETM+ Imagery of the Wet Tropics. *Coop. Res. Cent. Trop. Rainfor. Ecol. Manag. Rainfor. CRC, Cairns.* 44 pp. <https://doi.org/10.1155/2010/468147>
- Bryan-Brown, D.N., Connolly, R.M., Richards, D.R., Adame, F., Friess, D.A., Brown, C.J., 2020. Global trends in mangrove forest fragmentation. *Sci. Rep.* 10, 1–8. <https://doi.org/10.1038/s41598-020-63880-1>
- Buckley, R.C., 1982. Patterns in north Queensland mangrove vegetation. *Aust. J. Ecol.* 7, 103–106. <https://doi.org/10.1111/j.1442-9993.1982.tb01306.x>
- Bullock, E.L., Fagherazzi, S., Nardin, W., Vo-Luong, P., Nguyen, P., Woodcock, C.E., 2017. Temporal patterns in species zonation in a mangrove forest in the Mekong Delta, Vietnam, using a time series of Landsat imagery. *Cont. Shelf Res.* 147. <https://doi.org/10.1016/j.csr.2017.07.007>
- Bunt, J.S., Williams, W.T., 1980. Studies in the analysis of data from Australian tidal forests ('Mangroves'). II. The use of an asymmetric monothetic divisive classificatory program. *Aust. J. Ecol.* 5, 391–396. <https://doi.org/10.1111/j.1442-9993.1980.tb01262.x>
- Bunt, J.S., Williams, W.T., Bunt, E.D., 1985. Mangrove species distribution in relation to tide at the seafront and up rivers. *Mar. Freshw. Res.* 36, 481–492.

- Bunting, P., Rosenqvist, A., Lucas, R.M., Rebelo, L.M., Hilarides, L., Thomas, N., Hardy, A., Itoh, T., Shimada, M., Finlayson, C.M., 2018. The global mangrove watch - A new 2010 global baseline of mangrove extent. *Remote Sens.* 10. <https://doi.org/10.3390/rs10101669>
- Cao, Y; Larsen, DP; Thorne, R., 2001. Rare species in multivariate analysis for bioassessment : *J. North Am. Benthol. Soc.* 20, 144–153.
- Capdeville, C., Abdallah, K., Buffan-Dubau, E., Lin, C., Azemar, F., Lambs, L., Fromard, F., Rols, J.L., Leflaive, J., 2018. Limited impact of several years of pretreated wastewater discharge on fauna and vegetation in a mangrove ecosystem. *Mar. Pollut. Bull.* 129, 379–391. <https://doi.org/10.1016/j.marpolbul.2018.02.035>
- Cárdenas, N.Y., Joyce, K.E., Maier, S.W., 2017. Monitoring mangrove forests: Are we taking full advantage of technology? *Int. J. Appl. Earth Obs. Geoinf.* 63, 1–14. <https://doi.org/10.1016/j.jag.2017.07.004>
- Castaneda-Moya, E., Rivera-Monroy, V.H., Twilley, R.R., 2006. Mangrove Zonation in the Dry Life Zone of the Gulf of. *Estuaries and coasts* 29, 751–764.
- Chalermchatwilai, B., Pongpam, S., Patanaponpaiboon, P., 2011. Distribution of fine-root necromass in a secondary mangrove forest in Trat province, eastern Thailand. *ScienceAsia* 37, 1–5. <https://doi.org/10.2306/scienceasia1513-1874.2011.37.001>
- Chazdon, R.L., Brancalion, P.H.S., Laestadius, L., Bennett-Curry, A., Buckingham, K., Kumar, C., Moll-Rocek, J., Vieira, I.C.G., Wilson, S.J., 2016. When is a forest a forest? Forest concepts and definitions in the era of forest and landscape restoration. *Ambio* 45, 538–550. <https://doi.org/10.1007/s13280-016-0772-y>
- Chen, B., Xiao, X., Li, X., Pan, L., Doughty, R., Ma, J., Dong, J., Qin, Y., Zhao, B., Wu, Z., Sun, R., Lan, G., Xie, G., Clinton, N., Giri, C., 2017. A mangrove forest map of China in 2015: Analysis of time series Landsat 7/8 and Sentinel-1A imagery in Google Earth Engine cloud computing platform. *ISPRS J. Photogramm. Remote Sens.* 131, 104–120. <https://doi.org/10.1016/j.isprsjprs.2017.07.011>
- Chen, G., Thill, J.C., Anantsuksomsri, S., Tontisirin, N., Tao, R., 2018. Stand age estimation of rubber (*Hevea brasiliensis*) plantations using an integrated pixel- and object-based tree growth model and annual Landsat time series. *ISPRS J. Photogramm. Remote Sens.* 144, 94–104. <https://doi.org/10.1016/j.isprsjprs.2018.07.003>
- Chen, L., Zeng, X., Tam, N.F.Y., Lu, W., Luo, Z., Du, X., Wang, J., 2012. Comparing carbon sequestration and stand structure of monoculture and mixed mangrove plantations of *Sonneratia caseolaris* and *S. apetala* in Southern China. *For. Ecol. Manage.* 284, 222–229. <https://doi.org/10.1016/j.foreco.2012.06.058>
- Chen, Q., Yu, R., Hao, Y., Wu, L., Zhang, W., Zhang, Q., Bu, X., 2018. A new method for mapping aquatic vegetation especially underwater vegetation in Lake Ulansuhai using GF-1 satellite data. *Remote Sens.* 10. <https://doi.org/10.3390/rs10081279>
- Chen, R., Twilley, R.R., Twilley, R., 2011. development forest model of mangrove A gap dynamic resources and nutrient of soil salinity along gradients. *Society* 86, 37–51. <https://doi.org/10.1046/j.1365-2745.1998.00233.x>
- Cihlar, J., 2000. Land cover mapping of large areas from satellites : status and research. *Int. J. Remote Sens.* 21, 1093–1114.

- Cintrón, G., Schaeffer Novelli, Y., 1984. Methods for studying mangrove structure, in: Snedaker, S.C. (Ed.) *The mangrove ecosystem: research methods* 8, 91–113.
- Clarke, K.R., Somerfield, P.J., Gorley, R.N., 2008. Testing of null hypotheses in exploratory community analyses: similarity profiles and biota-environment linkage. *J. Exp. Mar. Bio. Ecol.* 366, 56–69. <https://doi.org/10.1016/j.jembe.2008.07.009>
- Collins, D.S., Avdis, A., Allison, P.A., Johnson, H.D., Hill, J., Piggott, M.D., Hassan, M.H.A., Damit, A.R., 2017. Tidal dynamics and mangrove carbon sequestration during the Oligo-Miocene in the South China Sea. *Nat. Commun.* 8, 1–12. <https://doi.org/10.1038/ncomms15698>
- Congalton, R.G., 1991. A review of assessing the accuracy of classifications of remotely sensed data. *Remote Sens. Environ.* 37, 35–46. [https://doi.org/10.1016/0034-4257\(91\)90048-B](https://doi.org/10.1016/0034-4257(91)90048-B)
- Corbane, C., Politis, P., Kempeneers, P., Simonetti, D., Soille, P., Burger, A., Pesaresi, M., Sabo, F., Syrris, V., Kemper, T., 2020. A global cloud free pixel- based image composite from Sentinel-2 data. *Data Br.* 31, 105737. <https://doi.org/10.1016/j.dib.2020.105737>
- Craft, C., 2016. 9 - Mangroves, in: Craft, C. (Ed.), *Creating and Restoring Wetlands*. Elsevier, Boston, pp. 233–263. <https://doi.org/https://doi.org/10.1016/B978-0-12-407232-9.00009-9>
- Csillik, O., Kumar, P., Mascaro, J., O’Shea, T., Asner, G.P., 2019. Monitoring tropical forest carbon stocks and emissions using Planet satellite data. *Sci. Rep.* 9, 1–12. <https://doi.org/10.1038/s41598-019-54386-6>
- Curtis, J., McIntosh, R., 1950. The Interrelations of Certain Analytic and Synthetic Phytosociological Characters Author (s): J . T . Curtis and R . P . McIntosh Published by : Ecological Society of America Stable URL : <http://www.jstor.org/stable/1931497> . *Ecology* 31, 434–455.
- Dahdouh-Guebas, F., Koedam, N., 2008. Long-term retrospection on mangrove development using transdisciplinary approaches: A review. *Aquat. Bot.* 89, 80–92. <https://doi.org/10.1016/j.aquabot.2008.03.012>
- Dainelli, R., Toscano, P., Di Gennaro, S.F., Matese, A., 2021. Recent advances in unmanned aerial vehicles forest remote sensing—a systematic review. Part ii: Research applications. *Forests* 12. <https://doi.org/10.3390/f12040397>
- Dale, M.R.T., 1999. *Spatial Pattern Analysis in Plant Ecology*, Cambridge Studies in Ecology. Cambridge University Press. <https://doi.org/10.1017/CBO9780511612589>
- Dale, M.R.T., Fortine, M., 2014. *Spatial Analysis, Spatial Analysis A guide for ecologist*. <https://doi.org/10.1201/9781420070408.ch4>
- Dale, P.E.R., Knight, J.M., Dwyer, P.G., 2014. Mangrove rehabilitation: a review focusing on ecological and institutional issues. *Wetl. Ecol. Manag.* 22, 587–604. <https://doi.org/10.1007/s11273-014-9383-1>
- Danise, S., Twitchett, R.J., Little, C.T.S., Clémence, M.E., 2013. The Impact of Global Warming and Anoxia on Marine Benthic Community Dynamics: An Example from the Toarcian (Early Jurassic). *PLoS One* 8. <https://doi.org/10.1371/journal.pone.0056255>
- Darmawan, S., Takeuchi, W., Vetruta, Y., Wikantika, K., Sari, D.K., 2015. Impact of topography and tidal height on ALOS pascars polarimetric measurements to estimate aboveground biomass of mangrove forest in Indonesia. *J. Sensors* 2015. <https://doi.org/10.1155/2015/641798>
- Daru, B.H., Yessoufou, K., Mankga, L.T., Davies, T.J., 2013. A Global Trend towards the Loss of

Evolutionarily Unique Species in Mangrove Ecosystems. PLoS One 8.
<https://doi.org/10.1371/journal.pone.0066686>

- Das, L., Patel, R., Salvi, H., Kamboj, R.D., 2019. Assessment of natural regeneration of mangrove with reference to edaphic factors and water in Southern Gulf of Kachchh, Gujarat, India. *Heliyon* 5, e02250. <https://doi.org/10.1016/j.heliyon.2019.e02250>
- Dat Pham, T., Xia, J., Thang Ha, N., Tien Bui, D., Nhu Le, N., Tekeuchi, W., 2019. A review of remote sensing approaches for monitoring blue carbon ecosystems: Mangroves, sea grasses and salt marshes during 2010–2018. *Sensors (Switzerland)* 19. <https://doi.org/10.3390/s19081933>
- Department of Marine and Coastal Resources (DMCR), 1991. *Trat Mangrove Forest, Success Model, 747 "Community Power"* [WWW Document]. URL <https://www.dmcr.go.th/detailAll/2545/nws/16> (accessed 9.17.19).
- DeVries, B., Decuyper, M., Verbesselt, J., Zeileis, A., Herold, M., Joseph, S., 2015. Tracking disturbance-regrowth dynamics in tropical forests using structural change detection and Landsat time series. *Remote Sens. Environ.* 169, 320–334. <https://doi.org/10.1016/j.rse.2015.08.020>
- Di Nitto, D., Neukermans, G., Koedam, N., Defever, H., Pattyn, F., Kairo, J.G., Dahdouh-Guebas, F., 2014. Mangroves facing climate change: Landward migration potential in response to projected scenarios of sea level rise. *Biogeosciences* 11, 857–871. <https://doi.org/10.5194/bg-11-857-2014>
- Díaz-Delgado, R., Múcher, S., 2019. Editorial of special issue “drones for biodiversity conservation and ecological monitoring.” *Drones* 3, 1–4. <https://doi.org/10.3390/drones3020047>
- Diniz, C., Cortinhas, L., Nerino, G., Rodrigues, J., Sadeck, L., Adami, M., Souza-Filho, P.W.M., 2019. Brazilian mangrove status: Three decades of satellite data analysis. *Remote Sens.* 11. <https://doi.org/10.3390/rs11070808>
- Donato, D.C., Kauffman, J.B., Murdiyarto, D., Kurnianto, S., Stidham, M., Kanninen, M., 2011. Mangroves among the most carbon-rich forests in the tropics. *Nat. Geosci.* 4, 293–297. <https://doi.org/10.1038/ngeo1123>
- Duke, N.C., 2017. Mangrove Floristics and Biogeography Revisited: Further Deductions from Biodiversity Hot Spots, Ancestral Discontinuities, and Common Evolutionary Processes, in: Rivera-Monroy, V.H., Lee, S.Y., Kristensen, E., Twilley, R.R. (Eds.), *Mangrove Ecosystems: A Global Biogeographic Perspective: Structure, Function, and Services*. Springer International Publishing, Cham, pp. 17–53. https://doi.org/10.1007/978-3-319-62206-4_2
- Duke, N.C., Ball, M.C., Ellison, J.C., 1998. Factors influencing biodiversity and distributional gradients in mangroves. *Glob. Ecol. Biogeogr. Lett.* 7, 27–47. <https://doi.org/10.2307/2997695>
- Duke, N.C., Meynecke, J.-O., Dittmann, S., Ellison, A.M., Anger, K., Berger, U., Cannicci, S., Diele, K., Ewel, K.C., Field, C.D., Koedam, N., Lee, S.Y., Marchand, C., Nordhaus, I., Dahdouh-Guebas, F., 2007. A World Without Mangroves? *Science* (80-.). 317, 41b–42b. <https://doi.org/10.1126/science.317.5834.41b>
- Ellison, A.M., 2002. Macroecology of mangroves: Large-scale patterns and processes in tropical coastal forests. *Trees - Struct. Funct.* 16, 181–194. <https://doi.org/10.1007/s00468-001-0133-7>
- Ellison, A.M., 2000. Mangrove restoration: Do we know enough? *Restor. Ecol.* 8, 219–229. <https://doi.org/10.1046/j.1526-100X.2000.80033.x>

- Ellison, A.M., Farnsworth, E.J., 1996. Anthropogenic Disturbance of Caribbean Mangrove Ecosystems: Past Impacts, Present Trends, and Future Predictions. *Biotropica* 28, 549. <https://doi.org/10.2307/2389096>
- Ellison, A.M., Felson, A.J., Friess, D.A., 2020. Mangrove Rehabilitation and Restoration as Experimental Adaptive Management. *Front. Mar. Sci.* 7, 1–19. <https://doi.org/10.3389/fmars.2020.00327>
- Ellison, A.M., Mukherjee, B.B., Karim, A., 2000. Testing patterns of zonation in mangroves: Scale dependence and environmental correlates in the Sundarbans of Bangladesh. *J. Ecol.* 88, 813–824. <https://doi.org/10.1046/j.1365-2745.2000.00500.x>
- Elwin, A., Bukoski, J.J., Jintana, V., Robinson, E.J.Z., Clark, J.M., 2019. Preservation and recovery of mangrove ecosystem carbon stocks in abandoned shrimp ponds. *Sci. Rep.* 9, 1–10. <https://doi.org/10.1038/s41598-019-54893-6>
- Ewel, K.C., Bourgeois, J.A., Cole, T.G., Zheng, S., 2013. and vegetation characteristics in environmental Variation Kosrae , Micronesia forests , high-rainfall 7, 49–56.
- FAO, 2019. Restoring forest landscapes through assisted natural regeneration (ANR) – A practical manual. Bangkok.
- FAO, 2016. Map Accuracy Assessment and Area Estimation Map Accuracy Assessment and Area Estimation : A Practical Guide.
- FAO, 2007. The world’s mangroves 1980–2005; Technical Report; Food and Agriculture Organization of the United Nations. Rome, Italy.
- Fassnacht, F.E., Latifi, H., Stereńczak, K., Modzelewska, A., Lefsky, M., Waser, L.T., Straub, C., Ghosh, A., 2016. Review of studies on tree species classification from remotely sensed data. *Remote Sens. Environ.* 186, 64–87. <https://doi.org/10.1016/j.rse.2016.08.013>
- Fatoyinbo, T.E., Simard, M., Washington-Allen, R.A., Shugart, H.H., 2008. Landscape-scale extent, height, biomass, and carbon estimation of Mozambique’s mangrove, forests with Landsat ETM+ and Shuttle Radar Topography Mission elevation data. *J. Geophys. Res. Biogeosciences* 113, 1–13. <https://doi.org/10.1029/2007JG000551>
- Feller, I.C., Lovelock, C.E., Berger, U., McKee, K.L., Joye, S.B., Ball, M.C., 2010. Biocomplexity in mangrove ecosystems. *Ann. Rev. Mar. Sci.* 2, 395–417. <https://doi.org/10.1146/annurev.marine.010908.163809>
- Ferrentino, E., Nunziata, F., Zhang, H., Migliaccio, M., 2020. On the ability of polsar measurements to discriminate among mangrove species. *IEEE J. Sel. Top. Appl. Earth Obs. Remote Sens.* 13, 2729–2737. <https://doi.org/10.1109/JSTARS.2020.2989872>
- Field, C.D., 1999. Mangrove rehabilitation: Choice and necessity. *Hydrobiologia* 413, 47–52. <https://doi.org/10.1023/A:1003863415354>
- Foody, G.M., 2020. Remote Sensing of Environment Explaining the unsuitability of the kappa coefficient in the assessment and comparison of the accuracy of thematic maps obtained by image classification. *Remote Sens. Environ.* 239, 111630. <https://doi.org/10.1016/j.rse.2019.111630>
- Foody, G.M., 2002. Status of land cover classification accuracy assessment. *Remote Sens. Environ.* 80, 185–201. [https://doi.org/10.1016/S0034-4257\(01\)00295-4](https://doi.org/10.1016/S0034-4257(01)00295-4)
- Forkuo, E.K., Frimpong, A., 2012. Analysis of Forest Cover Change Detection 2, 82–92.

- Friess, D.A., Rogers, K., Lovelock, C.E., Krauss, K.W., Hamilton, S.E., Lee, S.Y., Lucas, R., Primavera, J., Rajkaran, A., Shi, S., 2019. The State of the World's Mangrove Forests: Past, Present, and Future. *Annu. Rev. Environ. Resour.* 44, 89–115. <https://doi.org/10.1146/annurev-environ-101718-033302>
- Fu, Z., Li, D., Hararuk, O., Schwalm, C., Luo, Y., Yan, L., Niu, S., 2017. Recovery time and state change of terrestrial carbon cycle after disturbance. *Environ. Res. Lett.* 12. <https://doi.org/10.1088/1748-9326/aa8a5c>
- Funk, J.M., Aguilar-Amuchastegui, N., Baldwin-Cantello, W., Busch, J., Chuvastov, E., Evans, T., Griffin, B., Harris, N., Ferreira, M.N., Petersen, K., Phillips, O., Soares, M.G., van der Hoff, R.J.A., 2019. Securing the climate benefits of stable forests. *Clim. Policy* 19, 845–860. <https://doi.org/10.1080/14693062.2019.1598838>
- Gao, B., 1996. NDWI A Normalized Difference Water Index for Remote Sensing of Vegetation Liquid Water From Space 266, 257–266. [https://doi.org/10.1016/S0034-4257\(96\)00067-3](https://doi.org/10.1016/S0034-4257(96)00067-3)
- Gao, J., 1998. A hybrid method toward accurate mapping of mangroves in a marginal habitat from SPOT multispectral data. *Int. J. Remote Sens.* 19, 1887–1899. <https://doi.org/10.1080/014311698215045>
- Ghosh, M.K., Kumar, L., Roy, C., 2016. Mapping long-term changes in mangrove species composition and distribution in the Sundarbans. *Forests* 7. <https://doi.org/10.3390/f7120305>
- Gibbons, P., Freudenburger, D., 2006. An overview of methods used to assess vegetation condition at the scale of the site. Philip Gibbons. 2006; *Ecological Management & Restoration - Wiley InterScience. Ecol. Manag. Restor.* 7, 10–17. <https://doi.org/10.1111/j1442-8903.2006.00286.x>
- Gilman, E.L., Ellison, J., Duke, N.C., Field, C., 2008. Threats to mangroves from climate change and adaptation options: A review. *Aquat. Bot.* 89, 237–250. <https://doi.org/10.1016/J.AQUABOT.2007.12.009>
- Giri, C., Long, J., Abbas, S., Murali, R.M., Qamer, F.M., Pengra, B., Thau, D., 2015. Distribution and dynamics of mangrove forests of South Asia. *J. Environ. Manage.* 148, 101–111. <https://doi.org/10.1016/j.jenvman.2014.01.020>
- Giri, C., Ochieng, E., Tieszen, L.L., Zhu, Z., Singh, A., Loveland, T., Masek, J., Duke, N., 2011. Status and distribution of mangrove forests of the world using earth observation satellite data. *Glob. Ecol. Biogeogr.* 20, 154–159. <https://doi.org/10.1111/j.1466-8238.2010.00584.x>
- Giri, C., Pengra, B., Zhu, Z., Singh, A., Tieszen, L.L., 2007. Monitoring mangrove forest dynamics of the Sundarbans in Bangladesh and India using multi-temporal satellite data from 1973 to 2000. *Estuar. Coast. Shelf Sci.* 73, 91–100. <https://doi.org/10.1016/j.ecss.2006.12.019>
- Giri, S., Mukhopadhyay, A., Hazra, S., Mukherjee, S., Roy, D., Ghosh, S., Ghosh, T., Mitra, D., 2014. A study on abundance and distribution of mangrove species in Indian Sundarban using remote sensing technique. *J. Coast. Conserv.* 18, 359–367. <https://doi.org/10.1007/s11852-014-0322-3>
- Goessens, A., Satyanarayana, B., Van Der Stocken, T., Zuniga, M.Q., Mohd-Lokman, H., Sulong, I., Dahdouh-Guebas, F., 2014. Is Matang Mangrove Forest in Malaysia sustainably rejuvenating after more than a century of conservation and harvesting management? *PLoS One* 9. <https://doi.org/10.1371/journal.pone.0105069>
- Goldberg, L., Lagomasino, D., Thomas, N., Fatoyinbo, T., 2020. Global declines in human-driven mangrove loss. *Glob. Chang. Biol.* 26, 5844–5855. <https://doi.org/10.1111/gcb.15275>

- Goldblatt, R., You, W., Hanson, G., Khandelwal, A.K., 2016. Detecting the boundaries of urban areas in India: A dataset for pixel-based image classification in google earth engine. *Remote Sens.* 8, 1–28. <https://doi.org/10.3390/rs8080634>
- Göltenboth, F., Schoppe, S., 2006. 10 - MANGROVES, in: Göltenboth, F., Timotius, K.H., Milan, P.P., Margraf, J. (Eds.), *Ecology of Insular Southeast Asia*. Elsevier, Amsterdam, pp. 187–214. <https://doi.org/https://doi.org/10.1016/B978-044452739-4/50011-5>
- Gomariz-Castillo, F., Alonso-Sarría, F., Pedro Montávez, J., Lorente-Plazas, R., 2019. An open-source web mapping tool to estimate wind energy in the Iberian Peninsula. *J. Spat. Sci.* 64, 153–172. <https://doi.org/10.1080/14498596.2017.1386597>
- Gomes, V.C.F., Queiroz, G.R., Ferreira, K.R., 2020. An overview of platforms for big earth observation data management and analysis. *Remote Sens.* 12, 1–25. <https://doi.org/10.3390/RS12081253>
- Gotelli, N., Hart, E., Ellison, A., Maintainer, J., 2015. Title Null Model Analysis for Ecological Data. R Packag. <https://doi.org/10.5281/zenodo.16522>
- Graf, W., Kleinn, C., Schall, P., Nauss, T., Detsch, F., Magdon, P., 2019. Analyzing the relationship between historic canopy dynamics and current plant species diversity in the herb layer of temperate forests using long-term Landsat time series. *Remote Sens. Environ.* 232, 111305. <https://doi.org/10.1016/j.rse.2019.111305>
- Grafström, A., Saarela, S., Ene, L.T., 2014. Efficient sampling strategies for forest inventories by spreading the sample in auxiliary space. *Can. J. For. Res.* 44, 1156–1164. <https://doi.org/10.1139/cjfr-2014-0202>
- Green, E.P., Clark, C.D., Mumby, P.J., Edwards, a. J., Ellis, a. C., 1998. Remote sensing techniques for mangrove mapping. *Int. J. Remote Sens.* 19, 935–956. <https://doi.org/10.1080/014311698215801>
- Griffiths, P., Kuemmerle, T., Baumann, M., Radeloff, V.C., Abrudan, I. V., Lieskovsky, J., Munteanu, C., Ostapowicz, K., Hostert, P., 2014. Forest disturbances, forest recovery, and changes in forest types across the carpathian ecoregion from 1985 to 2010 based on landsat image composites. *Remote Sens. Environ.* 151, 72–88. <https://doi.org/10.1016/j.rse.2013.04.022>
- Gu, J., Congalton, R.G., 2020. Analysis of the impact of positional accuracy when using a single pixel for thematic accuracy assessment. *Remote Sens.* 12, 1–21. <https://doi.org/10.3390/rs12244093>
- Guo, Q., Su, Y., Hu, T., Guan, H., Jin, S., Zhang, J., Zhao, X., Xu, K., Wei, D., Kelly, M., Coops, N.C., 2021. Lidar Boosts 3D Ecological Observations and Modelings: A Review and Perspective. *IEEE Geosci. Remote Sens. Mag.* 9, 232–257. <https://doi.org/10.1109/MGRS.2020.3032713>
- Hauff, R.D., Ewel, K.C., Jack, J., 2006. Tracking human disturbance in mangroves: Estimating harvest rates on a Micronesian Island. *Wetl. Ecol. Manag.* 14, 95–105. <https://doi.org/10.1007/s11273-005-2567-y>
- Hauser, L.T., Binh, N.A., Hoa, P.V., Quan, N.H., Timmermans, J., 2020. Gap-free monitoring of annual mangrove forest dynamics in ca mau province, vietnamese mekong delta, using the landsat-7-8 archives and post-classification temporal optimization. *Remote Sens.* 12, 1–16. <https://doi.org/10.3390/rs12223729>
- Heenkenda, M.K., Joyce, K.E., Maier, S.W., Bartolo, R., 2014. Mangrove species identification: Comparing WorldView-2 with aerial photographs. *Remote Sens.* 6, 6064–6088. <https://doi.org/10.3390/rs6076064>
- Held, A., Ticehurst, C., Lymburner, L., Williams, N., 2003. High resolution mapping of tropical mangrove

- ecosystems using hyperspectral and radar remote sensing. *Int. J. Remote Sens.* 24, 2739–2759. <https://doi.org/10.1080/0143116031000066323>
- Helmer, E.H., Rufenacht, B., 2005. Cloud-free satellite image mosaics with regression trees and histogram matching. *Photogramm. Eng. Remote Sens.* 71, 1079–1089. <https://doi.org/10.14358/PERS.71.9.1079>
- Heumann, B.W., 2011. An Object-Based Classification of Mangroves Using a Hybrid Decision Tree – Support Vector Machine Approach. *Remote Sens.* 3, 2440–2460. <https://doi.org/10.3390/rs3112440>
- Hickey, D., Bruce, E., 2010. Examining Tidal Inundation and Salt Marsh Vegetation Distribution Patterns using Spatial Analysis (Botany Bay, Australia). *J. Coast. Res.* 261, 94–102. <https://doi.org/10.2112/08-1089.1>
- Higginbottom, T.P., Symeonakis, E., 2014. Assessing land degradation and desertification using vegetation index data: Current frameworks and future directions. *Remote Sens.* 6, 9552–9575. <https://doi.org/10.3390/rs6109552>
- Hill, M.O., 1973. Diversity and Evenness: A Unifying Notation and Its Consequences. *Ecology* 54, 427–432. <https://doi.org/10.2307/1934352>
- Hogarth, P.J., 2013. Mangrove Ecosystems, in: Levin, S.A. (Ed.), *Encyclopedia of Biodiversity* (Second Edition). Academic Press, Waltham, pp. 10–22. <https://doi.org/https://doi.org/10.1016/B978-0-12-384719-5.00247-1>
- Holdridge, L.R., 1967. Life zone ecology. *Trop. Sci. Cent.* 206. <https://doi.org/Via 10.1046/j.1365-2699.1999.00329.x>
- Hong, S.H., Kim, H.O., Wdowinski, S., Feliciano, E., 2015. Evaluation of polarimetric SAR decomposition for classifying wetland vegetation types. *Remote Sens.* 7, 8563–8585. <https://doi.org/10.3390/rs70708563>
- Hu, T., Sun, X., Su, Y., Guan, H., Sun, Q., Kelly, M., Guo, Q., 2020. Development and Performance Evaluation of a Very Low-Cost UAV-Lidar System for Forestry Applications. *Remote Sens.* 13, 77. <https://doi.org/10.3390/rs13010077>
- Huang, C., Goward, S.N., Masek, J.G., Thomas, N., Zhu, Z., Vogelmann, J.E., 2010. Remote Sensing of Environment An automated approach for reconstructing recent forest disturbance history using dense Landsat time series stacks 114, 183–198. <https://doi.org/10.1016/j.rse.2009.08.017>
- Huang, X., Zhang, L., Wang, L., 2009. Evaluation of morphological texture features for mangrove forest mapping and species discrimination using multispectral IKONOS imagery. *IEEE Geosci. Remote Sens. Lett.* 6, 393–397. <https://doi.org/10.1109/LGRS.2009.2014398>
- Ifo, S.A., Moutsambote, J.M., Koubouana, F., Yoka, J., Ndzai, S.F., Bouetou-Kadilamio, L.N.O., Mampouya, H., Jourdain, C., Bocko, Y., Mantota, A.B., Mbemba, M., Mouanga-Sokath, D., Odende, R., Mondzali, L.R., Wenina, Y.E.M., Ouissika, B.C., Joel, L.J., 2016. Tree Species Diversity, Richness, and Similarity in Intact and Degraded Forest in the Tropical Rainforest of the Congo Basin: Case of the Forest of Likouala in the Republic of Congo. *Int. J. For. Res.* 2016. <https://doi.org/10.1155/2016/7593681>
- Islam, M.M., Borgqvist, H., Kumar, L., 2019. Monitoring Mangrove forest landcover changes in the coastline of Bangladesh from 1976 to 2015. *Geocarto Int.* 34, 1458–1476. <https://doi.org/10.1080/10106049.2018.1489423>

- Jackson, T.J., Chen, D., Cosh, M., Li, F., Anderson, M., Walthall, C., Doriaswamy, P., Hunt, E.R., 2004a. Vegetation water content mapping using Landsat data derived normalized difference water index for corn and soybeans. *Remote Sens. Environ.* 92, 475–482. <https://doi.org/10.1016/j.rse.2003.10.021>
- Jennerjahn, T.C., Gilman, E., Krauss, K.W., Lacerda, L.D., Nordhaus, I., Wolanski, E., 2017. Mangrove Ecosystems under Climate Change, in: Rivera-Monroy, V.H., Lee, S.Y., Kristensen, E., Twilley, R.R. (Eds.), *Mangrove Ecosystems: A Global Biogeographic Perspective: Structure, Function, and Services*. Springer International Publishing, Cham, pp. 211–244. https://doi.org/10.1007/978-3-319-62206-4_7
- Jhonnerie, R., Siregar, V.P., Nababan, B., Prasetyo, L.B., Wouthuyzen, S., 2015. Random Forest Classification for Mangrove Land Cover Mapping Using Landsat 5 TM and Alos Palsar Imageries. *Procedia Environ. Sci.* 24, 215–221. <https://doi.org/10.1016/j.proenv.2015.03.028>
- Ji, L., Zhang, L., Wylie, B.K., Rover, J., 2011. On the terminology of the spectral vegetation index $(NIR - SWIR)/(NIR + SWIR)$. *Int. J. Remote Sens.* 32, 6901–6909. <https://doi.org/10.1080/01431161.2010.510811>
- Jia, M., Wang, Z., Wang, C., Mao, D., Zhang, Y., 2019. A new vegetation index to detect periodically submerged mangrove forest using single-tide Sentinel-2 imagery. *Remote Sens.* 11, 1–17. <https://doi.org/10.3390/rs11172043>
- Jia, M., Wang, Z., Zhang, Y., Mao, D., Wang, C., 2018. Monitoring loss and recovery of mangrove forests during 42 years: The achievements of mangrove conservation in China. *Int. J. Appl. Earth Obs. Geoinf.* 73, 535–545. <https://doi.org/10.1016/j.jag.2018.07.025>
- Jia, M., Zhang, Y., Wang, Z., Song, K., Ren, C., 2014. Mapping the distribution of mangrove species in the Core Zone of Mai Po Marshes Nature Reserve, Hong Kong, using hyperspectral data and high-resolution data. *Int. J. Appl. Earth Obs. Geoinf.* 33, 226–231. <https://doi.org/10.1016/j.jag.2014.06.006>
- Jiang, J., DeAngelis, D.L., Smith, T.J., Teh, S.Y., Koh, H.L., 2012. Spatial pattern formation of coastal vegetation in response to external gradients and positive feedbacks affecting soil porewater salinity: A model study. *Landsc. Ecol.* 27, 109–119. <https://doi.org/10.1007/s10980-011-9689-9>
- Joint Research Center, 2019. Sentinel2 L1C cloud-free composites 2015-2020 [WWW Document]. *Sentin. L1C cloud-free Compos. 2015-2020*. URL https://forobs.jrc.ec.europa.eu/recaredd/S2_composite.php (accessed 1.1.20).
- Joshi, H.G., Ghose, M., 2014. Community structure, species diversity, and aboveground biomass of the Sundarbans mangrove swamps. *Trop. Ecol.* 55, 283–303.
- Kaartinen, H., Hyypä, J., Vastaranta, M., Kukko, A., Jaakkola, A., Yu, X., Pyörälä, J., Liang, X., Liu, J., Wang, Y., Kaijaluoto, R., Melkas, T., Holopainen, M., Hyypä, H., 2015. Accuracy of kinematic positioning using global satellite navigation systems under forest canopies. *Forests* 6, 3218–3236. <https://doi.org/10.3390/f6093218>
- Kanniah, K.D., Sheikhi, A., Cracknell, A.P., Goh, H.C., Tan, K.P., Ho, C.S., Rasli, F.N., 2015. Satellite images for monitoring mangrove cover changes in a fast growing economic region in southern Peninsular Malaysia. *Remote Sens.* 7, 14360–14385. <https://doi.org/10.3390/rs71114360>
- Kaufman, L., Rousseeuw, P., 2009. *Finding groups in data: an introduction to cluster analysis*. John Wiley & Sons Inc.
- Köhl, M., Magnussen, S., Marchetti, M., 2006. *Sampling Methods, Remote Sensing and GIS Multiresource*

Forest Inventory, Springer-Verlag Berlin Heidelberg New York.

- Kovacs, J.M., Liu, Y., Zhang, C., Flores-Verdugo, F., de Santiago, F.F., 2011. A field based statistical approach for validating a remotely sensed mangrove forest classification scheme. *Wetl. Ecol. Manag.* 19, 409–421. <https://doi.org/10.1007/s11273-011-9225-3>
- Kovacs, J.M., Vandenberg, C. V., Flores-Verdugo, F., 2006. Assessing fine beam RADARSAT-1 backscatter from a white mangrove (*Laguncularia racemosa* (Gaertner)) canopy. *Wetl. Ecol. Manag.* 14, 401–408. <https://doi.org/10.1007/s11273-005-6237-x>
- Krauss, K.W., Osland, M.J., 2019. Tropical cyclones and the organization of mangrove forests: a review. *Ann. Bot.* 125, 213–234. <https://doi.org/10.1093/aob/mcz161>
- Kuenzer, C., Bluemel, A., Gebhardt, S., Quoc, T.V., Dech, S., 2011. Remote sensing of mangrove ecosystems: A review. *Remote Sens.* 3, 878–928. <https://doi.org/10.3390/rs3050878>
- Kuenzer, C., Ottinger, M., Wegmann, M., Guo, H., Wang, C., Zhang, J., Dech, S., Wikelski, M., 2014. Earth observation satellite sensors for biodiversity monitoring: potentials and bottlenecks. *Int. J. Remote Sens.* 35, 6599–6647. <https://doi.org/10.1080/01431161.2014.964349>
- Kumari, P., Singh, J.K., Pathak, B., 2020. Chapter 1 - Potential contribution of multifunctional mangrove resources and its conservation, in: Patra, J.K., Mishra, R.R., Thatoi, H. (Eds.), *Biotechnological Utilization of Mangrove Resources*. Academic Press, pp. 1–26. <https://doi.org/https://doi.org/10.1016/B978-0-12-819532-1.00001-9>
- Lawley, V., Lewis, M., Clarke, K., Ostendorf, B., 2016. Site-based and remote sensing methods for monitoring indicators of vegetation condition: An Australian review, in: *Ecological Indicators*. Elsevier Ltd, pp. 1273–1283. <https://doi.org/10.1016/j.ecolind.2015.03.021>
- Lee, S Y, Jones, E.B.G., Diele, K., Castellanos-Galindo, G.A., Nordhaus, I., 2017. Biodiversity, in: Rivera-Monroy, V.H., Lee, Shing Yip, Kristensen, E., Twilley, R.R. (Eds.), *Mangrove Ecosystems: A Global Biogeographic Perspective: Structure, Function, and Services*. Springer International Publishing, Cham, pp. 55–86. https://doi.org/10.1007/978-3-319-62206-4_3
- Leempoel, K., Satyanarayana, B., Bourgeois, C., Zhang, J., Chen, M., Wang, J., Bogaert, J., Dahdouh-Guebas, F., 2013. Dynamics in mangroves assessed by high-resolution and multi-temporal satellite data: A case study in Zhanjiang Mangrove National Nature Reserve (ZMNNR), P. R. China. *Biogeosciences* 10, 5681–5689. <https://doi.org/10.5194/bg-10-5681-2013>
- Legendre, P., Legendre, L., 2012. Numerical Ecology Ch 6 - Multidimensional qualitative data, in: *Developments in Environmental Modelling*. pp. 337–424. <https://doi.org/10.1016/B978-0-444-53868-0.50008-3>
- Leong, Rick C., Friess, D.A., Crase, B., Lee, W.K., Webb, E.L., 2018. High-resolution pattern of mangrove species distribution is controlled by surface elevation. *Estuar. Coast. Shelf Sci.* 202, 185–192. <https://doi.org/10.1016/j.ecss.2017.12.015>
- Lewis, R.R., Brown, B.M., Flynn, L.L., 2019. *Methods and Criteria for Successful Mangrove Forest Rehabilitation, Coastal Wetlands*. Elsevier B.V. <https://doi.org/10.1016/b978-0-444-63893-9.00024-1>
- Li, H.T., Brunner, P., Kinzelbach, W., Li, W.P., Dong, X.G., 2009. Calibration of a groundwater model using pattern information from remote sensing data. *J. Hydrol.* 377, 120–130. <https://doi.org/10.1016/j.jhydrol.2009.08.012>

- Li, W., El-Askary, H., Qurban, M.A., Li, J., ManiKandan, K.P., Piechota, T., 2019. Using multi-indices approach to quantify mangrove changes over the Western Arabian Gulf along Saudi Arabia coast. *Ecol. Indic.* 102, 734–745. <https://doi.org/10.1016/j.ecolind.2019.03.047>
- Liu, Z., Li, J.B., Lim, B., Seng, C., Inbaraj, S. and Sun, Z. (2008), 2008. Local Spatial Statistics for Remotely Sensed Image Classification. *Int. Arch. of the Photogramm. Remote Sens. Spat. Inf. Sci.* XXXVII.
- Liu, Y., Gong, W., Hu, X., Gong, J., 2018. Forest type identification with random forest using Sentinel-1A, Sentinel-2A, multi-temporal Landsat-8 and DEM data. *Remote Sens.* 10, 1–25. <https://doi.org/10.3390/rs10060946>
- Long, J.B., Giri, C., 2011. Mapping the Philippines' mangrove forests using Landsat imagery. *Sensors* 11, 2972–2981. <https://doi.org/10.3390/s110302972>
- López-Medellín, X., Ezcurra, E., 2012. The productivity of mangroves in northwestern Mexico: A meta-analysis of current data. *J. Coast. Conserv.* 16, 399–403. <https://doi.org/10.1007/s11852-012-0210-7>
- López-Portillo, J., Lewis, R.R., Saenger, P., Rovai, A., Koedam, N., Dahdouh-Guebas, F., Agraz-Hernández, C., Rivera-Monroy, V.H., 2017. Mangrove Forest Restoration and Rehabilitation, in: Rivera-Monroy, V.H., Lee, S.Y., Kristensen, E., Twilley, R.R. (Eds.), *Mangrove Ecosystems: A Global Biogeographic Perspective: Structure, Function, and Services*. Springer International Publishing, Cham, pp. 301–345. https://doi.org/10.1007/978-3-319-62206-4_10
- Lovelock, C.E., Adame, M.F., Bennion, V., Hayes, M., Reef, R., Santini, N., Cahoon, D.R., 2015. Sea level and turbidity controls on mangrove soil surface elevation change. *Estuar. Coast. Shelf Sci.* 153, 1–9. <https://doi.org/10.1016/j.ecss.2014.11.026>
- Lucas, R., Carreiras, J., Proisy, C., Bunting, P., 2009. ALOS PALSAR applications in the tropics and subtropics: Characterisation, mapping and detecting change in forests and coastal wetlands. Eur. Sp. Agency, (Special Publ. ESA SP 664 SP).
- Lucas, R., Lule, A.V., Rodríguez, M.T., Kamal, M., Thomas, N., Asbridge, E., Kuenzer, C., 2017. Spatial Ecology of Mangrove Forests: A Remote Sensing Perspective, in: Rivera-Monroy, V.H., Lee, S.Y., Kristensen, E., Twilley, R.R. (Eds.), *Mangrove Ecosystems: A Global Biogeographic Perspective: Structure, Function, and Services*. Springer International Publishing, Cham, pp. 87–112. https://doi.org/10.1007/978-3-319-62206-4_4
- Lucas, R., Rebelo, L.M., Fatoyinbo, L., Rosenqvist, A., Itoh, T., Shimada, M., Simard, M., Souza-Filho, P.W., Thomas, N., Trettin, C., Accad, A., Carreiras, J., Hilarides, L., 2014. Contribution of L-band SAR to systematic global mangrove monitoring. *Mar. Freshw. Res.* 65, 589–603. <https://doi.org/10.1071/MF13177>
- Lucas, R.M., Mitchell, A.L., Rosenqvist, A., Proisy, C., Melius, A., Ticehurst, C., 2007. The potential of L-band SAR for quantifying mangrove characteristics and change: case studies from the tropics. *Aquat. Conserv. Mar. Freshw. Ecosyst.* 17, 245–264. <https://doi.org/https://doi.org/10.1002/aqc.833>
- Luo, Z., Sun, O.J., Xu, H., 2010. A comparison of species composition and stand structure between planted and natural mangrove forests in Shenzhen Bay, South China. *J. Plant Ecol.* 3, 165–174. <https://doi.org/10.1093/jpe/rtq004>
- Lymburner, L., Bunting, P., Lucas, R., Scarth, P., Alam, I., Phillips, C., Ticehurst, C., Held, A., 2020. Mapping the multi-decadal mangrove dynamics of the Australian coastline. *Remote Sens. Environ.* 238, 111185.

<https://doi.org/10.1016/j.rse.2019.05.004>

- Ma, W., Wang, W., Tang, C., Chen, G., Wang, M., 2020. Zonation of mangrove flora and fauna in a subtropical estuarine wetland based on surface elevation. *Ecol. Evol.* 1–15. <https://doi.org/10.1002/ece3.6467>
- Macintosh, D.J., Ashton, E.C., 2002. A Review of Mangrove Biodiversity Conservation and Management. *Ecosystems*.
- Macintosh, D.J., Ashton, E.C., Havanon, S., 2002. Mangrove rehabilitation and intertidal biodiversity: A study in the Ranong mangrove ecosystem, Thailand. *Estuar. Coast. Shelf Sci.* 55, 331–345. <https://doi.org/10.1006/ecss.2001.0896>
- Manna, S., Raychaudhuri, B., 2020. Retrieval of Leaf area index and stress conditions for Sundarban mangroves using Sentinel-2 data. *Int. J. Remote Sens.* 41, 1019–1039. <https://doi.org/10.1080/01431161.2019.1655174>
- Masek, J.G., Wulder, M.A., Markham, B., McCorkel, J., Crawford, C.J., Storey, J., Jenstrom, D.T., 2020. Landsat 9: Empowering open science and applications through continuity. *Remote Sens. Environ.* 248. <https://doi.org/10.1016/j.rse.2020.111968>
- Matasci, G., Hermosilla, T., Wulder, M.A., White, J.C., Coops, N.C., Hobart, G.W., Bolton, D.K., Tompalski, P., Bater, C.W., 2018. Three decades of forest structural dynamics over Canada’s forested ecosystems using Landsat time-series and lidar plots. *Remote Sens. Environ.* 216, 697–714. <https://doi.org/10.1016/j.rse.2018.07.024>
- Mateo, R.G., Mokany, K., Guisan, A., 2017. Biodiversity Models: What If Unsaturation Is the Rule? *Trends Ecol. Evol.* 32, 556–566. <https://doi.org/10.1016/j.tree.2017.05.003>
- Matese, A., 2020. Editorial for the special issue “forestry applications of unmanned aerial vehicles (UAVs).” *Forests* 11, 10–12. <https://doi.org/10.3390/F11040406>
- Matese, A., 2019. *Forestry Applications of Unmanned Aerial Vehicles (UAVs)*.
- Mather, P.M., Koch, M., 2011. *Computer processing of remotely sensed images*, Wiley-Blackwell is an imprint of John Wiley & Sons. John Wiley & Sons, Ltd. <https://doi.org/10.1227/00006123-197707000-00015>
- Maurya, K., Mahajan, S., Chaube, N., 2021. Remote sensing techniques: mapping and monitoring of mangrove ecosystem—a review. *Complex Intell. Syst.* <https://doi.org/10.1007/s40747-021-00457-z>
- McFeeters, S.K., 1996. The use of the Normalized Difference Water Index (NDWI) in the delineation of open water features. *Int. J. Remote Sens.* 17, 1425–1432. <https://doi.org/10.1080/01431169608948714>
- McGuinness, A.K.A., 1997. *International Association for Ecology Dispersal, Establishment and Survival of Ceriops tagal Propagules in a North Australian Mangrove Forest* Published by: Springer in cooperation with International Association for Ecology Stable URL : <http://www.jstor>. 109, 80–87.
- McKee, K.L., Faulkner, P.L., 2000. Restoration of biogeochemical function in mangrove forests. *Restor. Ecol.* 8, 247–259. <https://doi.org/10.1046/j.1526-100X.2000.80036.x>
- McMahon, D.E., Jackson, R.B., 2019. Management intensification maintains wood production over multiple harvests in tropical Eucalyptus plantations. *Ecol. Appl.* 29, 1–15. <https://doi.org/10.1002/eap.1879>

- Midekisa, A., Holl, F., Savory, D.J., Andrade-pacheco, R., Gething, W., Bennett, A., Sturrock, H.J.W., 2017. Mapping land cover change over continental Africa using Landsat and Google Earth Engine cloud computing 1–15.
- Miettinen, J., Stibig, H.J., Achard, F., 2014. Remote sensing of forest degradation in Southeast Asia—Aiming for a regional view through 5–30 m satellite data. *Glob. Ecol. Conserv.* 2, 24–36. <https://doi.org/10.1016/j.gecco.2014.07.007>
- Miller, G.J., Morris, J.T., Wang, C., 2019. Estimating aboveground biomass and its spatial distribution in coastal wetlands utilizing planet multispectral imagery. *Remote Sens.* 11. <https://doi.org/10.3390/rs11172020>
- Morris, E.K., Caruso, T., Buscot, F., Fischer, M., Hancock, C., Maier, T.S., Meiners, T., Müller, C., Obermaier, E., Prati, D., Socher, S.A., Sonnemann, I., Wäschke, N., Wubet, T., Wurst, S., Rillig, M.C., 2014. Choosing and using diversity indices: Insights for ecological applications from the German Biodiversity Exploratories. *Ecol. Evol.* 4, 3514–3524. <https://doi.org/10.1002/ece3.1155>
- Mullissa, A., Vollrath, A., Odongo-Braun, C., Slagter, B., Balling, J., Gou, Y., Gorelick, N., Reiche, J., 2021. Sentinel-1 SAR Backscatter Analysis Ready Data Preparation in Google Earth Engine. *Remote Sens.* 13, 1954. <https://doi.org/10.3390/rs13101954>
- Murray, N.J., Phinn, S.R., Clemens, R.S., Roelfsema, C.M., Fuller, R.A., 2012. Continental scale mapping of tidal flats across east Asia using the landsat archive. *Remote Sens.* 4, 3417–3426. <https://doi.org/10.3390/rs4113417>
- Mwita, E., Menz, G., Misana, S., Nienkemper, P., 2012. Detection of Small Wetlands with Multi Sensor Data in East Africa. *Adv. Remote Sens.* 01, 64–73. <https://doi.org/10.4236/ars.2012.13007>
- Myint, S.W., Giri, C.P., Wang, L., Zhu, Z., Gillette, S.C., 2008. Identifying Mangrove Species and Their Surrounding Land Use and Land Cover Classes Using an Object-Oriented Approach with a Lacunarity Spatial Measure. *GIScience Remote Sens.* 45, 188–208. <https://doi.org/10.2747/1548-1603.45.2.188>
- Nehru, P., Balasubramanian, P., 2018. Mangrove species diversity and composition in the successional habitats of Nicobar Islands, India: A post-tsunami and subsidence scenario. *For. Ecol. Manage.* 427, 70–77. <https://doi.org/10.1016/j.foreco.2018.05.063>
- NESDB, 2000. Mangrove Resources Management Plan for Sustainable Development. Bangkok, Thailand.
- Neukermans, G., Dahdouh-Guebas, F., Kairo, J.G., Koedam, N., 2008. Mangrove species and stand mapping in gazi bay (kenya) using quickbird satellite imagery. *J. Spat. Sci.* 53, 75–86. <https://doi.org/10.1080/14498596.2008.9635137>
- Nfotabong-Atheull, A., Din, N., Dahdouh-Guebas, F., 2013. Qualitative and Quantitative Characterization of Mangrove Vegetation Structure and Dynamics in a Peri-urban Setting of Douala (Cameroon): An Approach Using Air-Borne Imagery. *Estuaries and Coasts* 36, 1181–1192. <https://doi.org/10.1007/s12237-013-9638-8>
- Nguyen, H.H., McAlpine, C., Pullar, D., Johansen, K., Duke, N.C., 2013. The relationship of spatial-temporal changes in fringe mangrove extent and adjacent land-use: Case study of Kien Giang coast, Vietnam. *Ocean Coast. Manag.* 76, 12–22. <https://doi.org/10.1016/j.ocecoaman.2013.01.003>
- Nóbrega, G.N., Ferreira, T.O., Siqueira Neto, M., Mendonça, E. de S., Romero, R.E., Otero, X.L., 2019. The

- importance of blue carbon soil stocks in tropical semiarid mangroves: a case study in Northeastern Brazil. *Environ. Earth Sci.* 78, 1–10. <https://doi.org/10.1007/s12665-019-8368-z>
- Oh, R.R.Y., Friess, D.A., Brown, B.M., 2017. The role of surface elevation in the rehabilitation of abandoned aquaculture ponds to mangrove forests , Sulawesi , Indonesia 100, 325–334. <https://doi.org/10.1016/j.ecoleng.2016.12.021>
- Ohlmann, M., Miele, V., Dray, S., Chalmandrier, L., O'Connor, L., Thuiller, W., 2019. Diversity indices for ecological networks: a unifying framework using Hill numbers. *Ecol. Lett.* 22, 737–747. <https://doi.org/10.1111/ele.13221>
- Oksanen, A.J., Blanchet, F.G., Friendly, M., Kindt, R., Legendre, P., Mcglinn, D., Minchin, P.R., Hara, R.B.O., Simpson, G.L., Solymos, P., Stevens, M.H.H., Szoecs, E., 2020. Package 'vegan' .
- Oldeland, J., Wesuls, D., Rocchini, D., Schmidt, M., Jürgens, N., 2010. Does using species abundance data improve estimates of species diversity from remotely sensed spectral heterogeneity? *Ecol. Indic.* 10, 390–396. <https://doi.org/10.1016/j.ecolind.2009.07.012>
- Olofsson, P., Foody, G.M., Herold, M., Stehman, S. V., Woodcock, C.E., Wulder, M.A., 2014. Good practices for estimating area and assessing accuracy of land change. *Remote Sens. Environ.* 148, 42–57. <https://doi.org/10.1016/j.rse.2014.02.015>
- Osland, M.J., Feher, L.C., Griffith, K.T., Cavanaugh, K.C., Enwright, N.M., Day, R.H., Stagg, C.L., Krauss, K.W., Howard, R.J., Grace, J.B., Rogers, K., 2017. Climatic controls on the global distribution, abundance, and species richness of mangrove forests. *Ecol. Monogr.* 87, 341–359. <https://doi.org/https://doi.org/10.1002/ecm.1248>
- Osland, M.J., Feher, L.C., López-Portillo, J., Day, R.H., Suman, D.O., Guzmán Menéndez, J.M., Rivera-Monroy, V.H., 2018. Mangrove forests in a rapidly changing world: Global change impacts and conservation opportunities along the Gulf of Mexico coast. *Estuar. Coast. Shelf Sci.* 214, 120–140. <https://doi.org/10.1016/j.ecss.2018.09.006>
- Otero, V., Van De Kerchove, R., Satyanarayana, B., Martínez-Espinosa, C., Fisol, M.A. Bin, Ibrahim, M.R. Bin, Sulong, I., Mohd-Lokman, H., Lucas, R., Dahdouh-Guebas, F., 2018. Managing mangrove forests from the sky: Forest inventory using field data and Unmanned Aerial Vehicle (UAV) imagery in the Matang Mangrove Forest Reserve, peninsular Malaysia. *For. Ecol. Manage.* 411, 35–45. <https://doi.org/10.1016/j.foreco.2017.12.049>
- Otero, V., Van De Kerchove, R., Satyanarayana, B., Mohd-Lokman, H., Lucas, R., Dahdouh-Guebas, F., 2019. An analysis of the early regeneration of mangrove forests using Landsat time series in the matang mangrove forest reserve, Peninsular Malaysia. *Remote Sens.* 11, 1–18. <https://doi.org/10.3390/rs11070774>
- Otsu, N., 1979. A threshold selection method from gray-level histogram. *IEEE Trans. Syst. Man Cybern.* 9, 62–66. <https://doi.org/10.1109/TSMC.1979.4310076>
- Ottinger, M., Kuenzer, C., 2020. Spaceborne L-Band synthetic Aperture Radar Data for geoscientific analyses in coastal land applications: A review. *Remote Sens.* 12, 1–36. <https://doi.org/10.3390/rs12142228>
- Palmer, M.W., Earls, P.G., Hoagland, B.W., White, P.S., Wohlgemuth, T., 2002. Quantitative tools for perfecting species lists. *Environmetrics* 13, 121–137. <https://doi.org/10.1002/env.516>

- Pasquarella, V.J., Holden, C.E., Kaufman, L., Woodcock, C.E., 2016. From imagery to ecology: leveraging time series of all available Landsat observations to map and monitor ecosystem state and dynamics. *Remote Sens. Ecol. Conserv.* 2, 152–170. <https://doi.org/10.1002/rse2.24>
- Peiman, R., 2011. Pre-classification and post-classification change-detection techniques to monitor land-cover and land-use change using multi-temporal Landsat imagery: A case study on Pisa Province in Italy. *Int. J. Remote Sens.* 32, 4365–4381. <https://doi.org/10.1080/01431161.2010.486806>
- Pelletier, C., Valero, S., Inglada, J., Champion, N., Dedieu, G., 2016. Assessing the robustness of Random Forests to map land cover with high resolution satellite image time series over large areas. *Remote Sens. Environ.* 187, 156–168. <https://doi.org/10.1016/j.rse.2016.10.010>
- Peters, R., Lovelock, C., López-Portillo, J., Bathmann, J., Wimpler, M.C., Jiang, J., Walther, M., Berger, U., 2020a. Partial canopy loss of mangrove trees: Mitigating water scarcity by physical adaptation and feedback on porewater salinity. *Estuar. Coast. Shelf Sci.* 248. <https://doi.org/10.1016/j.ecss.2020.106797>
- Peters, R., Walther, M., Lovelock, C., Jiang, J., Berger, U., 2020b. The interplay between vegetation and water in mangroves: new perspectives for mangrove stand modelling and ecological research. *Wetl. Ecol. Manag.* 28, 697–712. <https://doi.org/10.1007/s11273-020-09733-0>
- Pham, T.D., Xia, J., Baier, G., Le, N.N., Yokoya, N., 2019a. Mangrove Species Mapping Using Sentinel-1 and Sentinel-2 Data in North Vietnam. *Int. Geosci. Remote Sens. Symp.* 6102–6105. <https://doi.org/10.1109/IGARSS.2019.8898987>
- Pham, T.D., Yokoya, N., Bui, D.T., Yoshino, K., Friess, D.A., 2019b. Remote sensing approaches for monitoring mangrove species, structure, and biomass: Opportunities and challenges. *Remote Sens.* 11, 1–24. <https://doi.org/10.3390/rs11030230>
- Phan, S.M., Nguyen, H.T.T., Nguyen, T.K., Lovelock, C., 2019. Modelling above ground biomass accumulation of mangrove plantations in Vietnam. *For. Ecol. Manage.* 432, 376–386. <https://doi.org/10.1016/j.foreco.2018.09.028>
- Pianka, E.R., 1973. The Structure of Lizard communities. *Annu. Rev. Ecol. Syst.* 1–39. https://doi.org/10.1007/978-0-387-49985-7_1
- Pimple, U., 2020. Dataset on plot inventories of species diversity and structural parameters of natural and rehabilitated mangrove forest in the Trat province of Thailand. *Data Br.* 30. <https://doi.org/10.1016/j.dib.2020.105500>
- Pimple, U., Leadprathom, K., Simonetti, D., Sitthi, A., Pungkul, S., Pravinongvuthi, T., Dessard, H., Peters, R., Berger, U., Siri-on, K., Kemacheevakul, P., Gond, V., 2021. Assessing mangrove species diversity, intertidal zonation and functional indicators in response to natural, regenerated, and rehabilitated succession. Manuscript submitted for publication.
- Pimple, U., Simonetti, D., Hinks, I., Oszwald, J., Berger, U., Pungkul, S., Leadprathom, K., Pravinongvuthi, T., Maprasoap, P., Gond, V., 2020. A history of the rehabilitation of mangroves and an assessment of their diversity and structure using Landsat annual composites (1987–2019) and transect plot inventories. *For. Ecol. Manage.* 462, 118007. <https://doi.org/10.1016/j.foreco.2020.118007>
- Pimple, U., Simonetti, D., Sitthi, A., Pungkul, S., Leadprathom, K., Skupek, H., Som-ard, J., Gond, V., Towprayoon, S., 2018. Google Earth Engine Based Three Decadal Landsat Imagery Analysis for Mapping of Mangrove Forests and Its Surroundings in the Trat Province of Thailand. *J. Comput.*

Commun. 06, 247–264. <https://doi.org/10.4236/jcc.2018.61025>

- Pimple, U., Sitthi, A., Simonetti, D., Pungkul, S., Leadprathom, K., Chidthaisong, A., 2017. Topographic Correction of Landsat TM-5 and Landsat OLI-8 Imagery to Improve the Performance of Forest Classification in the Mountainous Terrain of Northeast Thailand. *Sustainability* 9, 258. <https://doi.org/10.3390/su9020258>
- Piou, C., Feller, I.C., Berger, U., Chi, F., 2006. Zonation patterns of Belizean offshore mangrove forests 41 years after a catastrophic hurricane. *Biotropica* 38, 365–374. <https://doi.org/10.1111/j.1744-7429.2006.00156.x>
- Pirti, A., Gümüş, K., Erkaya, H., Hoşbaş, R.G., 2010. Evaluating repeatability of RTK GPS/GLONASS Near/Under forest environment. *Croat. J. For. Eng.* 31, 23–33.
- Polgar, G., Jaafar, Z., 2018. Endangered Forested Wetlands of Sundaland, Endangered Forested Wetlands of Sundaland. <https://doi.org/10.1007/978-3-319-52417-7>
- Polidoro, B.A., Carpenter, K.E., Collins, L., Duke, N.C., Ellison, A.M., Ellison, J.C., Farnsworth, E.J., Fernando, E.S., Kathiresan, K., Koedam, N.E., Livingstone, S.R., Miyagi, T., Moore, G.E., Nam, V.N., Ong, J.E., Primavera, J.H., Salmo, S.G., Sanciangco, J.C., Sukardjo, S., Wang, Y., Yong, J.W.H., 2010. The loss of species: Mangrove extinction risk and geographic areas of global concern. *PLoS One* 5. <https://doi.org/10.1371/journal.pone.0010095>
- Pool, D. J., Snedaker, S. C., Lugo, A.E., 1977. Structure of Mangrove Forests in Florida, Puerto Rico, Mexico, and Costa Rica. *Biotropica* 9, 195–212. <https://doi.org/10.2307/2387881>
- Poos, M.S., Jackson, D.A., 2012. Addressing the removal of rare species in multivariate bioassessments: The impact of methodological choices, in: *Ecological Indicators*. Elsevier Ltd, pp. 82–90. <https://doi.org/10.1016/j.ecolind.2011.10.008>
- Proffitt, C.E., Devlin, D.J., 2005. Long-term growth and succession in restored and natural mangrove forests in southwestern Florida. *Wetl. Ecol. Manag.* 13, 531–551. <https://doi.org/10.1007/s11273-004-2411-9>
- Proisy, C., Coutron, P., Fromard, F., 2007. Predicting and mapping mangrove biomass from canopy grain analysis using Fourier-based textural ordination of IKONOS images. *Remote Sens. Environ.* 109, 379–392. <https://doi.org/10.1016/j.rse.2007.01.009>
- Proisy, C., Viennois, G., Sidik, F., Andayani, A., Enright, J.A., Guitet, S., Gusmawati, N., Lemonnier, H., Muthusankar, G., Olagoke, A., Prospero, J., Rahmania, R., Ricout, A., Soulard, B., Suhardjono, 2018. Monitoring mangrove forests after aquaculture abandonment using time series of very high spatial resolution satellite images: A case study from the Perancak estuary, Bali, Indonesia. *Mar. Pollut. Bull.* 131, 61–71. <https://doi.org/10.1016/j.marpolbul.2017.05.056>
- Python Core Team, 2020. Python: A dynamic, open source programming language.
- R Core Team, 2021. R: A language and environment for statistical computing. R Foundation for Statistical Computing.
- Rabinowitz, D., 1978. Early Growth of Mangrove Seedlings in Panama, and an Hypothesis Concerning the Relationship of Dispersal and Zonation. *J. Biogeogr.* 5, 113–133. <https://doi.org/10.2307/3038167>
- Rahman, M.M., Lagomasino, D., Lee, S.K., Fatoyinbo, T., Ahmed, I., Kanzaki, M., 2019. Improved assessment of mangrove forests in Sundarbans East Wildlife Sanctuary using WorldView 2 and

- TanDEM-X high resolution imagery. *Remote Sens. Ecol. Conserv.* 5, 136–149. <https://doi.org/10.1002/rse2.105>
- Rakotomavo, A., Fromard, F., 2010. Dynamics of mangrove forests in the Mangoky River delta, Madagascar, under the influence of natural and human factors. *For. Ecol. Manage.* 259, 1161–1169. <https://doi.org/10.1016/j.foreco.2010.01.002>
- Rani, V., Sreelekshmi, S., Asha, C. V., Bijoy Nandan, S., 2018. Forest Structure and Community Composition of Cochin Mangroves, South-West Coast of India. *Proc. Natl. Acad. Sci. India Sect. B - Biol. Sci.* 88, 111–119. <https://doi.org/10.1007/s40011-016-0738-7>
- Rao, B.R.M., Dwivedi, R.S., Kushwaha, S.P.S., Bhattacharya, S.N., Anand, J.B., Dasgupta, S., 1999. Monitoring the spatial extent of coastal wetlands using ERS-1 SAR data. *Int. J. Remote Sens.* 20, 2509–2517. <https://doi.org/10.1080/014311699211903>
- Raulings, E.J., Morris, K., Roache, M.C., Boon, P.I., 2010. The importance of water regimes operating at small spatial scales for the diversity and structure of wetland vegetation. *Freshw. Biol.* 55, 701–715. <https://doi.org/10.1111/j.1365-2427.2009.02311.x>
- Reis-Neto, A.S., Meireles, A.J. d. A., Cunha-Lignon, M., 2019. Natural regeneration of the mangrove vegetation on abandoned salt ponds in Ceará, in the semi-arid region of northeastern Brazil. *Diversity* 11. <https://doi.org/10.3390/d11020027>
- Ren, H., Jian, S., Lu, H., Zhang, Q., Shen, W., Han, W., Yin, Z., Guo, Q., 2008. Restoration of mangrove plantations and colonisation by native species in Leizhou bay, South China. *Ecol. Res.* 23, 401–407. <https://doi.org/10.1007/s11284-007-0393-9>
- Ricklefs, R.E., Latham, R.E., 1993. Global patterns of diversity in mangrove floras. *Species Divers. Ecol. communities* 215–229.
- Ricklefs, R.E., Schwarzbach, A.E., Renner, S.S., Url, S., 2006. Rate of Lineage Origin Explains the Diversity Anomaly in the World ' s Mangrove Vegetation . *Rate of Lineage Origin Explains the Diversity Anomaly in the World ' s Mangrove Vegetation. Diversity* 168, 805–810.
- Rivera-Monroy, Victor H., Kristensen, E., Lee, S.Y., Twilley, R.R., 2017. Mangrove ecosystems: A global biogeographic perspective: Structure, function, and services, *Mangrove Ecosystems: A Global Biogeographic Perspective: Structure, Function, and Services.* <https://doi.org/10.1007/978-3-319-62206-4>
- Rivera-Monroy, Victor H, Lee, S.Y., Kristensen, E., Twilley, R.R., 2017a. Introduction, in: Rivera-Monroy, V.H., Lee, S.Y., Kristensen, E., Twilley, R.R. (Eds.), *Mangrove Ecosystems: A Global Biogeographic Perspective: Structure, Function, and Services.* Springer International Publishing, Cham, pp. 1–16. https://doi.org/10.1007/978-3-319-62206-4_1
- Rivera-Monroy, Victor H, Osland, M.J., Day, J.W., Ray, S., Rovai, A., Day, R.H., Mukherjee, J., 2017b. Advancing Mangrove Macroecology, in: Rivera-Monroy, V.H., Lee, S.Y., Kristensen, E., Twilley, R.R. (Eds.), *Mangrove Ecosystems: A Global Biogeographic Perspective: Structure, Function, and Services.* Springer International Publishing, Cham, pp. 347–381. https://doi.org/10.1007/978-3-319-62206-4_11
- Robert, E.M.R., Oste, J., Stocken, T. Van Der, Ryck, D.J.R. De, Quisthoudt, K., Kairo, J.G., Dahdouh-guebas, F., Koedam, N., Schmitz, N., 2015. Journal of Experimental Marine Biology and Ecology Viviparous mangrove propagules of *Ceriops tagal* and *Rhizophora mucronata* , where both Rhizophoraceae

- show different dispersal and establishment strategies. *J. Exp. Mar. Bio. Ecol.* 468, 45–54. <https://doi.org/10.1016/j.jembe.2015.03.014>
- Robertson, A.I., Alongi, D.M., 1992. *Tropical Mangrove Ecosystems*. American Geophysical Union, Washington, DC. <https://doi.org/https://doi.org/10.1029/CE041p0007>
- Robinson, N.P., Allred, B.W., Jones, M.O., Moreno, A., Kimball, J.S., Naugle, D.E., Erickson, T.A., Richardson, A.D., 2017. A dynamic landsat derived normalized difference vegetation index (NDVI) product for the conterminous United States. *Remote Sens.* 9, 1–14. <https://doi.org/10.3390/rs9080863>
- Rodriguez, W., Feller, I.C., Cavanaugh, K.C., 2016. Spatio-temporal changes of a mangrove–saltmarsh ecotone in the northeastern coast of Florida, USA. *Glob. Ecol. Conserv.* 7, 245–261. <https://doi.org/10.1016/j.gecco.2016.07.005>
- Rogers, K., Lymburner, L., Salum, R., Brooke, B.P., Woodroffe, C.D., 2017. Mapping of mangrove extent and zonation using high and low tide composites of Landsat data. *Hydrobiologia* 803, 49–68. <https://doi.org/10.1007/s10750-017-3257-5>
- Roslani, M.A., Mustapha, M.A., Lihan, T., Wan Juliana, W.A., 2013. Classification of mangroves vegetation species using texture analysis on RapidEye satellite imagery. *AIP Conf. Proc.* 1571, 480–486. <https://doi.org/10.1063/1.4858701>
- Ruokolainen, L., Blanchet, G., 2014. *Introduction to ecological multivariate analysis*. University of Helsinki.
- Rybczyk, J.M., Callaway, J.C., Day, J.W., 1998. A relative elevation model for a subsiding coastal forested wetland receiving wastewater effluent. *Ecol. Modell.* 112, 23–44. [https://doi.org/10.1016/S0304-3800\(98\)00125-2](https://doi.org/10.1016/S0304-3800(98)00125-2)
- Ryo, M., Aguilar-Trigueros, C.A., Pinek, L., Muller, L.A.H., Rillig, M.C., 2019. Basic Principles of Temporal Dynamics. *Trends Ecol. Evol.* 34, 723–733. <https://doi.org/10.1016/j.tree.2019.03.007>
- Sagar, S., Phillips, C., Bala, B., Roberts, D., Lymburner, L., 2018. Generating continental scale pixel-based surface reflectance composites in coastal regions with the use of a multi-resolution tidal model. *Remote Sens.* 10. <https://doi.org/10.3390/rs10030480>
- Sagar, S., Roberts, D., Bala, B., Lymburner, L., 2017. Extracting the intertidal extent and topography of the Australian coastline from a 28 year time series of Landsat observations. *Remote Sens. Environ.* 195, 153–169. <https://doi.org/10.1016/j.rse.2017.04.009>
- Saintilan, N., Williams, R.J., 2010. Short Note: The decline of saltmarsh in southeast Australia: Results of recent surveys. *Wetl. Aust.* 18, 49. <https://doi.org/10.31646/wa.228>
- Salmo, S.G., Lovelock, C., Duke, N.C., 2013. Vegetation and soil characteristics as indicators of restoration trajectories in restored mangroves. *Hydrobiologia* 720, 1–18. <https://doi.org/10.1007/s10750-013-1617-3>
- Sandilyan, S., Kathiresan, K., 2012. Mangrove conservation: A global perspective. *Biodivers. Conserv.* 21, 3523–3542. <https://doi.org/10.1007/s10531-012-0388-x>
- Santiago, F., Kovacs, J.M., Lafrance, P., 2013. An object-oriented classification method for mapping mangroves in Guinea, West Africa, using multipolarized ALOS PALSAR L-band data. *Int. J. Remote Sens.* 34, 563–586. <https://doi.org/10.1080/01431161.2012.715773>
- Sarker, S.K., Reeve, R., Paul, N.K., Matthiopoulos, J., 2019. Modelling spatial biodiversity in the world's

- largest mangrove ecosystem—The Bangladesh Sundarbans: A baseline for conservation. *Divers. Distrib.* 25, 729–742. <https://doi.org/10.1111/ddi.12887>
- Schmiegelow, J.M.M., Giancesella, S.M.F., 2014. Absence of zonation in a mangrove forest in southeastern Brazil. *Brazilian J. Oceanogr.* 62, 117–131. <https://doi.org/10.1590/S1679-87592014058806202>
- Schmitt, K., Duke, N.C., 2020. *Tropical Forestry Handbook*. Trop. For. Handb. 1–29. <https://doi.org/10.1007/978-3-642-41554-8>
- Shah, K., Mustafa Kamal, A.H., Rosli, Z., Hakeem, K.R., Hoque, M.M., 2016. Composition and diversity of plants in Sibuti mangrove forest, Sarawak, Malaysia. *Forest Sci. Technol.* 12, 70–76. <https://doi.org/10.1080/21580103.2015.1057619>
- Shannon, C.E., Weaver, W.W., 1963. *The mathematical theory of communications*. University of Illinois Press, Urbana, p. 117 P.879 853.
- Shapiro, A.C., Trettin, C.C., Küchly, H., Alavinapanah, S., 2015. The Mangroves of the Zambezi Delta : Increase in Extent Observed via Satellite from 1994 to 2013 16504–16518. <https://doi.org/10.3390/rs71215838>
- Shelestov, A., Lavreniuk, M., Kussul, N., Novikov, A., Skakun, S., 2017. Exploring Google Earth Engine Platform for Big Data Processing: Classification of Multi-Temporal Satellite Imagery for Crop Mapping. *Front. Earth Sci.* 5, 1–10. <https://doi.org/10.3389/feart.2017.00017>
- Shen, W., Li, M., Huang, C., Wei, A., 2016. Quantifying Live Aboveground Biomass and Forest Disturbance of Mountainous Natural and Plantation Forests in Northern Guangdong, China, Based on Multi-Temporal Landsat, PALSAR and Field Plot Data. *Remote Sens.* 8, 595. <https://doi.org/10.3390/rs8070595>
- Sillanpää, M., Vantellingen, J., Friess, D.A., 2017. Vegetation regeneration in a sustainably harvested mangrove forest in West Papua, Indonesia. *For. Ecol. Manage.* 390, 137–146. <https://doi.org/10.1016/j.foreco.2017.01.022>
- Simard, M., 2019. Radar Remote Sensing of Mangrove Forests: SAR Handbook: Comprehensive Methodologies for Forest Monitoring and Biomass Estimation., in: Eds. Flores, A., Herndon, K., Thapa, R., Cherrington, E. (Ed.), . NASA.
- Simard, M., Zhang, K., Rivera-Monroy, V.H., Ross, M.S., Ruiz, P.L., Castañeda-Moya, E., Twilley, R.R., Rodriguez, E., 2006. Mapping height and biomass of mangrove forests in Everglades National Park with SRTM elevation data. *Photogramm. Eng. Remote Sensing* 72, 299–311. <https://doi.org/10.14358/PERS.72.3.299>
- Simonetti, D., Pimple, U., Langner, A., Marelli, A., 2021. Pan-tropical Sentinel-2 cloud-free annual composite datasets. *Data Br.* 39, 107488. <https://doi.org/10.1016/j.dib.2021.107488>
- Simonetti, D., Simonetti, E., Szantoi, Z., Lupi, A., Eva, H.D., 2015. First Results from the Phenology-Based Synthesis Classifier Using Landsat 8 Imagery. *IEEE Geosci. Remote Sens. Lett.* 12, 1496–1500. <https://doi.org/10.1109/LGRS.2015.2409982>
- Simpson, E.H., 1949. Measurement of diversity. *Nature* 163–688.
- Singh, A., 1989. Review Article: Digital change detection techniques using remotely-sensed data. *Int. J. Remote Sens.* 10, 989–1003. <https://doi.org/10.1080/01431168908903939>

- Slagter, B., Tsendbazar, N.-E., Vollrath, A., Reiche, J., 2020. Mapping wetland characteristics using temporally dense Sentinel-1 and Sentinel-2 data: A case study in the St. Lucia wetlands, South Africa. *Int. J. Appl. Earth Obs. Geoinf.* 86, 102009. <https://doi.org/10.1016/j.jag.2019.102009>
- Smith, T.J., 1987. Effects of light and intertidal position on seedling survival and growth in tropical tidal forests. *J. Exp. Mar. Bio. Ecol.* 110, 133–146. [https://doi.org/10.1016/0022-0981\(87\)90024-4](https://doi.org/10.1016/0022-0981(87)90024-4)
- Snedaker, S.C., 1989. Overview of ecology of mangroves and information needs for Florida Bay. *Bull. Mar. Sci.* 44, 341–347.
- Snedaker, S.C., 1982. Mangrove species zonation: why?, in: Sen, D.N., Rajpurohit, K.S. (Eds.), *Contributions to the Ecology of Halophytes*. Springer Netherlands, Dordrecht, pp. 111–125. https://doi.org/10.1007/978-94-009-8037-2_8
- Son, N.T., Chen, C.F., Chang, N. Bin, Chen, C.R., Chang, L.Y., Thanh, B.X., 2015. Mangrove mapping and change detection in ca mau peninsula, vietnam, using landsat data and object-based image analysis. *IEEE J. Sel. Top. Appl. Earth Obs. Remote Sens.* 8, 503–510. <https://doi.org/10.1109/JSTARS.2014.2360691>
- Spalding, M., Blasco, F., Field, C., 1997. *World mangrove atlas*. International Society for Mangrove Ecosystems, WCMC, National Council for Scientific Research, Paris.
- Sreelekshmi, S., Nandan, S.B., Kaimal, S. V., Radhakrishnan, C.K., Suresh, V.R., 2020. Mangrove species diversity, stand structure and zonation pattern in relation to environmental factors — A case study at Sundarban delta, east coast of India. *Reg. Stud. Mar. Sci.* 35, 101111. <https://doi.org/10.1016/j.rsma.2020.101111>
- Srikanth, S., Lum, S.K.Y., Chen, Z., 2016. Mangrove root: adaptations and ecological importance. *Trees - Struct. Funct.* 30, 451–465. <https://doi.org/10.1007/s00468-015-1233-0>
- Sternberg, L.D.S.L., Teh, S.Y., Ewe, S.M.L., Miralles-Wilhelm, F., DeAngelis, D.L., 2007. Competition between hardwood hammocks and mangroves. *Ecosystems* 10, 648–660. <https://doi.org/10.1007/s10021-007-9050-y>
- Su, Y., Guo, Q., Fry, D.L., Collins, B.M., Kelly, M., Flanagan, J.P., Battles, J.J., 2016. A Vegetation Mapping Strategy for Conifer Forests by Combining Airborne LiDAR Data and Aerial Imagery. *Can. J. Remote Sens.* 42, 1–15. <https://doi.org/10.1080/07038992.2016.1131114>
- Suchewaboripont, V., Pongparn, S., Patanaponpaiboon, P., 2011. Zonal variation in leaf-litter decomposition in a secondary mangrove forest. *Tropics* 20, 1–10. <https://doi.org/10.3759/tropics.20.1>
- Sulong, I., Mohd-Lokman, H., Mohd-Tarmizi, K., Ismail, a., 2002. Mangrove mapping using Landsat imagery and aerial photographs: Kemaman District, Terengganu, Malaysia. *Environ. Dev. Sustain.* 4, 135–152. <https://doi.org/10.1023/A:1020844620215>
- Szuster, B.W., 2006. A Review of Shrimp Farming in Central Thailand and its Environmental Implications, in: *Shrimp Culture: Economics, Market, and Trade*. Leung, P. S. & Engle, C. (eds), Oxford OX4 2DQ, UK, pp. 155–166. <https://doi.org/10.1002/9780470277850.ch11>
- Tang, W., Zheng, M., Zhao, X., Shi, J., Yang, J., Trettin, C.C., 2018. Big geospatial data analytics for global mangrove biomass and carbon estimation. *Sustain.* 10, 1–17. <https://doi.org/10.3390/su10020472>
- Teh, S.Y., DeAngelis, D.L., Sternberg, L. da S.L., Miralles-Wilhelm, F.R., Smith, T.J., Koh, H.L., 2008. A

- simulation model for projecting changes in salinity concentrations and species dominance in the coastal margin habitats of the Everglades. *Ecol. Modell.* 213, 245–256. <https://doi.org/10.1016/j.ecolmodel.2007.12.007>
- Thampanya, U., Vermaat, J.E., Sinsakul, S., Panapitukkul, N., 2006. Coastal erosion and mangrove progradation of Southern Thailand. *Estuar. Coast. Shelf Sci.* 68, 75–85. <https://doi.org/10.1016/j.ecss.2006.01.011>
- Thomas, N., Bunting, P., Lucas, R., Hardy, A., Rosenqvist, A., Fatoyinbo, T., 2018. Mapping mangrove extent and change: A globally applicable approach. *Remote Sens.* 10, 1–20. <https://doi.org/10.3390/rs10091466>
- Thompson, S.D., Nelson, T.A., White, J.C., Wulder, M.A., 2015. Mapping Dominant Tree Species over Large Forested Areas Using Landsat Best-Available-Pixel Image Composites. *Can. J. Remote Sens.* 41, 203–218. <https://doi.org/10.1080/07038992.2015.1065708>
- Tian, Y., Chen, G., Tang, F., Zheng, C., Ye, Y., 2018. Effects of different types of nutrient effluent from shrimp ponds on the seedling growth of *Kandelia obovata*. *Acta Oceanol. Sin.* 37, 112–120. <https://doi.org/10.1007/s13131-018-1207-3>
- Tomlinson, P.B., 2016. *The Botany of Mangroves*, 2nd ed. Cambridge University Press. <https://doi.org/10.1017/CBO9781139946575>
- Tomlinson, P.B., 1986. *The Botany of Mangroves*. Cambridge University Press, 32 East 57th St., New York, NY 10022.
- Torres-Fernández del Campo, J., Olvera-Vargas, M., Figueroa-Rangel, B.L., Cuevas-Guzmán, R., Iñiguez-Dávalos, L.I., 2018. Patterns of Spatial Diversity and Structure of Mangrove Vegetation in Pacific West-Central Mexico. *Wetlands* 38, 919–931. <https://doi.org/10.1007/s13157-018-1041-6>
- Torresani, M., Rocchini, D., Sonnenschein, R., Zebisch, M., Marcantonio, M., Ricotta, C., Tonon, G., 2019. Estimating tree species diversity from space in an alpine conifer forest: The Rao's Q diversity index meets the spectral variation hypothesis. *Ecol. Inform.* 52, 26–34. <https://doi.org/10.1016/j.ecoinf.2019.04.001>
- Triest, L., Van der Stocken, T., Allela Akinyi, A., Sierens, T., Kairo, J., Koedam, N., 2020. Channel network structure determines genetic connectivity of landward–seaward *Avicennia marina* populations in a tropical bay. *Ecol. Evol.* 10, 12059–12075. <https://doi.org/10.1002/ece3.6829>
- Turschwell, M.P., Tulloch, V.J.D., Sievers, M., Pearson, R.M., Andradi-Brown, D.A., Ahmadi, G.N., Connolly, R.M., Bryan-Brown, D., Lopez-Marcano, S., Adame, M.F., Brown, C.J., 2020. Multi-scale estimation of the effects of pressures and drivers on mangrove forest loss globally. *Biol. Conserv.* 247, 108637. <https://doi.org/10.1016/j.biocon.2020.108637>
- Twilley, R., Snedaker, S., Yáñez-Arancibia, A., Medina, E., 1996. Biodiversity and ecosystem processes in tropical estuaries: perspectives of mangrove ecosystems.
- Twilley, R.R., 2018. Mangrove wetlands. *Encycl. Ecol.* 546–556. <https://doi.org/10.1016/B978-0-444-63768-0.00346-2>
- Twilley, R.R., 2008. Mangrove wetlands. *Encycl. Ecol.* 2, 546–556. <https://doi.org/10.1016/B978-0-444-63768-0.00346-2>

- Twilley, R.R., Castañeda-Moya, E., Rivera-Monroy, V.H., Rovai, A., 2017. Productivity and Carbon Dynamics in Mangrove Wetlands, in: Rivera-Monroy V., Lee S., Kristensen E., Twilley R. (Eds) Mangrove Ecosystems: A Global Biogeographic Perspective. Springer, Cham.
- Twilley, R.R., Rivera-Monroy, V.H., 2005. Developing performance measures of mangrove wetlands using simulation models of hydrology, nutrient biogeochemistry, and community dynamics. *J. Coast. Res.* 21, 79–93.
- United Nations Environment Program, 2014. The importance of mangroves to people: A call to action, United Nations Environment Programme World Conservation Monitoring Centre.
- Vaiphasa, C., De Boer, W.F., Skidmore, A.K., Panitchart, S., Vaiphasa, T., Bamrongrugs, N., Santitamont, P., 2007. Impact of solid shrimp pond waste materials on mangrove growth and mortality: A case study from Pak Phanang, Thailand. *Hydrobiologia* 591, 47–57. <https://doi.org/10.1007/s10750-007-0783-6>
- Valderrama-Landeros, L., Flores-de-Santiago, F., Kovacs, J.M., Flores-Verdugo, F., 2018. An assessment of commonly employed satellite-based remote sensors for mapping mangrove species in Mexico using an NDVI-based classification scheme. *Environ. Monit. Assess.* 190. <https://doi.org/10.1007/s10661-017-6399-z>
- Valiela, I., Bowen, J.L., York, J.K., 2001. Mangrove Forests: One of the World's Threatened Major Tropical Environments. *Bioscience* 51, 807. [https://doi.org/10.1641/0006-3568\(2001\)051\[0807:MFOOTW\]2.0.CO;2](https://doi.org/10.1641/0006-3568(2001)051[0807:MFOOTW]2.0.CO;2)
- Van Loon, A.F., Te Brake, B., Van Huijgevoort, M.H.J., Dijkema, R., 2016. Hydrological classification, a practical tool for mangrove restoration. *PLoS One* 11, 1–26. <https://doi.org/10.1371/journal.pone.0150302>
- Vancutsem, C., Achard, F., Pekel, J.-F., Vieilledent, G., Carboni, S., Simonetti, D., Gallego, J., Aragao, L., Nasi, R., 2020. Long-term (1990–2019) monitoring of tropical moist forests dynamics. *bioRxiv*. <https://doi.org/10.1101/2020.09.17.295774>
- Viennois, G., Proisy, C., Féret, J.B., Prospero, J., Sidik, F., Suhardjono, Rahmania, R., Longépé, N., Germain, O., Gaspar, P., 2016. Multitemporal Analysis of High-Spatial-Resolution Optical Satellite Imagery for Mangrove Species Mapping in Bali, Indonesia. *IEEE J. Sel. Top. Appl. Earth Obs. Remote Sens.* 9, 3680–3686. <https://doi.org/10.1109/JSTARS.2016.2553170>
- Vo, Q.T., Kuenzer, C., Vo, Q.M., Moder, F., Oppelt, N., 2012. Review of valuation methods for mangrove ecosystem services. *Ecol. Indic.* 23, 431–446. <https://doi.org/10.1016/j.ecolind.2012.04.022>
- Vogt, J., Piou, C., Berger, U., 2014. Comparing the influence of large- and small-scale disturbances on forest heterogeneity: A simulation study for mangroves. *Ecol. Complex.* 20, 107–115. <https://doi.org/10.1016/j.ecocom.2014.09.008>
- Wallner, A., Elatawneh, A., Schneider, T., Kindu, M., Ossig, B., Knoke, T., 2018. Remotely sensed data controlled forest inventory concept. *Eur. J. Remote Sens.* 51, 75–87. <https://doi.org/10.1080/22797254.2017.1403295>
- Walters, B.B., 2000. Local mangrove planting in the Philippines: Are fisherfolk and fishpond owners effective restorationists? *Restor. Ecol.* 8, 237–246. <https://doi.org/10.1046/j.1526-100X.2000.80035.x>
- Walters, B.B., Walters, B.B., 2004. Local Management of Mangrove Forests in the Philippines. *Hum. Ecol.*

- Wang, D., Wan, B., Qiu, P., Su, Y., Guo, Q., Wang, R., Sun, F., Wu, X., 2018. Evaluating the performance of Sentinel-2, Landsat 8 and Pléiades-1 in mapping mangrove extent and species. *Remote Sens.* 10. <https://doi.org/10.3390/rs10091468>
- Wang, L., Jia, M., Yin, D., Tian, J., 2019. A review of remote sensing for mangrove forests: 1956–2018. *Remote Sens. Environ.* 231. <https://doi.org/10.1016/j.rse.2019.111223>
- Wang, L., Silván-Cárdenas, J.L., Sousa, W.P., 2008. Neural network classification of mangrove species from multi-seasonal Ikonos imagery. *Photogramm. Eng. Remote Sensing* 74, 921–927. <https://doi.org/10.14358/PERS.74.7.921>
- Wang, L., Sousa, W.P., Gong, P., 2004. Integration of object-based and pixel-based classification for mapping mangroves with IKONOS imagery. *Int. J. Remote Sens.* 25, 5655–5668. <https://doi.org/10.1080/014311602331291215>
- Wang, Le, Sousa, W.P., Gong, P., Biging, G.S., 2004. Comparison of IKONOS and QuickBird images for mapping mangrove species on the Caribbean coast of Panama. *Remote Sens. Environ.* 91, 432–440. <https://doi.org/10.1016/j.rse.2004.04.005>
- Wang, R., Gamon, J.A., 2019. Remote sensing of terrestrial plant biodiversity. *Remote Sens. Environ.* 231. <https://doi.org/10.1016/j.rse.2019.111218>
- Wang, T., Zhang, H., Lin, H., Fang, C., 2016. Textural-spectral feature-based species classification of mangroves in Mai Po nature reserve from worldview-3 imagery. *Remote Sens.* 8, 1–15. <https://doi.org/10.3390/rs8010024>
- Wang, Y., Imhoff, M.L., 1993. Simulated and observed L-HH radar backscatter from tropical mangrove forests. *Int. J. Remote Sens.* 14 (15), 2819–2828. <https://doi.org/http://dx.doi.org/10.1080/01431169308904311>
- Watson, J.C., 1928. Mangrove forests of the Malay peninsula. *Malay. For. Rec.* 6, 1–275.
- Weiss, J., 2009. *The Economics of Climate Change in Southeast Asia: A Regional Review.* <https://doi.org/http://hdl.handle.net/11540/179>
- White, J.C., Saarinen, N., Kankare, V., Wulder, M.A., Hermosilla, T., Coops, N.C., Pickell, P.D., Holopainen, M., Hyypä, J., Vastaranta, M., 2018. Confirmation of post-harvest spectral recovery from Landsat time series using measures of forest cover and height derived from airborne laser scanning data. *Remote Sens. Environ.* 216, 262–275. <https://doi.org/10.1016/j.rse.2018.07.004>
- White, J.C., Wulder, M.A., Hobart, G.W., Luther, J.E., Hermosilla, T., Griffiths, P., Coops, N.C., Hall, R.J., Hostert, P., Dyk, A., Guindon, L., 2014. Pixel-based image compositing for large-area dense time series applications and science. *Can. J. Remote Sens.* 40, 192–212. <https://doi.org/10.1080/07038992.2014.945827>
- Wijedasa, L.S., Sloan, S., Michelakis, D.G., Clements, G.R., 2012. Overcoming limitations with landsat imagery for mapping of peat swamp forests in sundaland. *Remote Sens.* 4, 2595–2618. <https://doi.org/10.3390/rs4092595>
- Wolanski, E., Spagnol, S., Thomas, S., Moore, K., Alongi, D.M., Trott, L., Davidson, A., 2000. Modelling and visualizing the fate of shrimp pond effluent in a mangrove-fringed tidal creek. *Estuar. Coast. Shelf*

Sci. 50, 85–97. <https://doi.org/10.1006/ecss.1999.0535>

- Wu, Q., Jin, Y., Fan, H., 2016. Evaluating and comparing performances of topographic correction methods based on multi-source DEMs and Landsat-8 OLI data. *Int. J. Remote Sens.* 37, 4712–4730. <https://doi.org/10.1080/01431161.2016.1222101>
- Wulder, M.A., Loveland, T.R., Roy, D.P., Crawford, C.J., Masek, J.G., Woodcock, C.E., Allen, R.G., Anderson, M.C., Belward, A.S., Cohen, W.B., Dwyer, J., Erb, A., Gao, F., Griffiths, P., Helder, D., Hermosilla, T., Hipple, J.D., Hostert, P., Hughes, M.J., Huntington, J., Johnson, D.M., Kennedy, R., Kilic, A., Li, Z., Lymburner, L., McCorkel, J., Pahlevan, N., Scambos, T.A., Schaaf, C., Schott, J.R., Sheng, Y., Storey, J., Vermote, E., Vogelmann, J., White, J.C., Wynne, R.H., Zhu, Z., 2019. Current status of Landsat program, science, and applications. *Remote Sens. Environ.* 225, 127–147. <https://doi.org/10.1016/j.rse.2019.02.015>
- Xia, Q., Qin, C.Z., Li, H., Huang, C., Su, F.Z., 2018. Mapping mangrove forests based on multi-tidal high-resolution satellite imagery. *Remote Sens.* 10. <https://doi.org/10.3390/rs10091343>
- Xia, Q., Qin, C.Z., Li, H., Huang, C., Su, F.Z., Jia, M.M., 2020. Evaluation of submerged mangrove recognition index using multi-tidal remote sensing data. *Ecol. Indic.* 113. <https://doi.org/10.1016/j.ecolind.2020.106196>
- Xiong, J., Thenkabail, P.S., Tilton, J.C., Gumma, M.K., Teluguntla, P., Oliphant, A., Congalton, R.G., Yadav, K., Gorelick, N., 2017. Nominal 30-m cropland extent map of continental Africa by integrating pixel-based and object-based algorithms using Sentinel-2 and Landsat-8 data on google earth engine. *Remote Sens.* 9, 1–27. <https://doi.org/10.3390/rs9101065>
- Yaney-Keller, A., Tomillo, P.S., Marshall, J.M., Paladino, F. V., 2019. Using unmanned aerial systems (Uas) to assay mangrove estuaries on the pacific coast of Costa Rica. *PLoS One* 14, 1–20. <https://doi.org/10.1371/journal.pone.0217310>
- Yang, C., Everitt, J.H., Fletcher, R.S., Jensen, R.R., Mausel, P.W., 2007. Mapping black mangrove along the south Texas Gulf coast using AISA+ hyperspectral imagery. *Indiana State Univ. - 21st Bienn. Work. Aer. Photogr. Videogr. High Resolut. Digit. Imag. Resour. Assess.* 2007 75, 143–153.
- Ye, S., Rogan, J., Sangermano, F., 2018. Monitoring rubber plantation expansion using Landsat data time series and a Shapelet-based approach. *ISPRS J. Photogramm. Remote Sens.* 136, 134–143. <https://doi.org/10.1016/j.isprsjprs.2018.01.002>
- Yilmaz, M.T., Hunt, E.R., Goins, L.D., Ustin, S.L., Vanderbilt, V.C., Jackson, T.J., 2008. Vegetation water content during SMEX04 from ground data and Landsat 5 Thematic Mapper imagery. *Remote Sens. Environ.* 112, 350–362. <https://doi.org/10.1016/j.rse.2007.03.029>
- Yirdaw, E., Monge Monge, A., Austin, D., Toure, I., 2019. Recovery of floristic diversity, composition and structure of regrowth forests on fallow lands: implications for conservation and restoration of degraded forest lands in Laos. *New For.* 50, 1007–1026. <https://doi.org/10.1007/s11056-019-09711-2>
- Zhang, C., Kovacs, J.M., Liu, Y., Flores-Verdugo, F., Flores-de-Santiago, F., 2014. Separating mangrove species and conditions using laboratory hyperspectral data: A case study of a degraded mangrove forest of the Mexican Pacific. *Remote Sens.* 6, 11673–11688. <https://doi.org/10.3390/rs61211673>
- Zhang, H., Wang, T., Liu, M., Jia, M., Lin, H., Chu, L.M., Devlin, A.T., 2018. Potential of combining optical and dual polarimetric SAR data for improving mangrove species discrimination Using Rotation

Forest. *Remote Sens.* 10. <https://doi.org/10.3390/rs10030467>

- Zhang, H.K., Roy, D.P., Yan, L., Li, Z., Huang, H., Vermote, E., Skakun, S., Roger, J.C., 2018. Characterization of Sentinel-2A and Landsat-8 top of atmosphere, surface, and nadir BRDF adjusted reflectance and NDVI differences. *Remote Sens. Environ.* 215, 482–494. <https://doi.org/10.1016/j.rse.2018.04.031>
- Zhang, X., Tian, Q., 2013. A mangrove recognition index for remote sensing of mangrove forest from space. *Curr. Sci.* 105, 1149–1155.
- Zhang, X., Treitz, P.M., Chen, D., Quan, C., Shi, L., Li, X., 2017. Mapping mangrove forests using multi-tidal remotely-sensed data and a decision-tree-based procedure. *Int. J. Appl. Earth Obs. Geoinf.* 62, 201–214. <https://doi.org/10.1016/j.jag.2017.06.010>
- Zhao, C., Qin, C.Z., 2020. 10-m-resolution mangrove maps of China derived from multi-source and multi-temporal satellite observations. *ISPRS J. Photogramm. Remote Sens.* 169, 389–405. <https://doi.org/10.1016/j.isprsjprs.2020.10.001>
- Zhen, J., Liao, J., Shen, G., 2018. Mapping mangrove forests of dongzhaigang nature reserve in china using landsat 8 and radarsat-2 polarimetric SAR data. *Sensors (Switzerland)* 18. <https://doi.org/10.3390/s18114012>
- Zhu, C., Zhang, X., Zhang, N., Hassan, M.A., Zhao, L., 2018. Assessing the defoliation of pine forests in a long time-series and spatiotemporal prediction of the defoliation using Landsat data. *Remote Sens.* 10. <https://doi.org/10.3390/rs10030360>
- Zhu, X., Helmer, E.H., 2018. An automatic method for screening clouds and cloud shadows in optical satellite image time series in cloudy regions. *Remote Sens. Environ.* 214, 135–153. <https://doi.org/10.1016/j.rse.2018.05.024>
- Zhu, Z., Woodcock, C.E., 2012. Object-based cloud and cloud shadow detection in Landsat imagery. *Remote Sens. Environ.* 118, 83–94. <https://doi.org/10.1016/j.rse.2011.10.028>
- Zong, Y., 2006. Sea-levels, late quaternary | Tropics. *Encycl. Quat. Sci.* 3087–3095. <https://doi.org/10.1016/B0-44-452747-8/00149-6>

Title : Spatio-temporal dynamics of mangrove forest in Trat Province of Thailand

Keywords : Trat province ; mangrove species diversity Thailand ; automatic regrowth monitoring algorithm ; Landsat annual composites ; Rehabilitated mangroves ; Google Earth Engine ; systematic field inventories ; tidal influence ; ecosystem restoration

Abstract :

In the United Nations decade on ecosystem restoration 2021–2030, coastal ecosystems such as mangroves are listed as a priority for biodiversity restoration. Therefore, understanding large-scale mangrove species diversity and temporal changes are important for predicting ecosystem health, viability, and resilience against changing climate and human pressure. However, it is also crucial to understand the effects of conservation interventions when considering future conservation efforts and policies for mangroves. To address these concerns, we must improve our ability to gather reliable forest inventory measurements, spatial scale biodiversity predictions, and good practices for using Earth observation data. In this study, we investigated the knowledge gaps considering potential spatial diversity, intertidal zonation, and the historic state of mangrove forest species, and tested the role of environmental settings such as topography and anthropogenic (rehabilitation or plantation) settings on diversification. We have successfully integrated historic multi-satellite data, current ecological data, and micro-topographic measurements to establish a historic state and zonation for the mangrove forests in the Trat Province of Thailand. The method introduced in this study allows us to overcome the technical limitations of monitoring protocols and provides a powerful decision-support system to assess the forest recovery period, structural growth, and species composition of plantations and natural native stands over three decades. This study also identifies the main influencing factors that hinder the quality of Earth observation data and propose best practices specific to mangrove ecosystem monitoring. In addition, we developed the “automatic regrowth monitoring algorithm (ARMA)” tool and summarized the functional indicators (secondary succession) by type. ARMA can identify plantation years, recovery period, age, and structural development of rehabilitated mangroves compared with their adjacent natural and naturally regenerated mangroves. We believe that our study makes a significant contribution to mangrove biodiversity research, as it has several potential applications for restoration management planning, and therefore will be a useful tool to measure and evaluate biodiversity and thereby improve ecosystem-based mangrove forest management.

Titre : Dynamique spatio-temporelle de la forêt de mangrove dans la province de Trat en Thaïlande

Mots-clés: Province de Trat; diversité des espèces de mangroves en Thaïlande; algorithmes de suivi automatique de la repousse; composites annuels Landsat; mangroves réhabilitées; moteur Google Earth; inventaires systématiques sur le terrain; influence des marées; restauration des écosystèmes.

Résumé:

Dans le programme 2021-2030 des Nations Unies sur la restauration des écosystèmes, les mangroves sont identifiées comme une priorité pour la conservation et la restauration de la biodiversité. Il est donc important d'en comprendre la diversité spatiale et temporelle en espèces afin d'en évaluer la résilience face aux changements climatiques et aux pressions anthropiques. Il est également crucial de comprendre les effets des actions précédemment menées lorsque l'on envisage le développement de politiques ambitieuses de conservation et de restauration. Pour répondre à ces préoccupations, nous avons dû développer des méthodes d'inventaire forestier fiables, prédire spatialement la biodiversité et utiliser de façon adéquate les données d'observation de la Terre. Dans cette étude, nous avons analysé les lacunes de connaissances concernant l'organisation spatiale, la zonation intertidale et l'histoire récente des mangroves de la province de Trat. Nous avons étudié l'impact, sur la diversification forestière, des paramètres environnementaux comme la topographie et les paramètres anthropiques comme la réhabilitation des peuplements ou les plantations. Nous avons réussi à intégrer des données multi-satellites historiques, des données écologiques actuelles et des mesures micro-topographiques pour établir un état et décrire l'organisation spatiale des mangroves de la province de Trat. La méthode présentée dans cette étude nous permet de surmonter les limites techniques des protocoles de surveillance et fournit un puissant système d'aide à la décision pour évaluer la période de récupération de la forêt, la croissance et la composition en espèces des plantations et des peuplements naturels sur trois décennies. Cette étude identifie également les principaux facteurs d'influence qui nuisent à la qualité des données d'observation de la Terre et propose de meilleures pratiques spécifiques à la surveillance des écosystèmes de mangrove. En outre, nous avons développé l'outil "automatic regrowth monitoring algorithm (ARMA)" et résumé les indicateurs fonctionnels (succession secondaire) par type de peuplement. ARMA peut identifier les années de plantation, la période de récupération, l'âge et le développement des mangroves réhabilitées par rapport aux mangroves naturelles ou régénérées naturellement. Nous pensons que notre étude apporte une contribution significative à la recherche sur

caractérisation de la biodiversité des mangroves, car elle a plusieurs applications potentielles pour la planification et la gestion de la restauration forestière. Cet outil est utile pour mesurer et évaluer la biodiversité et pourra ainsi améliorer la gestion des forêts de mangroves.